Divergent regulations of c-Kit receptor by TPO and CD9 in megakaryocytic cells : implication in the dynamic control of the balance proliferation/differentiation

Azza Chaabouni

Année 2015

Thèse présentée à l'Université Claude Bernard Lyon1

ECOLE DOCTORALE BIOLOGIE MOLECULAIRE INETGRATIVE ET CELLULAIRE

Pour l'obtention du titre de

DOCTEUR DE L'UNIVERSITE LYON1

SPECIALITE : Biologie cellulaire et Hématologie

Date de soutenance : 6 Octobre 2015

N° d'ordre : 144-2015

Azza CHAABOUNI

Régulations divergentes du récepteur c-Kit par la TPO et la tétraspanine CD9 : Implication dans le contrôle de la balance prolifération/maturation mégacaryocytaire

Directeur de thèse : Dr François MORLE

Jury de thèse :

Mme Michèle SOUYRI	**Rapporteur**
Mme Evelyne LAURET	**Rapporteur**
Mme Kathrin GIESELER	**Examinateur**
Mr. Boris GUYOT	**Examinateur**
Mr. François MORLE	**Examinateur**

UNIVERSITE CLAUDE BERNARD - LYON 1

Président de l'Université	**M. François-Noël GILLY**
Vice-président du Conseil d'Administration	M. le Professeur Hamda BEN HADID
Vice-président du Conseil des Etudes et de la Vie Universitaire	M. le Professeur Philippe LALLE
Vice-président du Conseil Scientifique	M. le Professeur Germain GILLET
Directeur Général des Services	M. Alain HELLEU

COMPOSANTES SANTE

Faculté de Médecine Lyon Est – Claude Bernard	Directeur : M. le Professeur J. ETIENNE
Faculté de Médecine et de Maïeutique Lyon Sud – Charles Mérieux	Directeur : Mme la Professeure C. BURILLON
Faculté d'Odontologie	Directeur : M. le Professeur D. BOURGEOIS
Institut des Sciences Pharmaceutiques et Biologiques	Directeur : Mme la Professeure C. VINCIGUERRA
Institut des Sciences et Techniques de la Réadaptation	Directeur : M. le Professeur Y. MATILLON
Département de formation et Centre de Recherche en Biologie Humaine	Directeur : Mme. la Professeure A-M. SCHOTT

COMPOSANTES ET DEPARTEMENTS DE SCIENCES ET TECHNOLOGIE

Faculté des Sciences et Technologies	Directeur : M. F. DE MARCHI
Département Biologie	Directeur : M. le Professeur F. FLEURY
Département Chimie Biochimie	Directeur : Mme Caroline FELIX
Département GEP	Directeur : M. Hassan HAMMOURI
Département Informatique	Directeur : M. le Professeur S. AKKOUCHE
Département Mathématiques	Directeur : M. le Professeur Georges TOMANOV
Département Mécanique	Directeur : M. le Professeur H. BEN HADID
Département Physique	Directeur : M. Jean-Claude PLENET
UFR Sciences et Techniques des Activités Physiques et Sportives	Directeur : M. Y.VANPOULLE
Observatoire des Sciences de l'Univers de Lyon	Directeur : M. B. GUIDERDONI
Polytech Lyon	Directeur : M. P. FOURNIER
Ecole Supérieure de Chimie Physique Electronique	Directeur : M. G. PIGNAULT
Institut Universitaire de Technologie de Lyon 1	Directeur : M. le Professeur C. VITON
Ecole Supérieure du Professorat et de l'Education	Directeur : M. le Professeur A. MOUGNIOTTE
Institut de Science Financière et d'Assurances	Directeur : M. N. LEBOISNE

Remerciements

J’aimerai remercier Dr Michèle SOUYRI et Dr Evelyne LAURET pour avoir accepté d’évaluer mon travail de thèse et la qualité de ce manuscrit. J’aimerai aussi remercier Pr Kathrin GIESELER d’avoir bien voulu évaluer mon travail en participant au jury de thèse.

Je remercie les Dr. Véronique MAGUER-SATTA et Thomas MERCHER pour leurs conseils précieux transmis lors des comités de thèse.

Je ne saurai exprimer l’ampleur de ma gratitude à mon directeur de thèse le Dr. François MORLE tout d’abord pour m’avoir accepté dans son équipe, mais aussi d’avoir toujours été disponible, de s’être montré patient, d’avoir bien voulu m’apprendre le métier et me transmettre ses connaissances. Merci pour les discussions toujours enrichissantes, mais aussi de vous être accroché pour faire face aux temps difficiles. Merci d’être passionné par ce que vous faites.

Je remercie énormément le Dr. Boris GUYOT pour s’être montré très patient, d’avoir pris le temps de m’expliquer les choses et pour les nombreux échanges m’ayant permis de progresser à de nombreux moments au cours de ma thèse. Merci pour ta franchise.

Je suis reconnaissante envers Guy Mouchiroud et Michèle pour leur aide à différents moments de ma thèse.

Un grand merci à tous les anciens et nouveaux membres de l’équipe, de même que les membres du laboratoire CGPhiMC pour la chaleureuse ambiance créée rendant ainsi le quotidien plus agréable.

Je remercie sincérement pour leur encouragement et leur soutien mes amis qui sont aussi entrain de traverser cette épreuve.

Je remercie aussi ma tante de m’avoir assez intrigué pour que je me lance dans cette aventure et pour ses nombreux conseils.

Un grand merci à Raphael pour m’avoir toujours encouragé, m’avoir épaulé et rassuré et sans qui je n’aurai pu m’accrocher pour continuer à avancer durant cette épreuve.

Je remercie par-dessus tous mes parents pour m’avoir toujours épaulé, toujours poussé à aller de l’avant, pour leur soutien infaillible et leurs conseils.

Régulations divergentes du récepteur c-Kit par la TPO et la tétraspanine CD9 : Implication dans le contrôle de la balance prolifération/maturation mégacaryocytaire

La thrombopoïétine (TPO) favorise successivement la prolifération et la maturation des progéniteurs mégacaryocytaires, soulevant la question du mécanisme expliquant cette dualité d'action. La signalisation SCF/ c-Kit est essentielle pour la prolifération de tous les progéniteurs hématopoïétiques, alors que l'extinction de l'expression du récepteur c-Kit est requise pour l'engagement en différenciation terminale. Réciproquement, l'équipe a montré que la stimulation de la voie Notch affecte une sous-population de progéniteurs bipotents érythro-mégacaryocytaires exprimant fortement CD9 (tétraspanine induite durant la maturation mégacaryocytaire) et favorise la reprise de leurs divisions au détriment de leur différenciation mégacaryocytaire terminale. Cet effet de la voie Notch s'accompagne d'une augmentation de l'expression de c-Kit. Ces observations m'ont conduite à m'intéresser aux mécanismes de régulation de c-Kit par la TPO en m'appuyant sur un modèle de progéniteurs bipotents immortalisés et dont la prolifération est strictement dépendante de la TPO (cellules G1ME). Les travaux réalisés durant ma thèse m'ont permis d'établir que (i) La stimulation des cellules G1ME par le ligand de Notch DLL1 favorise l'expression de c-Kit et réprime celle de CD9 (ii) L'activation inattendue de c-Kit par la TPO contribue à la prolifération (iii) c-Kit contribue activement à restreindre la polyploïdisation des cellules G1ME en présence de TPO (iv) La tétraspanine CD9 elle-même réprime l'expression de c-Kit à la membrane. Sur la base de ces résultats, nous proposons le modèle selon lequel, la TPO participerait à la fois à la prolifération des progéniteurs du fait de sa capacité à activer c-Kit, mais contribue aussi à l'augmentation de l'expression de CD9 qui en atteignant un seuil suffisant conduit à l'extinction de l'expression de c-Kit à la surface, entrainant alors l'arrêt des divisions et la différenciation mégacaryocytaire terminale.

Mots-clés : TPO, Notch, c-Kit, tétraspanine, CD9, différenciation érythro-mégacaryocytaire

Divergent regulations of c-Kit receptor by TPO and CD9 in megakaryocytic cells: Implication in the dynamic control of the balance proliferation/differentiation

The Thrombopoietin (TPO) favors both the proliferation and the maturation of megakaryocytic progenitors, raising the question of the molecular mechanism explaining its dual function. SCF/ c-Kit signaling is essential for all hematopoietic progenitors amplification, whereas terminal differentiation requires the extinction of c-Kit receptor expression. Reciprocally, we evidenced in our team that Notch stimulation enables the induction of c-Kit expression and act on a particular subpopulation of bipotent erythro-megakaryocytic progenitors highly expressing the tetraspanin CD9 (induced during megakaryocytic maturation) and favors their re-entry in a cycling state by blocking their megakaryocytic maturation. These observations lead to the investigation of the molecular mechanism of c-Kit regulation by TPO in a cellular model of bipotent progenitors immortalized and dependent on TPO, the G1ME cells. During my thesis, I evidenced that: i) Notch stimulation induces the expression of c-Kit while repressing CD9 expression; ii) Surprisingly TPO is able to activate c-Kit allowing its contribution to cell proliferation; iii) c-Kit also represses megakaryocytic polyploidization (endomitosis characterizing megakaryocytic maturation) of G1ME cells; iv) The tetraspanin CD9 represses the expression of c-Kit. The ensemble of these data allows us to propose the following model wherein TPO activates c-Kit allowing the proliferation of megakaryocytic progenitors, while concomitantly induces the expression of the tetraspanin CD9 that will reach a sufficient level to provoke the extinction of c-Kit expression at the cell surface, thus enabling the arrest of cell cycling progress and the engagement into terminal megakaryocytic maturation.

Keywords:TPO, Notch, c-Kit, tetraspanin, CD9, erythro-megakaryocytic differentiation

Résumé

Même dans un environnement stable, tout progéniteur se divise un nombre limité de fois avant de s'engager irrémédiablement en différenciation, suggérant ainsi l'existence d'une horloge cellulaire contrôlant son maintien à l'état indifférencié.

Dans notre équipe, nous nous sommes interrogés sur les mécanismes moléculaires permettant le maintien à l'état indifférencié avant le basculement définitif en différenciation terminale et avons choisi comme modèle d'étude les progéniteurs hématopoïétiques bipotents érythro-mégacaryocytaires (MEP). Dans ce contexte, la voie de signalisation Notch étant connue comme un intervenant crucial du choix de destinée cellulaire, nous avons choisi de l'utiliser comme outil pour disséquer les mécanismes moléculaires contrôlant la balance prolifération/ différenciation des MEP.

Ainsi, précédemment à mon intégration, des travaux de l'équipe ont mis en évidence un rôle positif de la voie Notch sur l'amplification de la descendance bipotente E/MK des progéniteurs MEP murins. Cette observation nous a amené à rechercher le mécanisme d'action de la voie Notch permettant l'amplification des MEP. Dans ce contexte, des travaux de l'équipe avaient permis de montrer que la destinée cellulaire des progéniteurs MEP reposait essentiellement sur l'antagonisme fonctionnel entre les deux facteurs de transcription Fli-1 et EKLF, tous deux requérant leur interaction avec un partenaire commun GATA1, afin d'induire respectivement la différenciation soit mégacaryocytaire soit érythrocytaire. De plus, l'action de la voie Notch sur l'amplification des MEP s'est avéré strictement dépendant de la présence de SCF, le ligand du récepteur c-Kit dont l'expression a été augmentée, suggérant l'intervention d'un axe Notch/c-Kit dans l'amplification des progéniteurs MEP. Par ailleurs, des travaux plus récents ont montré un effet plus prononcé de la voie Notch sur une sous-population de MEP exprimant fortement la tétraspanine CD9, initialement biaisée vers la différenciation mégacaryocytaire, suggérant ainsi une interaction fonctionnelle entre CD9 et la voie Notch impliquée dans le contrôle de la balance prolifération/ différenciation mégacaryocytaire.

Ces observations ont amené plusieurs questions et les objectifs de ma thèse ont été premièrement d'explorer l'implication de GATA1 en aval de la voie Notch au cours de l'amplification des MEP, deuxièmement d'étudier la régulation de c-Kit par Notch et son

implication dans le contrôle de la balance prolifération/différenciation et enfin d'explorer l'interaction fonctionnelle entre Notch, CD9 et TPOR, ce dernier étant connu pour avoir un rôle double à la fois sur la prolifération et la différenciation des progéniteurs mégacaryocytaires.

Ainsi, au cours de ma thèse j'ai étudié dans un premier temps la capacité de la voie Notch à réguler l'expression de GATA1 en formulant comme hypothèse que l'augmentation de son niveau d''expression ou de phosphorylation permettrait de diminuer la stringence entre les facteurs Fli-1 et EKLF expliquant ainsi le maintien de l'état bipotent. Parallèlement, nous avons testé l'implication de la phosphorylation de GATA1 dans l'effet pro-amplificateur de Notch sur les MEP en utilisant un modèle murin exprimant une forme non-phosphorylable. J'ai pu observer que la stimulation des cellules L8057 par la voie Notch n'induit l'augmentation ni des niveaux d'expression ni de phosphorylation de GATA1. De plus, l'expression d'une forme non-phosphorylable de GATA1 n'a pas affecté la capacité de la voie Notch à induire l'amplification des progéniteurs bipotents MEP, permettant ainsi d'exclure l'implication de la phosphorylation de GATA1 dans l'effet pro-amplificateur de Notch sur les MEP. Au contraire de notre hypothèse de départ, j'ai pu démontrer un effet répresseur de la voie Notch sur l'expression de GATA1 dans les cellules L8057, qui a pu être confirmé dans les MEP natifs. Ces résultats suggérent ainsi l'intervention potentielle de taux diminués de GATA1 dans l'amplification des MEP.

Dans un deuxième temps, j'ai exploré la régulation de c-Kit par la voie Notch et la TPO dans la lignée bipotente E/MK G1ME immortalisée en absence de GATA1 et en présence de TPO. Ainsi, j'ai pu démontrer que la voie Notch régule positivement l'expression de c-Kit directement au niveau transcriptionnel et cet effet s'est avéré indépendant des régulateurs les plus connus de c-Kit GATA2 et SCL. De plus, cet effet s'est accompagné par une répression de l'expression de marqueurs de différenciation mégacaryocytaire terminale comme CD9 et PF4. De manière plus importante, en couplant une stratégie d'ARN interférence et d'inhibiteurs pharmacologique, j'ai pu mettre en évidence l'implication critique de c-Kit dans la prolifération TPO-dépendante des cellules G1ME. De plus, j'ai pu mettre en évidence une activation de c-Kit non par son ligand canonique le SCF mais par la TPO. Conjointement à son effet pro-prolifératif, c-Kit contribuerait à la répression de la différenciation mégacaryocytaire des cellules G1ME comme suggéré par l'augmentation de la population polyploïde en présence d'un inhibiteur de c-Kit, le Masitinib. De manière

originale, j'ai pu mettre en évidence un nouveau rôle de la tétraspanine CD9 dans la répression de l'expression de surface de c-Kit, comme attesté par la forte corrélation inverse de leurs niveaux d'expression observée suite à la transfection des cellules G1ME avec des siARN ciblant les transcrits de CD9.

L'ensemble de ces résultats nous a permis de proposer un modèle expliquant le rôle double de la TPO sur le contrôle à la fois de la prolifération et de la différenciation mégacaryocytaire. Ainsi, nous proposons qu'au cours de la progression vers la différenciation mégacaryocytaire, la TPO par le biais de l'activation de c-Kit permet l'amplification des progéniteurs mégacaryocytaires tout en restreignant leur différenciation terminale. Concomitamment, l'augmentation progressive de l'expression de CD9 cause la diminution progressive de l'expression de c-Kit jusqu'à atteindre un niveau seuil causant la perte totale de son expression et signant ainsi l'engagement définitif en différenciation terminale.

En somme, mes travaux de thèse ont permis de mettre en évidence l'intégration de signaux Notch et TPO sur la régulation de GATA1, c-Kit, et CD9. Ces acteurs feraient partie d'un même réseau qui contribuerait à la régulation de la balance prolifération/ différenciation des progéniteurs bipotents MEP. Nous proposons que la voie Notch permette le maintien des MEP en restreignant leur différenciation à la fois érythrocytaire et mégacaryocytaire par la répression de l'interaction de GATA1 avec les facteurs de transcription Fli-1 et EKLF. D'un autre côté, nous proposons que Notch induise l'expression de c-Kit en réprimant l'expression de ses régulateurs négatifs GATA1 ou CD9, définissant ainsi un axe Notch/c-Kit favorable à l'amplification des progéniteurs à l'état bipotent.

En nous basant sur des études récentes mettant en évidence l'implication de CD9 dans le contrôle de certaines voies de signalisation à travers le contrôle de leur sécrétion sous forme d'exosomes, ainsi que l'intense activité sécrétoire précédemment décrite des mégacaryocytes, mon travail de thèse ouvre sur une nouvelle perspective impliquant le contrôle de l'engagement en différenciation mégacaryocytaire signée par le contrôle par CD9 de la sécrétion de c-Kit sous forme d'exosomes.

Abbreviations list

ACK-2: Anti c-Kit antibody

ADAM: A disintegrin And Metalloproteinase

AKT: Activated Kinase

AMKL: Acute Megakaryoblastic Leukemia

AML: Acute Myelgenous Leukemia

CRA: Competitive Repopulation Assay

DSL: Delta, Serrate, Lag-1

E/ MK: Erythro-megakaryocytic

EPO: Erythropoietin

ERK: Extracellular signal-regulated kinase

FOXO: Forkhead box O

Grb2: Growth factor receptor-bound protein

HSC: Hematopoietic stem cell

ICN: Intracellular Notch

JAK: Janus Kinase

JNK: c-Jun N-terminal Kinase

MAML: Mastermind-Like

MAPK: Mitogen Activated Protein Kinase

MK: Megakaryocytes

MMP: Matrix Metallo-Proteinase

MPD: Myeloproliferative disorder

MSPC: Mesenchymal stem and progenitor cell

mTOR: mammalian target of rapamycin

NICD: Notch IntraCellular Domain

PF4: Platelet Factor 4

PI3K: Phosphoinositide 3 Kinase

PKC: Protein Kinase C

RBC: Red Blood Cells

RTK: Receptor with Tyrosine Kinase activity

SCF: Stem cell factor

SFK: Src Family Kinase

SHC: Src homology 2 domain containing

SOCS: Suppressors of cytokines signaling

SOS: Son of sevenless

STAT: Signal Transducers and Activators of Transcription

TACE: TNF-α converting enzyme

T-ALL: T cell Acute Lymphoblastic Leukemia

TPO: Thrombopoietin

List of figures and tables

INTRODUCTION

Table of content

INTRODUCTION

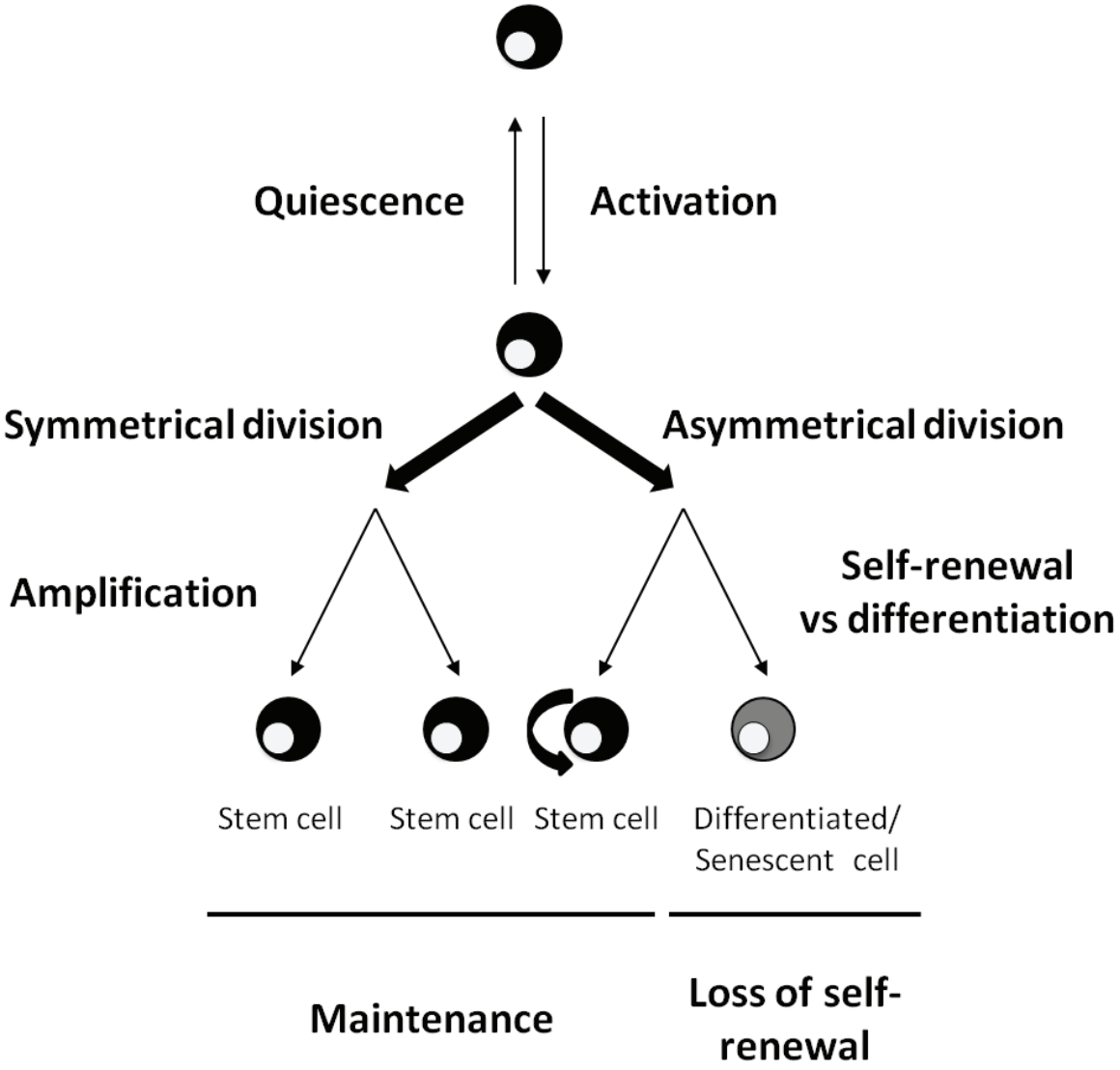

Figure 1: The different fates of hematopoietic stem cells

Stem cells transit between active (cell cycling) and dormant (quiescence) states. By exiting the cell cycle and entering in a quiescent state, stem cells are protected from external damaging agents. By symmetrical divisions, stem cells can generate two identical stem cells and amplify their pool without losing their multipotency. By asymmetrical divisions, stem cells generate a stem cell with conserved multipotency (self-renewal) and a second cell which can either differentiate inducing the progressive loss of oligopotency and self-renewal abilities or becomes senescent.

1 Hematopoiesis

The hematopoietic system is responsible for the production of all mature blood cells, which have to be renewed continuously in steady state condition because of their limited lifespan or in stress condition when facing infections or hemorrhage. Mature blood cells derive from hematopoietic stem cells (HSC) which irrevocably lose their multipotency or die by senescence after multiple cell cycles. As presented in **Figure 1**, HSCs can be maintained through either cell cycle exit and entering a quiescent state, or through self-renewing (asymmetrical division) and amplification (symmetrical division). Consequently, HSCs can replenish blood cells compartment throughout all individual lifespan. Thus, the balance between quiescence, amplification/self-renewal and differentiation has to be tightly regulated in order to avoid stem cell pool exhaustion.

Mature blood cells (including lymphocytes, macrophages, granulocytes, platelets and red blood cells) are produced in a hierarchical manner through the successive differentiation of the multipotent hematopoietic stem cell into pluripotent then bipotent and monopotent progenitors. This hierarchical model implies that HSC has to be activated in order to generate all mature blood cells. Nevertheless, recent studies pointed out unexpected overlap between stem and progenitor cells properties, HSC pool heterogeneity and special properties of megakaryocytic biased HSC. In the first part of this chapter I will present our current understanding of megakaryocytic cells production according to the classical hierarchical model of hematopoiesis, while in the second part I will summarize recent observations highlighting the proximity between HSC and megakaryocytic lineage.

1.1 Hierarchical processing of hematopoiesis

The hierarchical model was built from progeny analyses of hematopoietic stem/progenitor cells either *in vivo* by transplantation or *in vitro*by colony assays. These techniques were allowed and complemented by HSC and progenitors purification upon their fractionation based on different sets of cell surface markers. Using serial or competitive transplantation assay, different subtypes of HSC were discovered depending on their self-renewal/maintenance ability: Long-term HSCs (LT-HSCs) are the most primitive and differentiate into

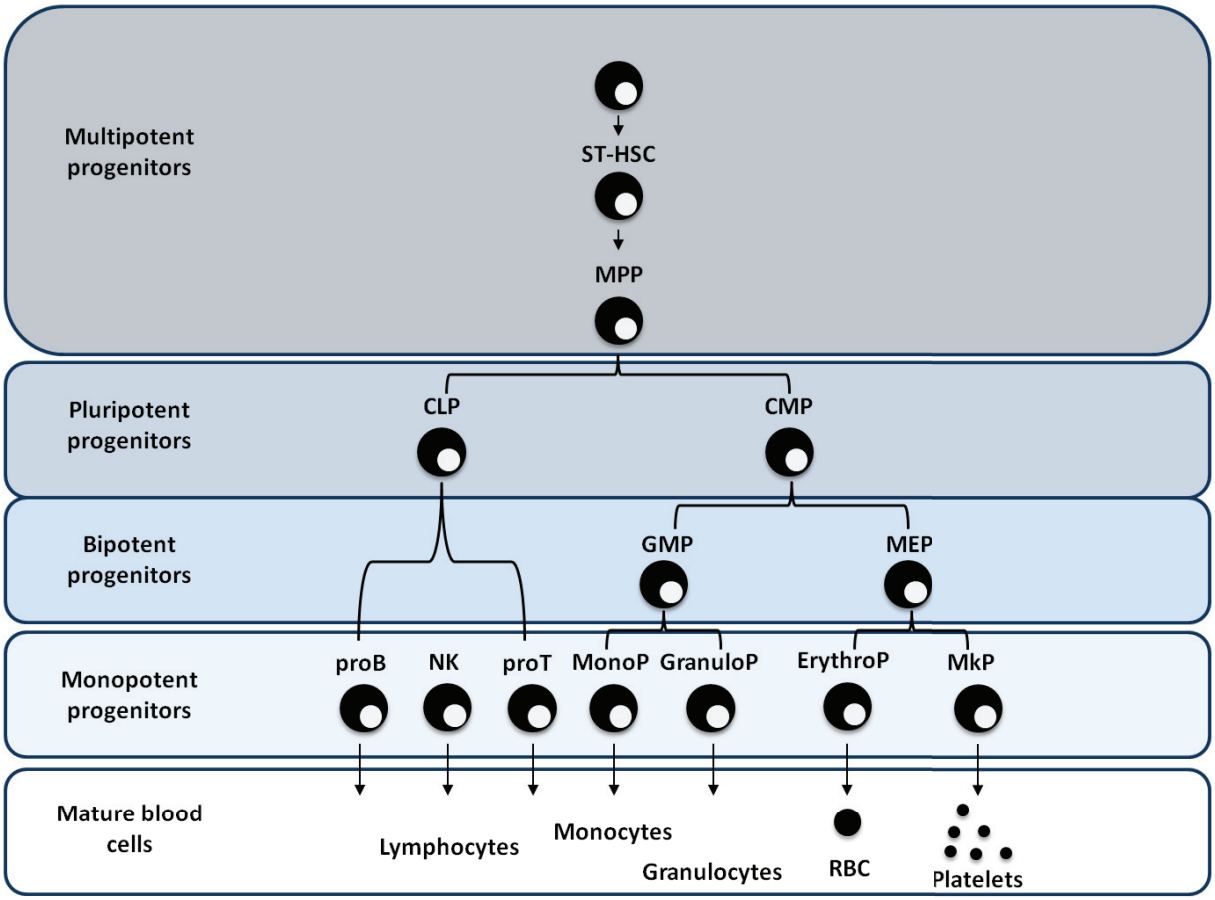

Figure 2: The standard hierarchical model of hematopoiesis

Multipotent hematopoietic stem cells with long-term self-renewal ability (LT-HSC) differentiate and lose progressively their self-renewal capacity giving rise to short-term (ST-) HSCs and multipotent progenitors (MPP). MPP give rise to either common lymphoid (CLP) or common myeloid pluripotent progenitors (CMP). CLP further differentiate into monopotent progenitors responsible for the generation of B or T lymphocytes or Natural Killer cells (NK). CMP further differentiate into bipotent progenitors either common to granulocytes and monocytes (GMP), or common to erythrocytes and megakaryocytes (MEP). Monopotent erythrocytic progenitors terminally differentiate into red blood cells, while megakaryocytic progenitors differentiate into platelets.

less self-renewing short-term HSCs (ST-HSCs), then into multipotent progenitors (MPP). Both *in vivo* and *in vitro* studies showed specific lineage-combinations, thus suggesting the existence of common pluri- or bi-potent progenitors. Indeed, MPP differentiate into either common lymphoid progenitor from which B and T lymphocytes and Natural Killer cells are derived, or into common myeloid progenitor (CMP) from which bipotent megakaryocyte erythrocyte progenitor (MEP) and granulocyte monocyte progenitor (GMP) are derived. The bipotent MEP further differentiates into monopotent erythrocytic (producing red blood cells (RBC) or monopotent megakaryocytic progenitor (producing platelets) and the bipotent GMP further differentiate into monopotent granulocytic progenitor (producing all types of granulocytes) or into monopotent monocytic progenitor (producing monocytes/ macrophages when infiltrated into tissues) **(Figure 2)**(Akashi et al., 2000).

1.2 Main regulators of HSC cell fate

Whether remaining in a quiescent state, proliferating or differentiating into one or another lineage, HSCs and progenitors choice is governed by a complex and permanent crosstalk between external signals (represented by the microenvironment including cytokines) and internal signals (represented by signaling pathways and their influence on transcription factors and micro-RNAs networks). Given the huge number of studies on HSCs cell fate maintenance and differentiation, here I will only exemplify some general regulation mechanisms and cite some main important actors controlling HSCs cell fates.

1.2.1 Cytokines and receptors

Hematopoietic stem and progenitor cells are under the influence either of common cytokines necessary for their proliferation and survival such as the Stem Cell Factor (SCF), or of lineage-specific cytokines acting also on progenitors' maturation such as Interleukin-7 for lymphocytes B and T, Granulocyte Macrophage Colony Stimulating Factor (GM-CSF) for granulocytes and monocytes, erythropoietin (EPO) for red blood cells and thrombopoietin (TPO) for platelets **(Figure 3)**. The integration of external signals is ensured at the cell membrane by receptors which haveselective affinity for their specific ligands.For example, SCF binds to c-Kit receptor, EPO to EPO-R and thrombopoietin (TPO) to c-MPL. This level of

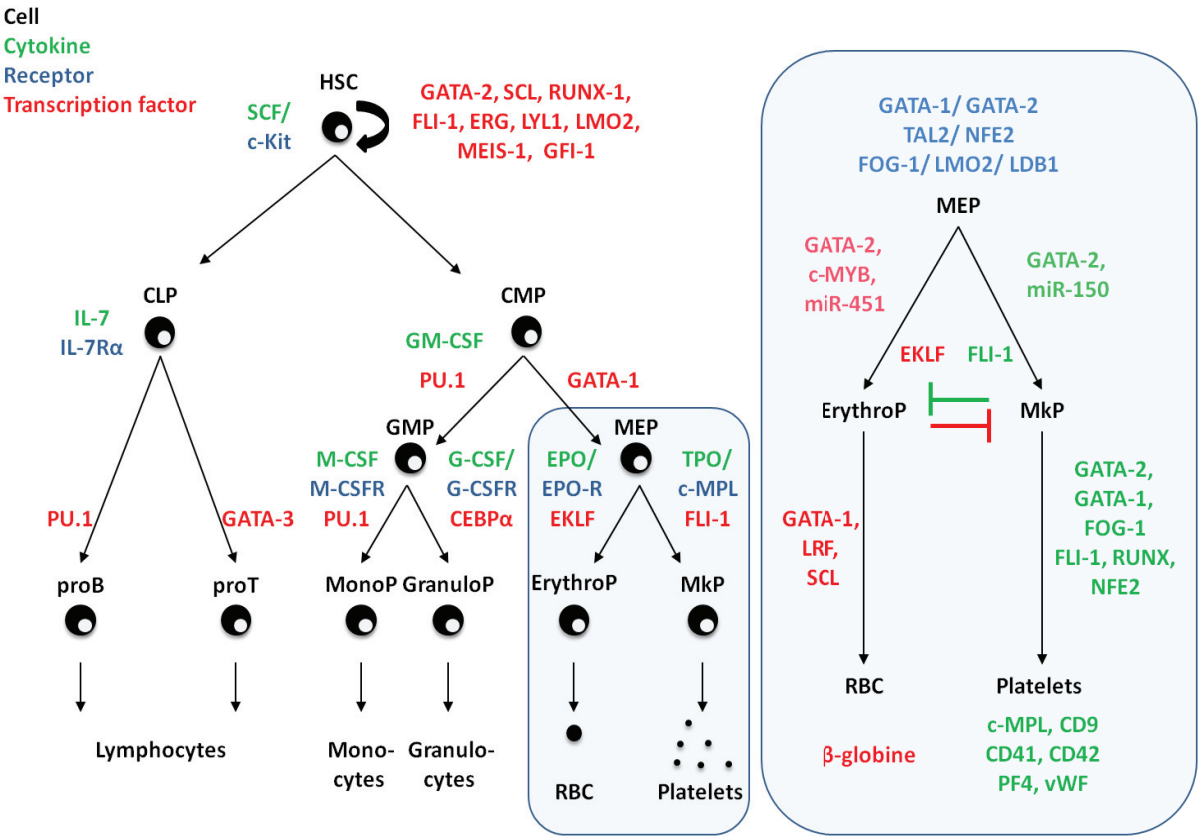

Figure 3: Main cytokines, cytokine receptors and transcription factors controlling hematopoiesis

A: Hematopoietic tree on which are indicated the main cytokines (green), cytokine-receptors (blue) and transcription factors (red) contributing to each lineage commitment and identity.

B: Focus on the main transcription factors and miRNA controlling bipotent (blue), erythrocytic (red) or megakaryocytic (green) lineages identity. Functional cross-antagonism between FLI-1 and EKLF is one of the main transcriptional mechanisms involved in the commitment between erythrocytic and megakaryocytic lineages. Few specific differentiation markers expressed in mature red blood cells or platelets are indicated at the bottom.

specificity is complemented by selectiveexpression of eachcytokine/receptor couple for each lineagewhich can mediate different cellular responses depending on the cell context or history. As a matter of fact, the same signaling pathway can induce opposed effects when comparing two different cellular contexts. For instance, TPO can both induce proliferation or quiescence of HSC (Yoshihara et al., 2007)and SCF/c-Kit stimulates proliferation and survival in stem and all hematopoietic progenitors, whereas it is essential for mast cells differentiation (Serve et al., 1995)(Papadimitriou et al., 1995)

1.2.2 Transcription factors

Transcription factors, which levels can be modulated in response to cytokines, act in combination by forming activating or repressing complexes and inter-regulate their expression in order to define lineage specific transcriptional programs (reviewed in (Sarrazin and Sieweke, 2011). For instance, HSCs and myeloid progenitors identity is defined notably by common transcription factors members of GATA and ETS families such as GATA-2 and FLI-1. Otherwise, PU.1 transcription factor is essential for B-Lymphopoiesis and monopoiesis and is repressed by GATA-1 at the level of the pluripotent CMP or by GATA-1 and GATA-2 at the level of megakaryocytic progenitors in order to maintain cell identity. Among other important lineage-specific transcription factors we can cite GATA-3 for T-lymphopoiesis, CEBP-α for granulopoiesis, EKLF for erythropoiesis and FLI-1 for megakaryopoiesis **(Figure 3)**.

1.2.3 The hematopoietic niche

The activity of HSCs is regulated by external signals provided by their microenvironment which is located into the bone marrow and called hematopoietic niche(reviewed in (Boulais and Frenette, 2015)**(Figure 4)**. The hematopoietic niche is innerved by the sympathetic nervous system and vascularised by specialized venules called sinusoids and by arterioles. Principal cell types composing the hematopoietic niche are notably osteoblasts, endothelial cells, mesenchymal progenitors but also hematopoietic cells such as megakaryocytes and macrophages.

The hypothesis of low oxygenic niche (hypoxia) being essential for the maintenance of HSCs by quiescence and self-renewal is mainly based on the correlation between gradual cell cycle staining and distance from blood flow. Indeed, on the contrary to short-term cycling

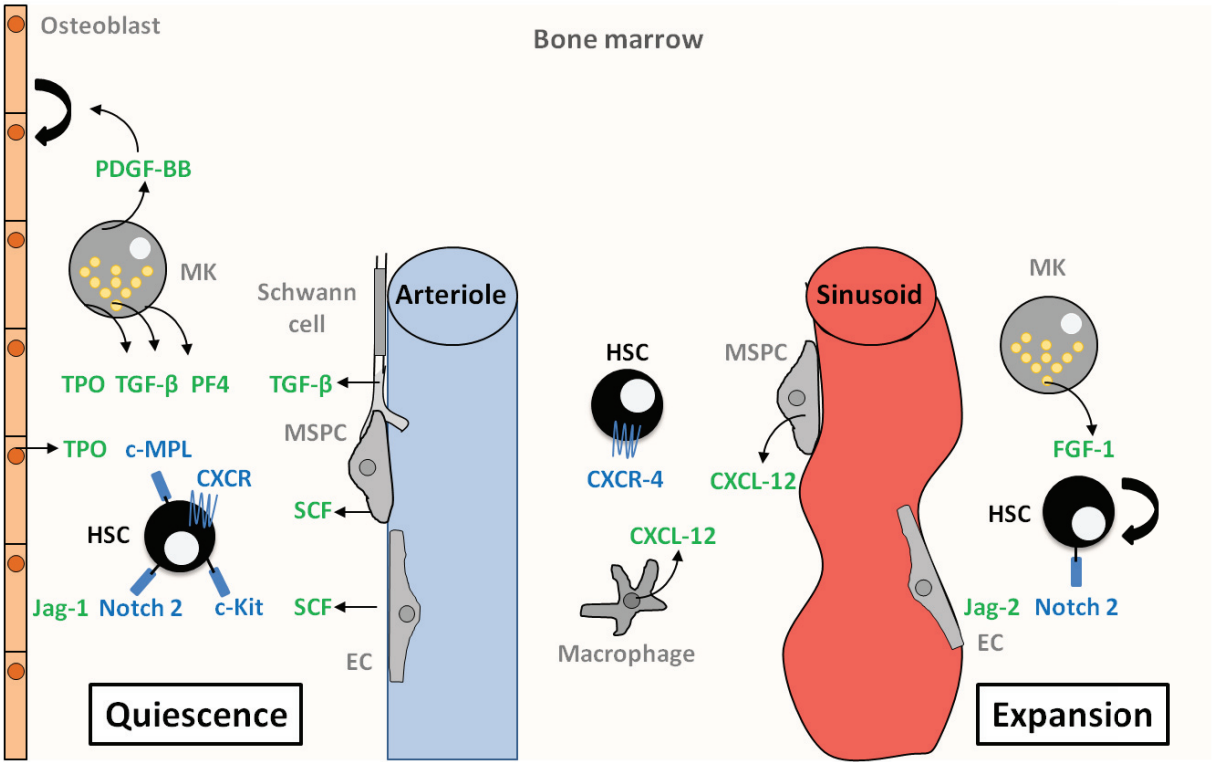

Figure 4: The hematopoietic niche : Cellular and molecular components affecting HSCs function

HSCs (black) evolve in a specialized microenvironment called niche which is located into the bone marrow. The niche is vascularized by arterioles (blue) and specialized veinules called sinusoids (red), as well as innerved by the sympathetic system represented here by Schwann cells. The cellular components of the niche influencing HSCs function are osteoblasts (brown) and several other hematopoietic or non hematopoietic cells (grey) including endothelial cells (EC), Mesenchymal stem and progenitor cell (MSPC), as well as megakaryocytes (MK) and macrophages. Niche cells affect HSCs function by secreting different factors, or through the expression of different ligands (in green) which bind to their specific receptor (in blue) on HSCs.

HSCs, quiescent long-term HSCs were located far from blood flow(Winkler et al., 2010). Furthermore, they were characterized by a hypoxic profile based on low mitochondrial activity (Simsek et al., 2010), location into a sub-fraction of the bone marrow positively stained with pimonidazole (Parmar et al., 2007)(chemical agent forming complexes only into reduced environment) and a high level of hypoxia induced factors (HIF-1 α) (Takubo et al., 2010).

This hypothesis was recently reassessed based on the refinement of HSCs location in relation to the vasculature and the reinterpretation of the hypoxic profile.As a matter of fact, HSCs are located into the endosteum (bone surface) with no preferential association with sinusoids or arterioles (Nombela-Arrieta and Silberstein, 2014). A complementary study showed that HSCs location depends on their cycling state as quiescent LT-HSCs are enriched into the endosteum and preferentially associated with arterioles, whereas their activation induces their migration next to sinusoids (Kunisaki et al., 2013).Besides, direct measurement of O_2 concentration confirmed the global hypoxic state of the niche but highlighted its heterogeneity. Surprisingly, O_2 concentration was lower next to sinusoids and higher next to arterioles (Spencer et al., 2014). Additionally, global hypoxia into the niche and the hypoxic profile of HSC can be explained by a combination of intrinsic and extrinsic factors. Intrinsically, HIF-1 expression is stabilized by MEIS-1 (Simsek et al., 2010), a co-factor for HOX transcription factors (Shen et al., 1999). Extrinsically, SCF (Pedersen et al., 2008) and TPO (Kirito and Kaushansky, 2005)induce HIF-1α expression.

SCF is mostly produced by endothelial and perivascular cells and is essential for the maintenance of HSCs(Ding et al., 2012). Endothelial cells also express Notch ligands which regulate HSCs maintenance(Bowers et al., 2015; Butler et al., 2010; Chiang et al., 2013). TPO is produced by osteoblasts (Yoshihara et al., 2007)and megakaryocytes(Nakamura-Ishizu et al., 2014b) and induces HSCs quiescence (Qian et al., 2007). The regulation of HSC activity by megakaryocytes will be detailed in the following chapters.

Population name	Molecular marker	Reference
MEP	Lin- Sca1- cKit+ IL7R- CD34-CD16/32 low	(Akashi et al., 2000)
PEM	Lin- Sca1- cKit+ CD34-CD16/32 low	(Sanchez et al., 2006)
PreMegE	Lin- Sca1-cKit+ Flk2- IL7Rα- CD34- CD41- CD150+ CD105 low	(Pronk et al., 2007)
BEMP	Lin- Sca1- cKit+ Flt3- IL7Rα- CD150+ CD105 low CD9 low	(Ng et al., 2012)
MERP HSC	Lin- cKit+ CD34- Sca1+ CD150+ CD41 +/-	(Yamamoto et al., 2013)

Table 1: Prospective purification of bipotent erythro-megakaryocytic progenitors identified in mice

Membrane markers used for mouse bipotent erythro-megakaryocytic progenitors prospective purification by FACS and the corresponding references describing their phenotype are indicated. Functional data indicate that PreMegE and BEMP largely overlap, whereas MEP subset is included in the PreMegE/BEMP. PEM are bipotent cells derived from MEP identified in stress conditions and are unable to proliferate *in vitro*. MERP HSCs have been identified by single cell transplantation showing long term repopulation activity with only erythroid and megakaryocytic potential. MERP differ from other bipotent progenitors by the expression of stem cell marker Sca1.

1.3 The main regulators of the bipotent MEP cell fate

1.3.1 The bipotent megakaryocyte erythrocyte progenitor (MEP)

The existence of a bipotent erythrocytic megakaryocytic progenitor was first evidenced by *in vitro* observation of mixed colonies containing both erythrocytic and megakaryocytic cells, following flow-cytometry sorting of human bone marrow cells according to CD34 and CD38 markers (Debili et al., 1996). Next, the purification of murine MEPs was reported from different sources like spleen, bone marrow from normal or anemia-stressed mice(Akashi et al., 2000)(Vannucchi et al., 2000) or fetal liver (Traver et al., 2001).As recapitulated in **Table 1**, combinations of cell surface markers were used for MEPs purification including CD34, CD16/32 (Akashi et al., 2000), CD9 and CD150 (Ng et al., 2012). Interestingly, when seeded *in vitro*, MEP progenitors generate not only mixed colonies but also uni-lineage erythrocytic and megakaryocytic colonies, suggesting low stability of the bipotent state leading to rapid commitment toward either lineage.

1.3.2 Erythropoiesis

Erythropoiesis is the process allowing the production of red blood cells (RBC) which are responsible for tissue oxygenation. RBCs highly express hemoglobin, an iron-containing molecule which is able to bind oxygen.

1.3.2.1 The cooperation between SCF and EPO signaling

As schematized in **Figure 5**, the most immature erythrocytic progenitors are BFU-E (Burst-Forming-Unit-Erythroid) from which are derived CFU-E (Colony-Forming-Unit-Erythroid). Both of BFU-E and CFU-E progenitors depend on the cooperation between SCF/c-Kit and EPO/EPO-R signaling for their survival and expansion in normal and stress erythropoiesis(Broudy et al., 1996; Huddleston et al., 2003). In hypoxic conditions, EPO production by the kidney is increased favoring the survival of CFU-E progenitors and subsequent increase of BFU-E production (Mide et al., 2001). While renewing divisions of erythrocytic progenitors requires both SCF and EPO, differentiation into mature erythrocytes requires the presence of EPO alone and concomitant loss of c-Kit expression (Muta et al., 1995).

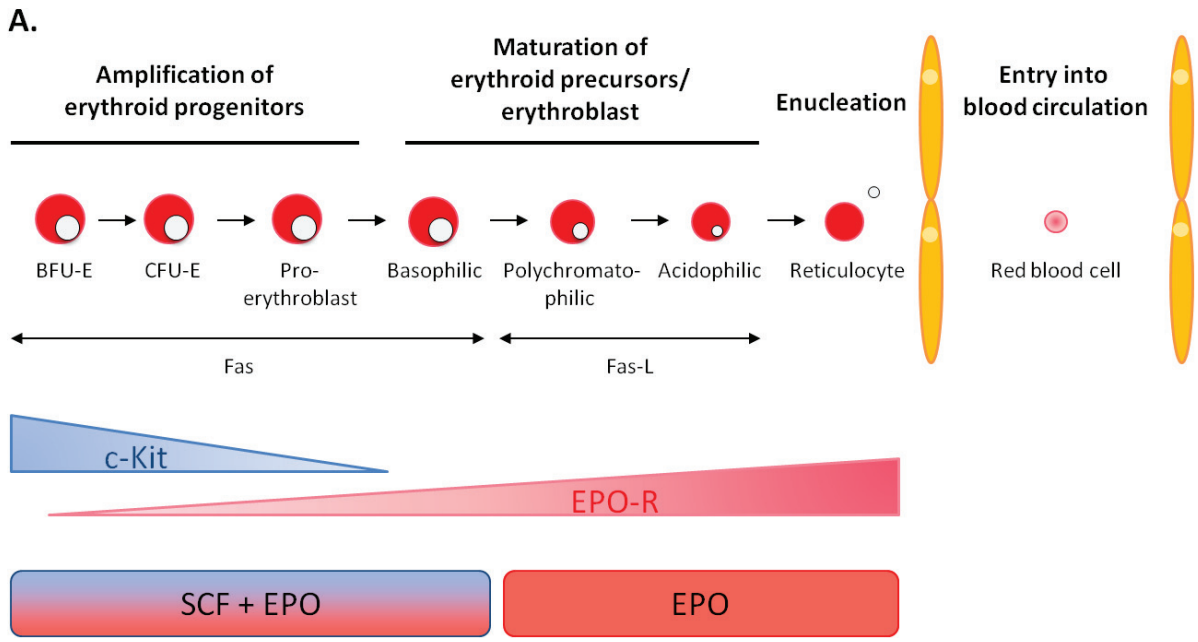

Figure 5: The erythrocytic differentiation steps and cytokine dependency

A.The cooperation between Erythropoietin (EPO) and Stem cell factor (SCF) allows the proliferation of erythrocytic progenitors BFU-E (Burst-Forming-Unit-Erythrocyte), CFU-E (Cell-Forming-Unit-Erythrocyte) and pro-erythroblasts which express both c-Kit and EPO-R receptors. The transition to erythroid precursors is characterized by the loss of c-Kit expression (blue triangle) and the increase of EPO-R expression (red triangle). The extinction of c-Kit expression marks the dependency upon EPO alone (red rectangle) and the engagement into terminal erythroid divisions. During terminal maturation, the nucleus is condensed until its enucleation from the reticulocytes which then enter into circulation to generate mature red blood cells. The size of erythroid progenitors' pool is regulated by apoptosis of early Fas expressing progenitors induced by late progenitors expressing FasL.

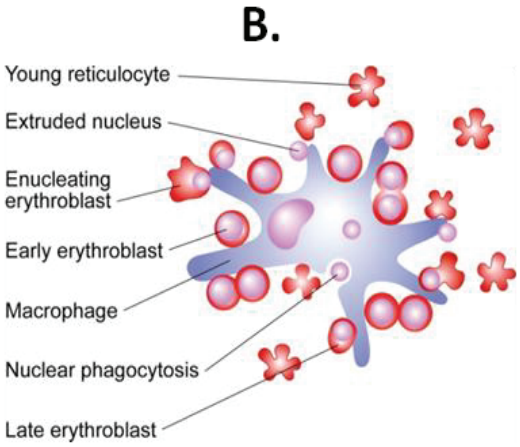

B. Schematic representation of the erythroid island wherein a central macrophage is surrounded by erythroid cells at different stages of maturation (adapted from (Chasis and Mohandas, 2008)).

In vitro studies establish the role of SCF/c-Kit signaling during the expansion of pro-erythroblasts by stimulating cell cycle progression mediated by c-Myc (Munugalavadla and Kapur, 2005). The cooperation between EPO and c-Kit can be illustrated by the stabilization of EPO-R by SCF/c-Kit signaling, which allows the induction of Bcl-xL and the survival of erythroid progenitors (Kapur and Zhang, 2001). Furthermore, c-Kit and EPO-R associate physically and SCF induces the phosphorylation of EPO-R in 32D myeloid cell line (Wu et al., 1995). Additionally, co-stimulation by EPO and SCF shows synergistic effect on downstream signaling molecules such as JAK-2 (Arcasoy and Jiang, 2005), STAT-5 (Boer et al., 2003)and MAPK ERK-1/2 (Sui et al., 1998). During erythroid differentiation, c-Kit expression is down-regulated by the combination of transcriptional repression by GATA-1 ((Munugalavadla et al., 2005) and depletion from thecell surfaceand subsequent degradation induced by EPO through Lyn kinase (Kosmider et al., 2009) and c-CBL(Masson et al., 2006; Odai et al., 1995; Zeng et al., 2005).Consequently, the absence of SCF/c-Kit signaling and the stimulation by EPO/ EPO-R signaling induces cell cycle arrest, partly mediated by p27 (Tamir et al., 2000), and engagement into maturation.

1.3.2.2 From erythroblasts to RBC

Erythroblasts undergo terminal divisions which are accompanied by cell size reduction and hemoglobin accumulation rendering the cytoplasm more and more acidophilic. The acidophilic erythroblast extrudes its nucleus becoming a reticulocyte which will lose its organelles (mitochondria and endoplasmic reticulum) and enter blood flow as a red blood cell.

1.3.2.3 The erythroblastic niche

The erythroblastic island is constituted of a central macrophage surrounded by erythroid cells at all stages of maturation(Chasis and Mohandas, 2008)(Bessis, 1958)(Mohandas and Prenant, 1978)**(Figure 5)**. The regulation of RBC production rate is allowed by cell to cell interactions. Indeed, while undergoing terminal divisions, erythroblasts (Fas-Ligand positive cells) negatively regulate the number of erythrocytic progenitors (Fas receptor positive cells) by inducing their apoptosis through Fas/Fas-L interaction(De Maria et al., 1999).

Besides, macrophages regulate many aspects all along erythropoiesis such as proliferation (Rhodes et al., 2008)adhesion-dependent survival (Fabriek et al., 2007; Hanspal et al., 1998) of erythroid progenitors, iron-uptake (Leimberg et al., 2008), as well as their maturation

(Chow et al., 2013), nucleus extrusion (Soni et al., 2006);(Yoshida et al., 2005) and finally senescent RBC phagocytosis in the liver and spleen.

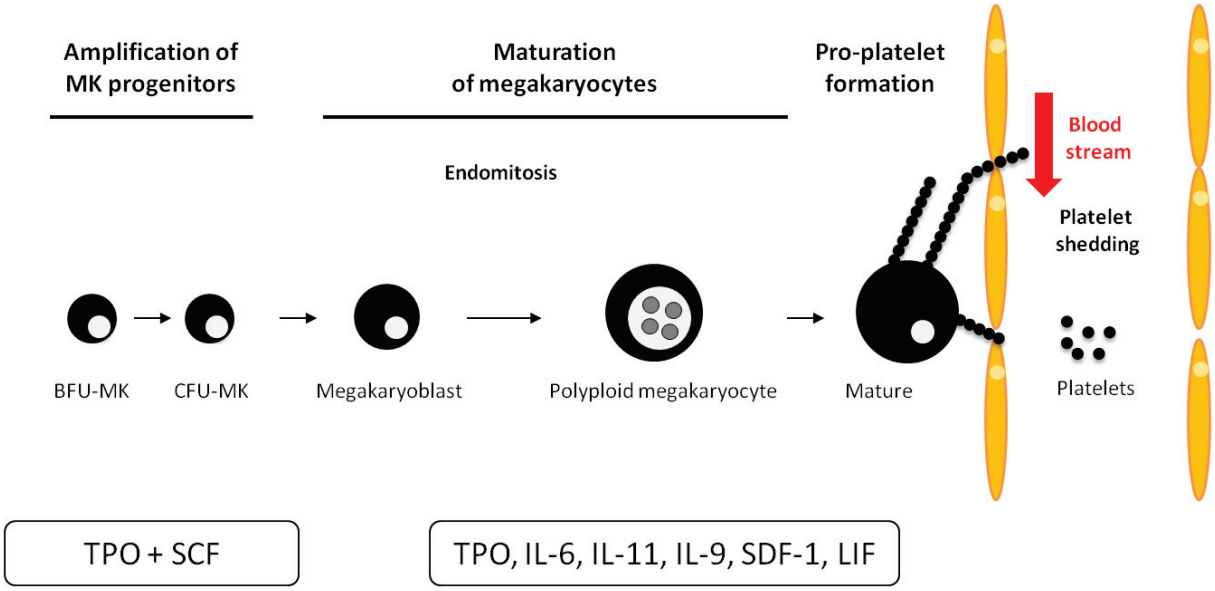

Figure 6: The megakaryocytic differentiation steps and cytokine dependency

Megakaryocytic progenitors amplify under TPO and SCF signals and generate megakaryocytes which maturation depends onthe cooperation between TPO and other cytokines. Megakaryocytes' maturation is characterized by endomitosis, the increase of cytoplasm/ nucleus ratio and the formation of membrane extensions, called pro-platelets which expand between endothelial cells and are shredded into platelets notably under the effect of blood stream.

1.3.2.4 Transcription factors essential for erythropoiesis

At the MEP level, EKLF transcription factor antagonizes FLI-1 activity allowing the specification of erythrocytic versus megakaryocytic cell fate (Bouilloux et al., 2008; Frontelo et al., 2007)**(Figure 3)**. During the amplification of erythrocytic progenitors, GATA-2 allows the expression of c-Kit and the progress into cell-cycle(Munugalavadla et al., 2005). The engagement into final maturation is characterized by the replacement of GATA-2 by GATA-1 notably on GATA-2 (Grass et al., 2003)and c-Kit (Jing et al., 2008)transcription regulatory sequences, inducing their transcriptional repression. Along with its co-factors (FOG-1, LMO2, LDB1) and other transcription factors such as LRF, TAL-1, RUNX-1 and SCL, GATA-1 and EKLF induce the expression of erythrocytic genes responsible for heme synthesis, cytoskeletal modifications and energy production (Hodge et al., 2006)(Tallack et al., 2012)(Dore et al., 2012).

1.3.3 Megakaryopoiesis

Megakaryopoiesis is the process allowing the production of platelets, important for blood vessel repair due to their expression of adhesion proteins, their aggregation and pro-inflammatory functions. Megakaryopoiesis is an active process allowing the production of approximately 10^{11} platelets per day in humans, a number that can be induced 10 timesupon emergency(Kaushansky, 2005).

1.3.3.1 From megakaryocytic progenitors to platelets

As schematized in **Figure 6**, the most immature megakaryocytic progenitors are BFU-MK (Burst-Forming-Unit-Megakaryocyte) from which are derived CFU-MK (Colony-Forming-Unit-Megakaryocyte). Both CFU-MK and BFU-MK progenitors amplify under TPO/c-MPL(Ng et al., 2014)and SCF/c-Kit (Zeuner et al., 2007) signals. Differentiation of CFU-MK allows the generation of megakaryoblasts which undergo variable number of cytokinesis-abortive mitosis,also called endomitosis, inducing the increase of cell ploidy up to 16N in average in mammals. Following important accumulation of granules and membrane into the cytoplasm accompanied by nucleus size reduction, mature megakaryoblasts migrate next to blood vessels and extrude membrane extensions called pro-platelets which expand between the endothelial cells. By the help of blood stream, pro-platelets are shredded and platelets

released into the circulation where they will circulate during 7 to 10 days in humans before their degradation in the spleen (reviewed in (Chang et al., 2007)).

1.3.3.2 Main Cytokines involved in megakaryopoiesis

The TPO/c-MPL couple drives early steps of megakaryopoiesis as it allows the specification and amplification of megakaryocytic progenitors, their maturation (de Sauvage et al., 1996); (Gurney et al., 1994) and the control of platelets number (Ng et al., 2014). However, TPO and c-MPL knock-out mice stillhave 10% of the normal platelets count and do not suffer from hemorrhage(Bunting et al., 1997), suggesting the contribution of other cytokines to platelet production. For instance, the administration of Interleukin IL-6 (Neben et al., 1993) and IL-11 (Ishibashi et al., 1989) to mice enhanced megakaryocytes maturation. Additionally, numerous *ex-vivo* studies aiming to derive great number of platelets from human cord or peripheral blood for transplantation-recovery purposes pointed out different combinations of cytokines (Panuganti et al., 2013) that help the expansion and maturation of megakaryocytes, including CXCL-12, IL-9, EPO (Cortin et al., 2005; Fujiki et al., 2002), IL-3 (Panuganti et al., 2010), Flt-3L (Proulx et al., 2003), GM-CSF (Lennartsson et al., 2004), and SCF (Minamiguchi et al., 2001).

SCF contribution to megakaryopoiesis is based on several arguments. For instance, mutant mice with conditional deletion of SCF show slight thrombocytopenia (cited in (Kaushansky, 2009)). Furthermore, enforced expression of constitutively active c-Kit mutant (D816V) in murine bone marrow cells enhances megakaryocytic differentiation (Ferrao et al., 2003). Additionally, SCF protects megakaryocytes from chemotherapy-induced apoptosis (Zeuner et al., 2007)(Bartucci et al., 2011). The most striking evidence for a role of c-Kit in megakaryopoiesis comes from HSCs progeny analysis in transplantation assay, where HSCs expressing high levels of c-Kit produce high amounts of platelets (Shin et al., 2014b). Except few *in vitro* studies showing the synergy between TPO and SCF to activate STAT-5 and JAK-2 (Drayer et al., 2005) or MAPK (Minamiguchi et al., 2001), the molecular mechanism of TPO and SCF cooperation is poorly characterized, contrarily to EPO-SCF synergy.

1.3.3.3 Main transcription factors involved in megakaryopoiesis

The identity of megakaryocytic progenitors is ensured by GATA-1 and GATA-2 transcription factors which antagonize the expression of lymphocytic-monocytic transcription factor SPI-1/PU.1 (Chou et al., 2009; Iwasaki et al., 2003). All steps of megakaryopoiesis require the cooperation between GATA (1 and 2), ETS (Fli-1) and RUNX-1 transcription factors **(Figure 3)**. GATA-1 interaction with its co-factor FOG-1 regulates megakaryocytic amplification, cytoplasmic maturation and platelet formation. While early steps are characterized by a high GABPα/Fli-1 ratio, this ratio is inverted during later steps. The endomitosis step is regulated notably by RUNX-1 and its target MYH-10 as well as by Tal-1 and its targets p21 and STAT-1. The formation of proplatelets is regulated by Tal-1, SRF, NF-E2 and Fli-1 and the activation of platelets is regulated by Runx-1 (reviewed in (Tijssen and Ghevaert, 2013). The expression of megakaryocytic markers such as CD41, CD42, GPIX, c-MPL and PF-4 is principally regulated by GATA-1, GATA-2, Tal-1, Runx-1 and Fli-1 (reviewed in (Szalai et al., 2006)

1.4 HSC and megakaryocytic lineage proximity

1.4.1 HSC heterogeneity

The hematopoietic stem cell was initially identified with the observation of CFU-S, clones of lymphoid and myeloid potential forming nodules into the spleen of lethally irradiated mice, offering them radioprotection. The clones composing these nodules were maintained over serial transplantation into multiple recipients and showed low cycling activity, defining HSCs as unique cells with self-renewal ability and multipotency maintained by quiescence (reviewed in (Eaves, 2015)).

1.4.1.1 Heterogeneity in repopulation kinetic

Transplantation assays of bone marrow cells into irradiated recipient mice allowed the identification of different sub-populations of HSCs with some displaying only rapid replenishment of blood cells with transient splenic activity, while others displayed more long term reconstitution (Osawa et al., 1996). Moreover, quantification of long-term repopulating ability at the single cell level showed that stem cells progeny possess lower activity than parental cells, indicating limited self-renewal potential of HSC (Ema et al., 2014). The

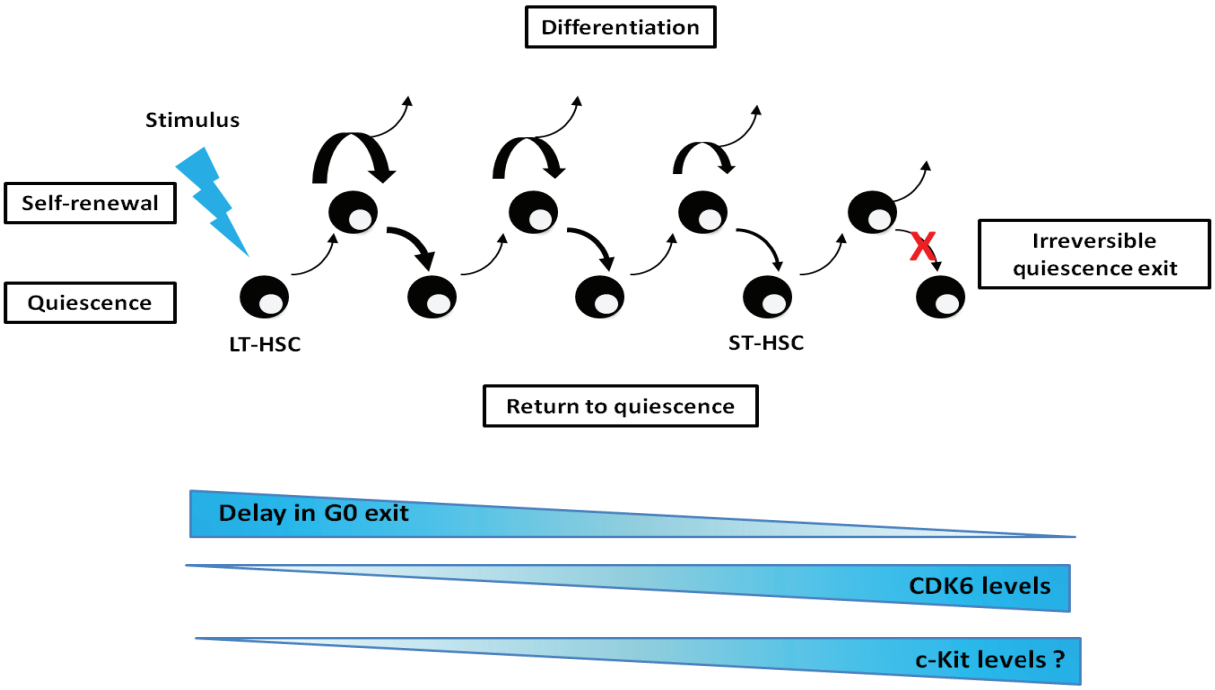

Figure 7: Continuous loss of HSCs self-renewal ability correlates with progressive G0 exit delay until irreversible quiescence exit

Quiescent HSCs are stimulated by external stimulus (lightning) inducing their cycling, but once activated some HSCs can return into quiescence instead of proliferate and differentiate. A recent study (Laurenti et al, 2015) has shown that LT-HSCs differ from ST-HSCs by shorter delay in G0 exit which is at least partially determined by lower levels of CDK6. Based on this study and other data, we propose the following model wherein HSCs would progressively lose their self-renewal potential by accumulating CDK6, until their irreversible exit from quiescence following several iterative cycles of activation.

c-Kit levels have also been shown to be higher in ST-HSC than in LT-HSC thus further suggesting that c-Kit levels might also increase during the successive rounds of stimulation of HSCs. Given the strong megakaryocytic bias of c-Kit ^{High} HSCs (Shin et al, 2014b), this model raises the intriguing possibility that megakaryocytic biased HSCs could correspond to “old” HSCs that have undergone a high number of reactivation rounds. Alternatively, different lineage bias of HSCs could reflect a sort of memory of all previous stimuli that led to their generation allowing the maintenance ofa specific subset that can be more rapidly activated upon emergency. For example, “old” HSC resulting from preferential EPO or TPO stimulation history could contribute to maintain specific erythroid or megakaryocytic stem cells, respectively.

transplantation of phenotypically enriched HSC population showed different duration of clone's persistence defining retrospectively the parental cells as long-term HSC when sustained for over than ten months, intermediate-term HSC when sustained for six to eight months (Benveniste et al., 2010) and short-term HSC that extinguishes after only four to six weeks (Osawa et al., 1996)

1.4.1.2 Heterogeneity in self-renewal ability and quiescence

Quiescence is defined as the inability of cells to pass the restriction check point into G1 cell cycle phase and their exit into the so called G0 quiescent state which is accompanied by a low metabolic activity. Quiescent cells can be detected using different methods such as fluorescent labeling of mitochondrial activity (Rhodamine-123: (Nibley and Spangrude, 1998), dual labeling of DNA (Hoechst 33342) with nucleolar marker Ki-67 or with RNA marker (Pyronin-Y: (Gothot et al., 1997), DNA synthesis monitoring (Thymidine ^{3}H, BrdU incorporation(Passegue et al., 2005)), or nucleosome labeling (inducible H2B-GFP (Foudi et al., 2009). The use of labeling strategies either *in vivo* or *ex-vivo* before transplantation into myelo-ablated mice showed not only the heterogeneity of HSCs considering their cycling state, but also established that in contrast to short-term HSCs, long-term multilineage HSCs are mostly found in a quiescent state. The differences in methods and the duration or periodicity of labeling resulted in different estimations of HSC cycling frequency ranging from one cell division per 1 or 12 months (reviewed in (Nakamura-Ishizu et al., 2014a). The association of BrdU labeling and pulse-chase chromatin labeling using inducible H2B-GFP expression evidenced the existence of a deeply quiescent/dormant HSCs population that cycle upon stress and return to quiescence in steady state conditions (Wilson et al., 2008). Interestingly, the identification of non cell-cycle-related SLAM (Signaling Lymphocyte Activation Molecule) family members allowed prospective isolation of deeply quiescent HSCs standing in the $CD229^{low}$ $CD244^{low}$ (Oguro et al., 2013) sub-fraction of CD150+ CD48- CD41- LSK cells (Kiel et al., 2005) with maintained long-term repopulation potential over serial transplantation assay and lymphoid-myeloid reconstitution ability. However, a recent study using Pyronin-Y/Hoechst fractionation over serial transplantation assay argues that highly purified HSCs with the latter markers do not encompass all long-term reconstituting HSCs but causes a substantial loss of cycling HSCs able of long-term reconstitution (Goldberg et al., 2014). Contrarily to non-cell-cycle SLAM markers that allowed a modest refinement of

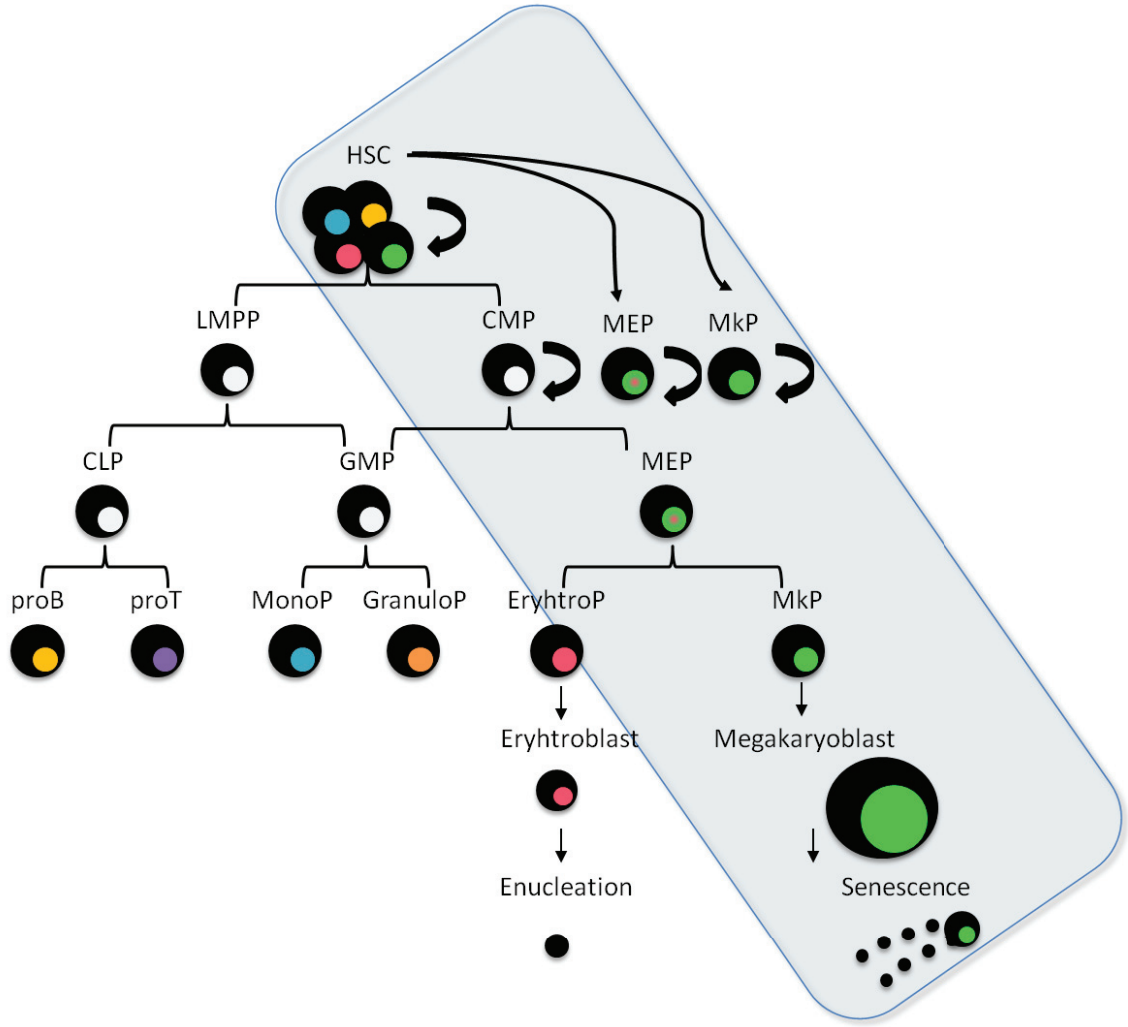

Figure 8: Progenitors' stemness and hierarchical proximity between HSCs and MK lineage

HSC is no longer considered as a unique cell, but is represented by a pool of heterogeneous transcriptionally primed cells that can give rise to self-renewable multipotent progenitors. The position of GMP was revised as it can derive either from a common lympho-myeloid progenitor (LMPP), or a common myeloid progenitor (CMP). Likewise, recent studies indicate that megakaryocytic cells can be generated either through the classical bipotent progenitor MEP derived from CMP or directly from megakaryocytic biased HSCs. Moreover, the existence of bipotent erythro-megakaryocytic and even monopotent megakaryocytic progenitors displaying long term repopulation activity has also been reported. These data highlight the striking proximity between HSCs and the megakaryocytic lineage (blue rectangle), as well as the less stringent frontier between the specific properties of stem cells and progenitors.

quiescent HSC population purity, the identification of cell-cycle marker CDK6 allowed resolving the heterogeneity of the latter population considering their delay of response to mitogenic signal which depended on their delay of exit from G0 quiescent state. Indeed, CDK6/CyclinD were found to be hierarchically expressed along the differentiation of HSC from LT-HSC (CDK6- CyclinD-) through ST-HSC (CDK6+ CyclinD-) to bipotent GMP (CDK6+ CyclinD+) (Laurenti et al., 2015). This study evidenced that the loss of self-renewal ability correlates with the decreased delay of exit from G0 quiescent state in a continuous manner along with the progressive expression of cell-cycle components **(Figure 7)**.

1.4.1.3 Preferential lineage output and transcriptional priming

Previously, the observation of preferential association between some lineages led to the definition of myeloid versus lymphoid dichotomy as a first step of differentiation and multipotency loss of HSCs, whereas increasing numbers of more recent studies show that all HSCs do not contribute equally to all hematopoietic lineages because of their heterogeneity**(Figure 8)**.

Depending on the lineage output of different HSCs clones over serial transplantation, a subset of HSCs appeared to be less efficient for lymphoid reconstitution and was called Myeloid-biased HSC (My-HSC), as opposed to Lymphoid-Biased HSCs and Balanced-HSCs(Muller-Sieburg et al., 2002). Another method consisted in *in vivo*tracking of HSCs progeny over serial transplantation of either single cell HSC or *in vitro* cultured HSCs clones confirming the existence of different subsets of HSCs skewed either towards myeloid or lymphoid differentiation and were named α, β, δ and ϒ (Dykstra and de Haan, 2008). Moreover, the myeloid/lymphoid ratio was preserved over serial transplantation suggesting its dependency upon intrinsic cues. Of note, aging is associated with increased self-renewal and myeloid over lymphoid bias of HSCs (Rossi et al., 2005), suggesting the proximity between myeloid lineage and stemness.

Contrarily to the previously spread idea of myeloid versus lymphoid dichotomy as the first differentiation choice faced by HSCs, the observation of preferential association between B lymphoid cells with mono-myeloid cells in CFU-S colonies (Jordan et al., 1990), the persistence of lymphoid potential in GMP and the lack of lymphoid and E/MK combination in prospectively isolated CD34 FLT3 (Adolfsson et al., 2005; Mansson et al., 2007) or CD150 HSCs (Morita et al., 2010), initiated the idea of E/MK potential exclusion as the first choice

faced by HSC, followed by lymphoid exclusion and ending by GM differentiation. These hypotheses were lately confirmed by single cell transplantation (Oguro et al., 2013)assay and transcriptome analysis.

First, both these analyses performed at the single cell level confirmed the heterogeneity of prospectively isolated HSC or pluripotent progenitors, independently of the phenotypic markers used (Guo et al., 2013; Mansson et al., 2007). Secondly, the comparison of the transcriptional profile of HSC sorted upon CD34 and FLT3 markers at the population and single cell levels showed a strong association between HSC and erythro-megakaryocytic programs, and virtually absent association between erythro-megakaryocytic and lymphoid programs. Granulo-monocytic program was equivalently associated with lymphocytic or E/MK program (Mansson et al., 2007). Transcriptional profiling of single cell sorted CD48- 150+ HSC showed that the most striking variation when facing E/MK versus lympho-myelocytic choice resides in the transcription factor GATA-2 which negatively correlates with lympho-myelocytic module (Flt3, Cebpa and Notch1) and positively correlates with both E/MK module (with GATA-1, Fli-1, c-MPL, CD41, CD150), and stem cells module (Runx-1 ,Meis-1, SCL) (Guo et al., 2013). Conversely, HSC priming toward lympho-myelocytic lineages is favored by transcription factor Ikaros (Ng et al., 2009), PU.1 and E2A (Dias et al., 2008), whereas HSC priming toward granulo-monocytic program is restricted notably by CEBPα (Hasemann et al., 2014). Thirdly, whereas E/MK transcriptional signature is associated with stemness, the restriction to lymphoid differentiation of HSC limits their self-renewal ability (van Galen et al., 2014).

1.4.1.4 Transcriptional priming and quiescence

Interestingly, transcriptome analysis on HSC sorted upon megakaryocytic markers shows a correlation with the quiescent state. For instance, CD34 Flt3 sorted long-term HSC sub-fractioned upon CD9 marker shows a correlation between high expression of CD9 and low expression of Ki-67 (a marker of nucleolar activity) and cyclins, suggesting a quiescent state (Karlsson et al., 2013). Moreover, transcriptional analysis of HSC sorted upon FLT3 and sub-fractioned depending on CD41 expression level complemented by transplantation studies from wild-type or CD41 knock-out mice evidenced that $CD41^+$ HSCs are less proliferative, participate to long-term reconstitution, are myeloid biased and able to generate $CD41^-$ HSCs which are more proliferative and lymphoid-biased (Gekas and Graf, 2013). Similarly,

multiplex-qPCR on single cell CD150+ CD48- HSCs revealed that vWF ^{High}HSCs present megakaryocytic transcriptional signature compared to vWF ^{Low} HSCs which express mainly lymphoid genes. Functional assay *invivo* revealed that vWF ^{High} HSCs are quiescent, depend on TPO for their reactivation and are highly biased toward platelet reconstitution on the short-term, but able to generate vWF^{Low} and all hematopoietic lineages on the long-term (Sanjuan-Pla et al., 2013). In summary, the fraction of HSCs expressing high levels of megakaryocytic markers tends to be quiescent, long-term reconstituting, platelet/myeloid biased and more primitive as it generates more proliferative and lymphoid biased HSCs.

Thus, HSCs are not unique cells, but a heterogeneous population of transcriptionally primed stem cells conditioning their cell-cycling and blood-cell type generation. Additionally, the hierarchical proximity between HSCs and bipotent E/MK or the transcriptional megakaryocytic priming of quiescent long-term HSCs suggests the ability of progenitors to act as stem cells.

1.4.2 Progenitors' stemness

1.4.2.1 Progenitors are able to self-renew

Contrarily to previous idea standing that HSCs are the only cells capable of multipotency and self-renewal, recent studies grant the self-renewal ability to progenitors themselves. Indeed, in anemia-induced stressed mice, a population of erythrocytic progenitors emerges into the spleen and is able of self-maintenance over long-term and serial transplantation proving its self-renewal ability (Harandi et al., 2010). Additionally, single cell transplantation of murine LSK HSCs sub-fractioned upon CD150 and CD41 markers into irradiated primary recipient followed by whole bone marrow transplantation into secondary irradiated recipient showed the existence of pluripotent (CMRP), megakaryo-erythrocytic bipotent (MERP) and megakaryocytic monopotent (MKP) progenitors displaying long term repopulation activity. These progenitors emerged from CD150+ CD41+ and CD41- subpopulation and sustainedover at least 8 weeks the production of myeloid, erythrocytes and megakaryocytes or only megakaryocytes, respectively (Yamamoto et al., 2013). Thus, even differentiation-restrained progenitors are able of self-renewal**(Figure 8)**.

1.4.2.2 Progenitors are the main contributors to steady-state hematopoiesis

Surprisingly, in steady state condition, HSCs are not activated every time that mature blood cells must be produced. A recent study set up a new murine model allowing the labeling of each individual cell at a given time with a unique inducible transposition event. By following HSCs progeny, this method allowed to determine the contribution of different clones to the renewal of different blood cell types at steady state. Using this approach, this study revealed that steady-state blood cells production is maintained by the successive recruitment of thousands of clones, with each clone contributing only transiently to mature progeny. Moreover this study revealed that in contrast to what occurs during transplantation, 95% of mature blood cells are generated directly from MPP and progenitors without activating HSCs division (Sun et al., 2014).

Given the existence of HSCs displaying strong lineage priming and of multipotent/bipotent progenitors displaying long-term self-renewalcapability, the distinction between stem cells and progenitors becomes much less contrasted than thought before.

1.4.3 Megakaryocytes are critical actors of HSC maintenance by acting directly into their niche

Megakaryocytes are located in close proximity to HSCs in the hematopoietic niche being either in direct contact (Zhao et al., 2014), or at less than 2.5 cell-diameters (Nakamura-Ishizu et al., 2014b)} or 25 microns (Bruns et al., 2014). Additionally,the treatment by diphteria-toxin of mice expressing the diphteria-toxin receptor under the control of Cre recombinase driven by the megakaryocytic PF4 promoter allowed the depletion of megakaryocytes which resulted in the reduction of quiescent HSCs number, the increase of their proliferation and the reduction of their long-term initiating potential. The HSCs of megakaryocyte-depleted mice displayed perturbed cell cycle due to the increase of Cyclin E/ CDK2 expression (Bruns et al., 2014)which is responsible for the entry in S phase. RNA-seq and ELISA assays revealed that the depletion of megakaryocytes actually induced a decrease of TPO levels in serum (Nakamura-Ishizu et al., 2014b), as well as TGF-β (Zhao et al., 2014) and CXCL4/PF4(Bruns et al., 2014) levels into the bone marrow. Furthermore, among all the cell types present into the niche, megakaryocytes were responsible for most of these cytokines production. The injection of these cytokines in megakaryocyte-depleted mice

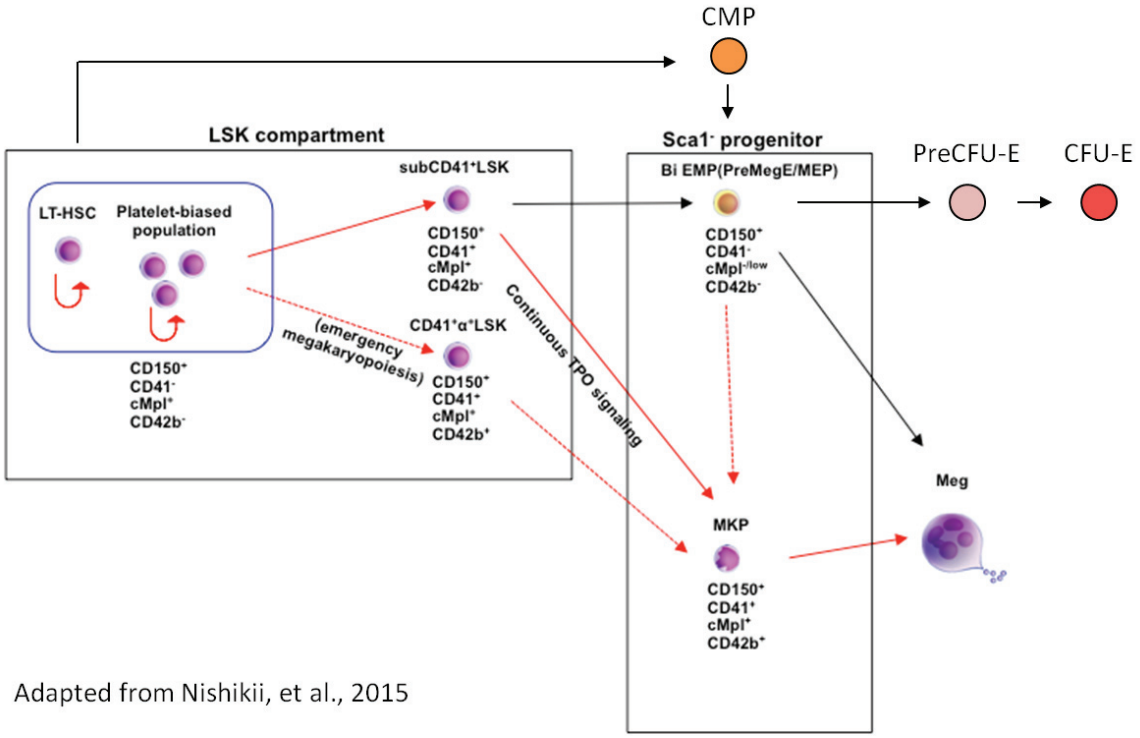

Figure 9: Progenitors with megakaryocytic potential

Numerous studies indicate that the main pathway (black arrows) contributing to the production of megakaryocytes (Meg) at steady state involves a bipotent erythro-megakaryocytic progenitor intermediate (named MEP, BiEMP or PreMegE depending onthe surface markers used for their prospective isolation) produced by multipotent stem cells through the CMP intermediate. However, recent studies indicate the existence of a specific subset of stem cells that while being multipotent are highly biased towards megakaryocytic lineage and directly generates unipotent megakaryocytic progenitor upon emergency. This alternative pathway (red arrows) thus contributes to the rapid and efficient restoration of platelets number during stress megakaryopoiesis (adapted from Nishikii et al, 2015).

restored the quiescence of LT-HSC and the implication of these molecules into HSCs quiescence was further confirmed in the corresponding knock-out mice models. (Bruns et al., 2014)(Kunisaki et al.,2013). Overall, these studies established thatseveral factors released by megakaryocytes are involved in the maintenance of HSCs quiescence in steady state conditions.

Yet, megakaryocytes also secrete pro-proliferative factors inducing the expansion of HSCs. Indeed, mature megakaryocytes secrete IGF-1 (Insulin-like Growth Factor) and IGFBP-3 (IGF Binding Protein) which induce the expansion of HSCs in steady state condition (Heazlewood et al., 2013). Furthermore, in myelo-ablated mice, megakaryocytes rapidly and transiently liberate FGF-1 which allows their own expansion and subsequent HSCs expansion(Zhao et al., 2014). Following total body irradiation, megakaryocytes migrate to the endosteal niche and secrete PDGF-BB which induces the expansion of osteoblasts. The blockade of c-MPL mediated megakaryocytes migration reduces HSCs engraftment, contrarily to the injection of TPO which improves it (Olson et al., 2013)**(Figure 4)**.

In summary, megakaryocytes evolve in close proximity to HSCs and secrete various factors that induce either their quiescence, or their expansion in response to injury.

1.4.4 Common features between HSC and megakaryocytic lineage

Overall, the hematopoietic stem cells and the megakaryocytic lineage share numerous features. Megakaryocytes secrete different factors that influence their own migration, cell fate and modulate the expansion of the osteoblastic niche. Megakaryocytes contribute to the niche of HSCs either through direct contact or in a paracrine fashion, participating to HSCs engraftment and regulating the balance between quiescence and proliferation in normal or stress conditions. As HSCs and megakaryocytes share the same niche, they are subject to common signals such as TPO, SCF, Notch ligands to which they are able to respond through the expression of c-MPL, c-Kit and Notch receptors. Both HSCs maintenance and megakaryocytes' differentiation depend on common transcription factors such as GATA-2, FLI-1, RUNX-1 and SCL. HSCs and megakaryocytes also share the expression ofseveral surface markers such as CD9, CD41, CD150 and vWF which make part of the transcriptional priming of HSCs that are characterized by quiescence, long-term maintenance and myeloid/megakaryocytic biased differentiation. The megakaryocytic marker CD9 is a known partner of CD81 tetraspanin, which is required for the re-entry into quiescence of HSCs after

injury (Lin et al., 2011). More strikingly, HSCs and megakaryocytes are hierarchically proximate as self-renewable megakaryocytic progenitors can derive directly from HSCs, a result demonstrated by paired daughter-cell transplantation (Yamamoto et al., 2013). Moreover, a recent study evidenced the existence of a subset of HSCs which express CD41, are able of multipotency and are skewed toward megakaryocytic differentiation in steady state conditions. In stress condition, CD41+ HSCs generate a second subset of HSCs expressing CD42b which is strongly skewed toward megakaryocytic differentiation and allows rapid and efficient platelets recovery (Nishikii et al., 2015)**(Figure 9)**.

All these data highlight the intriguing proximity between megakaryocytes and HSCs at different levels: physical, functional and hierarchical, although its relevance remains presently unclear. Among severalpossibilities, this proximity can indicate that common actors regulate both megakaryopoiesis and HSCs function, potentially through common mechanisms. In the next chapter of the introduction, I will present the different signaling pathways and the tetraspanin family and their role in the regulation of both HSCs and megakaryocytes cell fate.

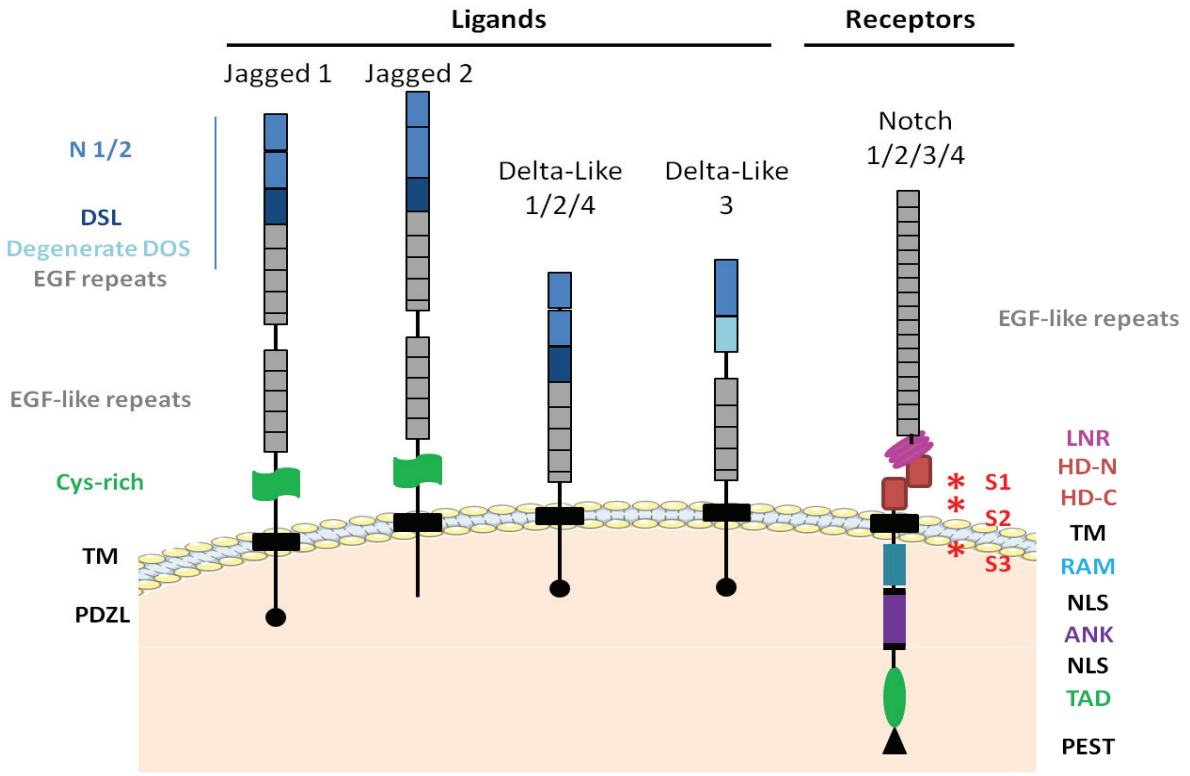

Figure 10: Notch ligands and receptors structure

Jag ligands differ from DLL ligands by the presence of a Cystein-rich (green flag) domain close to the transmembrane region (TM). Jag-1 harbors a PDZL domain in the C-terminal tail contrarily to Jag-2. DLL-3 differs from other DLL ligands by a degenerate DSL domain (Clear blue box). The domains common to both Jag and DLL ligands are indicated on the left: N1 (Cystein-containing) and N2 (non Cystein-containing), DSL (Delta-Serrate-Lag2) domain containing DOS (Delta_OSM-11 like proteins) motif, EGF-like repeats (Epidermal Growth Factor), transmembrane region and intracellular PDZL (PSD-95/ Dlg/ ZO-1) motif. N1, N2, DSL and the two first EFG-like repeats correspond to the domain of interaction with Notch receptor. The different domains of Notch receptors are indicated on the right: EGF-like repeats containing multiple glycosylation sites, LNR (LIN-12 Notch repeats) and HD (Hetero-dimerization domain). HD-N and –C are separated by S1 cleavage site and HD-C (C-terminal) harbors S2 cleavage site. S3 cleavage site follows the transmembrane region. Intracellular Notch comprises from top to bottom: RAM (Rbp associated molecule), ANK (ANKyrin repeats) surrounded by two NLS (Nuclear Localization Signal), TAD (Transactivation domain) and PEST sequence.

2 Notch signaling pathway

2.1 Notch signaling pathway

Notch signaling pathway plays a crucial role in binary cell fate decisions in all three developmental cell layers and their derived tissues both during development and adulthood. Notch is activated following cell to cell contact and different mechanisms allow the distinction between signal receiving and signal emitting cell which have two opposite and mutually exclusive cell fates. This process called lateral inhibition, controls the balance between proliferation and differentiation in numerous tissues.

2.1.1 Ligands and receptors

Notch signaling is activated following the interaction between one of the 4 Notch receptors (Notch 1/2/3/4) with one member of the Notch ligand families Jagged (Jag-1/2) or Delta-like (Dll- 1/2/3).

2.1.1.1 Ligands structure and maturation

Both families of canonical ligands include the DSL (Delta, Serrate, Lag-1) domain, with the exception of Delta-like 3 which is the most structurally divergent ligand**(Figure 10)**. In the N-terminus, both families of ligands have cysteine conserved residues and EGF-like repeats involved in the interaction with the receptor. Following the transmembranar region, the C-ter cytoplasmic tail includes the PDZL motif (PSD-95/ Dlg/ ZO-1 ligand)which allows the interaction with the cytoskeleton and plays a role independent of Notch. The presence of a Cysteine-rich domain in the juxta-membranar region characterizes Jagged (Jag) family members from their Delta-like counterparts.

Notch ligands glycosylation and ubiquitinylation are essential for their maturation, the definition of their affinity to receptor and for signal transduction, all steps being mediated by endocytosis**(Figure 11)**. Jagged and Delta-like ligands can also be proteolically cleaved by ADAM (A Disintegrin And Metalloproteinase) metalloprotease family members (9/10/12/17), generating soluble fragments which generally act as signaling inhibitors by competing for membrane-attached ligand binding (Reviewed (D'Souza et al., 2010)).

2.1.1.2 Non canonical ligands

Non canonical Notch ligands differ from their canonical counterparts by the absence of the DSL domain. Both canonical and non-canonical ligands share the capacity to interact with

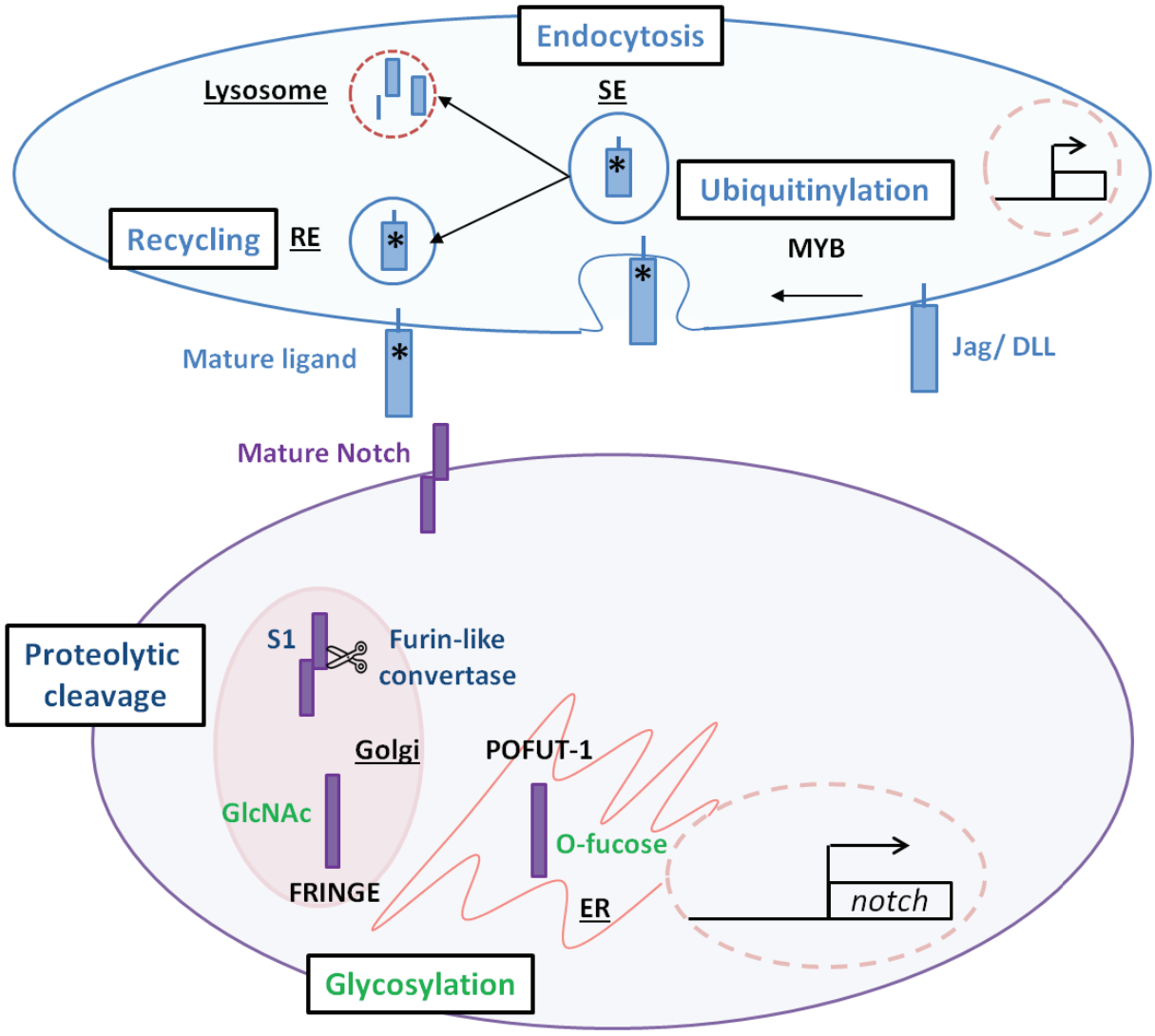

Figure 11: Biosynthesis of Notch ligands and receptors

Notch (purple rectangle) is O-fucosylated by POFUT-1 in the endoplasmic reticulum which is necessary for its N-glycosylation (Glucosamine N Acetyl GlcNAc) by Fringe in Golgi apparatus. Notch is cleaved at S1 site by Furin-like convertase enzyme generating a hetero-dimer non-covalently attached at the level of HD domain before its expression at the cell surface as a mature receptor.

Jag or DLL ligand (blue rectangle) is ubiquitinylated (black star) by the E3-Uquitin Ligase MYB, inducing its internalization into sorting endosome (SE) from which the ligand can be either targeted for lysosomal degradation or recycled to the cell surface into recycling endosome (RE). Ligand ubiquitinylation and recycling into the endosomal compartment are required for the activation of Notch receptor.

Notch receptors and to transduce Notch signals. Non-canonical ligands are structurally heterogeneous as they can be membrane-tethered or attached by GPI-anchor or secreted. Interestingly, some of the non-canonical ligands (such as DLK-1) were described as competitors for canonical ligands, whereas others (such as TSP-2) co-activate them (Reviewed in (D'Souza et al., 2010)).

2.1.1.3 Notch receptor structure and maturation

Notch receptors are synthesized as single-pass membrane-protein with a molecular mass ranging from 300 to 350 KDa. The receptor has to be glycosylated by POFUT-1 or Fringe to ensure its affinity and interaction ability to its ligand**(Figure 11)**. For example, Fringe induced-glycosylation favors the interaction of Notch receptor with Delta-like ligands instead of Jagged ligands. The receptor is then matured by proteolytic cleavage at the S1 site with furin-like convertase, inducing the formation of a heterodimer which will translocate to the cell-surface. The extracellular part of Notch receptor**(Figure 10)** is composed of EGF-like repeats which interact with the ligand, LNR domain (Lin12 Notch repeats) which is essential for the repression of the receptor in the absence of the ligand and hetero-dimerization domain (HD) which contains the S2 cleavage site. Following the transmembrane region which contains S3 cleavage site, intracellular domain of Notch is composed of RAMdomain (RBPJ associated molecule) essential for the binding to RBPJ-k, ankyrin repeats (ANK), surrounded by two Nuclear Localization Signal (NLS), transactivation domain (TAD) which allows transcriptional activation and PEST C-terminal domain which is ubiquitinylated allowing the degradation of the receptor (Reviewed in (Kovall and Blacklow, 2010).

2.1.2 Signal transduction

In absence ofthe ligand, Notch receptor adopts an inactive self-inhibited compacted conformation due to the LNR domain that forms a ring-shaped structure around the HD domain thus hiding the proteolytic site S2**(Figure 10)**.

Following receptor-ligand binding**(Figure 12)**, ligand ubiquitinylation by Neur or Mindbomb is essential for its clathrin and dynamin-dependent endocytosis in order to create the sufficient mechanical force and membrane constriction that triggers out the extracellular domain of the receptor and uncovers S2 cleavage site. For this reason, ligands have to be attached either to a membrane or coated on plastic support in order to allow Notch receptors activation. At the S2 site, Notch receptors are cleaved by a metalloprotease

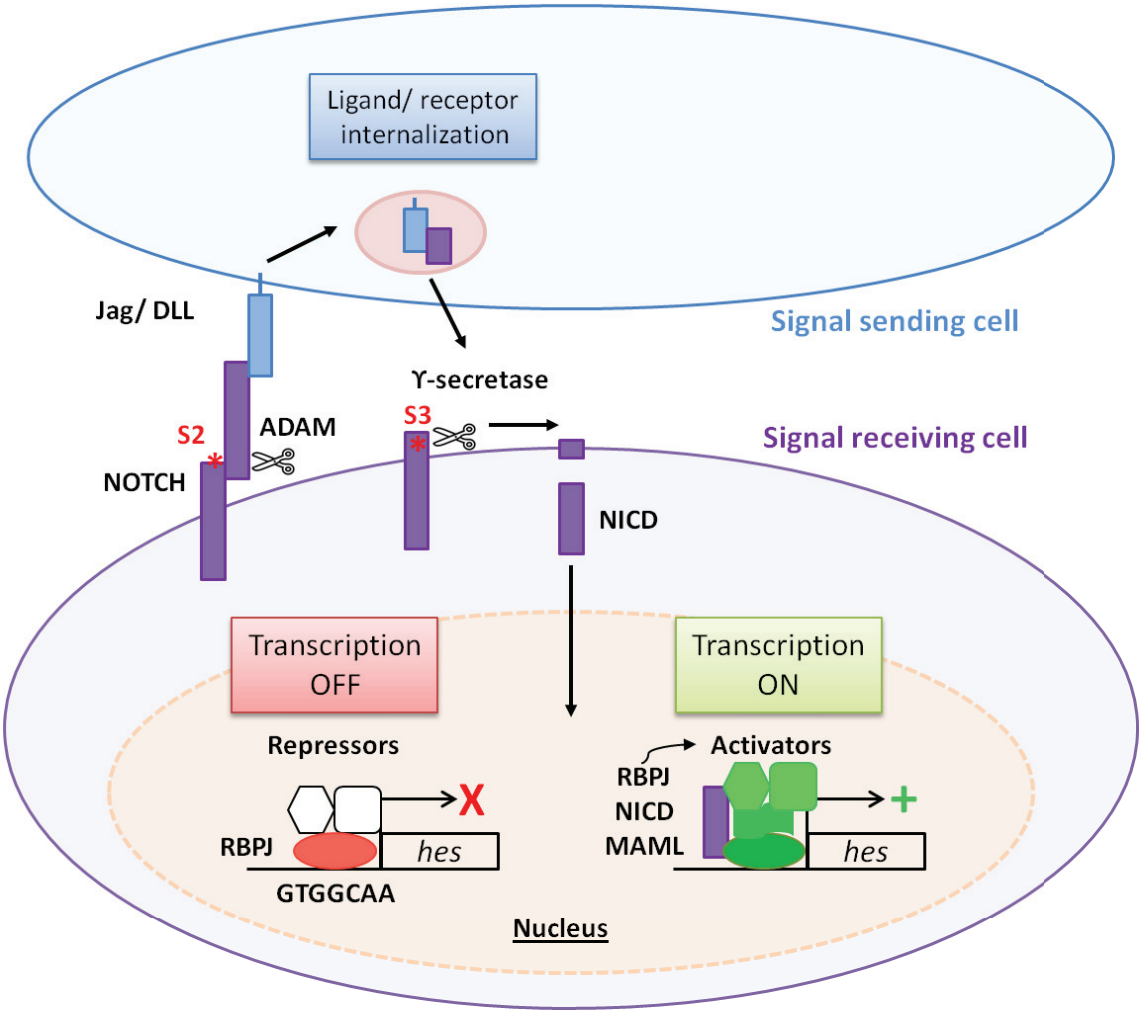

Figure 12: Notch signaling pathway: activation and signal transduction

Initially, Notch target gene (ie *hes*) transcription is repressed due to the binding of RBPJ-k (red oval) and transcriptional co-repressors (white squares) on its promoter. The interaction between Jag or DLL ligand and Notch receptor, through the interaction between signal sending cell (blue) and signal receiving cell (purple), induces the internalization of the ligand and the extracellular fragment of Notch into the signal sending cell, thus uncovering S2 cleavage site (red star) on Notch receptor. Following the cleavage by ADAM10 metalloprotease at the S2 site, Notch is further cleaved by the Υ-secretase complex at the S3 site, allowing the release of Notch Intracellular Domain (NICD). NICD translocates into the nucleus where it binds to Mastermind-Like (MAML) and RBPJ-k. The ternary complex recruits transcriptional activators (green squares) and the transcription of Notch target genes is activated.

member of the ADAM family, principally ADAM-10, generating a transmembranar fragment which will be further cleaved by the gamma-secretase complex. This complex is composed of Presenilin 1 and 2 catalytic subunit, Nicastrin which recognizes the substrate, APH2 that allows membrane localization and PEN2 which stabilizes the complex.

The liberated intracellular domain of Notch receptor (NICD or ICN) then translocates to the nucleus. NICD lacks DNA-binding domain but interacts with RBPJ-k through its RAM domain. Initially, RBPJ-k binds to DNA in specific but low affinity manner on its site (GTGGGAA) and represses the expression of Notch target genes, due to its cooperation with histone deacetylase (HDAC) machinery and transcriptional co-repressors such as N-Cor, ETO and SMRT which are gathered by MINT. The binding of NICD to RBPJ-k allows the recruitment of Mastermind-like (MAML) and the formation of a ternary complex that possess low transcriptional activation potential. Due to existence of head-to-head RBPJ-k binding sequences on the promoter of target genes (described for *hes-1* promoter) and the interaction between the ANK domains of multiple NICD molecules, the complex is stabilized and the signal can be amplified (Liu et al., 2010a). The ternary complex (NICD/RBPJ/MAML) recruits transcriptional activators such as the histone acetylase p300 and cooperates with tissue-specific transcriptional activators to induce the expression of Notch target genes (Reviewed in (Kovall and Blacklow, 2010)).

2.1.3 Notch target genes

Notch signaling directly activates the expression of Hes and Hey family members which correspond to the C class of transcriptional repressors from basic helix-loop helix (bHLH) protein family. This family also comprises transcriptional activators such as Myo-D and Mash-1 and Leucine zipper transcription factors such as c-Myc. There are 7 identified members of Hes family and 3 members of Hey family, but their direct activation by RBPJ-k/ NICD couple was assessed mostly for Hes-1, Hes-5, Hey-1 and Hey-2 (Reviewed in (Iso et al., 2003)).

Hes and Hey share common structure but can differ by their expression pattern and their mechanism of transcriptional repression. Both Hes and Hey are composed of bHLH and orange domains in their N-terminal region and a conserved tetrapeptide in the C-terminal region. They differ by a conserved residue in the basic region as Hes family members express a Proline residue, while Hey family members possess a Glycine residue**(Figure 13)**.

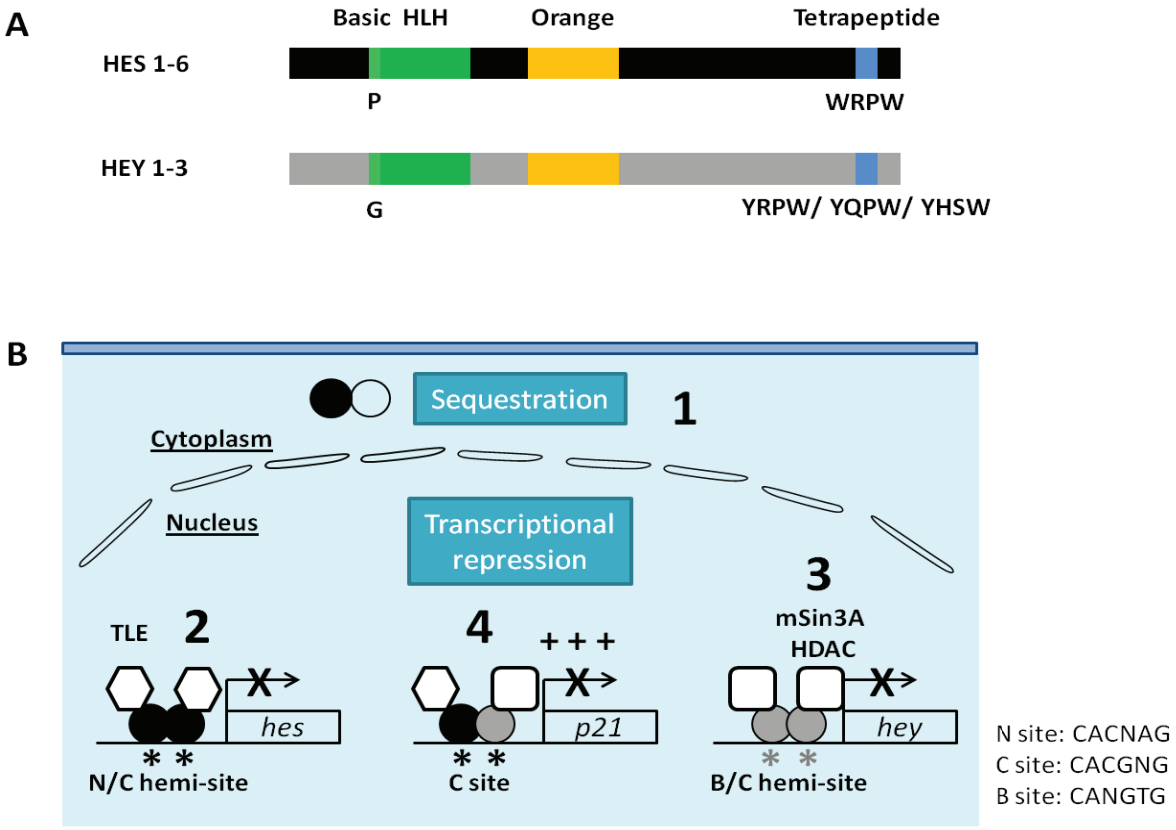

Figure 13: HES and HEY structure and mode of function

A. Schematic presentation of HES and HEY structures: HES and HEY are DNA binding proteins acting as transcriptional repressors that harbor a bHLH (basic Helix Loop Helix) domain, an Orange domain and a conserved tetrapeptide at the C-terminal extremity. HES and HEY proteins differ by the presence of a conserved Proline or Glycine residue at the same position in their N-terminal part. **B.** Schematic presentation of HES and HEY modes of action: 1- HES (black circle) are able to repress transcription by the sequestration of others b-HLH factor (blue circle). 2- HES homodimers can bind to N or C boxes and repress transcription through the recruitment of TLE co-repressor. 3- HEY homo-dimers can binds to B or C boxes and represses transcription through the recruitment of mSin3A repressor and HDAC. 4- HES and HEY (grey circle) can form hetero-dimers that bind to C boxes and repress transcription through the recruitment of TLE and HDACs (Histone Deacetylases). +++ indicate higher repression efficiency by HES/HEY heterodimers compared to homodimers. Nucleic sequence of the different consensussites is precised on the right.

bHLH proteins binds to DNA as dimers with each monomer attached to a specific half-site. Hes can bind to N and C consensus sites, while Hey mostly binds B and C consensus sites. Hes and Hey can act either as homodimers, or interact with each other to form a more efficient DNA-binding heterodimer that fix C consensus site. When forming homodimers Hes recruits principally TLE co-repressor protein, while Hey recruits N-CoR/ mSin3A repressor complex.

Hes repress transcriptional activity mostly through its tetrapeptide, while Hey uses mostly its bHLH domain. Hes uses different mechanisms to repress transcriptional activity either by direct binding to DNA and the recruitment of HDAC machinery (active repression), or by sequestrating other bHLH proteins preventing them to form functional complexes with their partners (passive repression), whereas Hey acts mostly by active repression mode. Both Hes and Hey control their own expression by direct binding on their respective promoters.Hes-1 and Hes-5 can have redundant functions on HSCs emergence as demonstrated by the absence of phenotype in simple mutant mice in contrast to double mutant mice ((Guiu et al., 2013). Interestingly, RBPJ-k binding sites were found on gene promoters different from Hes and Hey, and the corresponding genes were induced with Notch stimulation establishing the existence of supplementary direct targets. For instance, NICD/RBPJ axis directly activates the expression of genes with various functions such as cell cycle regulators(ie Cyclin-D3: (Joshi et al., 2009)or transcription factor (ie GATA-2: (Guiu et al., 2013)).

2.1.4 Signal downregulation

Mastermind induces the recruitment of Cyclin-C-CDK8 that phosphorylates Notch intracellular domain on Serine residue of the C-terminal PEST sequence, inducing its recognition by Fbw7 E3-Ubiquitin Ligase and its proteosomal degradation (Fryer et al., 2004)Furthermore, Mastermind can also be ubiquitinylated by UBC9 to downregulate Notch signaling. In addition, Hes phosphorylation on PKC consensus sites into the basic region can disrupt its DNA-binding (Strom et al., 1997)

2.1.5 Non canonical Notch signaling

The canonical Notch pathway implies the cleavage of Notch receptors at the cell surface by the gamma-secretase complex, its translocation into the nucleus and the activation of *hes* and *hey* transcription in an RBPJ-k dependent manner. Though, Notch is able to activate

signaling pathways and gene transcription by various other mechanisms, termed non-canonical Notch signaling (Reviewed in (Ayaz and Osborne, 2014)).

Increasing number of data illustrates the ability of non canonical Notch to activate different pathways. For instance, membrane-bound Notch induces AKT phosphorylation by mTORC2 allowing the survival of T lymphocytesfollowing cytokine deprival, whereas the retention of Notch-1 in the nucleus abolished the survival of Hela cells (Perumalsamy et al., 2009).Cytoplasmic Notch 1 interacts physically with CARMA-1, a component of T cells signalosome,thus allowing the activation of NF-κB (Shin et al., 2014a).The comparison between Notch and RBPJ-k conditional knock-out in mice evidenced the activation of NFκb by Notch independently of RBPJ-κ mediated gene transcription during CD4+ T cells amplification (Dongre et al., 2014). Moreover, the cooperation between Notch and YY1 transcription factor activates c-Myc transcription through non RBPJ-k binding-sites in K562 cells(Liao et al., 2007).

Besides, Notch signalingcan be activated independently of Notch receptors. For instance, c-Jun directly activates Hey-2 transcription as attested by promoter assay in K562 myeloid cell line, which in turn inhibits GATA-1 transcriptional auto-activation through direct physical interaction leading to the inhibition of erythrocytic differentiation of human derived CD34+ cells (Elagib et al., 2004).

2.2 Notch role in HSCs function

Given that mice deficient for the expression of Notch molecular components die before the emergence of definitive hematopoiesis, the development of conditional deleted mice models was necessary to investigate the role of Notch during hematopoiesis. The effects of Notch components' deletion on HSCs cell fate are detailed in **Table 3**.

2.2.1 Through the hematopoietic niche

Notch effect on HSCs can be mediated either by direct contact between niche cells and HSCs, or through the modulation of niche cells expansion (Reviewed in (Weber and Calvi, 2010)).

	HSC	Osteoblast	Endothelial cells	MSPC	Macrophages
Notch 1	X	X		X	X
Notch 2	X				
Notch 3	Not expressed				
Notch 4	Not expressed				
Jag-1	Weak	X	X	X	
Jag-2			X		
DL-1		X	X	X	
DL-4			X	X	
Fringe	X				X

Table 2: Expression profile of Notch receptors and ligands into the hematopoietic niche

(Reviewed in Liu et al., 2010; Weber et al., 2010). MSPC: Mesenchymal stem and progenitor cell.

As summarized in **Table 2**, Notch ligands (principally Jag-1, Jag-2, Dll-1 and Dll-4) and receptors (Notch 1 and 2) are expressed in HSCs and by diverse cells of the hematopoietic niche such as osteoblasts, endothelial and mesenchymal progenitor cells.

Striking evidence for the implication of Notch in the regulation of HSCs cell fate through the niche came from the pan-depletion of Notch signaling through the conditional knock-out of Mib-1 (essential for Notch ligands maturation), which induces the development of myeloproliferative disorder (MPD), notably characterized by extramedullary hematopoiesis with greatly enhanced proportion of HSCs. The development of MPD was due to defective microenvironment as attested by its emergence into irradiated mutant mice transplanted with wild-type bone marrow cells and its absence into wild-type irradiated mice transplanted with mutant bone marrow cells. Although Notch activation was comparable into the HSCs enriched population LSK from normal and MPD-developing mice, the expression of constitutively active Notch-1 receptor restored the survival and MPD-absence of Mib-1 deficient mice (Kim et al., 2008).

More precisely, Notch effect was mapped to the osteoblastic and endothelial niche components. The conditional depletion of Jag-1 in endothelial cells induces decreased number of Notch-2 expressing LT-HSCs, as well as their quiescence resulting in their exhaustion in serial transplantation assay (Poulos et al., 2013). Conversely, the expression of Notch ligands on endothelial cells induced the *ex vivo*expansion of HSCs and required the direct interaction between HSCs and endothelial cells (Butler et al., 2010). Additionally, the loss of Jag-1 expressing osteoblasts reduced HSCs quiescence and self-renewal ability (Bowers et al., 2015), while increased production of Jag-1 by osteoblasts induces the expansion of NICD-expressing HSCs and this effect required the interaction of HSCs with osteoblasts (Calvi et al., 2003).

Notch may regulate the osteoblastic niche, but with divergent effects depending on age and maturation stage (Reviewed in (Weber and Calvi, 2010). On one hand, pan-depletion of Notch signaling through the conditional depletion of Presenilin 1/2 (Gamma-secretase complex component) in osteoblasts induceslate-onset osteoporosis (decreased bone mass)(Engin et al., 2008).On the other hand, Presenilin 1/2 depletion in mesenchymal progenitors induced osteosclerosis (increased bone mass)(Hilton et al., 2008). Thus, Notch activation seems to inhibit osteoblastic differentiation of mesenchymal progenitors, while at later stage Notch would cause osteoclasts differentiation.

2.2.2 HSCs emergence

Notch signaling pathway is essential, when cooperating with BMP-4 and Wnt pathways, for the emergence of definitive hematopoiesis from hematopoietic clusters into the AGM region during development through the regulation of endothelial versus hematopoietic cell fate and in close relationship with arterial formation (reviewed in(Gering and Patient, 2010); (Ciau-Uitz et al., 2014)). Notch-1, but not Notch-2 (Kumano et al., 2003),as well as Jag-1 expression in the AGM are primordial for the emergence of HSCs through the control of GATA-2 expression (Robert-Moreno et al., 2007). Furthermore, the double mutation of *hes-1* and *hes-5* induces total loss of functional HSCs. Further analysis of *gata-2* promoter evidenced its double regulation by Notch, as Jag-1/Notch-1/RBPJ-k directly binds and induces the expression of GATA-2, whereas direct binding of HES-1 on a different region of the promoter represses *gata-2* transcription. In the AGM, GATA-2 expression is tightly regulated by Notch in two opposite ways. On one hand, HES-1 allows the emergence of pre-hematopoietic cells but inhibits their hematopoietic engagement through the repression of GATA-2. On the other hand, Jag-1/ Notch1/RBPJ-k signaling induces the expression of GATA-2 allowing the emergence of functional HSCs (Guiu et al., 2013). In summary, Notch participates to the control of the balance between emergence/differentiation in fetal life.

2.2.3 HSCs differentiation

The most robust effect of Notch activation in hematopoiesis is its positive role in the induction of T-cell development at the expense of B-cell differentiation (Reviewed in (Rothenberg, 2014)).This was first indicated by clinical studies showing that 50 and 20% of T-ALL (T cell Acute Lymphoblastic Leukemia) are associated with Notch-1 mutations either inducing increased expression of activated NICD-1 or affecting HD and LNR domains or PEST motif, respectively.Notch-1 expression is induced during lymphopoiesis with increased expression in T lymphocytes compared to B lymphocytes(Oh et al., 2013). Notch-1 regulates almost all steps of T-cells development such as amplification, cell fate decisions between α/β and ϒ/δ or T helper and T reg lymphocytes, as well as lymphocytes maturation from double negative to double positive CD4 CD8 stage.

Gene KO	Target	Mode of deletion	Phenotype	Cell autonomous	Reference
Notch 1	Receptor	Mx-Cre inducible	HSCs not affected at steady state No default of HSCs expansion after myeloablation	ND	Varnum-Finney, 2011
Notch 2	Receptor	Mx-Cre inducible	HSCs not affected at steady state Delay in recovery after 5FU Defect in reconstitution after irradiation	ND	Varnum-Finney, 2011
Jag-1	LIgand	Endothelial cells	Premature exhaustion of HSCs	Non-autonomous	Poulos, 2013
Notch1 and 2	Receptors	Mx-Cre inducible	Inhibition of T differentiation Chronic Myeloid Leukemia	ND	Klinakis, 2011; Oh, 2013
Nicastrin	Gamma-secretase	Vav-cre inducible	Defective response to stress erythropoiesis	ND	Oh, 2013
RBPJ-k	Notch nuclear target	Mx-Cre inducible	Myeloproliferative disorder Stromal-> miR-155 -> KRAS -> NFkb -> Inflammation	Autonomous	Wang, 2014
ADAM-10	Notch receptor cleavage	Mx-Cre inducible	Myeloproliferative disorder	Non autonomous	Weber, 2013
ADAM-10	Notch receptor cleavage	Mx-Cre inducible	Myeloproliferative disorder	Both	Yoda, 2011
POFUT-1	Notch fucosylation	Mx-Cre inducible	Myeloid hyperplasia	Both	Yao, 2011
MIB-1	Ligand endocytosis	MMTV-Cre Mx-Cre	Myeloproliferative disorder	Non autonomous	Kim, 2008
Presenilin 1 +/- Presenilin 2 -/-	Gamma-secretase	Constitutive	GMP amplification		Qyang, 2004
Nicastrin	Gamma-secretase	Mx-Cre inducible	Chronic MyeloMonocytic Leukemia	Autonomous	Klinakis, 2011
FX -/-	Ligand and receptor fucosylation	Constitutive	Myeloproliferative disorder HSCs: slight homing defect; increased cycling; Defect of HSCs regeneration	Autonomous	Zhou, 2008 Myers, 2010

Table 3: Hematopoietic phenotypes of murine knock-out models of various Notch signaling components

Each lane of the table indicates in the successive columns: the name of the deleted gene, its known implication in Notch signaling pathway, the type of deletion (constitutive, inducible or cell specific), the main hematopoietic phenotype observed, whether this phenotype is hematopoietic cell autonomous and the corresponding reference.

While Notch-1 activation induces T-cell development, Notch 1 and Notch 2 inactivation in murine models **(Table 3)** is associated with the development of myeloproliferative disorders affecting particularly the bipotent GMP and granulocytes (Klinakis et al., 2011). This is further confirmed by *exvivo* studies demonstrating the inhibitory role of Notch-1 in myeloid commitment (Stier et al., 2002). Myeloid commitment is rather favored by the induction of Notch-2 expression from HSCs to erythroid progenitors as elegantly demonstrated by expression profiling and functional analyses of 4 Notch receptors in murine models (Oh et al., 2013)**(Figure 14)**.

2.2.4 HSCs maintenance/ amplification

Several *ex-vivo* experiments using immobilized Notch ligands Jag-1, DLL-1 or DLL-4 argue for a positive role of Notch signaling during HSCs amplification ((Varnum-Finney et al., 2000); (Karanu et al., 2000; Karanu et al., 2003). Interestingly, a recent study using fed-batch culture strategy (dilution every 24h and replating every 4 days to test feed-back effects) assessed the negative effect of myeloid cells on HSCs expansion, while DLL-1 stimulation and subsequent STAT-3 activation led not only to the repression of myeloid granulomonocytic differentiation, but also allowed delayed expansion of most primitive progenitors CD34+ CD90+. Strikingly, the combination of DLL-1 stimulation with fed-batch culture allows the expansion of short-term HSCs in sublethally irradiated immunodeficient mice (Csaszar et al., 2014).

Notch contribution to HSCs maintenance is subject to divergent opinions. On one hand, Notch activity has been positively correlated with HSCs quiescence as Hes-1 transduced LSK produced a higher proportion of progenies able to exclude Hoechst label when transplanted into lethally irradiated mice (Kunisato et al., 2003). In accordance, the stimulation of HSCs *ex-vivo* by DLL-4 shows increased quiescent/proliferating LSK ratio concomitant to increased engraftment ability, short-term maintenance and increased expression of stemness over cyclines genes (Catelain et al., 2014). On the other hand, the conditional depletion of Notch ligands and receptors or pan-inactivation of Notch transducers through the conditional expression of a dominant negative form of MAML or the conditional depletion of RBPJ-k evidenced the absence of Notch effect on HSCs frequency and long-term-repopulating

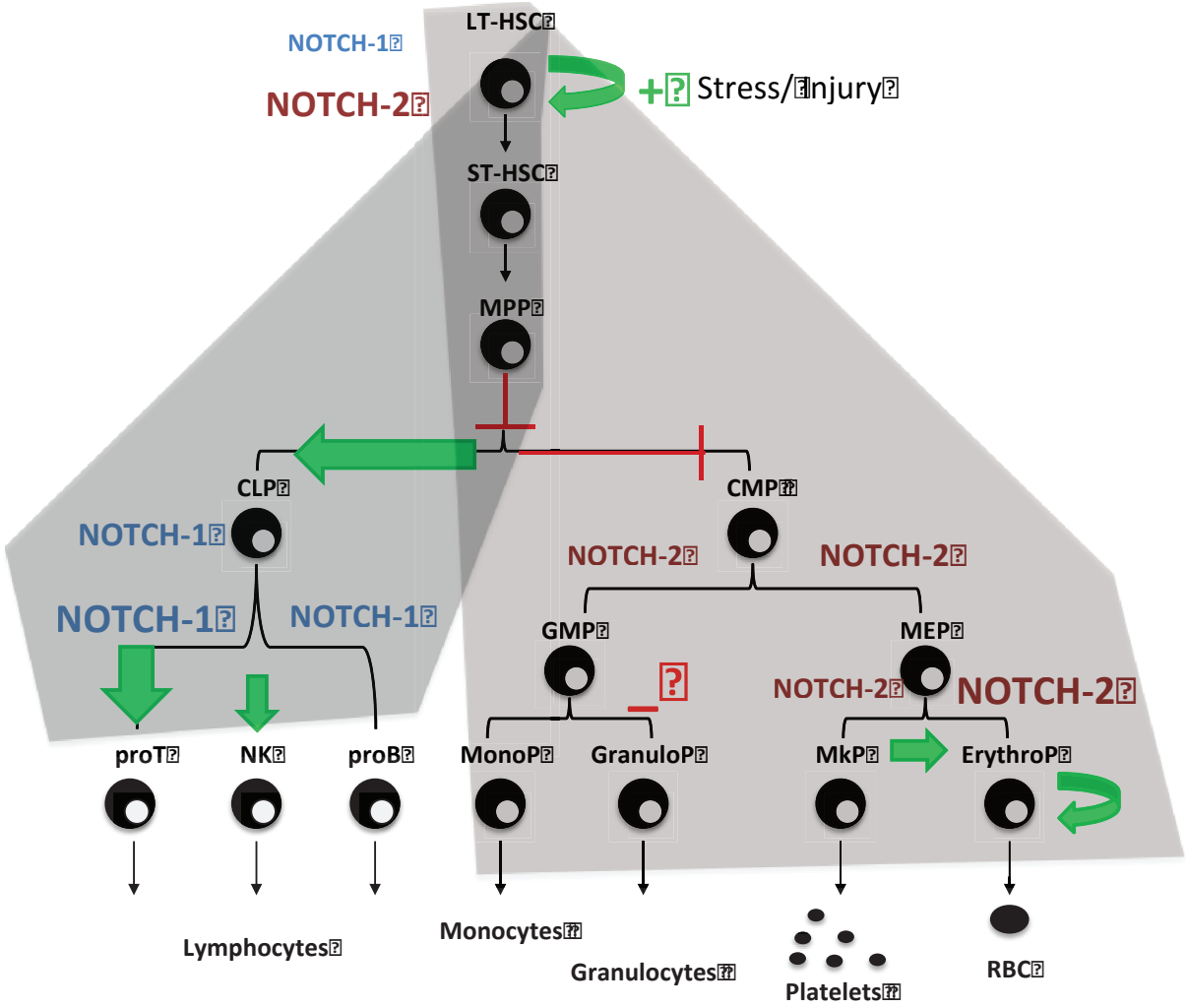

Figure 14: Mapping of Notch receptorrs expression and functions

Hematopoietic tree showing the differential expression of Notch-1 (blue area) in the lymphoid and Notch-2 (brown area) in the myeloid branches (relative expression levels are indicated by police sizes). The stimulating orrepressive effects of Notch signaling are indicated by green arrows or red inhibitory signs, respectively. The positive effect of Notchon self-renewal is indicated by curved green arrows and is mainly observed in stress conditions (adapted from (Oh et al., 2013)).

activity. These studies exclude the implication of Jag-1/Notch-1 during steady state hematopoiesis (Maillard et al., 2008; Mancini et al., 2005).Thus, the artificial activation of Notch is associated with positive effect on HSCs maintenance, while its repression argues for its dispensability in steady state condition. The apparent discrepancy of Notch implication in HSCs maintenance might be due to differences in signal intensities and kinetic of stimulation. Incidentally, when studying the effect of Notch on leukemia in a murine model of T-ALL, the authors evidenced that hyper-stimulation of Notch signaling induced only transient maintenance of LT-HSCs while sustained stimulation lead to their exit from quiescence and exhaustion (Chiang et al., 2013).

Interestingly, a study using conditional deletion of Notch-1 or Notch-2 seems to reconcile precedent discrepancy of Notch effect on the behavior of HSCs during either steady state or stress condition (Varnum-Finney et al., 2011). Actually, the preferential activation of Jag-1/ Notch-2/Hes-1 axis over Notch-1, potentially mediated by the maturation of Notch-2 by Fringe glycosyl-transferase, inhibits granulocytic myeloid differentiation. Confirming precedent results in conditional depletion models, neither Notch-1 nor Notch-2 affected the repopulating activity of LSK over serial transplantation, indicating the dispensable role of Notch in homeostatic condition. However, Notch-2 signaling allows the expansion of ST-HSCs and MPP in stress condition favoring a rapid recovery after induced-exit of quiescence or after myelosuppression.

In summary, Notch participates to the control of the balance between expansion and differentiation in adulthood by modulating HSCs niche and gene expression.Notch seems dispensable for HSCs maintenance in steady state conditions, while Notch-2 and DLL-1 allow rapid expansion of ST-HSCs in stress conditions. Notch delays HSCs differentiation, but strong induction of Notch-1 induces T lymphocytic differentiation, while Notch-2 activation allows myeloid commitment but represses granulo-monocytic lineages **(Figure 14)**.

2.3 Notch role in erythropoiesis

Notch role in erythropoiesis is difficult to appreciate from incoherent *in vitro* studies using cell lines with inducible expression of constitutively active Notch-1 ICD evidencing either

positive role on erythrocytic differentiation in FDCP-mix cells (Henning, 2007), or negative role in K562 cells (Ishiko et al., 2005).

The results from *ex-vivo* studies are more consistent when using immobilized Notch ligands DLL-4 or Jag-1 to stimulate CD34+ human progenitors derived from either cord blood (Poirault-Chassac et al., 2010; Sugimoto et al., 2006)fetal liver (Dando et al., 2005)or bone marrow (Walker et al., 1999). These studies show a positive effect of Notch signaling on the maintenance of erythrocytic progenitors while delaying their differentiation. Interestingly, one report used *ex-vivo* differentiation system to produce erythroblasts from human peripheral blood CD34+ cells, wherein SCF stimulation induces the expression of Notch-2 receptor, at the expense of Notch-1, which interacts with endogenous Jag-1 to delay erythrocytic maturation (Zeuner et al., 2011).

In-vivo studies support the positive role of Notch on erythropoiesis as murine models of pan-depletion of Notch signaling, through the conditional depletion of Notch modulators of endocytosis Mind-bomb-1 (Kim et al., 2008) or glycosylation (Zhou et al., 2008) show mild-anemia. Interestingly, using transgenic mice harboring a Hes1-GFP (reporter of Notch activated pathway)combined with deletion of either one of the 4 Notch receptors, a recent study evidenced the preferential expression of Notch-2 and Hes-1 in CFU-E and the association between Hes-1 expressing LSK with erythrocytic transcriptome signature. The conditional expression of ICN-2 increased CFU-E progenitors and erythroblasts in the bone marrow whereas the conditional depletion of Notch-2 receptor led to the opposite effect (Oh et al., 2013).Conversely, another study based on functional and chromatin-immunoprecipitation analyses on fetal liver derived from mice depleted for Ikaros transcription factor revealed the importance of Ikaros-mediated repression of Notch signaling for terminal erythroid differentiation (Ross et al., 2012). This study actually demonstrated the direct activation of Hes-1 by ICN/RBPJ-k during erythrocytic amplification, while erythrocytic terminal differentiation from the pro-erythroblast through the normoblast stage required the direct binding of Ikaros and the subsequent recruitment of GATA-1 and Ezh-2/ MI-2 complex inducing chromatin compaction and Hes-1 transcriptional repression.

Notch is also crucial for correct response to stress erythropoiesis. Indeed, conditional depletion of Nicastrin in the hematopoietic system delayed the recovery of red blood cells when acute stress anemia was induced by phenylhydrazine treatment.

Furthermore,sublethal irradiation causes increased Hes-1 expression into the bone marrow and Notch-2 expression in bipotent PreMegE progenitors. Additionally, Nicastrin -/- irradiated mice display virtually absent erythroid progenitors as well as basophilic and orthochromatic erythroblasts in the bone marrow. Finally, Notch2 -/- irradiated mice harbor small spleen and reduced proportion of erythroid progenitors, while other myeloid lineages are not affected, indicating specific effect on stress erythropoiesis(Oh et al., 2013).

The compilation of these data demonstrates the requirement of Notch-2 signaling for normal and stress erythroid progenitors' expansion, while its repression is needed to allow terminal differentiation.

2.4 Notch role in megakaryopoiesis

Notch role in megakaryopoiesis remains difficult to fully appreciate due to contradictory results obtained in mice or humanstudies.

On one hand,in a recent study (Mercher et al., 2008)Dll1 Notch ligand (either recombinant immobilized or expressed on the cell surface of OP9 stromal cells) was shown to stimulate the production of CD41+ megakaryocytic cells by murine LSK stem cells *in-vitro*. The same study showed that mice engrafted by LSK stem cells expressing dnMAML1 (a dominant negative repressing Notch signaling) displayed decreased production of megakaryocytic progenitors,contrarily to mice engrafted by HSC expressing ICN4 (cleaved activated Notch-4) which displayed increased production of megakaryocytic progenitors and increased ploidy in megakaryocytes. Though, in both inactivation and hyper-activation of Notch cases, blood platelets count did not vary.Interestingly, the activation of Notch pathway increased the number of MEP at the expense of GMP,reciprocally inhibition of Notch signaling by dnMAML1 decreased the proportion of MEP. Surprisingly, the number of multipotent progenitors CMP did not vary. Taken together, these data clearly indicate that the stimulation of Notch signaling favors megakaryocytic commitment of murine HSCs and erythro-megakaryocytic commitment of multipotent CMP at the expense of the granulo-monocytic lineages. Further studies showed thatthe short-cut allowing the generation of megakaryocytes from HSCs requires Notch induced activation of AKT while TPO seems dispensable, contrarily to the classical generation of megakaryocytes from CMPs which can

be initiated by TPO but is less dependent on AKT activation (Cornejo et al., 2011). More recently, part of the already known inhibitory effect of Ikaros on megakaryocytic lineage could be attributed to its ability to repress several downstream specific targets of Notch signaling, thus further strengthening the importance of Notch pathway in the positive control of megakaryocytic lineage specification (Malinge et al., 2013).

On the other hand(Poirault-Chassac et al., 2010), the stimulation of human CD34+ derived from umbilical cord blood or purified bipotent MEP byDLL-4 ligand(either immobilized or expressed on OP9 stromal cells)inhibited megakaryocytic terminal differentiation, as attested by the production of a reducednumber of CD41+ CD42+ cells, lower ploidy and reduced proplatelets formation. Though, the number and proportion of CFU-MK megakaryocytic progenitors did not vary. DLL-4 stimulation induced-phenotype was correlated with the induction of Hes-1 expression and the concomitant decrease of megakaryocytic markers such as Fli-1, NF-E2 and β-tubulin, thus confirming the negative effect of DLL4-mediated activation of Notch signaling on terminal megakaryocytic differentiation. Importantly, this study also showed, as previously shown for Dll1, that DLL-4 was also able to induce megakaryocytic differentiation of murine LSK stem cells. Whether these differences regarding the effect of Notch signaling on megakaryocytic lineage rely on different types of hematopoietic cells or to real differences in the function of Notch between human and mouse remains an open question (Malinge and Crispino, 2010).

2.5 Notch and Megakaryocytic Leukemia

Activating mutations of Notch-1 receptor have oncogenic effect on the development of acute T-lymphoblastic leukemia (reviewed in (Van Vlierberghe and Ferrando, 2012)), whereas the inactivation of Notch signaling is associated with myeloid leukemia**(Table 3)**. For instance, the alternative splicing of Notch-2 transcripts lead to the expression of a dominant negative form and the extinction of Hes-1 expression in the majority of AML samples (Adamia et al., 2014).

On the contrary, the constitutive activation of Notch is associated with the development of acute megakaryoblastic leukemia (AMKL). Indeed, the fusion oncogene OTT-MAL generated by the translocation t(1;22) (p13;q13) transcriptionally activates and physically interacts with

RBPJ-k, even in the absence of Notch stimulation. This aberrant activation of Notch signaling lead to the hyper-proliferation of the 6133 OTT-activated cell line established from a murine model of AMKL and was accompanied by an aberrant megakaryocytic specification. Though, the total transformation into AMKL required secondary oncogenic event such as the mutation W515L of c-MPL receptor (Mercher et al., 2009). These data are consistent with previously described positive effect of Notch on megakaryocytic specification from murine HSCs.

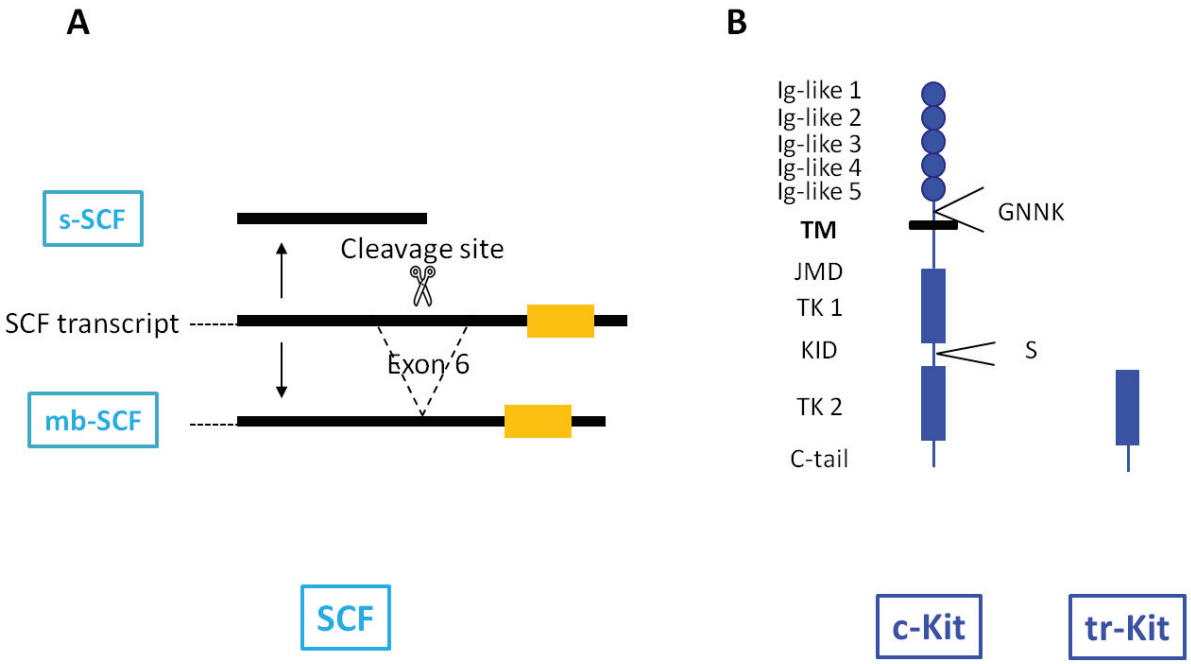

Figure 15: SCF and c-Kit receptor proteins structure and isoforms

A:The 6th exon of SCF transcript (black bar) encodes for a cleavage site. When present, SCF long isoform is cleaved producing a soluble and secreted form (s-SCF). Contrarily, the alternate spliced isoform lacking the 6th exon, and thus the cleavage site, produces a membrane-bound form of SCF (mb-SCF). Signal peptide is represented by hatched line and the transmembrane region is represented by orange box.

B: Schematic representation of c-Kit receptor structure and isoforms. The names of the different domains are indicated on the left: c-Kit receptor comprises 5 Ig-Like domains in the extracellular part, the transmembrane region (TM) and two tyrosine kinase domains (TK1 and TK2) separated by a kinase insert domain (KID) in the intracytoplasmic region. Alternative splicing events generate several isoforms differing by the presence or absence of either GNNK tetrapeptide in the extracellular part or of a serine residue in the KID domain. Alternative use of a cryptic promoter allows the production of a truncated protein called tr-Kit which contains only TK2 and C-terminal tail.

3 SCF/c-Kit signaling pathway

3.1 SCF/c-Kit signaling pathway

The SCF/c-Kit signaling pathway relies on the activation the Kit receptor by its specific ligand SCF. Beside important roles in the control of pigmentation, gut function and reproduction, this pathway is one of the most important pathways involved in the control of hematopoiesis.

3.1.1 SCF transcript and protein

3.1.1.1 Sl locus

SCF stands for Stem Cell factor, also called Kit-L for Kit Ligand, MGF for Mast Cell Growth Factor or SF for Steel factor. SCF is encoded by the Steel locus (*Sl*) the mutations of which lead to very similar phenotypes to that of c-kit mutations in mice(Williams et al., 1990). The *Sl* locus harbors 9 exons and maps on mouse chromosome 10 and on human chromosome 12.

3.1.1.2 SCF protein

SCF is mainly produced by fibroblasts and endothelial cells throughout the body. The relative production between soluble and membrane-bound SCF varies greatly between tissues. For instance, into the bone-marrow the production of soluble SCF is 4 times more abundant than the membrane-bound isoform. The dosage of circulating soluble SCF is approximately 3 ng/mL in normal human serum. SCF is highly glycosylated and circulates under the form of a non-covalently bound dimers with 4 Cysteine residues forming intra-molecular disulfide bounds contributing to maintain fully active conformation (Broudy, 1997).

3.1.1.3 SCF isoforms

SCF exists in two isoforms, one soluble and one membrane-bound which result from the alternative splicing of the 6th exon that contains the cleavage site required to generate the soluble form (Huang et al., 1992)**(Figure 15)**. Both isoforms are able to activate c-Kit receptor. However, a deletion in *Sl* locusinducing the production of only the soluble form causes anemia in *Sld* mice, thus highlighting the importance of the membrane-bound isoform for normal function of c-Kit (Brannan et al., 1991). For instance, membrane-bound

SCF induced the proliferation of 32D cells whichwas demonstrated to be specifically dependent onc-Kit residue Y728 involved in the binding toPLC-ϒ(Gommerman et al., 2000).

3.1.2 c-Kit transcript and protein

3.1.2.1 kit gene

kit gene harbors 21 exons and maps to chromosome 4 in human and to chromosome 5 in mouse.*kit* promoter has been thoroughly investigated (Cairns et al., 2003)and contains multiple binding sites for various transcription factorspositively regulating its expression such as SCL (Lecuyer et al., 2002). Most importantly, *kit* expression requires the concomitant activation of several enhancers, which arecontrolled either negatively by GATA-1(Munugalavadla et al., 2005)or positively by GATA-2 (Jing et al., 2008).

3.1.2.2 c-Kit protein

The protein productof *kit* gene is a tyrosine kinase receptor (RTK) belonging to the subclass III (along with PDGFR and FLT3 kinases) which is characterized by an extracellular region consisting of five immunoglobulin-like domains (encoded by exons 1 to 9), a single transmembrane domain (encoded by the exon 10) and an intracellular domain composed of two tyrosine kinase domains (encoded by exons 11-14 and 16-20) separated by an insert region (encoded by exon 15)**(Figure 15)**. During maturation, the 110 KD native c-Kit protein is heavily glycosylated at different N-glycosylation sites mainly located in the juxta-membranar region, and thus reaches 145 to 160 KDa when present at the membrane. c-Kitcontains 9 different ligand-induced phosphorylation sites on either Tyrosine or Serine, as well as ubiquitinylation sites essential for receptor internalization and degradation.

3.1.2.3 c-Kit isoforms

Alternative splicing of *kit* gene results in the production of several isoforms differing by the presence or absence of the tetrapeptide GNNK in the extracellular part of the juxtamembranar region. An additional isoform varies by the presence or absence of a serine residue in the kinase insert region. Furthermore, the use of a cryptic promoter in the 16th intron of murine *kit* gene (15th intron in human *Kit* gene) allows the production of a truncated form of the receptor (Tr-kit) that contains only the second part of the kinase domain and the C-terminal tail. Tr-kit was initially identified in post-meiotic germ cells of the testis (Rossi et al., 1992), but was later found specifically in hematopoietic stem and

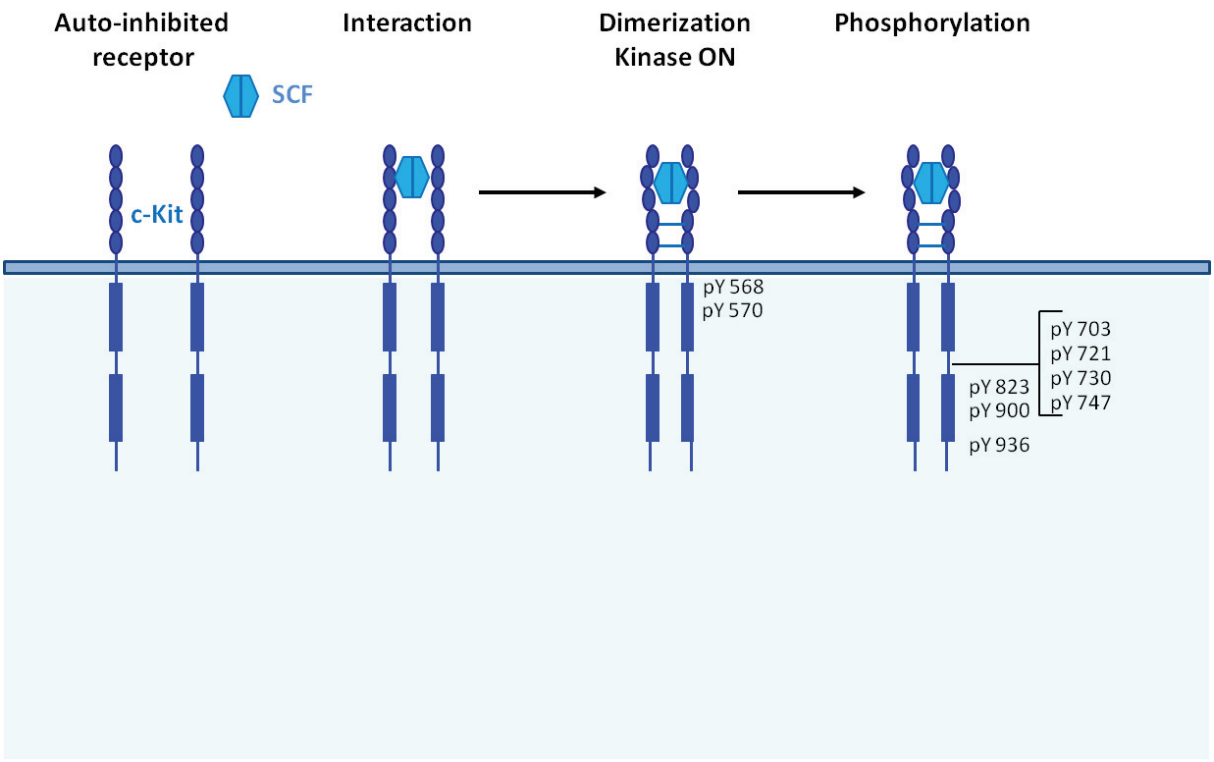

Figure 16: SCF-dependent activation of c-Kit kinase

In the absence of its ligand, c-Kit adopts a self-inhibited conformation. SCF dimers interact with Ig-like domains 1 to 3, and bring closer two c-Kit monomers. The two monomers dimerize through the 4th and 5th Ig-Like domain leading to the activation c-Kit tyrosine kinase activity. Activated c-Kit autophosphorylates first on Y568 and 570 then on the 7 remaining Tyrosine residues.

multipotent cells while its expression was lost in more committed progenitors(Zayas et al., 2008). Despite the fact that Tr-kit lacks a kinase domain, this isoform is able to signal by inducing the formation of a multimeric complex comprising SFK whencontributing to the transition from metaphasis to anaphasis during mouse egg activation (Paronetto et al., 2003).

3.1.3 Signal transduction

3.1.3.1 c-Kit kinase activation

In the inactive state, the juxtamembranar region of c-Kit receptor forms a hairpin loop that inserts into the active site avoiding the access to the ATP binding site and thereby suppressing the kinase activity (Reviewed in(Lennartsson and Ronnstrand, 2012))**(Figure 16)**.

SCF ligand, circulating as a homo-dimer, binds to the first three Ig-like domains of c-Kit receptor that shapes in a way favorable for the tight maintenance of SCF ligand interaction and brings two c-Kit monomers in close proximity. The two monomers dimerize through the 4^{th} and 5^{th} Ig-like domains, thus achieving the stabilization of c-Kit protein. The proximity between the two kinases domains of c-Kit induces their activation and trans-phosphorylation initially on the juxtamembranar Tyrosine residues 568 and 570. Next, trans-phosphorylation proceeds on the 7 remaining Tyrosine residues located in the kinase insert region (Tyr 703, 721, 730 and 747) , the kinase domain (Tyr 823 and 900) and the C-terminal tail (Tyr 936).

3.1.3.2 Downstream signaling

As illustrated in **Figure 18**, phosphorylated sites of activated c-Kit receptor function as docking sites for the binding of several adaptor proteins and kinases, thus activating transduction pathways which controls cell proliferation and survival. The three main signaling pathways acting downstream of c-Kit in hematopoiesis are detailed below and schematized in Figures 17/ 18.

PI3K/AKT pathway (Figure 17): SCF stimulation allows the activation of phosphoinositide 3 Kinase (PI3K), through the direct binding of the p85 regulatory subunit of PI3K on c-Kit Tyrosine residue 721 or indirectly through the adaptor protein Grb2 on Tyr 936. The phosphorylation of PIP2 (Phosphatidyl-inositol 4-5 diphosphate) into PIP3 (Phosphatidyl-

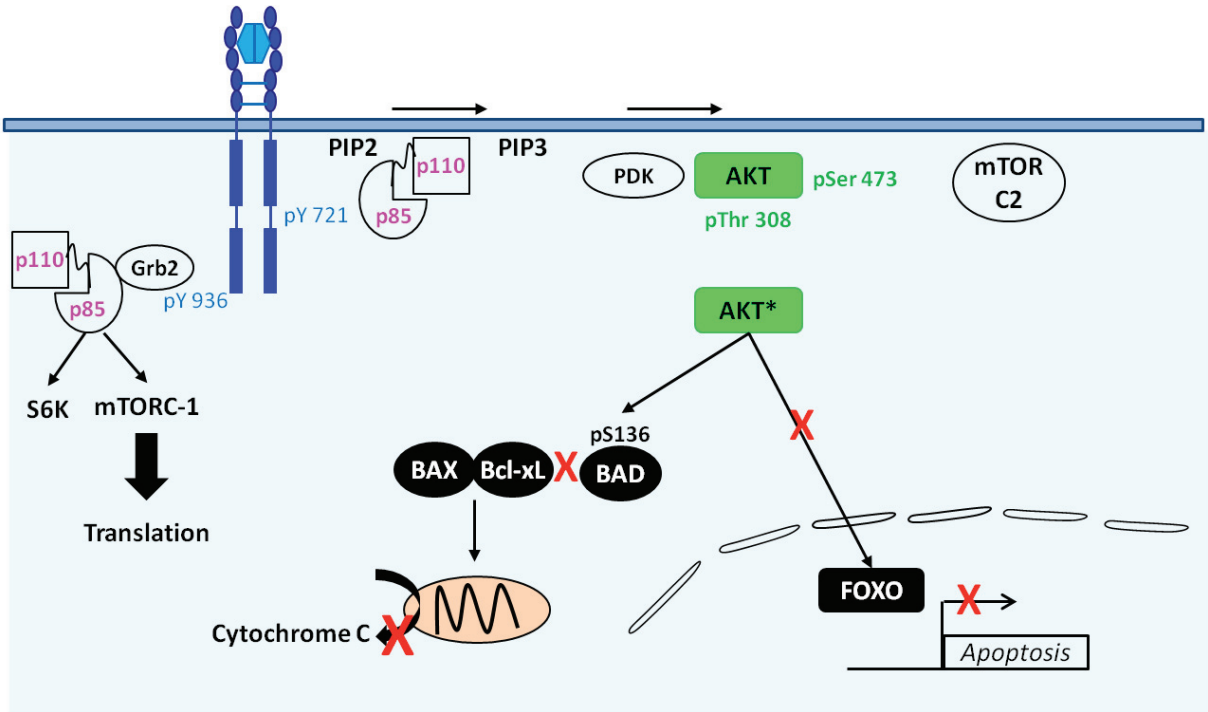

Figure 17: Role of c-Kit-activated PI3K/AKT pathway in cell survival

Activation of c-Kit induces the activation of PI3K (p85 pink sector + p110 pink square) which phosphorylates PIP2 into PIP3, allowing the activation of PDK-1 and the recruitment of AKT Ser/Thr kinase. PDK-1 and mTOC-2 activates AKT (green rectangle) by phosphorylation. Activated AKT (green rectangle with black star) sequestrates FOXO transcription factors preventing their translocation into the nucleus and thus the expression of pro-apoptotic genes. Activated AKT also sequestrates BAD disrupting its interaction with Bcl-xL. Bcl-xL interaction with BAX prevents the release of Cytochrome C (Curved black arrow) from the mitochondria (orange circle). Activated PI3K activates S6K and mTORC-1 allowing enhanced translation.

inositol 4-5 triphosphate) by p110 subunit of PI3K induces the recruitment of AKT a Ser/Thr kinase and the activation of PDK-1 (Phosphoinositide dependent kinase). AKT full activation is achieved by the phosphorylation on Thr-308 by PDK-1 and on Ser-473 by mTORC-2 (mammalian target of rapamycin complex-2), thereafter playing a pivotal role in cell survival through different mechanisms. The first mechanism involves the mitochondrial pathway as activated AKT phosphorylates Bad on Ser-136 disrupting its interaction with Bcl-xL, which in turn can inhibit the release of cytochrome C induced by Bax, finally leading to the inhibition of apoptosis. The second mechanism involves AKT-dependent phosphorylation of forkhead transcription factors (FOXO) inducing their sequestration into the cytoplasm, thus inhibiting their nuclear translocation and activation of pro-apoptotic genes. The third mechanism involves PI3K-dependent activation of mTORC-1 and S6K which in turn stimulate translation.

MAPK pathway: Mitogen Activated Protein Kinase pathway consists in three layers of signaling molecules,with cell-specific combinations, allowing signal transduction from the plasma membrane to the nucleus. c-Kit phosphorylation on Tyr 703 and 906 recruits the Grb2 adaptor, which is constitutively bound to the Sos (Son of Sevenless) guanine exchange factor, the latter being responsible for the recruitment of the small GTPase RAS. SCF stimulation induces the recruitment of another RAS guanine exchange factor, named vav-1 and induces its phosphorylation(Munugalavadla and Kapur, 2005). The proximity between Sos and RAS allows the latter protein to proceed to the exchange between GDP and GTP, inducing its conformational change and activation. Next, kinases are activated sequentially as RAS activates Raf which activates Mek-1 which in turn activates ERK-1 and 2. ERK-1 and 2 transcription factors translocate to the nucleus and induce the expression of target genes such as c-Fos and Elk-1, or act on cytoplasmic substrates such as RSK. c-Kit kinase also activates the three other major MAP kinases p38, JNK and ERK-5.

SFK pathway: The Src family of tyrosine kinases contains eight cytoplasmic kinases, some of which are ubiquitously expressed (Src, Yes and Fyn), while others have more restricted expression pattern such as Lck, Hck, Lyn, Fgr and Blk in the hematopoietic system (Ingley, 2008). They contain a unique membrane targeting domain, SH3 (Prolin-rich interacting domain), SH2 (phosphorylated Tyrosine interacting domain), a tyrosine kinase domain and a C-terminal tail with auto-inhibiting activity. SFK kinases interact directly with activated c-Kit receptor on Tyrosine 568/570 residues and their activity is rapidly increased within few

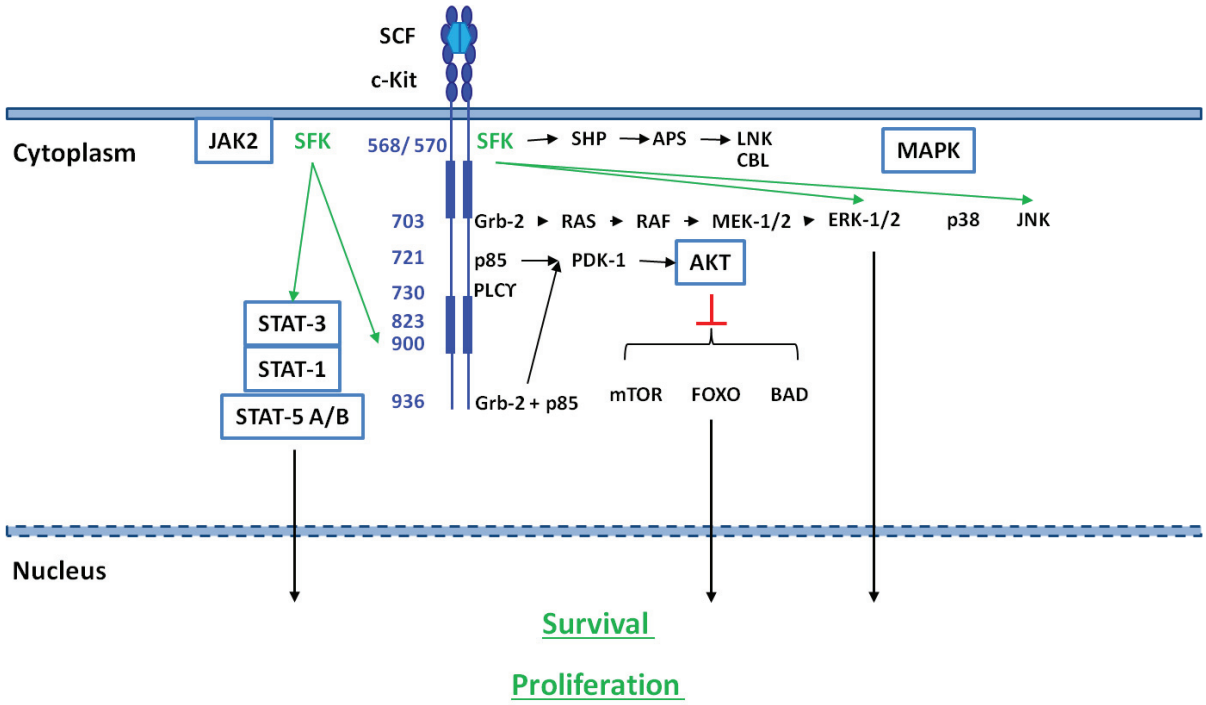

Figure 18: Main pathways activated by SCF/c-Kit signaling

Phosphorylated Tyrosine residues (blue) on activated c-Kit function as docking sites for the recruitment of specific adaptors or signaling molecules allowing the activation of at least three main pathways. The activation of JAK/STAT pathway is mediated either by JAK2 activation or through the recruitment and activation of Src family kinases (SFK), leading to the nuclear translocation of STATs factors. The PI3K/AKT pathway's activation results from the recruitment either directly of p85 subunit or indirectly through Grb2 adaptor, leading to the cytoplasmic retention of FOX factors.The MAPK/ERK pathway activation is mediated either by the recruitment of Grb2 adaptor or through SFK leading to the nuclear translocation of ILK and JUN factors among others. c-Kit signaling also leads to the activation of other MAPK: p38 and JNK.

minutes. SFK induces the phosphorylation of c-kit on Tyrosine 900 and enhance its kinase activity. SFK participate to several steps downstream of c-Kit signaling, such as the activation of AKT in a raft-dependent manner (Arcaro et al., 2007), JNK, p38 and ERK-1/2. SFK contribute to the pro-survival effect of SCF on erythroid precursors by suppressing Fas-mediated apoptosis signals(Endo et al., 2001; Nishio et al., 2001). Lyn member of SFK family can induce JNK and STAT-3 expression in mast cells and contributes to SCF-mediated effects on proliferation and migration. Lyn also promotes the cell cycle transition G1/S in the megakaryocytic cell line Mo7e(Linnekin et al., 1997).

JAK/ STAT: The Janus kinases are cytoplasmic Tyrosine kinases rapidly activated following ligand binding to RTK. JAKs interact and activate by phosphorylation members of the STATs family (Signal Transducers and Activators of Transcription). STATs transcription factors forms hetero-dimers between different members of the family and translocate to the nucleus where they activate gene transcription. JAK-2 is constitutively associated to c-Kit receptor and is transiently phosphorylated upon SCF stimulation. JAK-2 participates to SCF-induced proliferative response. STAT-1, STAT-5A and STAT-5B are activated by c-Kit kinase activity (Brizzi et al., 1999), inducing the enhancement of their DNA-binding. The co-stimulation of the megakaryoblastic cell line Mo7e with SCF and IL-9 induces the phosphorylation of STAT-3 on a serine residue and its nuclear translocation (Gotoh et al., 1996).

3.1.4 Signal downregulation

Following activation, SCF/c-Kit signaling is physiologically shut-down by different mechanisms allowing suitable signal intensity and duration of stimulation**(Figure 19)**.

When c-Kit kinase is still at the plasma membrane, PKC (Protein Kinase C) is activated by DAG (Diacylglycerol) release. PKC interacts with phosphorylated c-Kit on Tyrosine residue 570 and phosphorylates Serine 741 and 746 c-Kit residues inactivating its kinase activity. SHP-1 also interacts with pTyr-570 of c-Kit and dephosphorylates its Tyrosine residues. SHP-1 depletion in murine model induces the hyper-proliferation of hematopoietic progenitors (Shultz et al., 1997). In addition, SOCS-1 interacts with c-Kit, dephosphorylates JAK kinase (Endo et al., 1997)and inhibits SCF induced proliferation of mast cells (De Sepulveda et al., 1999).

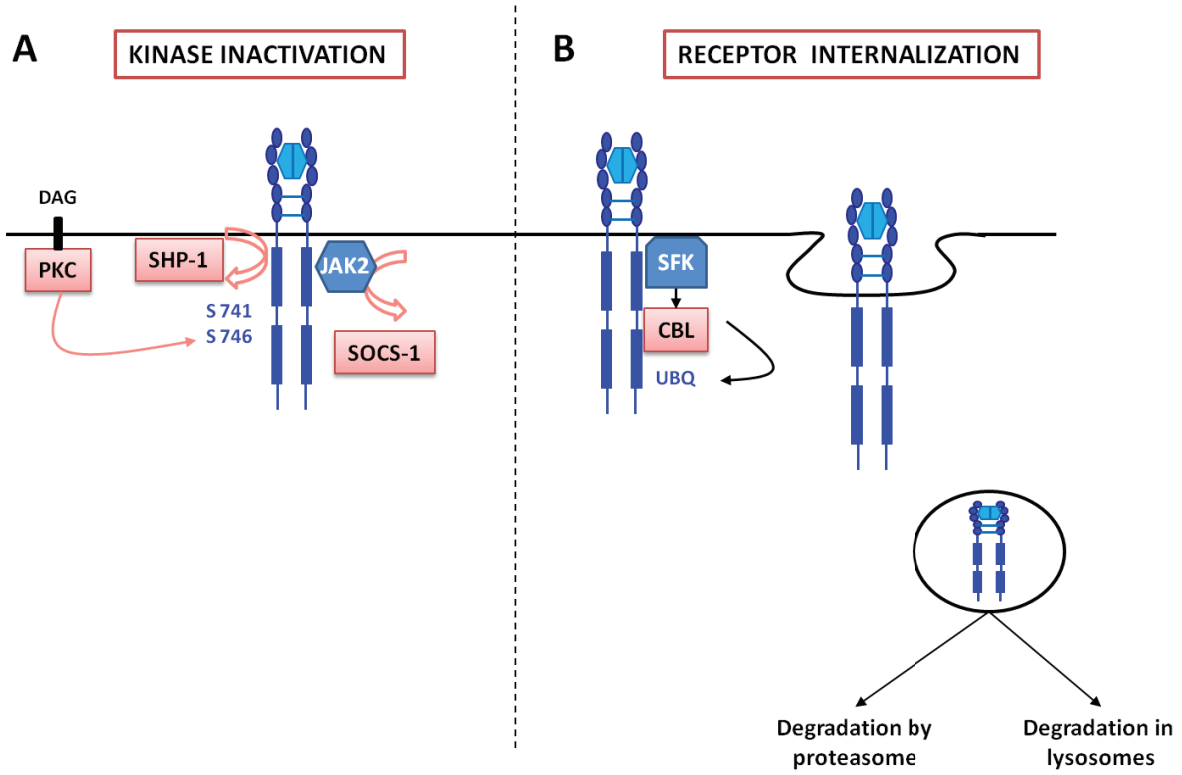

Figure 19: Downregulation mechanisms of SCF/c-Kit signaling

A: Downregulation mediated by kinase inactivation. Kinase inactivation can occur either by membrane-recruited PKC (through diacylglycerol DAG) which phosphorylates c-Kit (red arrow) or by dephosphosphorylation of c-Kit by SPH1 or JAK2 by SOCS1 phosphatases (curved double arrow).

B: Downregulation mediated by c-Kit internalization and degradation. Activation of c-Kit and subsequently SFK, induces the recruitment and activation of the E3-Ubiquitin Ligase CBL which then ubiquitinylates c-Kit inducing its internalization and degradation either by the lysosome or the proteasome.

In few minutes following SCF binding, SFK on Tyrosine residues 568/ 570 of activated c-Kit recruits c-CBL E3-Ubiquitin Ligase. The ubiquitinylation of c-Kit causes its internalization(Miyazawa et al., 1994) and degradation by the proteasome (D'Allard et al., 2013)or the lysosome (Zeng et al., 2005). The factors determining the balance between lysosomal or proteosomal degradation remains to be determined. Though, it is known that the inhibition of c-Kit kinase activity by Masitinib (Dubreuil et al., 2009)induces its lysosomal degradation (D'Allard et al., 2013).

3.1.5 c-Kit proteolytic cleavage

Membrane-bound c-Kit is cleaved by ADAM-17 (A Disintegrin and Metalloprotease)/ TACE (TNF-α converting enzyme) on the 5^{th} Ig-like domain releasing a soluble fragment of 100 KDa corresponding to the extracellular domain and which can be detected in human serum. This soluble form of c-Kit has been implicated in the survival of mast cells (Cruz et al., 2004), but the underlying mechanisms remain elusive. As both soluble and membrane-bound isoforms ofc-Kit have the same affinity for SCF, soluble c-Kit may act as a competitor of SCF. Alternatively, the cleavage of c-Kit may simply reduce the level of the full-length membrane-bound isoform available for activation by SCF (Turner et al., 1995).

3.1.6 c-Kit exosomal secretion

Interestingly, a few recent studies have shown that c-Kit can be secreted with exosomes and this form of secretion can mediate tumorigenesis. For example, when the conditioned medium of human mast cell line HMC-1 was harvested, c-Kit protein, but not transcripts, was found into exosomes. Furthermore, the culture of the human pulmonary adenocarcinoma cell line A549 with HMC-1 conditioned medium induced the activation of SCF/c-Kit signaling and the increase of their proliferation (Xiao et al., 2014). Similarly, activated phosphorylated c-Kit was detected in high amounts in the plasma of GIST-affected patients on the contrary tothe plasma of healthy donors. *In vitro* studies demonstrated that oncogenic activated c-Kit released in CD9-high exosomes are able to transform smooth muscle cells into gastric-like Cajal cells with increased invasiveness by allowing them to release metalloprotease MMP-1 in a c-Kit signaling dependent manner (Atay et al., 2014).

3.2 c-Kit role in hematopoiesis

3.2.1 In HSCs cell fate

The loss of c-Kit kinase activity in *W42* mutant mice which are viable and fertile, on the contrary to *W* mutant mice, is associated with extremely reduced number of HSCs and transplantation studies into sub-lethally or lethally irradiated mice suggest intrinsic defects of c-Kit deficient mice (Geissler et al., 1981). *Sl* mutant mice deficient in SCF expression have micro-environmental defect which would normally supports regenerative activity of CFU-S/ HSCs (McCulloch et al., 1965). Furthermore, the combination of low-dose irradiation with treatment by a monoclonal antibody (ACK2) blocking the interaction between SCF and c-Kit highly decreased competitive long-term HSCs and allowed for efficient transplant engraftment (Xue et al., 2010). These results suggest that the interaction between SCF and c-Kit modulates HSCs maintenance and engraftment.

3.2.1.1 HSCs emergence

Recent studies state the clear contribution of SCF/c-Kit signaling to HSCs emergence during fetal life. Indeed, c-Kit plays a critical role downstream of retinoic acid(RA) signaling during the emergence of the hemogenic endothelium in the AGM of embryos. Interestingly, the re-expression of c-Kit, which was lost in RA knock-out mice, was required to activate Notch signaling pathway, which in turn allowed the induction of p27 cell cycle regulator finally allowing the generation of the hemogenic endothelium and the maintenance of HSCs by quiescence (Marcelo et al., 2013).

A recent study investigatedthe murine placenta in whole embryo culture as a potential source of HSCs generation during the transition between AGM and fetal liver and the contribution of SCF/c-Kit signaling in this process (Sasaki et al., 2010). Interestingly, the inhibition of SCF/c-Kit signaling with ACK2 antibody decreased the transcripts levels of GATA-2, RUNX-1 (essential factors for HSCs establishment) and c-MYBinto placental hematopoietic cluster cells. Furthermore, SCF was shown to be produced by the endothelial cells surrounding placental hematopoietic clusters, suggesting their involvement in paracrine stimulation of HSC through the activation of SCF/kit signaling.

Interestingly, the transition between fetal and adult life is marked by increased requirement for SCF without variation of c-Kit expression level and could be rather partially explained by differential expression of Ink4 gene (Bowie et al., 2007).

3.2.1.2 HSCs maintenance

Loss of c-Kit kinase activity in *W41* mutant adult mice reduces the number of total LT-HSCs into the bone-marrow. Consequently, a 10-fold excess of mutant HSCs was necessary to accomplish a level of reconstitution comparable to wild-type HSCs in competitive transplantation assay. In addition to the loss of LT-HSCs following serial transplantation, these results evidence a major defect of self-renewal in *W41* mice. Cell cycle analysis revealed increased proportion of S/G2/M and decreased proportion of quiescent LT-HSCs in *W41* mice (Thoren et al., 2008). This study establishes the crucial role of c-Kit in the maintenance of LT-HSCs in steady state conditions. Similarly, the depletion of SHP-2, a protein activated by c-Kit signaling, also caused a decrease of bone marrow cellularity and major reconstitution defects in competitive reconstitution assay, as well as cell cycle deregulation. SHP2 -/- HSCs defect was associated with decreased expression of c-Kit. c-Kit expression was dependent on GATA-2 binding on its promoter, SHP-2 phosphatase activity, as well as PI3K and STAT-3 activation. Interestingly, this study reveals the existence of a kinase/phosphatase/kinase axis essential for HSCs maintenance (Zhu et al., 2011).

Consistent with the demonstration of HSCs heterogeneity, HSCs sorting upon c-Kit expression levels revealed the association between low levels of c-Kit protein and the quiescent state of HSCs (Matsuoka et al., 2011), suggesting that the above mentioned study describes a prevalent c-Kit^{Low} population. Furthermore, c-Kit^{Low} HSCs were responsible for the generation of HSCs with higher expression of c-Kit, the former displaying more powerful and sustained repopulation ability over serial transplantation assay, suggesting the retention of self-renewal ability by c-Kit^{Low} HSCs population on the contrary to their HSCs c-Kit^{High} progeny (Grinenko et al., 2014). Additionally, the transition from c-Kit^{Low} to c-Kit^{High} population was inhibited by the inhibitor of c-Kit signaling c-CBL (Shin et al., 2014b), confirming the requirement of c-Kit signaling activation for the generation of highly proliferative HSCs.

3.2.1.3 HSCs maintenance through the niche

SCF contributes to HSCs maintenance into their niche. The conditional depletion of SCF induced an important decrease in bone marrow and spleen cellularity and HSCs frequency. When using reporter mice for SCF expression, its production was mapped principally to endothelial and mesenchymal cells into the bone marrow. The maintenance of HSCs was independent of intrinsic cues and the conditional depletion of SCF specifically from the endothelial and perivascular cells lineage, on the contrary to the osteoblastic lineage, reproduced the defects in HSCs observed in SCF depleted mice(Ding et al., 2012). This study suggests the importance of SCF produced by the niche cells in the maintenance of HSCs. Interestingly, the matrix metalloproteinase MMP-9 was found to be responsible for the cleavage of membrane-bound SCF and its release by stromal cells. The depletion of MMP-9 delayed the response to myeloablative injury addressed by the percentage of HSCs in S phase of cell-cycle, thus suggesting the importance of soluble SCF in HSCs function during the response to injury (Heissig et al., 2002).

3.2.2 SCF/c-Kit role in bipotent MEP

Few studies specifically investigated the role of c-Kit during the amplification of erythro-megakaryocytic (E/MK) bipotent progenitors.*Ex-vivo* progeny analysis of murine HSCs (LSK CD150+) expressing different levels of c-Kit revealed that c-Kit^{High} HSCs generate an increased proportion of bipotent E/MK progenitors (preMegE) and unipotent megakaryocytic progenitors (MkP), but equivalent number of myeloid progenitors (preGM) when compared to c-Kit^{Low} HSCs. Theselective and level-dependentrole ofc-Kit during the generation of bipotent E/MK progenitors was further confirmed by comparing the progeny of sorted c-Kit^{High} and c-Kit^{Low} LSK populations transplanted into lethally irradiated mice(Shin et al., 2014b). Furthermore, transgenic mice harboring c-Kit $^{V558\Delta;\ T669I}$ gain-of-functionmutations show a selective increased frequency and number of bipotent MEPs, without significant changes in the proportion of pluripotents CMPs and bipotents GMPs (Deshpande et al., 2013). These results evidence the positive role of c-Kit in the amplification of bipotents MEPs.

3.2.3 SCF/c-Kit role in erythropoiesis

SCF/c-Kit signaling is crucial for normal erythropoiesis as evidenced by severe anemia in mice harboring homozygous mutations on *kit*(Antonchuk et al., 2004) or *Sl*(Rajaraman et al., 2002)locus. Based on physical and functional interactions between c-Kit and EPO-R, SCF and EPO act in synergy to stimulate the proliferation and survival of erythroid progenitors(Munugalavadla and Kapur, 2005). Moreover, SCF/kit signaling inhibits erythroid differentiation and downregulation of c-Kit constitutes a critical step for terminal differentiation.

Convergent studies argue for the pro-survival role of c-Kit during erythroid cells amplification. For instance, cytokines starvationinducedapoptosis of erythroid progenitors, generated *in-vitro* from human peripheral blood CD34+, can be partially rescued by SCF alone. SCF-induced survival of erythroid progenitors was cancelled by treatment with SFK inhibitor PP-2, which also induced a decrease of AKT activity (Endo et al., 2001). Similarly, SCF is able to suppress cell death of human primary erythroid progenitors induced by Fas-L mimetic molecule (CH11) and allowstheir expansion in a SFK dependent manner. Notably, the SFK member has been identified as Lyn which activity is induced by co-stimulation with both EPO and SCF (Nishio et al., 2001). Interestingly, co-stimulation of murine erythroid cells GIE-ER2 (erythroblastic cell line with inducible expression of GATA-1) by SCF and fibronectin peptide containing α4β1 integrin binding site allows their survival in an AKT and Bcl-xL dependent manner. In contrast, co-stimulation by SCF and fibronectin containing α5β1 integrin binding site allows their expansion through the sustained activation of FAK (Focal Adhesion Kinase) and ERK pathway(Kapur and Zhang, 2001), thus indicating that survival versus proliferation effect of SCF can be modulated by integrin signaling.

SCF is particularly important during stress erythropoiesis by allowing the massive expansion of stress erythroid progenitors in cooperation with EPO, BMP4 and hypoxia (Perry et al., 2007). Stress erythropoiesis resembles fetal erythropoiesis, notably through the re-induction of fetal hemoglobin expression. SCF/c-Kit signaling is also implicated in the re-expression of fetal hemoglobin during stress erythropoiesis as shown in sickle cell anemia (Miller et al., 1992)or in β-thalassemia(Gabbianelli et al., 2008). A recent study performed on human primary erythroid progenitors suggests that the induction of ϒ-globin expression by SCF relies on the repression of COUP-TFII repressor in an ERK-1/2 dependent manner(Aerbajinai et al., 2009). Interestingly, c-Kit expression was found to be lower in erythroid progenitors

generated by human CD34+ cells derived from peripheral bloodthan from cord blood. This decrease in c-Kit expression was also positively correlated with the decrease in fetal hemoglobin expression and inversely correlated with the expression of its inhibitor miR-221 (Gabbianelli et al., 2010). Taken together, these data indicate a dose-dependent contribution of SCF/c-Kit signaling to the expansion of erythroid progenitors and re-expression of fetal hemoglobin mediated at least partially through the activation of ERK pathway.

3.2.4 SCF/c-Kit role in megakaryopoiesis

Mice harboring partial loss-of-function mutations of c-Kit (Antonchuk et al., 2004)or SCF (Zsebo et al., 1990)or even inducible SCF gene deletion (Ding et al., 2012)present only discrete decrease or no alteration of platelets count in peripheral blood. However, both *Sl/Sl* and c-Kit *Wv/+*mutant mice fail to induce stressthrombopoiesis following 5FU treatment(Hunt et al., 1992). Accordingly, homozygous c-Kit mutant mice*Wv/Wv* display a drastic decrease of megakaryocytic progenitors' number in the spleen, but not into the bone marrow (Antonchuk et al., 2004). Thus, the majority of data indicate that SCF/c-Kit signaling is not required for steady state thrombopoiesis, while they clearly state its contribution to the amplification of megakaryocytic progenitors in stress conditions. Furthermore, numerous studies showed that SCF and TPO synergizes during the amplification of megakaryocytic progenitors *ex-vivo* (Reviewed in (Lee et al., 2014)).

3.3 c-Kit and hematological diseases

c-Kit activating mutations are involved in several hematological neoplasms as being the major cause of mastocytosis and the most frequent secondary mutations found in AML.

3.3.1 Mastocytosis

Mastocytosis is almost invariably due to c-Kit activating mutations (reviewed in (Soucie et al., 2015)). Mastocytosis is characterized by the deregulated proliferation and accumulation of mast cells in various organs and by the release of mast cell mediators. On the contrary to other hematologic lineages, the mast cell lineage is characterized by the maintenance of c-Kit during differentiation and SCF/c-Kit signaling is essential for survival and maturation of mast cells. Most of somatic c-Kit mutations in sporadic cases of mastocytosis in adult map to the kinase domain (D816V, D816Y and D820G) and promote ligand independent auto-

phosphorylation. Familial mastocytosis may occur in the absence of c-Kit mutations, while half of typical pediatric patients harbor an activating mutation on residue 839 (Longley et al., 1999). Mastocytosis affecting the dermis can also imply high dosage of soluble SCF (de Paulis et al., 1999), probably due to excessive cleavage of the membrane-bound isoform (Longley et al., 1993) (Reviewed in (Orfao et al., 2007)). Importantly, the c-Kit D816V mutation conferred significant growth advantage when associated with the loss of TET-2 DNA demethylating protein in murine mast cells derived from bone marrow (Soucie et al., 2012).

3.3.2 Acute Megakaryoblastic Leukemia (AMKL)

c-kit is the most frequently mutated RTK in AML (Acute Myelogenous Leukemia), wherein in most of cases it contributes to the deregulation of myeloblasts proliferation (Reviewed in (Malaise et al., 2009)).

AMKL is a heterogeneous subtype of AML and can be sub-classified into two main groups: a first group associated with Down-syndrome transient myeloproliferative disease and AMKL caused by the expression of a truncated GATA-1 protein (GATA-1s) and a second group associated with chromosomal translocation t(1;22)(p13;q13) resulting in the expression of the fusion protein OTT-MAL (Reviewed in(Shimizu et al., 2008)).

c-Kit mutations are rarely found in AMKL but aberrant regulation of GATA-1 target genes can affect c-Kit expression level. The proliferation of 6133 cells established from a murine model of AMKL with OTT-MAL fusion protein is dependent on SCF (Mercher et al., 2009)while its inhibition by IKAROS is associated with strong decrease of c-Kit expression (Malinge et al., 2013). Similarly, proliferation and survival of the cell line ZPAM, established from human patient presenting GATA-1s short isoform, were dependent on SCF and ERK activation, whereas SCF withdrawal caused apoptosis (Toki et al., 2009). These results suggest positive effect of SCF/c-Kit on megakaryoblastic proliferation without providing evidence for causative role of c-Kit signaling activation in the induction of AMKL.

4 TPO/c-MPL signaling pathway

c-MPL receptor is mainly expressed in HSCs and megakaryocytic cells. Through activation by its specific ligand thrombopoietin (TPO), c-MPL signaling mainly contributes to the maintenance of HSCs, as well as to the specification of megakaryocytic progenitors and the stimulation of their maturation into platelets.

4.1 c-MPL receptor and TPO ligand

4.1.1 The ligand Thrombopoietin

TPO was identified in the 50s as the humoral substance allowing the increase of platelets count into the peripheral blood. Numerous attempts to purify the protein failed, until the discovery of its receptor c-MPL in the 90s. The use of either affinity column purification (de Sauvage et al., 1994) or functional screening of cDNA librariesallowingc-MPL-dependent growth after transfection (Lok et al., 1994) allowed the purification of TPO and its cloning by different groups in 1994.

4.1.1.1 TPO protein structure and function

Circulating TPO is a secreted acidic glycoprotein produced mainly by the liver andto a less extent by kidneys. TPO is also produced in bone marrow by stromal cells, endothelial cells (Ding et al., 2012) and megakaryocytes (Nakamura-Ishizu et al., 2014a), thus contributing to the HSCs niche modulation.

TPO is a polypeptide of 353 amino-acids (AAs) in humans and 356 AAs in mice. TPO N-terminal domain contains 21 amino-acids corresponding to signal peptide and a conserved extracellular domain with high homology to EPO (Foster and Lok, 1996)**(Figure 20)**. The N-terminal domain forms 4 helices among which the first and forth are essential for the interaction with c-MPL receptor (Pearce et al., 1997). The C-terminal domain is rich in Proline, Serine and Threonine residues and massively glycosylated thereby facilitating the secretion (Linden and Kaushansky, 2000), as well as the stabilization (Elliott et al., 2003) of the protein.

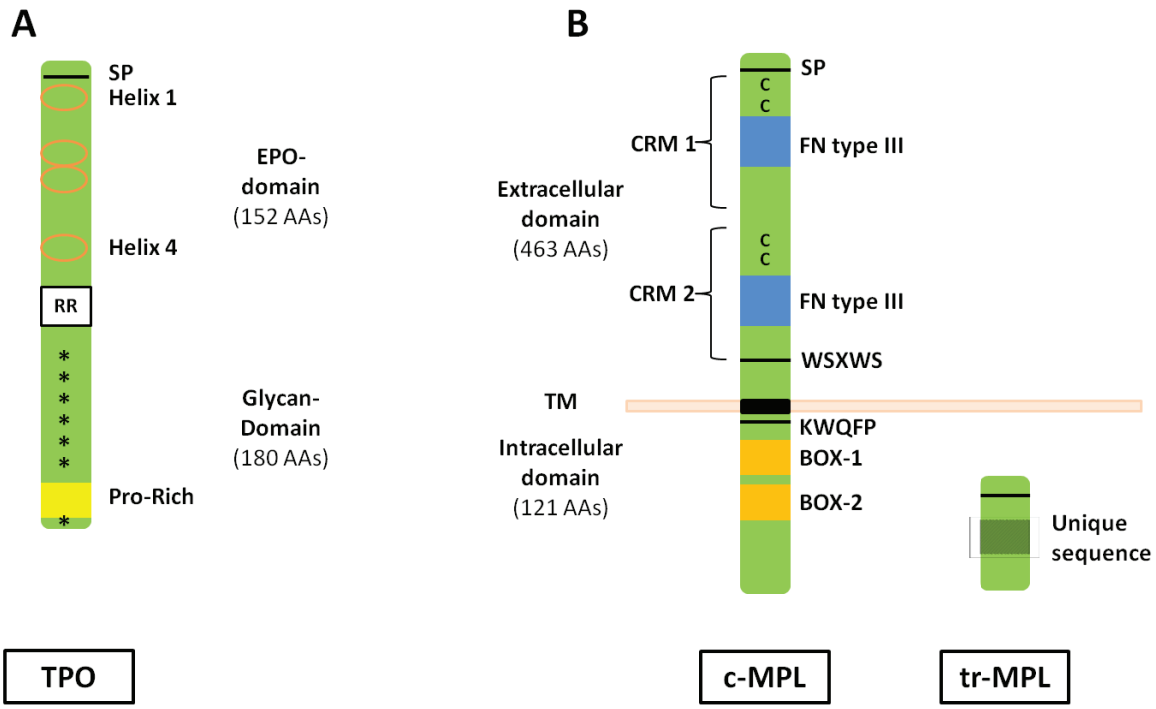

Figure 20: Structure of Thrombopoietin ligand TPO and its c-MPL receptor

A: TPO structure. TPO contains an EPO-domain with a signal peptide and 4 helices. RR: 2 conserved Arginine. The glycan-domain contains multiple glycosylation-modified residues and a Proline-rich domain (yellow box).

B: c-MPL structure and isoforms. The extracellular domain contains a Signal peptide (SP) followed by two Cytokine Receptor Modules (CRM) and a conserved WSXWS. Each CRM contains 2 conserved Cysteine residues (C) and Fibronectin type III domain (Blue box). The transmembrane region (TM) is followed by a conserved pentapeptide KWQFP. The intracellular domain is composed of 2 boxes (orange box). Tr-MPL isoform, generated by alternative splicing, contains a signal peptide and an unique intracellular domain (hatched box).

4.1.1.2 Regulation of TPO levels

The concentration of TPO in normal human serum is approximately95 pg/L in steady state condition. TPO stimulates platelets production and its level increases when platelets number decreases as observed in *mpl* knock-out mice (Gurney et al., 1994). However, this increase in TPO level is not due to increased production, but results from the escape of its capture and degradation by platelets themselves which express high levels of c-MPL receptor on their surface (approximately 30 receptors per platelet) (Broudy, 1997). By this way, platelets mass directly controls TPO level thus allowing the maintenance of platelets homeostasis (Reviewed in (Deutsch and Tomer, 2013)).

4.1.2 The receptor c-MPL

4.1.2.1 c-MPL receptor structure/function

c-MPL polypeptide is 635 AAs long in humans and 625 AAs in mice. c-MPL belongs to the subclass I of cytokine receptors along with EPO-R, GM-CSFR and Interleukins receptors such as IL-3R, IL-5R and IL-9R. As schematized in **Figure 20**, the extracellular domain of 466 AAs (in humans and 457 AAs in mice) is conserved among other members of the family and comprises a signal peptide of 25 AAs and two cytokine receptor modules (CRM). Each CRM is composed of 2 conserved Cysteine residues, a WSXWS motif essential for the interaction with TPO and a fibronectin-rich domain with multiple sites of glycosylation. The transmembrane region of 22 AAs and the juxtamembrane RWQFP motif are important for the maintenance of self-inhibited receptor in the absence of TPO. The intracellular domain of c-MPL of 122 AAs (in humans and 121 AAs in mice)is unique when compared to other members of the family and is characterized by the absence of kinase or phosphatase activity, but rather contains a Pro-X-X-Pro motif into the first box allowing its interaction with JAK kinase. The second box is rich in acidic amino-acids. The C-terminal intracytoplasmic end harbors phosphorylation sites (detailed in signaling cascade part). c-MPL protein is maturated by glycosylation which is important for its expression on the cell surface (Albu and Constantinescu, 2011). Of note, the most usually used annotation of c-MPL residues starts from the first cytoplasmic residue which will be used from herein. The conversion can be performed by the addition of 514 amino-acids.

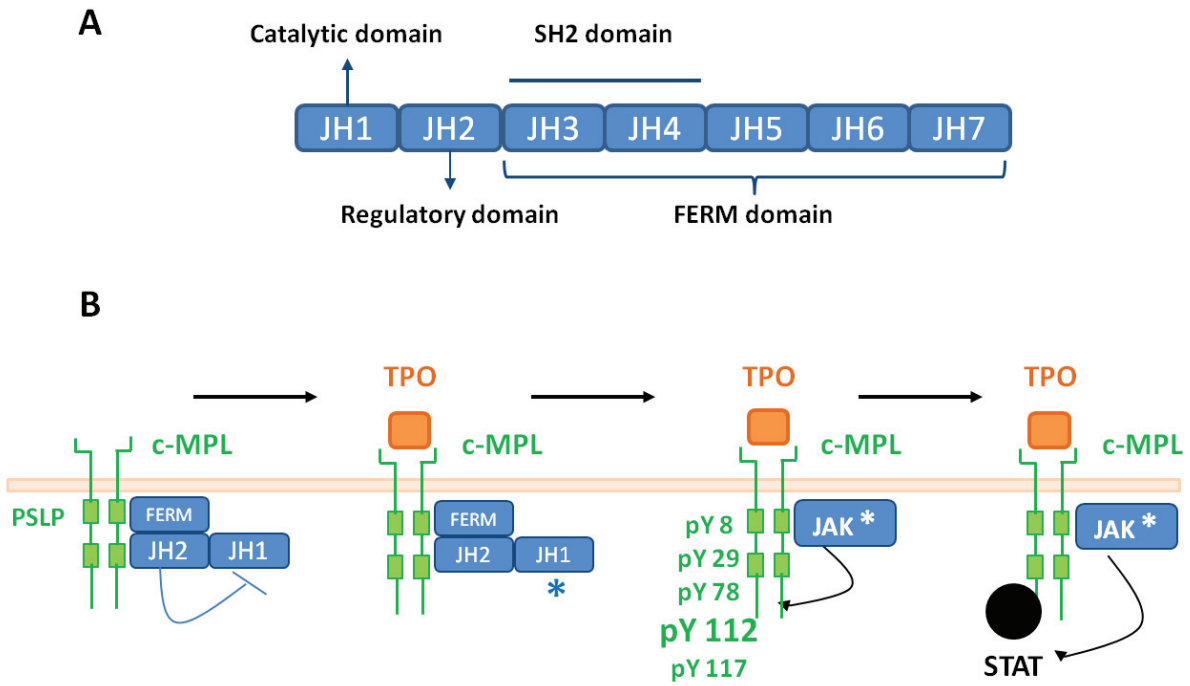

Figure 21: JAK2 structure and activation byTPO/c-MPL

A: JAK family members are composed of 7 JAK Homology domains (JH). The first domain corresponds to the catalytic subunit. JH2 inhibits the activity of JH1 in absence of ligand. The FERM domain (band 4.1/Ezrin/Radixin/Moesin) allows the interaction of JAK with c-MPL receptor on the motif PSLP into the box-1 (Green box). FERM domain contains JH3 and JH4 corresponding to an SH2-type domain allowing the interaction with phosphorylated Tyrosine residues.

B: JAK2 activation. In the absence of ligand, JAK2 is constitutively associated with c-MPL receptor (in green) in its inactive conformation through the tetrapeptide PSLP. TPO (Orange square) interaction with c-MPL allows the activation of JAK2 (star) which in turn phosphorylates c-MPL receptor on different residues (pY), the most important being Y112. STAT proteins (Black circle) are recruited on phospho-tyrosines residues of c-MPL and are activated by JAK2 kinase.

4.1.2.2 c-MPL isoforms

mpl locus encodes several alternate transcripts some of which are specific either of humans or mice. The only conserved isoform between humans (Vigon et al., 1992) and mice (Skoda et al., 1993) encodes a truncated protein called Tr-MPL which contains the signal peptide, lacks the transmembrane region and possess a unique sequence of 30 amino-acids in the cytoplasmic domain. Tr-MPL is retained into the cytoplasm and acts as a dominant negative for the full-length c-MPL by targeting it to lysosomal degradation, resulting in decreased cell growth (Coers et al., 2004).

4.1.3 TPO/c-MPL signaling

4.1.3.1 c-MPL activation

In the absence of ligand, c-MPL is expressed at the cell surface as a homo-dimer and adopts an auto-inhibited conformation with important contribution of the motif KWQFP. Even in the absence of TPO, JAK kinases are constitutively associated with c-MPL through the interaction of their FERM domain with the PSLP motif located in box-1 of c-MPL. In this inactive configuration, kinase activity of JAK (standing into the JH-1 domain) is inhibited by the regulatory domain JH-2 (Reviewed in (Wu and Sun, 2012)) **(Figure 21)**.

Upon TPO binding, c-MPL receptor dimers undergo a conformational shift allowing the close proximity of their two intracytoplasmic domains and subsequent activation of JAK kinases. As c-MPL lacks its own kinase activity, TPO signaling transduction is ensured by this activation of JAK kinases. TPO induces the activation of JAK-2 and TYK-2 JAK family members, though TYK-2 is not essential for TPO signaling (Drachman et al., 1999). Then, JAK-2 induces the phosphorylation of c-MPL on its Tyrosine residues 8, 29, 78, 112 and 117 in the intracytoplasmic domain. Signal transduction takes place mostly through Y112 residue whichfunctions as a docking site for adaptor and signaling molecules. These signaling proteins are alsophosphorylated by JAK-2 kinase (Reviewed in (Kaushansky, 2005)). The three major signaling pathways activated downstream of TPO/ c-MPL are detailed below and illustrated in **Figure 22**.

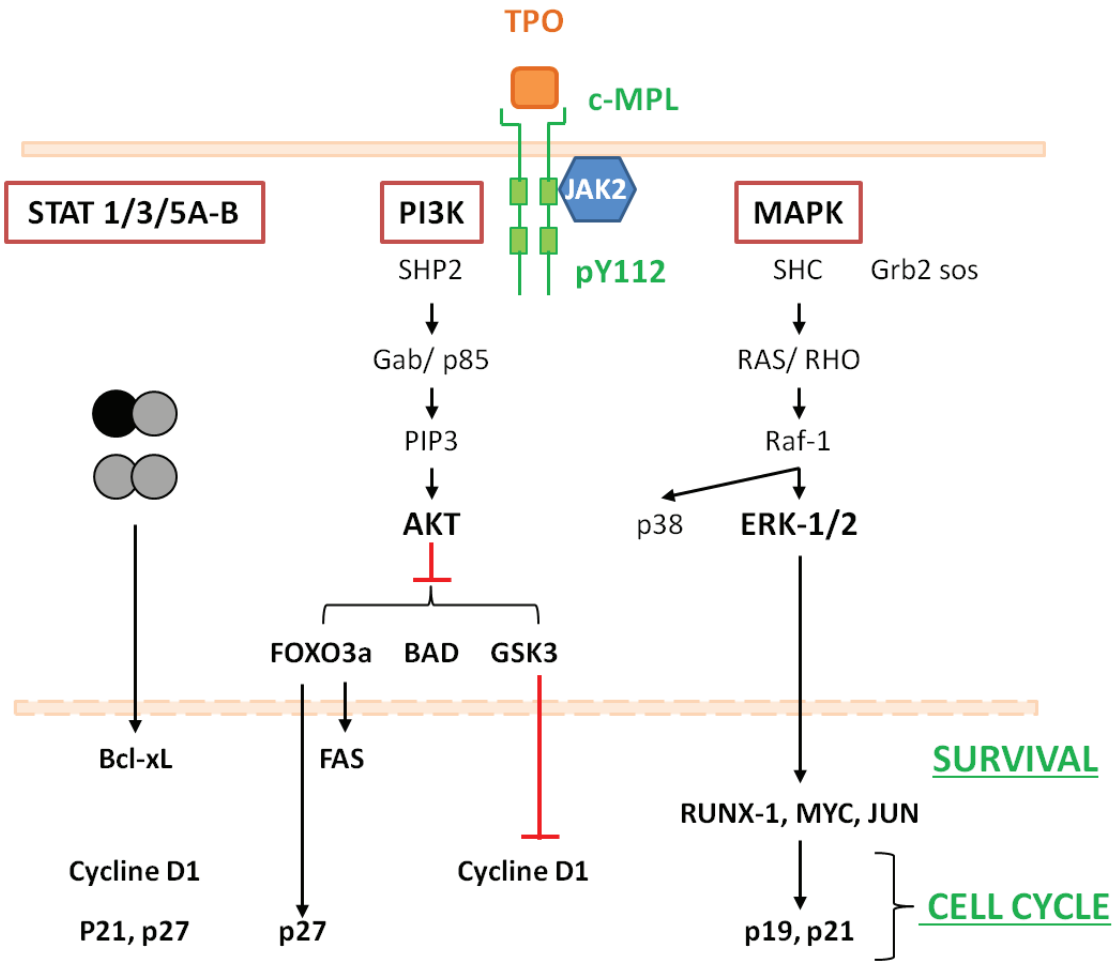

Figure 22: Main pathways activated by TPO/c-MPL

Phosphorylated Tyrosineresidues (here only pY112) of c-MPL receptor function as a docking site for the recruitment of adaptors and signaling molecules. STATs are recruited on c-MPL receptor and activated by JAK-2 allowing their activation and subsequent homo- or hetero-dimerization and nuclear translocation (grey or grey and black circles). STATs dimers then activate the expression of survival gene BcL-xL and cell cycle regulators p21 and p27. Activated SHP2 enhances the formation of p85 (PI3K subunit) and Gab adaptor protein allowing the activation of PI3K and subsequently of AKT kinase. AKT sequestrates FOXO3a transcription factors, BAD and GSK3-β, thus inhibiting the expression of their target pro-apoptotic genes FAS, p27 and Cyclin-D1. The adaptor complex SHC/Grb2 recruits GDP exchange factors Sos (Son Of Sevenless) allowing the sequential activation of MAP-Kinases: RAS, Raf-1 and ERK-1/2 as well as p38. ERK-1/2 activates the transcription factors RUNX-1, MYC and JUN allowing the expression of cell cycle regulators such as p19 and p21.

4.1.3.2 Signaling pathways activated by TPO/MPL:

JAK/ STAT pathway

STATs (Signal Transducers and Activators of Transcription) family members are recruited on phosphorylated Tyrosine residues of c-MPL receptor through their SH2 domain and are subsequently activated by JAK-2. Following their homo- or hetero-dimerization, STATs proteins translocate to the nucleus and bind to their target genes allowing their transcription. For example, STATs activation allows the expression of pro-survival Bcl-xL, as well as cell cycle regulators such as Cycline-D or p21, p27. STAT transcription factors also activate the expression of SOCS 1 and 3 responsible for the extinction of TPO/c-MPL signaling.

MAPK pathway

Rapid activation of the MAPK pathway is ensured by SHC (Src homology 2 domain containing)adaptor activationwhich bindsphosphorylated residue pY-122 of c-MPL. SHC activation by JAK-2 allows the recruitment of Grb-2 adaptor and exchange factor Sos,leading to the activation of Ras. Activated Ras activates Raf-1, which in turn activates p38 and ERK-1/2 MAP kinases. ERK-1/2 transcription factors translocate to the nucleus and phosphorylate their substrates notably Elk1, RUNX-1, MYC and JUN allowing their activation and the subsequent expression of cell cycle regulators such as Cycline-D1, c-Myc, p19 INK4 and p21. Noteworthy, slow activation of ERK-1/2 can occur independently of JAK-2 but through its interaction with pY-78 of c-MPL and subsequently to the activation of Rap-1 and B-Raf (Garcia et al., 2001).

PI3K pathway

SHP-2 docked on pY-112 is activated by JAK-2 and enhances the association between Gab adaptor protein and p85 subunit of PI3K allowing its activation. As explained in the chapter on c-Kit signaling transduction, PI3K allows the activation of AKT kinase which in turn phosphorylates several substrates controlling survival and cell cycle progression. Among important AKT substrates, FOXO3a is sequestrated into the cytoplasm allowing the de-repression of p27 and Fas genes transcription, BAD is inhibited inducing the liberation of the pro-survival protein Bcl-2 and GSK-3 is inhibited allowing increased expression of Cycline-D1.

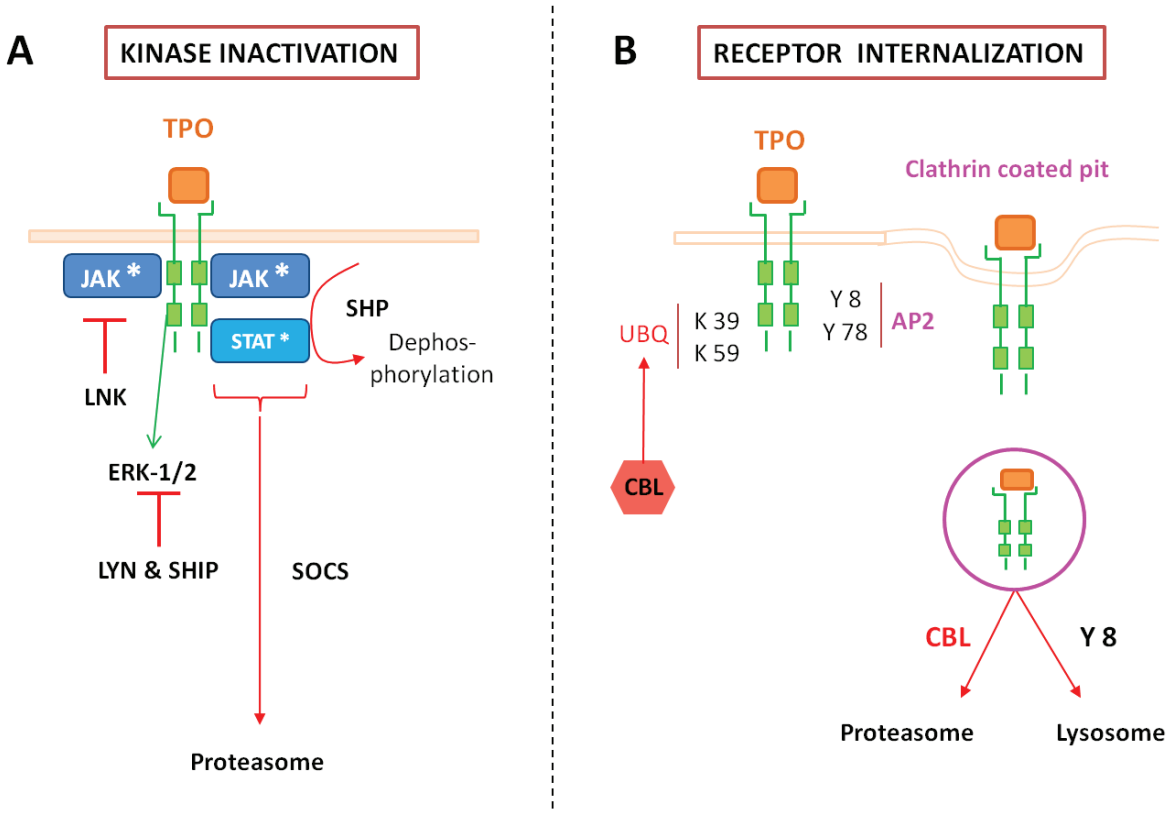

Figure 23: Mechanisms of TPO/c-MPL signaling downregulation

A: Downregulation by kinase inactivation. Kinase inactivation implicates the phosphatase SHP which targets JAK/STAT family members, SOCS proteins which target JAK/ STAT for degradation by the proteasome and the SFKs family members LNK and LYN which inhibit JAK and ERK-1/2, respectively.

B: Downregulation by internalization and degradation. Following c-MPL activation by TPO, c-MPL is ubiquitinylated and the TPO/c-MPL complex is internalized in clathrin-coated pits. CBL mediated ubiquitinylation also contributes to induce c-MPL degradation through the lysosome or proteasome pathways. The phosphorylated tyrosine residues Y8 and Y78 of c-MPL favor its interaction with AP2 and clathrin-dependent internalization of the complex, whereas phosphorylated residue Y8 targets the TPO/c-MPL complex for lysosomal degradation.

4.1.4 TPO/c-MPL signaling downregulation

TPO/c-MPL signaling is downregulated by two different ways: through the inactivation of kinase activity and through the degradation of the complex TPO/c-MPL **(Figure 23)**.

4.1.4.1 Inactivation of kinase activity

TPO stimulation induces the activation of STAT transcription factors leading to the expression of SOCS 1 and 3. SOCS proteins bind directly to the receptor or to the activated JAK and STATs through their SH2 domains and inhibit their activity either by competition or by proteasomoal degradation (reviewed in (Wormald and Hilton, 2004)). JAK-2 kinase activity is also inhibited by phosphatase SHP-1 which binds directly through its SH2 domain. The SFK family member LNK was also shown to inhibit TPO signaling through its binding to JAK-2 (Bersenev et al., 2008).The SFK LYN was shown to inhibit TPO/c-MPL mediated proliferation by inhibiting ERK-1/2, potentially through SHIP phosphatase and without affecting JAK-2 phosphorylation (Lannutti et al., 2006).

4.1.4.2 Internalization and degradation

Rapidly following TPO stimulation, AP-2 interacts with c-MPL receptor on the motifs RRL 8 and 78 of the intracellular domain, recruits Clathrin and induce its internalization. The recruitment of AP-2 on position 8 of intracellular c-MPL targets the receptor for lysosomal degradation (Hitchcock et al., 2008). In parallel, c-MPL can also be ubiquitinylated on its Lysine residues 39 and 59 by CBL inducing its degradation by the proteasome (Saur et al., 2010).

4.2 TPO/c-MPL signaling in the control of hematopoiesis

4.2.1 Role in HSCs function

Initial studies of mice harboring constitutive loss of either *mpl*(Alexander et al., 1996; Carver-Moore et al., 1996) or *thpo*(Carver-Moore et al., 1996) genes revealed a significant reduction of most multipotent and monopotent progenitors,already suggesting the impairment of HSCs function. Since then, several studies have clearly evidenced a role of TPO/c-MPL signaling in early amplification of HSCs during fetal life, as well as in maintenance

KO	Phenotype of HSCs	Phenotype of MK	Ref
Mpl	• Stemness capacity specific to MPL+ cells in murine fetal liver or human bone marrow •Defect in competitive repopulation capacity in murine fetal liver		Solar et al., 1998
Mpl	•Delayed production of HSCs in the AGM •Decreased self-renewal potential of Fetal Liver HSCs and progenitors at different stages		Petit-Cocault et al., 2007
Mpl	•Less CFU-S generated from BM Mpl -/- •Self-renewal defect in competitive BM TR		Kimura et al., 1998
KO Mpl cKit +/Wv	Synergy in Mpl and Kit loss on lesser number of HSCs needed in transplantation in competitive nonablative condition	Thrombocytosis, reduced MK progenitors in the BM	Antonchuk et al., 2004
Mpl TR Δ60 (no Tyrosine residues in cytoplasmic domain)	Reduction in long-term repopulating ability in competitive bone marrow transplantation in Mpl-/- mice also seen at lesser extent in Mpl TR Δ60 mice	Megakaryocytes with reduced ploidy	Tong et al., 2007
Thpo	•Four-fold BM HSC required for radioprotection of irradiated mice •Self-renewal defect quantified by limiting-dilution in secondary recipient cancelled by TPO restoration		Fox et al., 2002
Mpl		Thrombocytopenia with increased TPO serum concentration	Gurney et al., 1994
Thpo		Low number of MK progenitors, decreased ploidy	deSauvage et al., 1996
Mpl KO and transgenic Mpl	HSCs repopulation defect	Thrombocytosis due to increased TPO and JAK2/ STAT 3/5 signaling	Lannutti et al., 2009

Table 4: HSCs and megakaryocytic phenotypes in mouse models of c-MPL or TPO (thpo) knock-out

Each lane of the table indicates in the successive columns: the name of the deleted gene, the main impact either on HSCs quiescence or self-renewal or on megakaryocytic differentiation and the corresponding reference.

of adults HSCs by self-renewal and quiescence (reviewed in (de Graaf and Metcalf, 2011; Deutsch and Tomer, 2013)**(Table 4)**.

4.2.1.1 In fetal life

c-MPL transcripts are already detectable in hematopoietic clusters generated by AGM.Analyses of fetal liver cells showed that stemness activity segregates with c-MPL+ cells and that fetal liver c-Mpl -/- HSCs were unable to engraft into lethally irradiated mice in competitive repopulation assay (Solar et al., 1998). A more recent study performed at different times of development confirmed these results and further showed that c-MPL deficiency delayed the appearance of these defective long-term self-renewing HSCs in fetal liver (Petit-Cocault et al., 2007).

4.2.1.2 HSCs self-renewal

In adult mice, the self-renewal of HSCs is also controlled by TPO/c-MPL pathway. Indeed, loss of c-MPL dramatically reduced the number of CFU-S generated by bone marrow HSCs and impeded their competitiveness for proper long-term reconstitution in irradiated mice (Kimura et al., 1998). Similar defects were observed with HSCs expressing a truncated form of c-MPL which decreases TPO signaling (Tong et al., 2007). Moreover serial transplantation experiments performed in wild type or TPO-/- recipients elegantly confirmed that TPO/c-MPL signaling is required for long term self-renewal of HSCs (Fox et al., 2002). Altogether, these studies conducted in myeloablative conditions suggest a role of TPO/c-MPL in HSCs self-renewal after injury. Interestingly, loss of *mpl* has also been shown to reduce the number of bone marrow cells required for lymphomyeloid reconstitution in non-myeloablative competitive assay, thus confirming functional endogenous HSCs defect. Furthermore, concomitant loss of *mpl* and *kit* function further reduced the number of bone marrow cells required in these non-ablative competitive assays, indicating the cooperation between c-Kit and c-MPL during HSCs homing(Antonchuk et al., 2004).

4.2.1.3 Role in quiescence

Concordant results obtained by loss or gain of function *in vivo* and *ex-vivo* experiments on murine models strongly argue for a positive effect of TPO/c-MPL in maintaining HSCs quiescence and avoiding their exhaustion.

Constitutive loss of TPO induced specific and progressive loss of LT-HSCs from post-natal to adult life, suggesting its importance in HSCs maintenance. This effect was associated with concomitant increase of HSCs proliferation, as evidenced by increased number of BrdU labeled cells, and by reduced proportion of the most quiescent fraction ofHSCs(side-population or Ki-67^{Low} Hoechst^{Low} cells). Excessive proliferation was consistently accompanied by decreased expression of several negative regulatorsof cell cycle such as p57, p21 and p19 (Qian et al., 2007). Similarly, *ex-vivo* HSCs treatment with AMM2 (c-MPL blocking antibody) decreased p57 and p21 expression and increased c-Myc expression counteracting the positive effects of TPO. *In vivo,* AMM2 treatment reduced the number of side population HSC allowing exogenous HSC engraftment without irradiation, while concomitant 5-FU treatment was required for successful engraftment in competitive assay, thus suggesting efficient quiescence exit. Furthermore, quiescent HSCs were shown to reside in c-MPL+ sub-fraction, whereas their shift into proliferation reduced the percentage of c-MPL+ HSCs and p57 expression into the bone marrow. The quiescence of c-MPL+ HSCs requires their physical proximity with the osteoblastic niche which produces TPO(Yoshihara et al., 2007). Altogether, these results establish the implication of TPO/c-MPL signaling in the maintenance of long-term quiescent HSCs population.

Interestingly, the continuous injection of low dose of TPO in normal mice induced transient increase in quiescent over non-quiescent proportion of LSK HSCs after 4 days due to preferential survival of c-MPL+ cells, whereas one-time injection of high dose of TPO increased HSCs proliferation as soon as 2 days after treatment (Yoshihara et al., 2007). This latter study highlights the duality of the implication of TPO in fine-tuning the proliferation/quiescence balance of HSCs.

4.2.1.4 Role in DNA repair

A recent study evidenced the positive effect of TPO/c-MPL signaling on the protection of murine LSK from DNA damage and chromosomal abnormalities accumulation during recovery from irradiative stress on the long-term (de Laval et al., 2013). Indeed, irradiation induces DNA double strand breaks (DSB) in LSK from normal mice and the proportion of LSK cells harboring DSB increases in *mpl* -/- mice or in LSK cultured *in vitro* in absence of TPO. Irradiation-induced DSB in WT LSKwas canceled by TPO injection *in-vivo* or TPO addition *ex-vivo* and correlated with TPO-mediated enhancement of DNA repair efficiency by NHEJ (Non-

Homologous End Joining) mechanism. TPO protective role was also observed when analyzing chromosomal abnormalities in metaphasic LSK. Interestingly, loss of c-MPL induced the persistence of DSB induced by irradiation in LSK with aging. Furthermore, LSK cells derived from irradiated c-Mpl -/- mice failed to reconstitute LSK population in secondary lethally irradiated recipients in competitive assay. In contrast, TPO pre-treatment of wild type donor mice before irradiation enhances bone marrow chimerism obtained by LSK in competitive transplantation. This protective effect was specifically observed 4 months after transplantation, thus evidencing long-term protection of HSC. Noteworthy, TPO protection mainly concerned immature CD34- cells and could not be explained by enhanced LSK proliferation or quiescence.

A second study (de Laval et al., 2014) evidenced that TPO protective effect during NHEJ repair of irradiation-induced DSB was dependent on the formation of a ternary complex of DNA-PK (the catalytic subunit responsible for NHEJ) with ERK-1/2 and Iex1 (early actor of DNA-repair) which are transcriptionally activated in response to TPO.

4.2.2 Role in erythropoiesis

Some studies suggest a positive effect of TPO on erythrocytic progenitors' production. Infection of mice by mpl-transducing-retrovirus induces massive infiltration of erythroblasts in spleen and liver, causing hepatosplenomegaly and death (Cocault et al., 1996). The injection of TPO (Kaushansky et al., 1995) or the transplantation of TPO-treated (Fibbe et al., 1995) or mpl-transduced bone marrow cells (Yan et al., 1999)into irradiated mice accelerated red-blood cells recovery. The decrease of RBC in double mutant mpl -/- *kitWv*mice when compared to simple mutants (Antonchuk et al., 2004) suggest the synergy between TPO and SCF on erythroid cells production. However all these effects might be due to the expansion of bipotent or multipotent progenitors rather than specific effect on erythroid progenitors(Carver-Moore et al., 1996). Interestingly, the combination of TPO and SCF rescued the production of erythroid colonies by EPOR-deficient fetal liver cells (Kieran et al., 1996). TPO was also shown to stimulate the development of erythroid colonies derived from human peripheral blood mononuclear cells, but this stimulating effect was only observed in the presence of serum and was inhibited by either EPO or EPO-R antibodies (Liu et al., 1999). On one hand, TPO does not seem to be able to bind EPO-R. Indeed, radio-labeled TPO did not label human erythroblasts and excess of TPO failed to compete for EPO

binding to EPO-R in BaF-3/EPO-R cells (Broudy et al., 1997). On the other hand, BaF-3/EPO-R cells were shown to survive and to proliferate in the presence of TPO alone despite the absence of c-MPL expression. Intriguingly, the survival of BaF-3/EPO-R cells in TPO alone was strongly decreased by siRNA mediated knock-down of EPO-R (Rouleau et al., 2004). Taken together, these data suggest that TPO is able to mediate c-MPL-independent survival and proliferation of erythroid progenitors in EPO-R dependent but EPO-R binding-independent manner.

4.2.3 Role in megakaryopoiesis

4.2.3.1 Role in normal megakaryopoiesis

Both TPO -/- and c-MPL -/- mice show severe thrombocytopenia**(Table 4)**. Surprisingly, a recent study reported that mice harboring conditional deletion of c-MPL targeted only on megakaryocytes and platelets (induced by Cre recombinase expression driven by pf-4 promoter) paradoxically display megakaryocytosis and thrombocytosis (Ng et al., 2014). The excess of megakaryocytes and platelets could derive fromthe markedlyamplifiedc-Mpl expressing myeloid progenitors or LSK stem cells. Supporting this interpretation, LSKs fromc-Mpl pf-4 mice display a strong transcriptome signature indicative of TPO/c-MPL signaling activation, whereas paradoxically their circulating TPO levels are not increased. This study confirms that massive platelets production can readily occurwithout TPO and suggests the unexpected role of platelets and megakaryocytes in limiting available TPO to avoid the amplification of c-MPL-expressing myeloid progenitors.

4.2.3.2 Downstream signaling pathways involved in the dual role of TPO during the control of megakaryopoiesis

TPO/c-MPL signaling stimulates expansion, maturation and polyploidization of megakaryocytes. One intriguing but still unresolved question is whether the specific changes downstream ofTPO signaling can explainitsdual effects.

TPO/c-MPL signaling activates JAK2, STAT1, STAT3, STAT5-A and STAT5-B in megakaryocytic cells. Overexpression of a dominant negative mutant of STAT3 induced a decrease of megakaryocytic progenitors and platelets recovery after 5FU treatment while platelets count remained unaffected, suggesting the role of STAT3 in stress

megakaryopoiesis (Kirito et al., 2002). STAT5-A/-B knock-out mice display thrombocytopenia, but also overall defects of HSCs function (Snow et al., 2002). In contrast, STAT-1 knock-out mice show defective polyploidization of megakaryocytes thus indicating a specific requirement of STAT1 for megakaryocytic maturation(Huang et al., 2007)

Several other studies indicate that the duration and intensity of MAP kinase activation are important parameters to control the balance between proliferation and differentiation. Indeed, sustained activation of ERK-1/2 by Rap1 and B-Raf induces the expression of Elk-1 and is required for megakaryocytic maturation of UT7/c-MPL cells (Garcia et al., 2001). Similarly, sustained activation of ERK-1/2 by TPA or by forcing constitutively active MEK expression induced megakaryocytic differentiation of human K62 cells. Conversely, weak activation of ERK-1/2 induced by a mutant form of c-MPL lacking residues 71 and 94 on the intracytoplasmic domain in UT7/c-MPL cell line, or transient ERK1/2 inhibition by Bryostatin inhibited megakaryocytic differentiation (Rouyez et al., 1997)(Racke et al., 1997). Even though the latter studies performed in cell lines suggest the importance of sustained MAPK activation for differentiation, studies performed with primary cells reported contradictory results.

On one hand, TPO stimulation of cord blood CD34+ human progenitors induced strong activation of MAPK inducing megakaryocytic differentiation. Decreased activation of MEK and ERK-1/2 obtained by inhibition of MEK with low dose of PD-098059 increased the proliferation of megakaryocytes and delayed their differentiation, as attested by the increased proportion of blasts and immature CD34+ CD41+ CD42b- cells (Fichelson et al., 1999). On the other hand, the treatment of a pure megakaryocytic populationderived this time from peripheral blood CD34+ human progenitorswith the same dose of the same MEK inhibitor weakly inhibiting MEK and ERK1/2,leads in contrast to increased megakaryocytic polyploidization. Furthermore,the increased polyploidization was associated with strong increase of PI3K activation and was suppressed by rapamycin treatment (targeting mTOR). Thus, this study rather strongly suggests the pivotal role of the axis AKT/mTOR/S6K as the major actor of megakaryocytic polyploidization (Guerriero et al., 2006).

JAK2 activation level was also recently proposed as another important actor which controls the switch between megakaryocytic proliferation and terminal differentiation. Indeed, analyses of several spontaneously emerging sub-clones of UT7/c-MPL cells which proliferate instead of differentiate in the presence of TPO, revealed a systematic decrease of

JAK2 and c-MPL expression. Further experiments revealed that the restoration of megakaryocytic differentiation could be obtained by enforced expression of either JAK2 or c-MPL. Conversely, the stimulation by low dose of TPO or the treatment with low doses of JAK2 inhibitor allowed the proliferation of UT7/c-MPL cells. Importantly, low doses of JAK2 inhibitor was also shown to increase the number of megakaryocytes generated by human CD34+ progenitors cells *ex vivo,* as well as to increase the number of platelets in injected mice *in vivo*(Besancenot et al., 2014).

4.3 Pathological TPO/ c-MPL deregulation in the megakaryocytic lineage

Activating mutations of *mpl* are associated with myeloproliferative neoplasms (MPN) and hereditary thrombocytopenia (HT), whereas c-MPL loss of function is associated with congenital amegakaryocytic thrombocytopenia (CAMT).

In the case of MPN affecting the megakaryocytic compartment, *mpl* mutations are associated with 5% of essential thrombocytemia (ET) and 1% of primary myelofibrosis (PMF), whereas JAK2 constitutive activation is found in 50% of these two types of MPN. The most common c-MPL mutation is a substitution at the residue W515 which affects the juxtamembranar motif KWQFP, thus inducing receptor activation in the absence of TPO and subsequent activation of intracellular signaling. The transduction of irradiated mice with infected bone marrow cells harboring W515 mutation induced splenomegaly, increased expansion of megakaryocytic progenitors into the spleen and platelets count (Malinge et al., 2008). In the context of PMF and ET associated with JAK2 V617F and MPL W515 mutations, JAK2 and c-MPL expression was found decreased, whereas MPL expression was found increased in ET without any of these mutations.

In the case of hereditary mutations of *mpl*, a recent study investigated the effect of 3 mutations affecting the domain of interaction with TPO and proposed different mechanisms: P106L gain-of-function mutation is retained in the cytoplasm and able to induce cytokine-independent proliferative signals, whereas loss of function mutation F104S is still expressed at the cell surface but lose the capacity of activation by TPO and the R102P loss of function mutant form harbors defective glycosylation, cell-surface expression and dimerization ability (Stockklausner et al., 2015).

5 Tetraspanins

5.1 General presentation of tetraspanins family

Tetraspanins superfamily (TM4SF) comprises about 30 members and has been implicated in various physiological processes, including cell motility, adhesion and fusion, as well as tumor progression and metastasis (Reviewed in (Lazo, 2007)). Tetraspanins are cell surface proteins with 4 transmembrane regions, one intracellular and two extracellular loops. On the cell surface, tetraspanins are unable to transduce intracellular signaling, but rather dimerize between each other or with different members of the family and cluster, thus forming membrane specialized micro-domainswherein they provide a scaffold for receptors and signaling molecules assembly.

5.2 Tetraspanins in hematopoiesis

Tetraspanins CD9, CD63, CD81, CD82, CD151 are expressed in hematopoietic tissues. Some of them were shown to play a role in lymphocytes B and macrophages function(Lazo, 2007). Interestingly, CD9 is increasingly expressed during terminal megakaryocytic differentiation and preferentially expressed in a specific subset of HSCs displaying erythro-megakaryocytic lineage bias and being mostly in a quiescent state (Guo et al., 2013).

5.2.1 Regulation of HSCs engraftment and quiescence by tetraspanins CD9, CD81 and CD82

Several studies reported the contribution of some tetraspanins family members to HSCs homing and maintenance. For instance, CD9 transcripts were found to increase in human cord blood CD34+ HSCs exposed to SDF-1 stimulation *ex-vivo*. In addition, sorted CD34+ expressing low levels of CD9 are associated with decreased engraftment capacity into the bone marrow and spleen of sublethally irradiated NOD/SCID mice, when compared to total CD34+ HSCs (Leung et al., 2011).Likewise, whereas quiescent CD34+ HSC are associated with polarized expression of CD82 at the cell membrane, this polarized expression of CD82 is lost in cycling human G-CSF mobilized stem and progenitor cells (HSPCs) suggesting a positive role of CD82 in the maintenance of quiescence and homing capacity of HSPCs (Larochelle et

al., 2012). Additionally, Cd81 -/- HSC showed a marked engraftment defect when transplanted into secondary recipient mice and a significantly delayed return to quiescence when stimulated to proliferate with 5-fluorouracil (5-FU). As observed for CD82, CD81 proteins formed a polarized patch when HSCs were returning to quiescence. Complementary experiments further showed that the clustering of CD81 actually induced a decrease in AKT activity allowing nuclear translocation of FOXO-1a and subsequent increase of p19 and decrease of Cyclin-D1, thus at least partially explaining cell cycle exit(Lin et al., 2011).

These data suggest the contribution of tetraspanins in the maintenance of functional HSCs during homeostasis, as well as HSCs homing, re-entry into quiescence and self-renewal following injury.

5.2.2 Modulation of c-Kit response to SCF by CD9

Another interesting study suggests the regulation of c-Kit activation in response to SCF by CD9 (Anzai et al., 2002). c-Kit was found physically associated with several tetraspanins including CD9, CD63 and CD81 at the cell surface of Mo7e cell line. The colocalization of c-Kit and CD9 in Mo7e cells and c-Kit and CD81 in CD34+ cord blood progenitors was also observed by immunofluorescence. Co-immunoprecipitation assays further confirmed the direct interaction of c-Kit with CD9 and its indirect interaction with CD63 and CD81. Interestingly, in contrast to its unbound fraction, the fraction of c-Kit associated with CD9 was found to be slightly phosphorylated, but lacked kinase activity and was not activated or internalized in response to SCF stimulation. This study thus indicates that CD9 is able to physically interact with c-Kit and to alter its activity and turnover.

Main justification of my project

Even under stable environments, every type of progenitor only divide a limited number of times before irrevocably engaging into terminal differentiation thus suggesting the existence of intrinsic mechanisms or internal clocks controlling the balance between proliferation and differentiation. One of the main interests of our team is to understand the molecular mechanisms underlying these internal clocks using murine bipotent erythro-megakaryocytic progenitors (MEP) as a model system. Indeed, MEP are highly unstable progenitors and very rapidly commit into monopotent erythrocytic or megakaryocytic progenitors which themselves again only divide a limited number of times before terminal erythrocytic or megakaryocytic differentiation. Moreover, after commitment towards megakaryocytic lineage, thrombopoietin (TPO), the main cytokine controlling megakaryopoiesis, is involved in both proliferation and terminal differentiation raising the additional question of the mechanisms responsible for this intriguing dual function. One of the strategies developed in the team to address these questions has been to use Notch pathway activation as a molecular tool to modulate some parameters of these internal clocks controlling proliferation/differentiation balance and by this way try to understand how they work. First results indeed established that Notch pathway stimulation is actually able to increase the number of MEP divisions without losing their bipotency. More recently, we found that Notch pathway stimulation is also able to increase the number of divisions of committed megakaryocytic progenitors at the expense of their terminal differentiation. In that context, the main initial purpose of my work was to try to decipher the mechanisms by which Notch pathway sustains bipotency and favors the proliferation of megakaryocytic progenitors at the expense of their terminal differentiation.

Specifics aims and working hypotheses

1- Notch pathway and control of bipotency: testing the role of GATA1-levels

Previous results of the team established that the mutually exclusive erythro-megakaryocytic commitment of MEP mainly relies on functional cross-antagonism between Fli-1 and EKLF transcription factors which compete for limited amounts of the same partner GATA-1. Based on this functional antagonism, we hypothesized that Notch pathway might

lower the competition between Fli-1 and EKLF either by increasing GATA-1 levels or by modifying its phosphorylation state. The first specific aim of my work has been to test this hypothesis by studying the effect of Notch on the expression and phosphorylation of GATA-1 transcription factor in the murine megakaryoblastic cell line L8057.

2- Notch pathway and control of the proliferation/differentiation balance: deciphering mechanisms of c-Kit regulation

Other results of the team have shown that the stimulating effect of Notch pathway on MEP proliferation was strictly SCF-dependent and associated with increased expression of c-Kit receptor thus indicating that c-Kit regulation is a critical determinant in the control of proliferation/differentiation balance. Based on these results and the known functional duality of TPO, the second aim of my work was thus to determine the molecular mechanisms controlling the expression of c-Kit by Notch and TPO at both transcriptional and protein levels. For that purpose, I choose to conduct this study using G1ME cells which results from the spontaneous immortalization of GATA-1 deficient bipotent erythro-megakaryocytic progenitors and which proliferation depends on TPO only. The main results of this study concern the unexpected contribution of c-Kit to the TPO-dependent proliferation as well as the unexpected down regulation of c-Kit by the late megakaryocytic maker CD9. These results lead us to propose a new model explaining the functional duality of TPO through the dynamic regulation of c-Kit signaling.

RESULTS

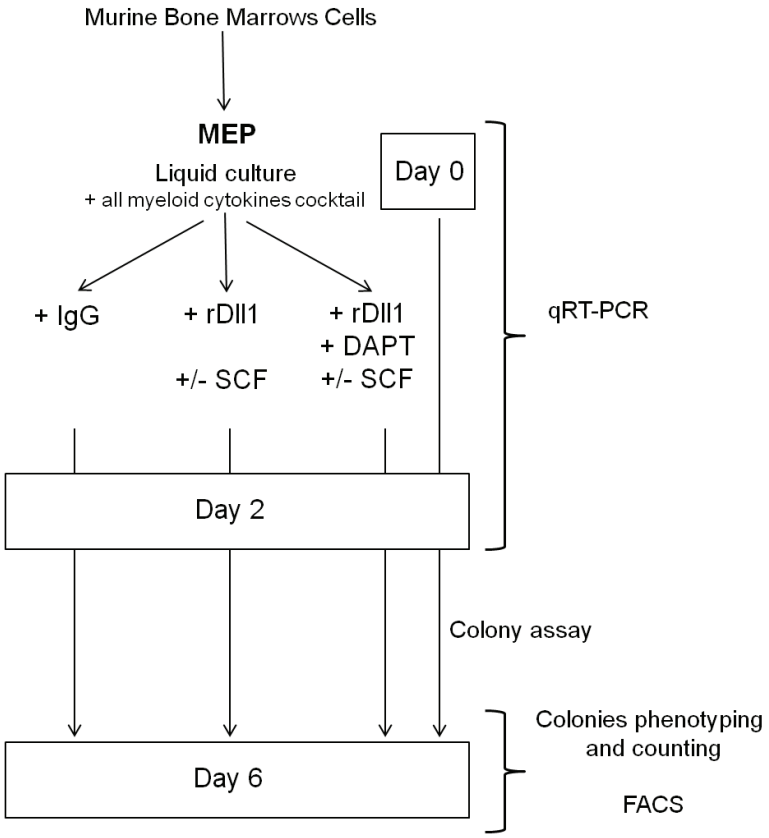

Figure 1: Schematic presentation of the protocol used to study the effect of Notch signaling on the proliferation and differentiation of MEP

Bipotent E/MK progenitors (MEP) are purified from murine bone marrow cells suspension by flow cytometry and seeded in liquid culture in presence of a full cocktail of myeloid cytokines (EPO, TPO, IL-3, IL-6, IL-11, GM-CSF and Flt-3L) either on control IgG or on recombinant Notch ligand rDll1 in presence or absence of Notch inhibitor DAPT with or without SCF. Freshly purified MEP (day 0), as well as their progeny generated following two days in liquid culture are either harvested for qRT-PCR analyses or seeded in semi-solid medium from which we quantified the number of mixed, erythrocytic and megakaryocytic colonies generated. Alternatively, MEPs are maintained 6 days in liquid cultures before cells counting and analysis of c-Kit expression by FACS.

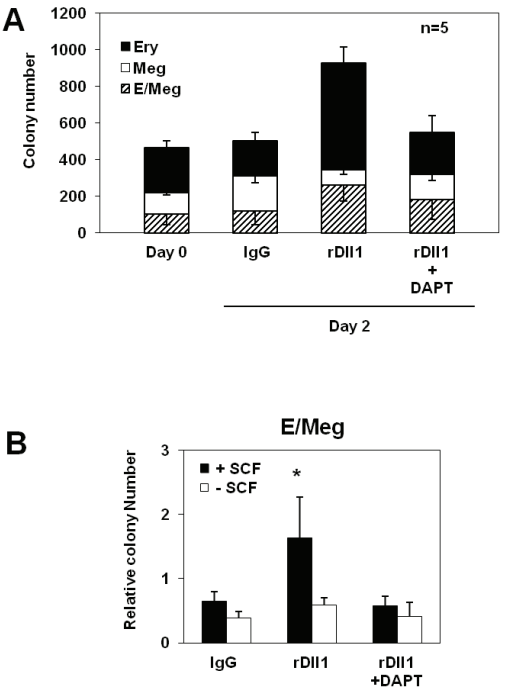

Figure 2: Notch signaling stimulates bipotent progenitor's amplification in a SCF-dependent manner

A: Progenitors present in sorted MEP populations before (Day 0) or after a two days liquid culture on either IgG or rDll1 (with or without DAPT) were numbered by colony assay as described in Figure 1. Results are presented as piled histograms showing the numbers of the different types of colonies (mixed, erythrocytic or megakaryocytic) generated from untreated cells (Day 0) and after a two days culture on IgG, rDll1 or rDll1 + DAPT (mean and standard deviations from 5 independent MEP preparations).

B: Same experiment as in A, except that MEPs were cultured either in presence or absence of SCF. Histograms show the fold variations in the relative numbers of mixed colonies obtained at Day 2 compared to the initial numbers at Day 0.

1. Main starting observations

Here, I will summarize the main results of our team (manuscript 1 in Annex 1) showing the SCF-dependent amplification of megakaryocytic-erythrocytic bipotent progenitors induced by Notch pathway stimulation and introducing the context of my study.

The protocol used to study the effect of Notch pathway stimulation on bipotent MEP cell fate is presented in Figure 1. Populations highly enriched in MEPs were sorted by FACS from murine bone marrow according to published protocol (Akashi et al., 2000). We then quantified the number of bipotent, erythrocytic and megakaryocytic progenitors present in this initial population (day 0) by counting the numbers of mixed (containing both erythrocytic and megakaryocytic cells), pure erythrocytic and pure megakaryocytic colonies obtained after seeding in semi-solid medium containing a full myeloid cytokines cocktail. Progenitors numbers were then compared to that obtained using the same colony assay performed after a 2 days liquid culture starting from the same cells number in the presence of coated recombinant Notch ligand rDll1 or IgG used as negative control. Duplicates cultures were also performed in the presence of ϒ-secretase inhibitor DAPT or in the absence of SCF to control that the changes induced by Notch ligand are due to the activation of the Notch pathway and to test their dependency on the SCF/c-Kit signaling respectively. Using this protocol, we observed that in absence of Notch stimulation (Day 0 or IgG day2), MEPs generated 1/3 of erythrocytic and 1/3 of megakaryocytic monopotent colonies but only 1/3 of mixed colonies (Figure 2 A), suggesting the low stability of the bipotent E/MK state. In contrast, the 2 days stimulation of MEPs by rDll1 increased the number of mixed colonies when compared to the initial number derived from freshly purified MEPs (Day 0) or to unstimulated MEPs (IgG) (Figure 2 A), thus indicating the positive effect of Notch on the stabilization of MEPs bipotency as well as on their amplification.

Besides, we found that Notch-induced amplification of MEPs required the addition of SCF (Figure 2 B). This observation suggests the cooperation between Notch and SCF pathways during the amplification of MEPs.

Cells counting and FACS analyses of MEP cultures after a 5 days stimulation by rDll1 revealed the SCF-dependent and selective amplification of c-Kit positive cells, which was a Notch-specific effect as it was reversed in presence of DAPT (Figure 3 A). Additionally, this SCF-dependent selective amplification of c-Kit positive progenitors was also associated with

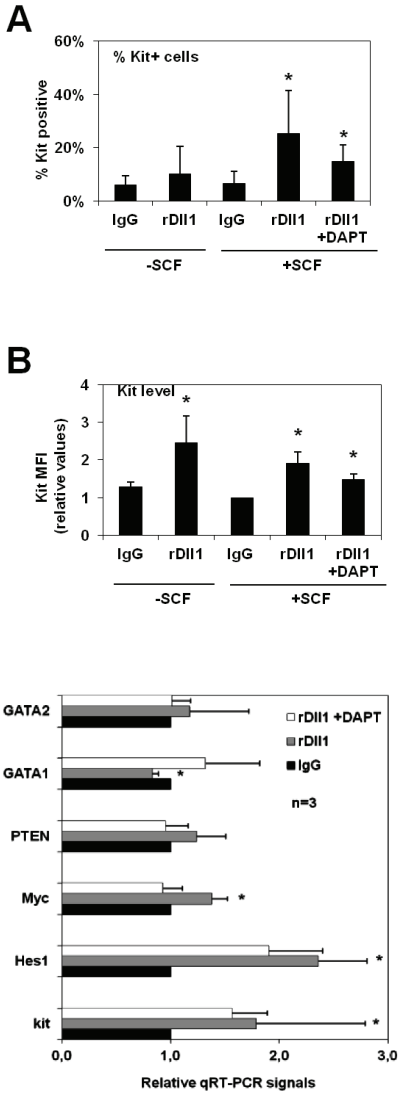

Figure 3: Notch modulates c-Kit protein levels in MEPs progeny

MEPs were cultured during 5 days in liquid culture in wells coated either with control IgG or with rDll1 ligand and in presence or absence of SCF or DAPT. At the end of the culture, cells were numbered and c-Kit expression was assessed by flow cytometry. **A.** Histogram showing the proportion of c-Kit positive cells B. Histogram presenting the relative median fluorescence intensities of c-Kit in the c-Kit positive population, showing that Notch stimulation induces the expression of c-Kit both in presence and absence of SCF.

Figure 4: Variations in transcript levels induced by Notch stimulation in MEPs

Transcripts levels were determined by qRT-PCR in MEP cultured two days on control IgG or rDll1 in presence or absence of DAPT as described in Figure 1. Histograms show the fold variations observed in the presence of Notch ligand rDll1 with or without Notch inhibitor DAPT. Means and strandard deviations from 3 independent experiments. Statistically significant results are indicated by asterisks.

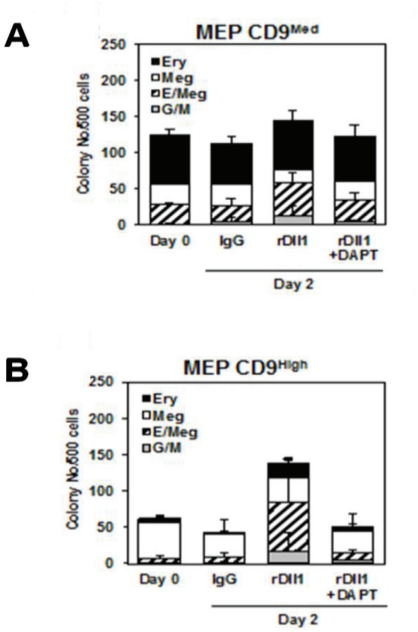

Figure 5: Strong induction of bipotent progenitors from MEPs subset expressing high levels of CD9

MEPs were sorted according to their medium **(A)** or high **(B)** levels of CD9 expression and their responses to Notch ligand were compared using the same protocol as described in Figure 2. Results are presented as piled histograms showing the numbers of the different types of colonies generated from untreated cells (Day 0) and after a two days culture in presence of IgG or rDll1 with or without DAPT. Means and standard deviations from 3 independent experiments

the SCF-independent increase of c-Kit expression per cell as attested by an increased c-Kit median of fluorescence in c-Kit positive population which again was reversed by DAPT treatment (Figure 3 B). Furthermore, MEPs stimulation by Notch ligand in presence of SCF induced an increase in c-Kit transcripts amounts (Figure 4). Taken together, these results indicated that the SCF-dependent amplification of MEP induced by Notch pathway activation is associated with an increased expression of c-Kit.

More recently, we observed that sorted MEPs populations are actually heterogeneous and can be subdivided in at least two subpopulations considering the level of expression of the CD9 tetraspanin. The majority MEPs subset expressing intermediate levels of CD9 ($CD9^{Med}$) closely resembles the unfractioned MEP population (Figure 5 A), while the subpopulation highly expressing CD9 is strongly skewed towards megakaryocytic differentiation as attested by the very high initial proportion of megakaryocytic colonies generated at Day 0 (Figure 5 B). Besides, the stimulation of the two subpopulations by Notch ligand rDll1 during two days led to a more pronounced increase in the proportion of mixed colonies in $CD9^{High}$ subpopulation when compared to $CD9^{Med}$ subpopulation (Figure 5). This observation reveals an increased sensitivity of the $CD9^{High}$ megakaryocytic biased MEP subpopulation to the stimulation by Notch leading to the amplification of bipotent progenitors.

In summary, these results indicate that MEPs bipotency is an unstable state which can be stabilized by Notch pathway stimulation leading concomitantly to their amplification. This effect requires the cooperation between Notch and SCF/c-Kit signaling and is accompanied by increased c-Kit transcripts and protein levels. Moreover, the stronger increase of bipotent progeny in the $CD9^{High}$ subpopulation of MEPs under Notch stimulation could suggest a functional interaction between Notch pathway and the tetraspanin CD9.

These observations led me to investigate the molecular mechanisms allowing Notch pathway to maintain bipotency and to stimulate MEP amplification by trying to answer the following questions: 1) is Notch pathway involved in the control of GATA-1 expression and/or phosphorylation and is GATA-1 phosphorylation implicated downstream to Notch in the stabilization of the bipotent state in MEPs? 2) How Notch pathway activates c-Kit expression? 3) Is c-Kit implicated in the balance proliferation/differentiation and what is the molecular basis of the functional interaction between Notch and CD9 ? To answer the two latter questions, I choose to conduct the study using the TPO-dependent G1ME cells resulting from the immortalization of GATA1 deficient murine bipotent progenitors.

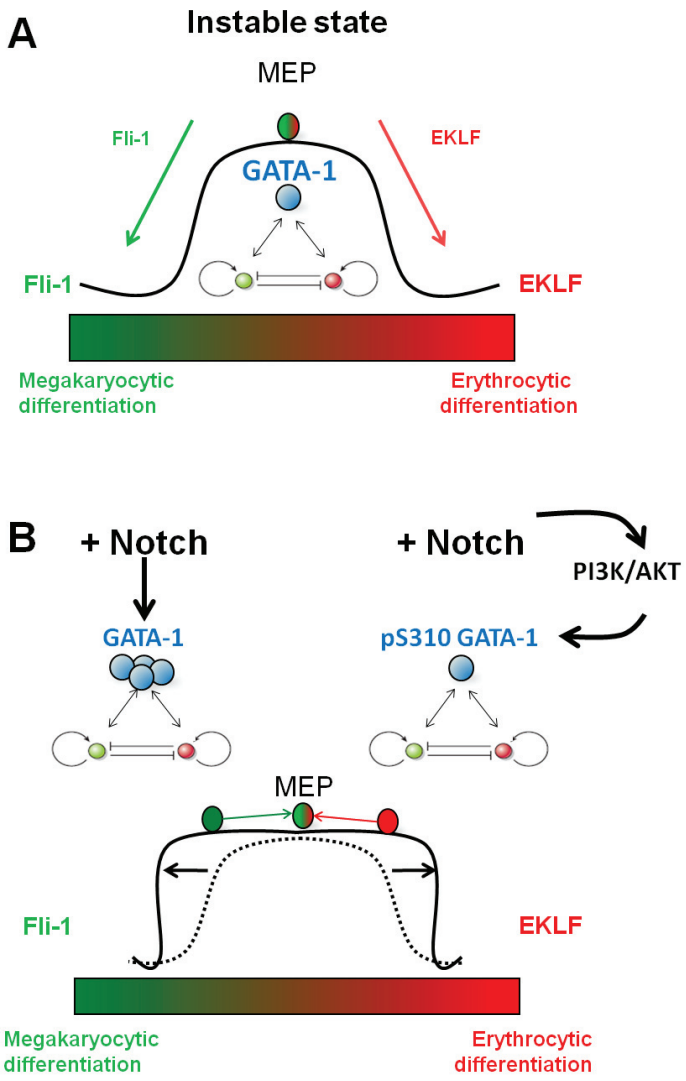

Figure 6: Working model on the stabilization of MEP bipotency

A- Cross-antagonism between Fli-1 and EKLF controlling MEP commitment:

Schematic presentation of the unstable balance between maintenance of MEPs bipotency and their commitment towards either erythrocytic or megakaryocytic differentiation based on the functional antagonism between Fli-1 and EKLF. EKLF (red circle) and Fli-1 (green circle) transcription factors inhibit each other expression, while inducing their own expression and both require their interaction with a common partner GATA-1 to induce either erythrocytic or megakaryocytic differentiation, respectively. This functional antagonism implies that Fli-1 and EKLF compete for their mutually exclusive interaction with GATA-1 thus causing the instability of the bipotent state (illustrated by the narrowness of the black curve plateau). Consequently, any small fluctuations in the level of Fli-1 or EKLF will be rapidly amplified causing increased capture of GATA-1 and inducing irreversible commitment towards either one lineage.

B. Hypotheses on the mechanisms possibly involved in the Notch-mediated stabilization of the bipotent state. Notch could stabilize the bipotent state (illustrated by the enlarged plateau of the black curve) by buffering the tolerated differential expression between Fli-1 and EKLF, before either EKLF or Fli-1 reach a sufficient level of expression inducing irrevocable engagement into differentiation. This buffering mechanism could be mediated either by enhancing the available quantity of GATA-1 (left panel), or by modulating GATA-1 phosphorylation affecting in turn the strength of its interactions with Fli-1 and EKLF (right panel).

2. Does Notch maintain MEPs bipotency through the regulation of GATA-1

2.1. Working hypotheses

We know that the mutually exclusive commitment of MEP towards erythrocytic or megakaryocytic differentiation is partly governed by the cross-antagonism between Fli-1 and EKLF transcription factors (Bouilloux et al., 2008; Frontelo et al., 2007). EKLF and Fli-1 transcription factors inhibit each other expression, while inducing their own expression and both require their interaction with a common partner GATA-1 to induce either erythrocytic or megakaryocytic differentiation, respectively (Figure 6). This functional antagonism suggests that Fli-1 and EKLF compete for their mutually exclusive interaction with GATA-1 thus causing the instability of the bipotent state. Consequently, any small fluctuation in the level of Fli-1 or EKLF will be rapidly amplified causing increased capture of GATA-1 and inducing irreversible commitment towards either one lineage (Figure 6 A). On the opposite, stabilization of the bipotent sate of MEP should be favored by situations allowing to reduce the competition between Fli-1 and EKLF for their interaction with GATA-1 (Figure 6 B).

Based on this model, we hypothesized that Notch pathway induces the maintenance of the MEP bipotency by acting directly on GATA1 in either quantitative or qualitative ways allowing to lower the competition between Fli1 and EKLF:

Our first hypothesis was that the Notch pathway could reduce the competition between Fli1 and EKLF by increasing GATA1 levels (Figure 6B left panel).

Our second hypothesis, was that the Notch pathway could modulate the strength of the interactions between GATA-1 with Fli-1 or EKLF by modulating GATA-1 phosphorylation (Figure 6 B right panel). Several previous studies were also compatible with this second hypothesis. One of these studies showed that Notch is indeed able to activate the AKT kinase through the repression of its inhibitor PTEN allowing the specification of the megakaryocytic lineage directly from murine HSCs (Cornejo et al., 2011). Other studies evidenced the AKT-dependent phosphorylation of GATA-1 on Serine 310 during erythroid differentiation in MEL cells treated with DMSO (Zhao et al., 2006), or in response to EPO in UT7 cell line (Kadri et al., 2005). Moreover, another study showed that GATA-1 phosphorylation on serine 310 was actually able to favor its preferential interaction with FOG1 instead of RB/E2F and by this

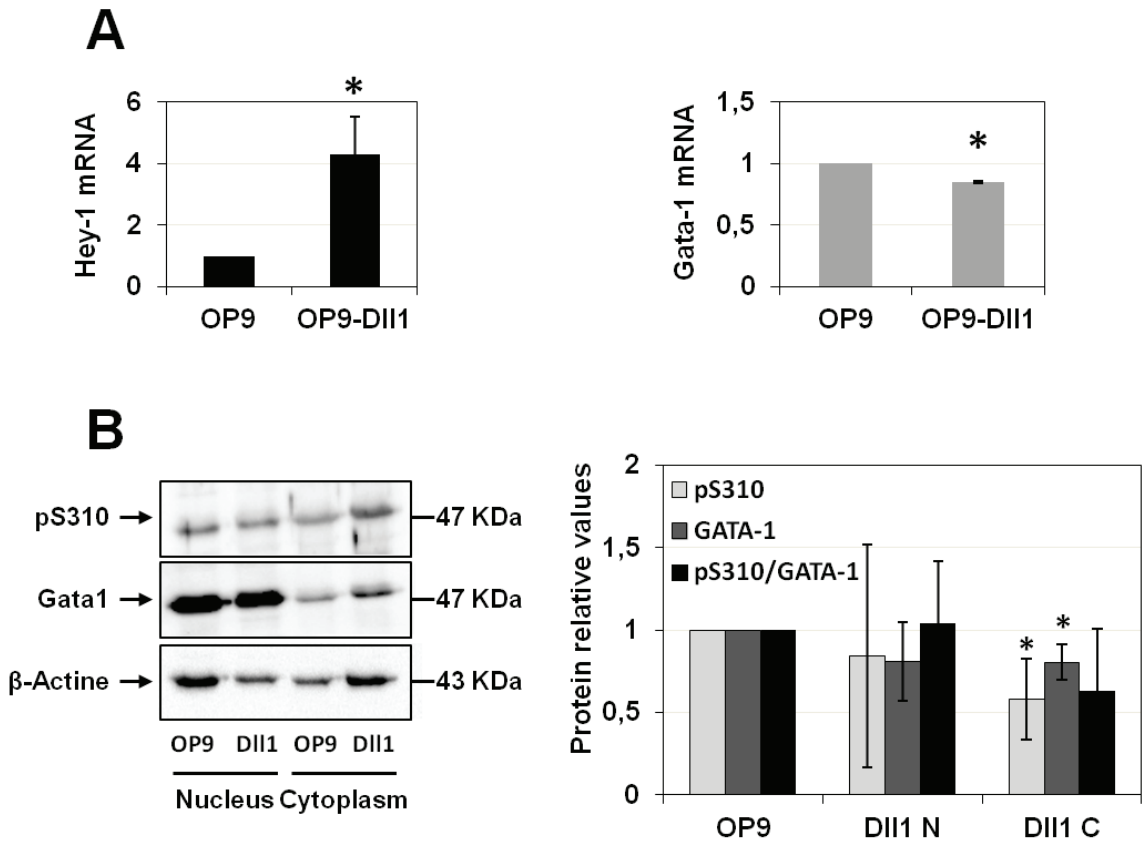

Figure 7: Notch does not modulate GATA-1 expression or phosphorylation in L8057 cells

L8057 megakaryocytic cells were cultured for one day on OP9 or OP9-Dll1 stromal cells and mRNAs or protein levels were quantified by qRT-PCR (A) or Western-Blot (B) respectively.

A. Culture of L8057 cells on OP9-Dll1 increases the transcript levels of Hey-1 (left histogram) attesting for Notch pathway activation and slightly reduces the expression of Gata-1 (right histogram). Means and standards deviations from three independent experiments with asterisk showing significant variation ($p<0.5\%$).

B. Left panel: Typical representative Western-Blot showing the levels of phosphorylation of GATA-1 on Serine 310, total GATA-1 or β-Actin in the nucleus or cytoplasm of L8057 cells cultured on either OP9 or OP9-Dll1 stromal cells. Right panel: Histograms showing the relative variations in the signals of GATA-1, phosphorylated GATA-1 and pGATA-1/GATA-1 ratios obtained after first standardization to β-Actin signal and then to values obtained on OP9 stromal cell.

way contribute to proliferation arrest and terminal erythroid differentiation (Kadri et al., 2009) (Lefevre, Thesis manuscript 2013).

2.2. Study of Notch effect on GATA-1 in L8057 cells

In order to test the effect of Notch stimulation on GATA-1 expression, I choose to conduct the study in the murine megakaryoblastic cell line L8057 (Ishida et al., 1993). First, I assessed their ability to respond to Notch stimulation. For that purpose, L8057 cells were co-cultured on murine OP9 stroma cells engineered to express Notch ligand Dll-1 (OP9-Dll1) or on control OP9 cells (OP9). Following 24 h of co-culture, L8057 cells were harvested and the expression of Notch target gene Hey-1 was assessed by qRT-PCR. As expected Hey-1 transcript levels in L8057 cells significantly increased by 4 fold in OP9-Dll1 compared to OP9 cocultures (Figure 7A left panel) thus attesting the activation of the Notch pathway.

Having validated the activation of Notch pathway, I then used the same coculture conditions to study the effect of Notch pathway activation on GATA-1 expression in L8057 cells. qRT-PCR analyses showed that the activation of Notch pathway in L8057 cells was accompanied by a slight and significant decrease of Gata-1 transcripts (15 % decrease on OP9-Dll1 compared to OP9 cocultures) (Figure 7 A right panel). Furthermore, cells lysates of L8057 cells harvested in the same conditions were fractioned into either nuclear or cytoplasmic fraction and used to quantify GATA-1 protein levels by Western blot. Quantification of Western-Blots signals revealed that the stimulation of L8057 cells by OP9-Dll1 induced a 15 % significant decrease of GATA-1 protein levels in the cytoplasmic fraction, whereas it did not affect the protein levels of GATA-1 in the nuclear fraction (Figure 7 B). Interestingly, parallel analyses performed on native bipotent MEP, revealed that their stimulation by recombinant ligand Dll1 during two days was also associated with a slight decrease of Gata-1 transcripts levels which was reversed by DAPT treatment (Figure 4).

In order to test the second hypothesis, I used the same lysates of L8057 cells harvested after co-culture on either OP9 or OP9-dll1 to quantify the levels of GATA-1 phosphorylated on residue 310 by Western-Blot analysis using a pSer 310 GATA-1 specific antibody. This analysis showed that the coculture of L8057 cells on OP9-Dll1 did not induce any significant change in the levels of phosphorylated GATA-1 or in the proportion of phosphorylated GATA-1 (pS310/total GATA-1 ratios) neither in the cytoplasm nor in the nucleus. However,

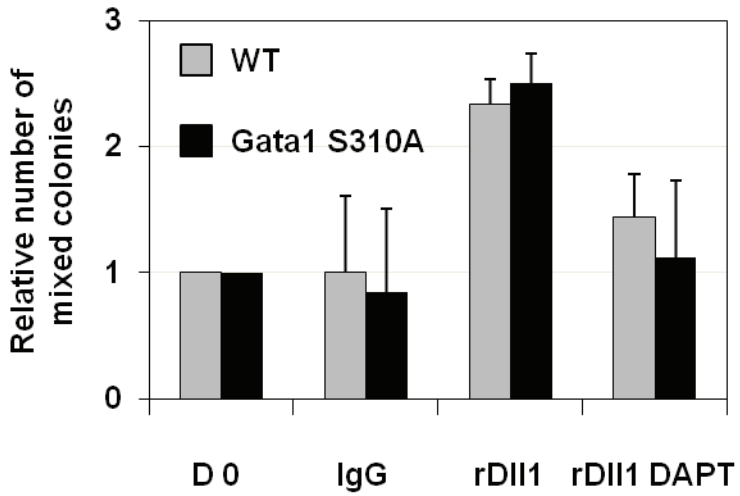

Figure 8: GATA-1 phosphorylation on S310 is dispensable for the stimulation of MEPs amplification induced by Notch pathway activation.

MEPs derived either from wild-type (grey bars) or GATA-1^{S310A} knock-in mice (Black bars) were purified and compared for their ability to increase the number of bipotent progenitors upon Notch pathway activation following the protocol described in Figure 1. Histograms show the relative variations in the number of mixed colonies obtained before (Day 0) and after 2 days of culture on either IgG, rDll1 with or without DAPT. Mean and standard deviations from three independent experiments showing no significant variations.

Notch activation induced a slight but significant decrease of GATA-1 phosphorylation in cytoplasmic but not in the nuclear fraction roughly following the variation observed on total GATA-1 protein levels (Figure 7 B).

We hypothesized that Notch activation induces the increase of GATA-1 expression levels and modulates its phosphorylation on S310 residue. Contrarily to this hypothesis, our results showed that Notch activation in L8057 cells slightly decreased GATA-1 transcripts and cytoplasmic GATA-1 protein levels to the same extent but did not change GATA1- protein levels in the nucleus. Moreover, we found that Notch activation in L8057 cells did not modulate the proportion of phosphorylated GATA-1 neither in the cytoplasm nor in the nucleus.

2.3. Study of the implication of S310 phosphorylated GATA-1 in Notch-mediated maintenance of MEPs

In order to directly assess the real implication of GATA-1 phosphorylation in the Notch-mediated maintenance of MEP bipotency, we took advantage of a murine knock-in model expressing a mutated form of GATA-1 in which Serine 310 has been change into Alanine thus disabling GATA1 phosphorylation on that residue (Rooke and Orkin, 2006) (kindly provided by S. Chretien).

As described before in Figure 1, MEP from either wild-type or GATA-1^{S310A} mice were purified and cultured on either IgG or Notch ligand rDll1 with or without Notch inhibitor DAPT. Following two days of stimulation, MEP progeny was seeded in semi-solid medium and colonies obtained were classified and counted. Again, we observed that Notch activation increased the proportion of mixed colonies when compared to freshly purified MEPs (Day 0) or unstimulated MEPs (IgG). This Notch-mediated maintenance and amplification of bipotent progeny of MEP persisted even in MEP derived from $GATA1^{S310A}$ mutant mice with no significant difference when compared to MEPs derived from wild-type mice (Figure 8). These results thus indicate that the phosphorylation of GATA-1 on its serine residue 310 is dispensable for Notch-mediated maintenance and amplification of the bipotent progenitors MEP.

Altogether these data indicate that, contrarily to our initial hypotheses, Notch activation does not increase GATA-1 protein levels or phosphorylation in L8057 cells. Moreover, loss of

GATA-1 phosphorylation on S310 does not alleviate the positive effect of Notch activation on native MEP maintenance and amplification. Based on these results, we conclude that the Notch-mediated amplification of MEP cannot be explained by increased GATA-1 protein levels or by changes in GATA-1 protein phosphorylation on S310 residue.

3. Study of the mechanisms by which c-Kit expression upregulation by Notch

The strong SCF-dependency of the Notch-mediated amplification of MEP prompted us to investigate the molecular mechanisms controlling c-Kit expression by Notch pathway. Moreover, knowing the functional duality of TPO in stimulating both proliferation and differentiation of megakaryocytic progenitors, we choose to extent our study of c-Kit regulation also in response to TPO. Given the very small number of MEP available from murine bone marrow (0.1% of total bone marrow cells), I choose to perform this study of c-Kit regulation using immortalized bipotent G1ME cells (Stachura et al., 2006). Before performing this study, I first verified the pertinence of this cellular model by controlling its erythro-megakaryocytic bipotency and its ability to mimic the upregulation of c-Kit observed in native MEP upon Notch activation.

3.1. Validation of G1ME cells as a cell model for the study of c-Kit regulation in bipotent progenitors

3.1.1. Verification of G1ME cells ability to differentiate towards E/MK lineages

G1ME bipotent progenitors cells were established from Gata-1 deficient murine embryonic stem cells immortalized in the presence of TPO (Stachura et al., 2006). Initial characterization of G1ME cells evidenced their expression of pluripotent markers such as c-Kit and GATA-2, as well as megakaryocytic markers such as CD9, CD41 and CD61, with no detectable expression of other hematopoietic lineages markers such as erythroid (Ter119), lymphoid (B220 and IL-7R), or granulo-monocytic (Mac-1 and Gr-1). Quite interestingly, the re-expression of GATA-1 transduced by retroviral infection allows G1ME cells to resume their

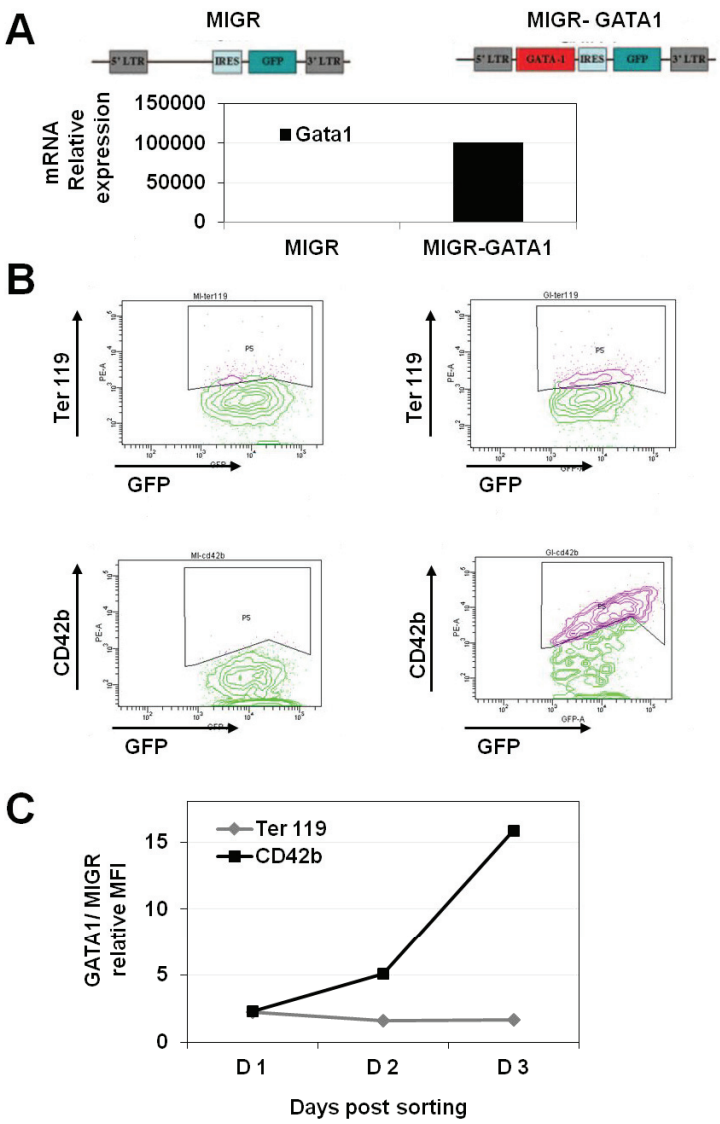

Figure 9: G1ME cells are still able to resume terminal erythroid and megakaryocytic differentiation upon GATA-1 re-expression

G1ME cells were infected by either retrovirus MIGR (transducing GFP) or MIGR-GATA-1 (transduction GFP and GATA-1). GFP positive infected cells were flow-sorted then re-seeded in a medium containing SCF, EPO, TPO, IL-3, IL-6 and IL-11. Their differentiation along the erythroid or megakaryocytic lineages was monitored by flow cytometry through the analysis of Ter119 or CD42b markers, respectively.

A. Schematic presentation of the retroviral vectors harboring either GFP alone (MIGR) or the coding sequence for GATA-1 coupled to GFP through an IRES sequence (MIGR-GATA1). The restoration of GATA-1 expression only in MIGR-GATA1 infected cells was checked at day 1 post-sorting by qRT-PCR as presented in the histogram.

B. FACS contour plots of the expression of GFP and either Ter119 (upper panels) or CD42b (lower panels) obtained after 2 and 4 days, respectively following infection with either MIGR (left panels) or MIGR-GATA1 (right panels) retroviruses. Gate P5 corresponds to GFP positive cells expressing significant levels of either Ter119 or CD42b when compared to control labeling with fluorescent IgG control isotypes.

C. Kinetic evolution of the ratios of the Ter119 (grey curve) and CD42b (black curve) median fluorescence intensities (MFI) between cells infected with MIGR-GATA1 and control MIGR retroviruses during the 3 days following infection.

differentiation only in erythrocytic and megakaryocytic lineages as assessed by the induction of Ter-119 erythroid marker and CD42b megakaryocytic marker observed by flow-cytometry.

First, I checked the phenoptype of G1ME cells (kindly provided by T. Mercher) by FACS analyses. As described in the initial study (Stachura et al., 2006), we observed that G1ME cells resembles E/MK bipotent progenitors as they express c-Kit, while they don't express CD34 and Sca-1 stem cells markers. Furthermore, they do express early megakaryocytic markers such as CD41 and CD61 as well as late megakaryocytic marker such as CD9, but no CD42b was detected. The double labeling of G1ME cells for erythroid markers CD71 and Ter119 showed that they are CD71+ Ter119 low. We also checked for the absence of granulo-monocytic markers Mac-1 and Gr-1 in G1ME cells cultured in TPO (data not shown).

I also tested the ability of G1ME cells to engage into both erythroid and megakaryocytic differentiation following their infection by retroviral vector transducing only GFP expression (MIGR) or by the same vector transducing both GATA-1 and GFP (MIGR-GATA1) (provided by T. Mercher). In a first experiment, transduction efficiency was determined by analyzing GFP expression by flow cytometry which revealed only transient persistence of GFP marker (data not shown), probably due to the overwhelming growth of GATA-1 -/- G1ME cells (Stachura et al., 2006). In a second experiment, G1ME cells were infected by MIGR or MIGR-GATA1 retroviral vectors followed by FACS-sorting of GFP positive cells that were seeded in a G1ME medium supplemented by full cocktail of erythro-megakaryocytic cytokines (SCF, EPO, TPO, IL-3, IL-6 and IL-11). We first checked by qRT-PCR at day 1 post-sorting the presence of GATA-1 transcripts in G1ME GFP+ cells infected by MIGR-GATA1 vector, whereas GATA-1 transcripts remained undetectable in G1ME GFP+ cells infected by MIGR control vector (Figure 9 A). Next, the expressions of the erythroid marker Ter119 and of the late megakaryocytic marker CD42b were monitored by flow cytometry during three days following the sorting of G1ME-GFP+ infected cells. This kinetic analysis showed that the median fluorescence of the megakaryocytic marker CD42b continuously increased in G1ME cells expressing GATA-1 when compared to their MIGR counterparts, whereas the median fluorescence of Ter119 was increased by 2 fold and was sustained at the same level during the three days following the sorting (Figure 9 C).

These results thus validated the ability of G1ME cells to engage into both erythroid and megakaryocytic lineages upon the restoration of GATA-1 transcription factor expression.

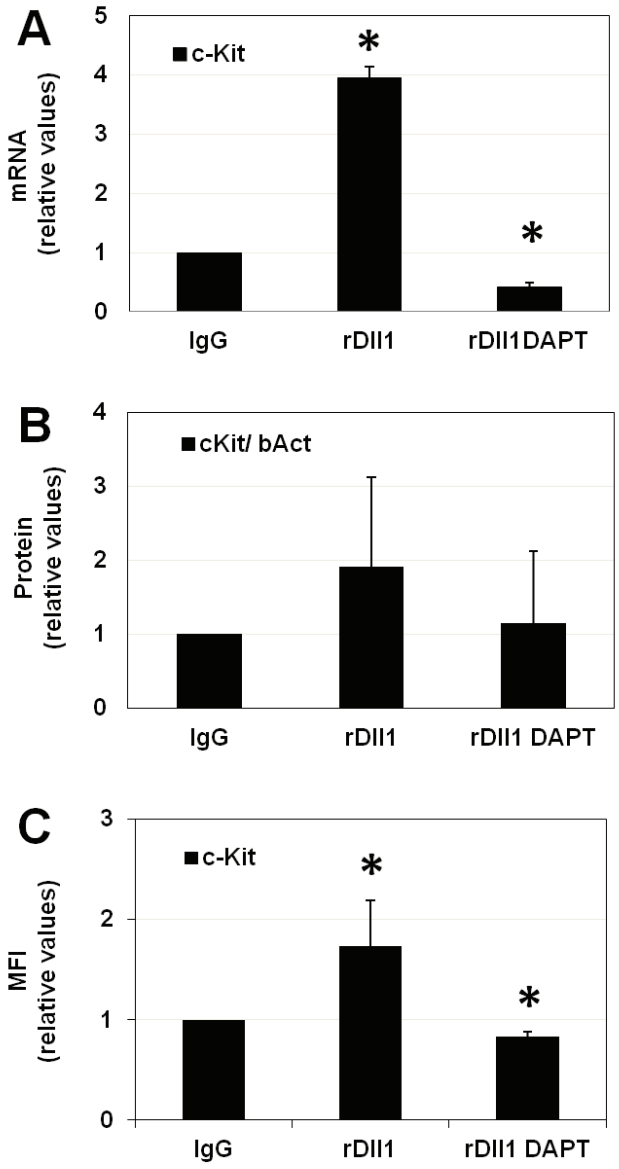

Figure 10: Notch activation upregulates c-Kit expression in G1ME cells

G1ME cells were cultured during two days in wells coated either with control IgG or recombinant Notch ligand rDll1 in presence or absence of Ɣ-secretase inhibitor DAPT, then harvested for the analysis of c-Kit transcripts and protein levels using qRT-PCR and FACS or Western-Blot, respectively.

A. Histogram showing the relative levels of c-Kit transcripts normalized to β-Actin and to IgG control condition.

B. Histogram showing the relative levels of c-Kit protein following quantification of Western-Blot signals of total c-Kit normalized to β-Actin and to IgG control condition.

C. Histogram showing the relative median of fluorescence intensities of c-Kit protein determined by FACS analyses. Results are presented as relative values calculated after deduction of background fluorescence and normalization to the IgG control condition.

For all histograms, (A, B, C) means and standards deviations from three independent experiments are presented and significant variations compared to control IgG indicated by an asterisk (Student t test $p<0.5\%$).

3.1.2. Validation of the ability of G1ME cells to induce c-Kit expression upon Notch activation

To test their ability to activate Notch pathway, G1ME cells were cultured either on control IgG or on Notch ligand rDll1 during two days and the expression of Notch target genes, Hey-1 and Hes-1, was monitored by qRT-PCR. Hey-1 transcripts were detected neither in control IgG nor in rDll1-stimulated G1ME cells (data not shown). By contrast, Hes-1 transcripts were detected at low level in unstimulated G1ME cells cultured on IgG and increased up to 7 fold in response to rDll1, this increase being reversed by DAPT treatment (Table 1).

This result thus attests that G1ME are able to activate the Notch pathway when they are cultured on Notch ligand rDll1.

Having validated the ability of G1ME cells to activate Notch pathway, I used the same culture protocol to investigate the effect of Notch activation on the expression of c-Kit at both mRNA and protein levels. qRT-PCR analyses revealed that the stimulation of G1ME cells by rDll1 ligand induced a significant 4 fold increase of c-Kit transcripts levels which was reversed by DAPT treatment (Figure 10 A). The analysis of c-Kit expression by Western-Blot revealed a 2 fold increase in c-Kit protein levels, though this effect was not significant (Figure 10 B). Finally, FACS analyses revealed that the stimulation of G1ME cells by rDll1 ligand induced a significant increase of the mean of florescence of c-Kit when compared to unstimulated G1ME cells (IgG) which was reversed in the presence of DAPT (Figure 10 C).These results thus validate that G1ME mimics the upregulation of c-Kit mRNA and c-Kit protein expression at the cell membrane which are observed upon Notch activation in native MEP.

To complete the characterization of the Notch response of G1ME cells, we combined additional qRT-PCR (Figure 11C) and FACS analyses (Figure 11A and B) to document the effect of Notch activation on the expression of the TPO receptor c-MPL as well as of the two other late megakaryocytic markers PF4 and CD9 in the same culture conditions.

We noticed that rDll1 induced a 2 fold decrease of the expression of c-MPL at the cell membrane which was however not reversed in the presence of DAPT (Figure 11A). Moreover, this decrease of c-MPL protein expression was associated with no significant variation in the levels of c-MPL transcripts (Figure 11C).

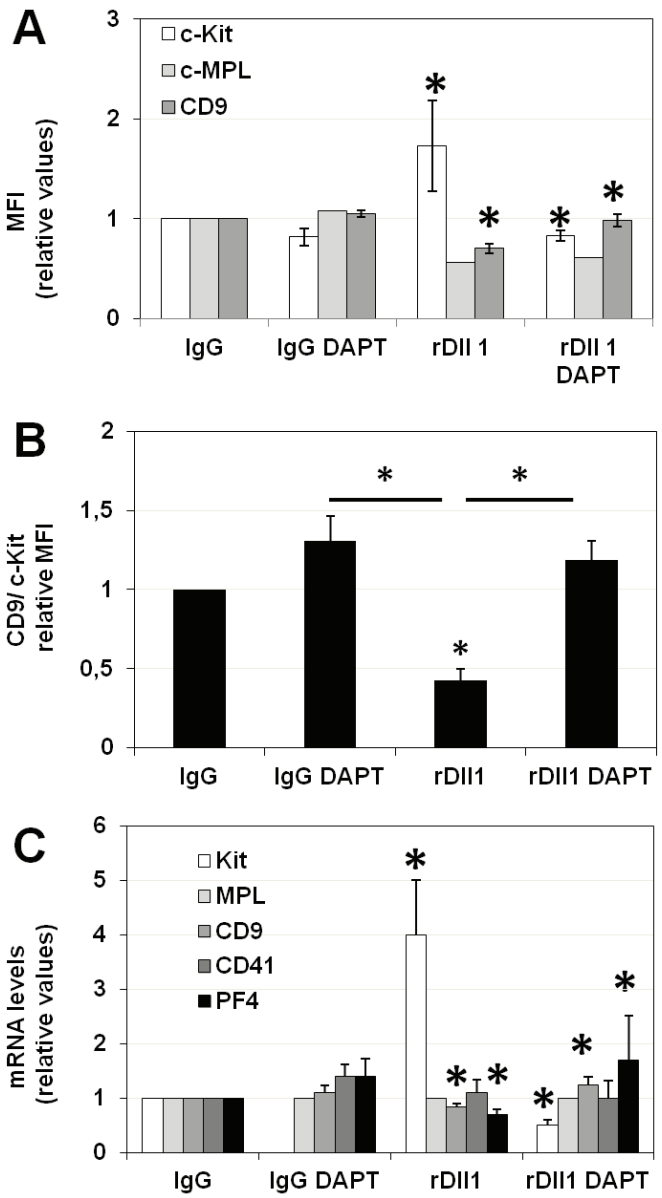

Figure 11: Notch stimulation increases c-Kit and decreases late megakaryocytic genes expression.

G1ME cells were cultured for two days either on recombinant Notch ligand rDll1 or control IgG in medium containing TPO and in the presence or absence of ϒ-secretase inhibitor DAPT as indicated. **A:** Median Fluorescence Intensities (MFI) of c-Kit, c-MPL and CD9 expression determined by FACS analyses (relative values standardized to the IgG condition). **B:** Same data as in A but presenting the ratio of median of fluorescence intensities of CD9 over c-Kit normalized to IgG control condition. **C:** mRNAs levels determined by qRT-PCR and normalized to β-actin (relative values standardized to the IgG condition). Mean and standard deviations from 3 independent experiments. Statistically significant differences from the IgG condition are indicated by asterisks ($p<0.05$ in Student t test).

More interestingly, we found that rDll1 induced a significant 30% decrease of the expression of CD9 at the cell membrane (Figure 11A) as well as a 20% decrease of CD9 mRNA levels (Figure 11C) which were both reversed in the presence of DAPT. This result revealed an intriguing divergent regulation of c-Kit and CD9 upon Notch activation raising the possibility that c-Kit and CD9 could modulate each other expression.

Knowing that CD9 expression strongly increases during terminal megakaryocytic differentiation, its decreased expression induced by rDll1 could reflect the inhibition of spontaneous megakaryocytic differentiation of G1ME cells. Supporting such a possibility, we found that rDll1 induced a significant 30% decrease in transcript levels of another late megakaryocytic gene Pf4 (Figure 11C) which again was reversed in the presence of DAPT. In contrast, CD41 and Fli-1 transcript levels, known to be activated earlier than CD9 and pf4, did not changed significantly in response to Notch activation (Table 1). These results tend to suggest that activation of the Notch pathway is involved in the repression of late megakaryocytic genes such as Cd9 and Pf4 that are spontaneously activated in G1ME cells cultured in presence of TPO.

In summary, these first analyses showing that G1ME cells are still able to differentiate exclusively into either erythroid or megakaryocytic cells as well as to mimic the behavior of native MEP in the upregulation of c-Kit expression upon Notch activation validate the use of these cells as a pertinent cellular model to study the regulation of c-Kit expression by Notch pathway. Moreover, these first results obtained on G1ME cells raise several interesting new questions regarding the putative interferences between c-Kit and CD9 expression as well as the putative implication of c-Kit in modulating the dual control of their proliferation or differentiation by TPO.

3.2. Study of c-Kit transcriptional regulation by Notch

In order to understand the molecular mechanisms allowing Notch pathway to induce c-Kit expression, I adopted a two steps strategy. First, I tried to get the best evidence that the upregulation of c-Kit does occur at the transcriptional level. Secondly, I investigated several transcription factors known to be involved in the regulation of c-Kit by analyzing their putative differential expression and/or recruitment on c-Kit gene chromatin in response to Notch activation.

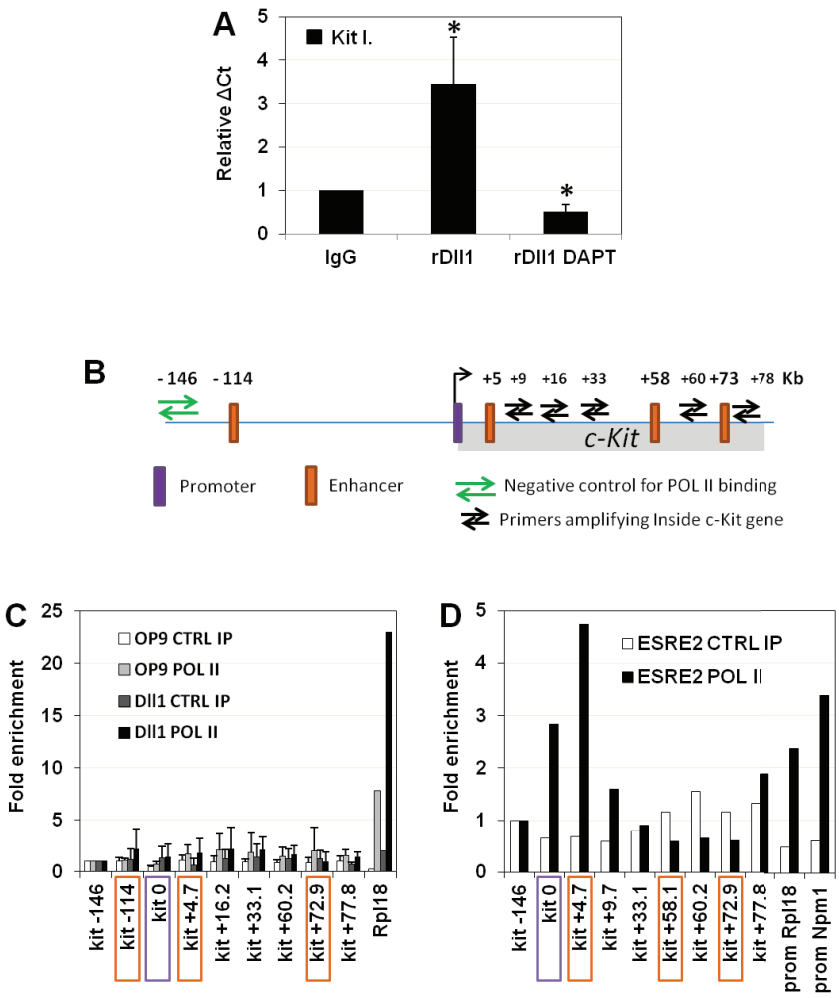

Figure 12: Notch regulates c-Kit expression at the transcriptional level

A .G1ME cells were cultured on IgG or rDll1 ligand with or without DAPT inhibitor during two days and the expression of c-Kit primary transcripts was quantified by qRT-PCR. Histogram presenting data normalized to the non-stimulated IgG condition with means and standards deviations from three independent experiments. Significant variations between rDll1 and IgG, as well as between rDll1 and rDll1+DAPT are represented by asterisk ($p< 0.001\%$ in Student test).

B. Schematic map showing the positions (in Kb) of the regions amplified using different primers in and around c-Kit gene.

C. G1ME cells were co-cultured either on OP9 or OP9-Dll1 stromal cells, harvested and analyzed by ChIP assay. Chromatin was precipitated by RNA POL-II antibody or control rabbit-IgG (CTRL IP). Enrichments in the RNA POL II chromatin of c-Kit gene enhancers (-114, +4.7, +72.9), promoter (c-Kit 0) or at regular intervals inside the coding sequence were quantified by qPCR. Enrichment data were normalized to the input amount of chromatin and to negative control for POL II binding on region (-146) Kb. RNA POL II enrichment on Rpl18 promoter was also analyzed as positive control for RNA POL II binding. Means and standards deviations are derived from 3 independent experiments.

D. Same protocol and presentation as in B except that the highly proliferating ESRE2 erythroid cells were used as positive control to test the efficiency of RNA POL II antibody in ChIP assay. Chromatin was precipitated using either RNA POL II antibody (Black bars) or rabbit control antibody (white bars) and qPCRs were performed on c-Kit gene and positivecontrol genes encoding proteins implicated in ribosome biogenesis (Rpl18 and Npm1) supposed to be highly transcribed.

3.2.1. Evidence for the transcriptional upregulation of c-Kit gene

To test the hypothesis that the upregulation of c-Kit mRNA is due to increased transcription of the c-Kit gene, I used qRT-PCR to quantify the upregulation of unspliced c-Kit primary transcripts. Indeed, unspliced primary transcripts are very rapidly degraded following transcription and for that reason their levels are a good indicatior of instantaneous transcription rate. Thus, we designed specific primers amplifying a region in the first intron of c-Kit gene and used these primers to quantify c-Kit primary transcripts in G1ME cells. Our results showed that the stimulation of G1ME cells by rDll1 induced a three fold increase in c-Kit primary transcripts when compared to unstimulated cells cultured on IgG, this increase being cancelled by DAPT treatment (Figure 12 A). These results strongly suggest that Notch actually regulates c-Kit expression directly at the transcriptional level.

In a different approach aimed to strengthen this conclusion, we tried to evidence an increase in the density of RNA Polymerase II (POL II) present on the promoter and along the c-Kit gene using chromatin immunoprecipitation assay (see methods). For that purpose, G1ME cells were cultured during two days on either OP9 or OP9-Dll1 stromal cells and harvested. Then, chromatin was cross-linked and immunoprecipitated using either RNA-POL II specific antibody or control rabbit antibody (used to estimate background level of immunoprecipitated chromatin due to unspecific antibody binding). Following crosslink reversion and DNA purification, I quantified by q-PCR the relative amounts of DNA amplified from c-Kit promoter or regularly interspaced regions inside c-Kit gene contained in POL II (Figure 12 B) or control chromatin and then calculated the relative enrichment of RNA POL II in these different regions following normalization to a negative non transcribed region outside c-Kit gene (-146 Kb upstream region). Unfortunately, the results of these RNA POLII ChIP analyses showed very low and non significant enrichments of RNA POL II on the promoter and all the regions tested inside c-Kit gene in both unstimulated (cultured on OP9) or Notch stimulated (cultured on OP9-Dll1) G1ME cells. In the same experiment, an 8 fold enrichment of RNA POL II was clearly detected on the promoter of the highly active RPL18 ribosomal protein gene which further increased up to 25 fold in Notch-stimulated G1ME cells thus attesting successful RNA POL II chromatin immunoprecipitation (Figure 12 C). In control experiments we used the same RNA POL II antibody to quantify RNA POL II recruitment on c-Kit gene in the SCF-dependent ESRE cells (Extensively Self-Renewing

Gene	IgG	rDll1	rDll1 + DAPT
Hes-1	1	15 .6 ± 3	0.81 ± 0.24
c-Myc	1	1. 29 ± 0.05	1. 04 ± 0.25
Gata-2	1	1. 24 ± 0.07	1. 27 ± 0.25
Pten	1	1.21 ± 0.1	1. 24 ± 0.1
Jak-2	1	1.2 ± 0.29	1.24 ± 0.45
Tal-1	1	1.15 ± 0.19	1.26 ± 0.29
Itga2b	1	1.1 ± 0.23	1 ± 0.32
Tr-Mpl	1	0. 96 ± 0.29	1.11 ± 0.18
miR-221	1	0.91 ± 0.19	1 ± 0.27
Fli-1	1	0.84 ± 0.11	0.98 ± 0.18
miR-451	1	0.78 ± 0.58	0.73 ± 0.94

Table 1: Gene expression variation according to stimulation by Notch ligand rDll1

G1ME cells were cultured during two days either on control IgG or on Notch ligand rDll1 in presence or absence of Notch inhibitor DAPT. The expression of the indicated genes (left column) was quantified by qRT-PCR. ΔCt of designated genes were normalized on β-Actin and IgG condition. Means and standard deviations from 3 independent experiments. Significant variations of rDll1 compared to IgG, or of rDll1+DAPT compared to rDll1 are shown by grey background.

Erythroid progenitors) expressing higher levels of c-Kit. In that case, a clear RNA POL II enrichment was observed on c-Kit promoter but this enrichment remained quite low as being only 4 fold above background and thus indicating a low loading of RNA POL II on the c-Kit gene (Figure 12 D).

Even if we could not quantify changes in RNA POL II recruitment on c-Kit gene by ChIP assay, we concluded from the induction of c-Kit primary transcripts that Notch pathway activation in G1ME cells upregulates c-Kit expression at the transcriptional level.

3.2.2. Looking for Notch-dependent regulation of known transcriptional regulators of c-Kit

As an attempt to identify the molecular actors allowing the induction of c-Kit gene transcription by Notch pathway, I adopted a gene/protein candidate strategy focused on several already known direct regulators of c-Kit gene transcription. For each candidate, I looked for putative changes in their expression using qRT-PCR and, when possible, directly quantified their enrichment on c-Kit gene using ChIP assays. Positive regulators candidates consisted in GATA-2 (Jing et al., 2008) and SCL (Lecuyer et al., 2002) which make part of the same complex that binds c-Kit gene on enhancer regions at position (-114), +5, +58 and +73 Kb (Jing et al., 2008) (Figure 13 A). Besides, knowing that Notch stimulation in G1ME cells induced the expression of Hes-1 which encodes for a transcriptional repressor, I analyzed the modulation of expression of c-Kit repressor such as miR-221 (Gabbianelli et al., 2010) or GATA-2 repressor miR-451 (Pase et al., 2009). miR-221 was an interesting candidate as it was shown to be negatively regulated by Notch pathway during angiogenesis (Nicoli et al., 2012). qRT-PCR analyses in G1ME cells stimulated during two days (rDll1) or not (IgG) by Notch revealed that none of these candidates' expression was modulated by Notch stimulation or by DAPT treatment (Table 1).

In a second complementary approach, I used ChIP assay to quantify the recruitment of GATA-2 and SCL on c-Kit promoter and enhancers in G1ME cells after a 2 days culture on either OP9 or OP9-Dll1 stromal cells. Chromatin was immuno-precipitated either by GATA-2 or SCL specific antibodies or by control rabbit antibody as described for previous RNA POL II ChIP assays. As above, primers amplifying the -146 Kb region were used as negative control for the binding of these two transcription factors. No significant recruitment of GATA-2

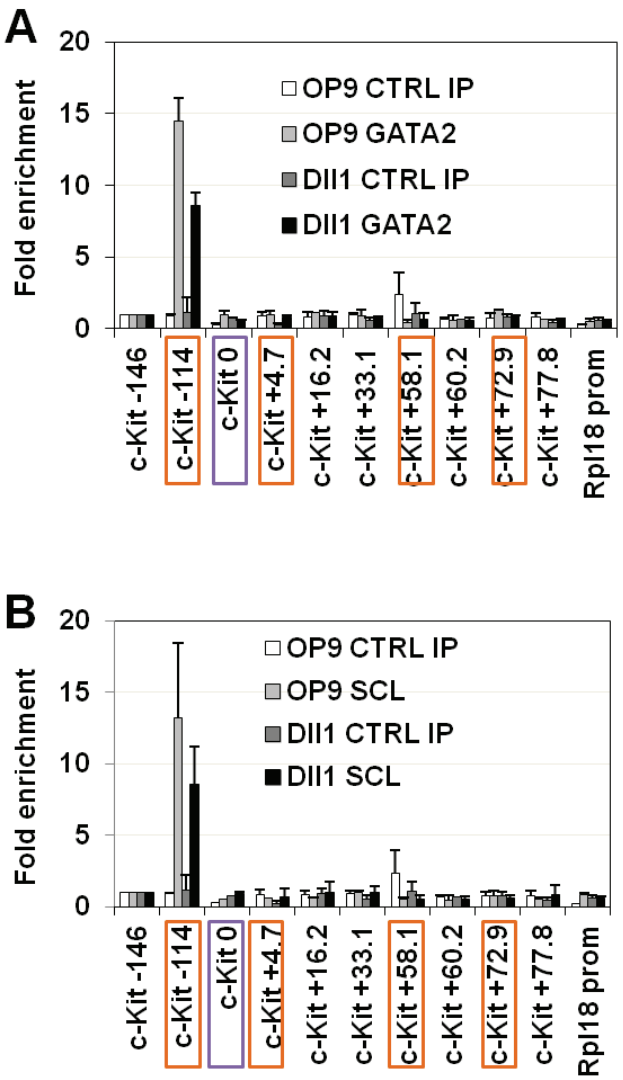

Figure 13: ChIP analyses of GATA-2 and SCL binding on c-Kit gene

Same protocol as in Figure 12 B except that immuno-precipitations were performed either using GATA-2 **(B)** or SCL specific antibodies **(C)** or control rabbit-IgG (CTRL IP).
Histograms show the relative enrichments of the different region for GATA-2 **(A)** or SCL **(B)** binding calculated after normalization to input chromatin and to the negative binding control region -146 Kb. Means and standards deviations from two independent experiments.

(Figure 13 A) or SCL (Figure 13 B) was detected on the c-Kit promoter and all along the c-Kit gene neither in unstimulated nor in stimulated G1ME cells. In contrast, strong enrichments indicating binding of both GATA2 and SCL were clearly detected on the -114 Kb enhancer in unstimulated cells (15 and 14 fold enrichments, respectively). Intriguingly however, these recruitments of GATA2 and SCL on the -114 enhancer were decreased in stimulated cells (down to 9 fold enrichment). Thus, although these results could confirm the expected binding of GATA2 and SCL to the -114 Kb c-Kit enhancer, we concluded that the transcriptional upregulation of c-Kit gene induced by Notch activation cannot be explained by the increased recruitment of either one of these two transcription factors.

In summary, we were able to show that the positive regulation of c-Kit by Notch originates at least partially at the transcriptional level but we failed to explain this increased transcription by an increased recruitment of the two known positive transcription regulators GATA2 or SCL. At this step of our study, we were aware that the pursuit of our investigation of additional candidates' regulators might be frustrating and possibly endless. Having no evident alternative to this candidate approach, we thus decided to refocus our project to investigate the putative contribution of c-Kit to the TPO-dependent proliferation of G1ME cells as well as the putative regulation of c-Kit by CD9.

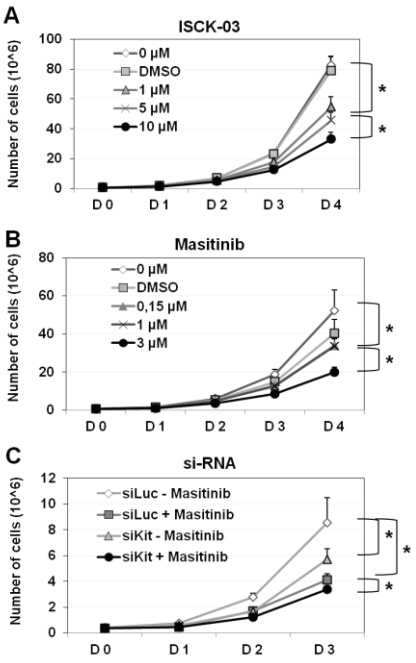

Figure 14: c-Kit is implicated in G1ME cells proliferation

A and B. G1ME cells were cultured in the presence of recombinant TPO with or without increasing doses of c-Kit inhibitors ISCK-03 (1.5 to 10 µM) **(A)** or Masitinib (0.15, 1 or 3 µM) **(B)** or control DMSO during 4 days. Cell concentration and cell viability were assessed every day of the kinetic and cell concentration was kept at 2.5 10^5 cells/ mL. The cumulated number of viable cells generated from the initial number of cells seeded was calculated based on the amplification factor from day to day. Mean and standard deviations from 3 independent experiments. Statistically significant differences of the cumulated number of cells at day 4 between the different conditions are indicated by asterisks (* $p < 1\%$). C. G1ME cells were submitted to 2 rounds of transfection at 24 hours interval with either c-Kit siRNA or control luciferase siRNA and re-seeded in medium containing TPO with or without 3 µM Masitinib. Figure shows the cumulated number of viable cells over 4 days after the first transfection.

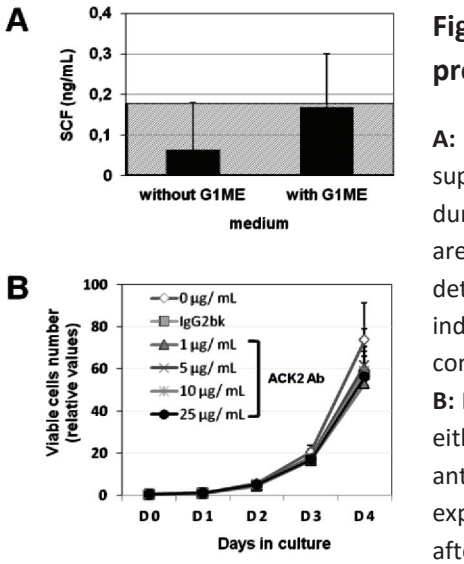

Figure15: SCF does not contributes to the TPO-dependent proliferation of G1ME cells

A: Quantification by Elisa immunoassay of SCF concentration in the supernatant of G1ME cells cultured in the presence of recombinant TPO during 24 hours compared to control medium without G1ME cells. Hatched area indicates the 95 % confidence interval of themean background value detected in control medium devoid of SCF. Mean and standard deviations of 4 independent experiments showing no significant difference of SCF concentration between normal medium and G1ME supernatant.

B: Proliferation curves of G1ME cells in the presence of recombinant TPO and either control IgG2bk or increasing doses of c-Kit blocking monoclonal antibody ACK2. Mean and standard deviations of three independent experiments showing no difference in the total number of cells generated after 4 days in the presence of control IgG2bk or ACK2 c-Kit antibody.

4. Study of c-Kit regulation by TPO, Notch and CD9 and its implication in G1ME cells proliferation/differentiation balance

TPO induces both proliferation and differentiation of megakaryocytic progenitors but the mechanisms underlying the switch between these two opposite effects remain poorly understood. Besides, the repression of c-Kit corresponds to a critical event signing the initiation of terminal differentiation of hematopoietic progenitors. These considerations prompted us to take advantage of the TPO-dependent proliferation of G1ME cells to investigate the putative contribution of c-Kit signaling in modulating the proliferative or differentiating effect of TPO. As reported above (Figure 11), we also noticed an intriguing divergent variations in the membrane expression levels of c-KIT and CD9 following the activation of Notch pathway in G1ME cells. This intriguing observation prompted us to investigate the putative involvement of CD9 in the down regulation of c-Kit. The results of these investigations are presented in a manuscript (manuscript 2) in which we propose a new model that could explain the dual function of TPO based on a dynamic regulatory interplay between TPO signaling, c-Kit and CD9. The full version of this manuscript is presented in the next section from which the main results are summarized in the following paragraphs.

First, I investigated the actual implication of c-Kit in G1ME cells proliferation and survival. For that purpose, I adopted two different strategies either the inhibition of c-Kit activity using specific chemical inhibitors or the inhibition of c-Kit expression by specific siRNA targeting c-Kit transcripts. The two strategies showed convergent results, as both the treatment of G1ME cells by ISCK03 or Masitinib inhibitors as well as the reduction of c-Kit expression by specific siRNA induced a dose dependent decrease of cell proliferation (Figure 14) with minimal effect on cell survival. These results demonstrate the active implication of c-Kit in G1ME cells proliferation.

Given that G1ME cells proliferate in the presence of TPO only but not in the presence of SCF, we were interested to identify the mode of activation of c-Kit. For that purpose, I looked for the putative secretion of SCF by G1ME cells. However, ELISA immuno-assay performed on G1ME cells conditioned medium revealed no detectable levels of SCF (Figure

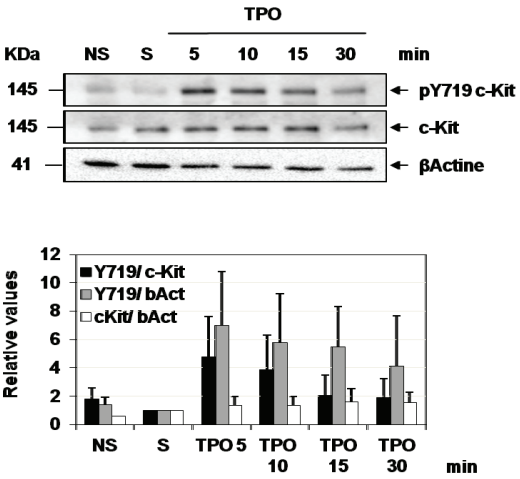

Figure 16: Stimulation of G1ME cells by TPO induces c-Kit receptor phosphorylation

G1ME cells were starved for 6 hours without TPO then re-stimulated by TPO during 5, 10, 15 or 30 minutes, followed by Western-Blot analysis of Y719 phosphorylated c-Kit, total c-Kit and β-Actin. NS: Non Starved cells; S: Starved cells. Upper part shows typical Western-Blot obtained after revelation of the same membrane with specific antibodies directed against either phosphorylated c-Kit on tyrosine Y719, or total c-Kit or β-Actin used as loading control. Histogram shown in lower part displays the variations of phosphorylated or total c-Kit or the ratio of phosphorylated over total c-Kit signal normalized to the ratio determined in the starved condition (mean and standard deviations from three independent experiments).

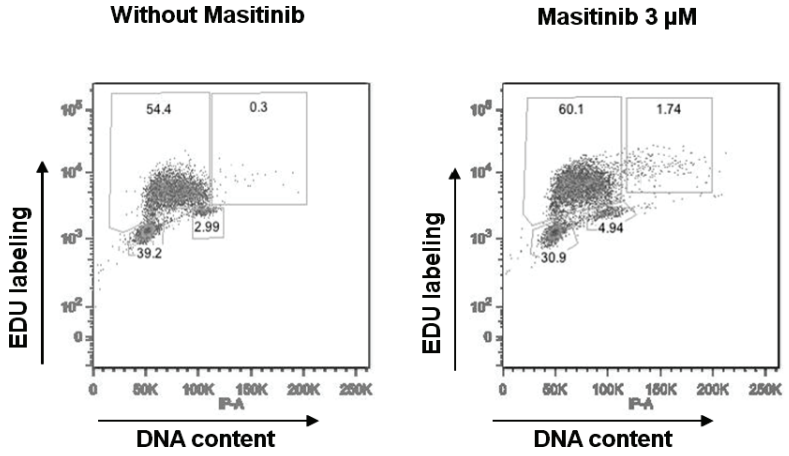

Figure 17: Masitinib stimulates polyploidization of G1ME cells

FACS dot-plots for EdU incorporation and DNA content.G1ME cells were cultured in the presence of Cos-TPO conditioned medium with or without Masitinib as indicated. Cell cycle analyses were performed by FACS after EdU pulse labeling followed by double labeling for EdU incorporation by Click-it reagent coupled to Alexafluor-647 and DNA content by propidium iodide. Numbers indicate the percentage of cells identified in the different phases of cell cycle including cells undergoing polyploidization (EdU labeled cells with DNA content higher than 4 N).

15 A). Moreover, blocking SCF to c-Kit interaction using ACK2 monoclonal c-Kit antibody did not affect G1ME cells proliferation (Figure 15 B), thus excluding a paracrine mechanism.

Thus, we hypothesized that TPO is able to directly activate c-Kit. To test this hypothesis, I analyzed by Western-Blot the levels of phosphorylation of c-Kit in response to TPO stimulation following G1ME cells starvation. These analyses demonstrated a significant increase in the proportion of Y719 phosphorylated c-Kit protein in response to TPO stimulation (Figure 16). To our knowledge, this result is the first demonstration that TPO can directly activate c-Kit phosphorylation.

At this step, these results established the implication of c-Kit in the TPO-dependent proliferation of G1ME cells. In order to determine whether c-Kit may be also implicated in the repression of G1ME cells differentiation, cells were treated with the c-Kit inhibitor the Masitinib and their cell cycle status was analyzed by FACS following the double labeling for EdU incorporation as well as DNA content using PI (Propidium Iodide). This analysis revealed that Masitinib actually stimulates the polyploidization of G1ME cells as indicated by an increased proportion of 4N cells still undergoing DNA synthesis (Figure 17). These results indicate that c-Kit participates to G1ME cells proliferation as well as restricts their spontaneous megakaryocytic differentiation.

Finally, I tested the hypothesis of a direct inhibition of c-Kit by CD9. For that purpose, G1ME cells were transfected by CD9 specific siRNA or control anti-Luciferase si-RNA and analyzed by flow cytometry the expression of c-Kit and CD9. I observed a strong negative correlation between CD9 and c-Kit expression as attested by the reciprocal decrease of CD9 and increase of c-Kit median of fluorescence (Figure 18). These results demonstrate that CD9 levels negatively regulate the levels of c-Kit expressed at the cell surface of G1ME cells.

In summary, this study allowed us to determine that c-Kit participates to the proliferation of G1ME cells following its activation not by its canonical ligand SCF, but directly by TPO. Furthermore, c-Kit restricted the low tendency of G1ME cells to differentiate along the megakaryocytic lineage. Additionally, this study evidenced that CD9 levels negatively regulate the levels of c-Kit expressed at the cell surface of G1ME cells.

Based on these results, we suggest a new model that could explain the dual function of TPO during the switch between proliferation and differentiation of megakaryocytic progenitors. According to this model, the proliferation of megakaryocytic progenitors would proceed under TPO-mediated c-Kit stimulation until reaching a threshold level of CD9

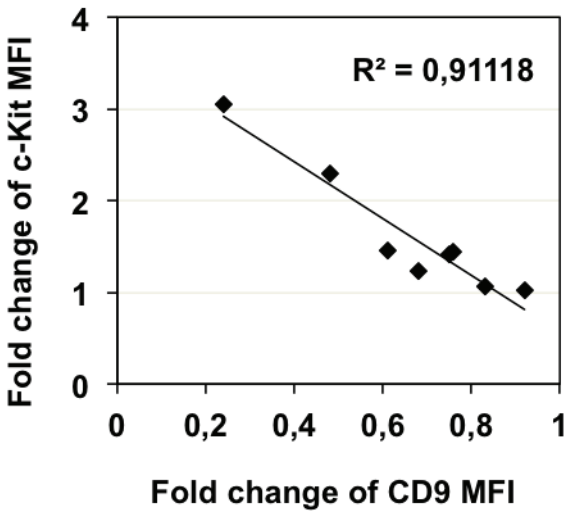

Figure 18: CD9 actively contributes to reduce c-Kit levels

G1ME cells were submitted to two rounds of transfection at 24 hours interval with either CD9 siRNA or control luciferase siRNA and re-seeded in medium containing TPO. The figureshows the compilation of data from three independent transfection experiments showing the striking correlation between the fold reduction of CD9 median of fluorescence and the fold increase in c-Kit median of fluorescence relative to si-Luciferase control condition.

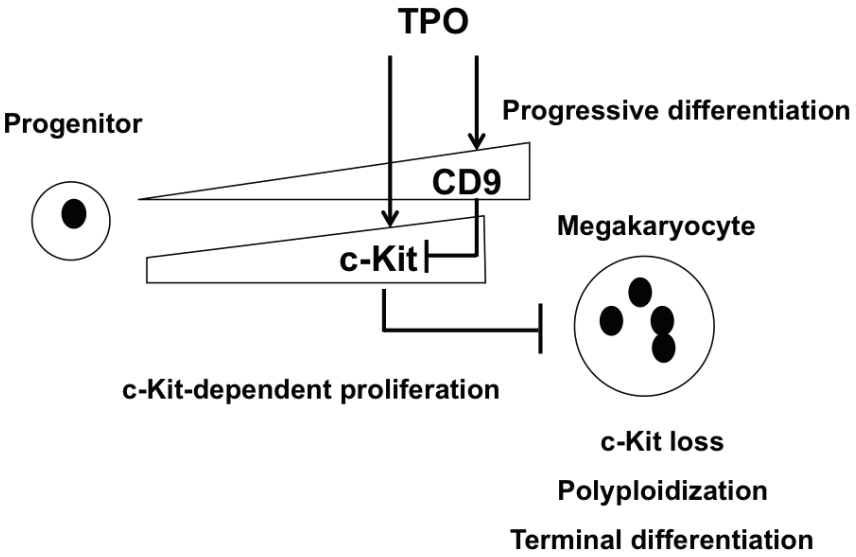

Figure 19: Working model of the dual control of c-Kit by TPOduring megakaryopoiesis

Our results showed that part of the proliferative effect of TPO is mediated through the activation of c-Kit signaling that concomitantly contributes to inhibit CD9 expression and polyploidization, while c-Kit itself is under the negative control of CD9. Based on these findings, we suggest that TPO stimulates the proliferation of megakaryocytic progenitors while progressively increasing CD9 expression until reaching a threshold level sufficient to inhibit c-Kit allowing in turn proliferation arrest and terminal differentiation.

sufficient to lower the expression of c-Kit at the cell surface and thereby to suppress the proliferative effect of TPO at the benefit of terminal differentiation (Figure 19).

MANUSCRIPT2:
c-Kit activation contributes to the TPO-dependent proliferation of megakaryocytic progenitors while c-Kit expression is limited by CD9 levels

c-Kit activation contributes to the TPO-dependent proliferation of megakaryocytic progenitors while c-Kit expression is limited by CD9 levels

Authors: Azza Chaabouni. Boris Guyot. Michèle Weiss-Gayet.and François Morlé

Authors' affiliation: Centre de Génétique et de Physiologie Moléculaire et Cellulaire. CGPhyMC. CNRS UMR 5534. Université Claude Bernard Lyon1. 16 Rue Dubois. 69622 Villeurbanne France

Running head: TPO activates c-Kit and CD9 limits its expression

Corresponding author: François Morlé.Centre de Génétique et de Physiologie Moléculaire et Cellulaire. CGPhyMC. CNRS UMR 5534. Université Claude Bernard Lyon1. 16 Rue Dubois. 69622 Villeurbanne France

Word counts:

Abstract: 250

Main text: 3899

Figures number: 8

Supplementary figures: 2

Supplementary tables: 2

Acknowledgements:

This work has been supported by grants from the CNRS and Université Claude Bernard Lyon1 and by specific grants from the Ligue Nationale contre le Cancer (Equipe labellisée 2009-2012 and Comités du Rhône. de la Drôme et du Cantal). MW and BG are permanent employees of CNRS while FM is permanent employee of INSERM. AC PhD student has been supported by a three years salary from the Ligue Nationale contre le Cancer (2011-2014) and by a 6 months salary from the Société Française d'Hématologie (2014-2015). Authors acknowledge Thomas Mercher for helpful suggestions and providing us G1ME cells, Bénédicte Chazaud for her help in recently hosting this project in her team as well as Didier Negre and Caroline Costa from UMS 3444 for lentiviral vectors production.

Abstract:

Despite the known dual contribution of Thrombopoietin (TPO) to both proliferation and terminal differentiation of megakaryocytic progenitors, the molecular event(s) controlling the switch between proliferation and differentiation remain poorly understood. In the present study, we addressed this question by exploring the contribution of c-Kit signaling to the TPO-dependent proliferation of G1ME cells (GATA1 deficient MEP progenitors immortalized in the presence of TPO). Using c-Kit signaling inhibitors Masitinib and ISCK03 or siRNA mediated knock down of c-Kit expression, we demonstrated that c-Kit signaling significantly contributes to the proliferative effect of TPO. In agreement with this finding, we showed that stimulation by TPO actually activates c-Kit phosphorylation in the absence of exogenous or secreted SCF. Moreover, we showed that CD9 expression and polyploidization of G1ME cells in the presence of TPO are induced by Masitinib, thus indicating that TPO-mediated c-Kit activation also contributes to limit their differentiation. Finally, we showed that siRNA mediated knock down of CD9 increased membrane expression of c-Kit in a strikingly dose-dependent manner. Taken together, these results indicate that TPO alone is able to activate c-Kit phosphorylation which in turn contributes to stimulate proliferation and concomitantly to inhibit polyploidization while c-Kit expression itself is limited by CD9 levels. Based on these results, we suggest that the proliferation of megakaryocytic progenitors proceeds under TPO-mediated c-Kit stimulation until reaching a threshold level of CD9 sufficient to lower the expression of c-Kit at the cell surface and thereby to suppress the proliferative effect of TPO at the benefit of terminal differentiation.

Introduction

During megakaryopoiesis, committed megakaryocytic progenitors undergo several divisions before terminal differentiation associated with polyploidization (1). Both proliferation and differentiation steps are under the main control of thrombopoietin (TPO) that acts through its specific receptor c-MPL (1-4). The molecular mechanisms underlying this dual function of TPO as well as the signal(s) inducing commitment from proliferation to terminal differentiation remain poorly understood.

One important change in the signaling events downstream to TPO/c-MPL allowing terminal differentiation is the sustained activation of the MAPK/ERK pathway that has been shown to be required for polyploidization (5-7). However, the underlying mechanisms controlling this change in signalization remains unknown.

Another important cytokine involved in the proliferation step of megakaryocytic progenitors is Stem Cell Factor (SCF) acting through its specific receptor c-Kit (8). While SCF and TPO synergize to stimulate the proliferation of megakaryocytic progenitors (9), terminal differentiation actually coincides with the drastic down-regulation of c-Kit expression at both transcriptional and protein levels (10). Moreover, several evidences indicate that c-Kit signaling not only contributes to stimulate proliferation but also concomitantly inhibits differentiation. Indeed, knock down of c-Kit accelerates the differentiation of megakaryocytic progenitors generated by human $CD34^+$ pluripotent stem cells in vitro as well as terminal differentiation of K562 cells induced by PMA (10). Transcriptional repression of c-Kit gene can be at least partially explained by the repressive effect of GATA-1 which levels increase during progression towards terminal megakaryocytic differentiation (11). Similarly, a recent study has shown that the human ZNF16 transcription factor which levels also increase during progression towards megakaryocytic differentiation is also actively involved in the active repression of c-Kit transcription (10). Unfortunately, given the lack of conservation of Znf16 in mouse (12), it remains currently unknown whether a similar factor is also involved in c-Kit repression during murine megakaryopoiesis. Interestingly, other recent studies have shown that hematopoietic stem cells (HSC) displaying the highest levels of c-Kit expression turned out to be strongly biased towards megakaryocytic differentiation (13). All together these data indicate that while c-Kit actively contributes to the proliferation step of megakaryocytic progenitors and its increasing levels accompany their progression towards terminal

differentiation, an active program is concomitantly activated that leads to its transcriptional repression and is required to allow terminal differentiation. Whether additional changes accompanying progression towards megakaryocytic differentiation further contribute to switch off c-Kit signaling remains an interesting possibility. For example, CD9 whose expression increases during progression towards megakaryocytic differentiation (14, 15), has been shown to sequester a fraction of c-Kit receptors into tetraspanin network thus rendering it unresponsive to SCF stimulation in MO7e cells (16).

In the present study, we used the GATA1 deficient G1ME cells (17) that proliferate in the presence of TPO only, as a cellular model to investigate the putative contribution of c-Kit signaling to the proliferative effect of TPO as well as the putative contribution of CD9 in the negative regulation of c-Kit. We showed that a significant part of the proliferative effect of TPO is actually mediated through the activation of c-Kit receptor that concomitantly contributes to inhibit polyploidization and that CD9 actively contributes to reduce c-Kit expression. Based on these results, we suggest that TPO dynamic control of proliferation and terminal differentiation during megakaryopoiesis relies on its dual property to activate c-Kit signaling contributing to proliferation instead of differentiation and to activate CD9 allowing the inhibition of c-Kit once a sufficient threshold level of CD9 is reached.

Material and Methods

Cell culture

G1ME cells (GATA-1 -/- Megakaryocyte Erythrocyte) were kindly provided by T. Mercher. G1ME cells were derived from GATA-1 deficient murine embryonic stem cells and immortalized in the presence of TPO the only cytokine needed for their proliferation and survival (17). G1ME cells were cultured in α-MEM Glutamax medium (GIBCO. Life Technologies) supplemented with 20 % fetal calf serum (PAA) and 1 % Peni-Streptomycin (PAA) in the presence of either 1% of Cos7-TPO conditioned medium (Kindly provided by T. Mercher) or 20 ng/ mL of murine recombinant TPO. Cells were cultured in 5 % CO_2 at 37°C and maintained between 5 10^5 and 1.5 10^6 cells/ mL by daily dilution. Inhibition of c-Kit signaling was performed by adding either chemical inhibitors Masitinib (18) (Clinisciences). [4-t- butylphenyl]-N-(4-imidazol-1-yl phenyl)sulfonamide (ISCK03; Sigma) (19-21) or c-Kit blocking antibody ACK2 (eBioscience).

Proliferation assay

Cell concentration was determined by double counting on hemocytometer. Cell viability was assessed by Trypan Blue exclusion (Sigma). Each day of the kinetic, 2.5 10^5 G1ME cells of each condition were reseeded in new wells. The cumulative numbers of viable cells were calculated from the increase of cell density determined after each passage.

Starvation and re-stimulation assays

A 5 to 6 hours starvation time was determined in pilot experiments as the maximal time allowing no more than 5% of starvation-induced cell death of G1ME cells as determined by Trypan blue exclusion in complete medium without TPO. Equal numbers of starved cells were harvested and resuspended in complete medium supplemented with 1 % TPO-conditioned medium or with 20 ng/mL of murine recombinant TPO for 5/ 10/ 15/ 30 minutes of re-stimulation at 37°C. Re-stimulation was stopped by adding ice-cold PBS containing a full cocktail of protease inhibitors (Complete mini EDTA-free tablets Roche) and phosphatase inhibitors (1 mM sodium pyrophosphate. 25 mM sodium beta-glycerophosphate and 50 mM of sodium fluoride (Sigma)).

Western-Blot

Whole cell lysates were prepared by lysing equal number of cells for each condition in Laëmmli lysis buffer supplemented with a full cocktail of protease inhibitors (Complete mini EDTA-free tablets. Roche) and phosphatase inhibitors (1 mM sodium pyrophosphate, 25 mM sodium beta-glycerophosphate and 50 mM of sodium fluoride). Proteins were denatured 5 minutes at 95 °C and stored at (-80 °C) until analysis. Proteins were separated on pre-casted 4-12% SDS-PAGE (Biorad) then transferred on PVDF membrane using Trans-Blot Turbo Transfer System (Biorad). Membranes were pre-incubated for 1 hour in blocking solution (5 % bovine serum albumin (BSA) in TBS-T) followed by overnight incubation at 4 °C with appropriate dilutions of c-Kit (Cell Signaling # 3074) or Y719 phospho-c-Kit (Cell Signaling # 3391) rabbit antibodies. After three washes in TBS-T (Tris Buffered Saline: 50 mM Tris pH 7.6. 300 mM NaCl and 0.1 % Tween-20), membranes were then incubated for 1 hour at room temperature (RT) with Goat anti-Rabbit coupled to horseradish peroxidase and washed three times in TBS-T. Signals were revealed using Clarity ECL substrate (Biorad) and recorded on Chemidoc instrument (Biorad) and quantified using the Image Lab software (Biorad). After c-

Kit signals recording, membranes were stripped 12 minutes at 50°C under shaking in strip buffer (62.5 mM Tris/HCl pH 6.8. 2% SDS and 100 mM β-mercaptoethanol). Stripped membranes were then preincubated for 30 minutes in 5 % nonfat-milk, incubated 1 hour at RT with anti-β-Actin (Millipore #MAB 1501) mouse antibody revealed and recorded as described above after 1 hour incubation at RT with Goat anti-Mouse secondary antibody coupled to horseradish peroxidase.

SCF dosage by ELISA

The supernatants of 2.10^5 G1ME cells cultured during 24 or 48 hours were harvested and SCF levels were determined on 100 □ L duplicate aliquots using commercial SCF mouse Elisa kit (ab100740; Abcam) following the recommendations of the manufacturer. Optical density at 450 nm was recorded on a Viktor luminometer (Perkin Elmer) and SCF concentration in each sample estimated by reference to standard curve established using murine recombinant SCF.

Flow cytometry

2.10^5 cells were washed twice in PBS containing 0.5 % BSA (Sigma) and 2 mM EDTA (PBE). Following 10 minutes of blocking with murine Fc-Block (Milteny), cells were incubated during 30 minutes with anti-CD117-PE, anti-CD117-APC, anti-CD9-PE, anti-CD9-APC or anti-CD110-PE fluorescent antibodies or with the corresponding fluorescent control IgGs. All antibodies were purchased from eBioscience. Labeled cells were washed and re-suspended in PBE buffer before analysis on FACS Aria II instrument (Becton Dickinson). Fluorescence signals were recorded on 10 000 viable labeled cells and analyzed using BDFACS-DIVAv5 and Flow Jo softwares.

Cell cycle analyses

Cells were plated in duplicate 48 hours before treatment then cultured in presence or absence of EdU (5-ethynyl-2'-deoxyuridine) at 10 µM during one hour. Cell cycle analysis was then performed using the Click-iT® EdU Alexa Fluor® 647 Flow Cytometry Assay Kit following the recommendations of the supplier (Molecular Probes, Life Technologies). Briefly, labeled cells were harvested, fixed and permeabilized to allow the detection of EdU by picolyl azide which is coupled to Alexa-Fluor-647 dye. After a 30 minutes treatment with RNase at 1 mg/mL, propidium iodide was added at 50 µg/mL just before analysis on FACS

Aria II flow cytometer (Becton Dickinson). Cell cycle analyses were performed using Flow Jo software.

RNA extraction and qRT-PCR

RNA was extracted from 10^5 cells using RNeasy Plus Micro Kit (Qiagen # 74034) following the manufacturer's recommendations. 100 ng of RNA were reverse transcribed using QuantiTect Reverse Transcription kit (Qiagen # 205313) followed by qPCR using LightCycler 480 SYBR Green Master I kit (Roche) on Mx 3000 version 6.22 thermocycler and analyzed on Mx-Pro-3000P software (Stratagen). Sequences of qRT-PCR primers are given in supplementary Table S1.

siRNA transfection

5.10^5 G1ME cells resuspended into 100 µL of Amaxa kit V reagent (Lonza) were transfected with 20 µM siRNA using program G-16 on Nucleofector device (Lonza). Cells were resuspended in full medium which was changed after 4 hours. After 24 hours, the same round of transfection was performed. At the indicated times following first transfection, cells were counted, their viability assessed by Trypan blue exclusion and then were harvested for qRT-PCR and flow cytometry analyses.

Statistics

Data were analyzed using Student t-test. Differences were considered significant if p-value was below 5 %.

Results

1- c-Kit signaling contributes to the TPO-dependent proliferation of G1ME cells

As previously reported by others (17), we found that G1ME cells were unable to survive and to proliferate in the presence of SCF only (Figure S1). However, this result did not exclude the putative contribution of c-Kit signaling to the proliferation of G1ME cells in response to TPO. In a first approach to address this possibility we investigated the effect of the two specific c-Kit inhibitors ISCK03 (19-21) and Masitinib (18) on the proliferation and viability of G1ME cells in the presence of TPO (Figure 1). The addition of increasing low doses of

ISCK03 (ranging from 1 to 10 □ M) led to a progressive decrease of G1ME cells proliferation reaching a 60% reduction of viable cells generated after a 4 days culture in the presence of 10 □ M ISCK03 (Figure 1A). Likewise, the addition of increasing low doses of Masitinib (ranging from 0.15 to 3 μM) led to a significant and dose-dependent decrease of G1ME cells proliferation reaching a 60% reduction of cumulated viable cells number generated after a 4 days culture in the presence of 3 □ M Masitinib (Figure 1B). Western blot analyses confirmed the presence of phosphorylated c-Kit protein at tyrosine residue 719 attesting of c-Kit activation and this phosphorylation was reduced by a treatment with c-Kit inhibitors ISCK03 (10 □ M) and Masitinib (3 □ M) (0.4 and 0.45 fold decrease compared to untreated cells. respectively; Figure 2B). Interestingly, FACS analyses further showed that Masitinib (Figure 2A, right panel) but not ISCK03 (Figure 2A, left panel) also led to a marked reduction (> 50%) of c-Kit levels expressed at the cell surface. In a second complementary approach, we decided to investigate the effect of reducing c-Kit expression directly at the transcriptional level by RNA interference. For that purpose, G1ME cells were submitted to two rounds of transient transfection at 24 hours interval using c-Kit specific siRNA or control luciferase siRNA. During the three days following the second transfection, cell proliferation was assessed and c-Kit transcripts and c-Kit cell surface levels were quantified by q-RT-PCR and FACS analysis, respectively (Figure 3). This protocol allowed us to obtain a transient downregulation of both c-Kit mRNA (Figure 3C) and c-Kit protein membrane levels (Figure 3D) which were both maximal (-60%) at 48 hours following the first round of transfection and approximately returned to initial levels at 96h. This transient downregulation of c-Kit was found associated with a significant reduction in the cumulated total number of viable cells generated during the two days following the second transfection (Figure 3A and 3B) with minimal reduction of cell viability (5 % decrease compared to untreated cells; data not shown). Combining c-Kit siRNA transfection with Masitinib treatment at 3 μM led to a greater reduction of c-Kit expression that was associated with greater reduction of cell proliferation (Figure 3A and 3B). Taken together, these results established that G1ME cells cultured in the presence of TPO displays activated c-Kit and that c-Kit activation significantly contributes to their proliferation despite the absence of added SCF.

2- TPO activates c-Kit receptor phosphorylation

Having established the contribution of c-Kit activation to the TPO-dependent proliferation of G1ME cells in the absence of added SCF, we tried to identify the origin of this c-Kit activation. One first possibility could be that c-Kit was activated through the secretion of SCF by G1ME cells. However, immuno-detection of SCF failed to reveal any significant SCF levels above 0.2 ng/mL (corresponding to the lower limit of SCF detection by Elisa test) in the conditioned medium of G1ME cells cultured in the presence of TPO (Figure 4A). Most importantly, addition of ACK2 c-Kit antibody, known to block the binding of SCF to c-Kit receptor (22), did not affect G1ME cells proliferation (Figure 4B). We therefore investigated the alternative possibility that TPO itself could contribute to c-Kit activation. For that purpose, we performed kinetics analyses of c-Kit phosphorylation on tyrosine 719 in G1ME cells that have been re-stimulated by either SCF or TPO after a 6 hours period of starvation in the absence of cytokine. Our results clearly showed the transient increase in c-Kit phosphorylation in response to TPO (Figure 5A) with a maximal of 5 fold mean increase after 5 minutes of TPO re-stimulation followed by gradual return to basal levels during the next 10 minutes. Transient increase in c-Kit phosphorylation was also observed in response to SCF with similar kinetics and no significantly different maximal mean of stimulation (Figure 5B). These results thus indicated that TPO actively contributes to c-Kit activation.

3- c-Kit activation restricts megakaryocytic differentiation

Having shown that c-Kit activation contributes to the TPO-dependent proliferation of G1ME cells, we next wanted to know whether c-Kit activation could also restrict their megakaryocytic differentiation. Terminal megakaryocytic differentiation involves two main aspects including increased transcription of late megakaryocytic genes and polyploidization. We therefore investigated whether c-Kit inhibition by Masitinib could stimulate the expression of late megakaryocytic genes and polyploidization in G1ME cells cultured in the presence of TPO. Interestingly, Masitinib treatment significantly increased Pf4 transcripts in G1ME cells (Figure 6A). Progression towards polyploidization was assessed by looking for cells with DNA content higher than 4 N and still undergoing DNA synthesis. For that purpose we performed pulse incorporation with EdU followed by its labeling as well as DNA content labeling using propidium iodide before FACS analyses (Figure 6B). Untreated G1ME cells contained at most 0.3 % of EdU labeled cells with DNA content higher than 4N (Figure 6B

left panel). In clear contrast, the low frequency of polyploid cells increased by more than 5 fold reaching 1.7 % when G1ME cells were treated by Masitinib (Figure 6B right panel). Taken together, these results thus indicated that c-Kit inhibition by Masitinib drives G1ME cells towards megakaryocytic terminal differentiation.

4- CD9 levels actively contribute to reduce c-Kit expression

A previous study performed in MO7e megakaryoblastic cells showed that a significant fraction of c-Kit receptor present at the cell surface is actually trapped into tetraspanins network notably composed of CD9 and that this fraction cannot be activated by SCF in contrast to the untrapped fraction (16). Moreover, when compared to the SCF-dependent cell lines EML (23) and ESRE2 (24), SCF-unresponsive G1ME cells appeared to display the highest level of CD9 and lowest level of c-Kit expression (Figure S2). Given these observations, we sought to determine whether CD9 could be actively involved in the negative regulation of c-Kit. To address this question, G1ME cells were submitted to two rounds of transient transfection using CD9 specific siRNA or control luciferase siRNA at 24 hours interval and c-Kit and CD9 expression levels were quantified by FACS during the next three days. This protocol allowed us to obtain efficient but transient downregulation of CD9 expression (Figure 7A) which progressively recovered initial levels. Interestingly, this transient decrease in CD9 expression was accompanied by a transient but significant increase of c-Kit expression two days following the first round of transfection (Figure 7A). Most interestingly, by compiling the results of several transfection experiments we found a striking correlation between the extent of CD9 decrease and the extent of c-Kit increase (Figure 7B). These results thus indicated that CD9 actively contributes to limit c-Kit expression at the cell surface of G1ME cells.

Discussion

G1ME cells result from the spontaneous unlimited outgrowth of bipotent MEP progenitors derived from Gata1 -/- ES cells induced to differentiate in the presence of TPO (17). Importantly, G1ME cells are still fully competent to terminally differentiate into both erythroid and megakaryocytic lineages upon re-expression of GATA1 (17). For these reasons G1ME cells remain a pertinent and useful model to understand the control of proliferation and

differentiation of bipotent MEP progenitors (17). In that context, our present study provides several new original findings showing the SCF-independent dual contribution of c-Kit in stimulating proliferation at the expense of terminal megakaryocytic differentiation downstream to TPO as well as its unexpected down regulation by CD9.

Several experimental evidences demonstrate that c-Kit activation does contribute to the stimulation of proliferation in response to TPO and in a SCF-independent manner. Indeed. the inhibition of c-Kit activity using either one of two different c-Kit specific chemical inhibitors ISCK03 and Masitinib (Figure 1) and most importantly the direct knock-down of c-Kit expression by specific siRNA (Figure 3) both induced a significant reduction of the TPO-dependent proliferation of G1ME cells. On one hand, the absence of detectable levels of SCF in the supernatant of G1ME cultures, as well as the absence of significant effect of ACK2 (anti-c-Kit antibody blocking the binding to SCF) (22) strongly indicate that the c-Kit contribution to cell proliferation is not mediated by its direct activation by secreted SCF. On the other hand, our results showing the transient phosphorylation of c-Kit at tyrosine residue Y719 upon re-stimulation of starved cells by TPO clearly indicate that TPO does contribute to c-Kit activation. Taken together our results strongly suggest that TPO-dependent proliferation is at least partially mediated through the activation of c-kit signaling. However, the additional contribution of low level of constitutive c-Kit activation cannot be formally excluded.. This raised in turn the question of how TPO leads to c-Kit activation. Interestingly, a few number of ligands other than SCF have been reported to be able to activate c-Kit including EPO (25), IL3 (26) or IL33 (27). In all cases, physical proximity of c-Kit with the specific receptors of these alternative activating ligands could be documented and would supposedly favor the trans-phosphorylation of c-Kit at the plasma membrane. Intriguingly, TPO has also been reported to stimulate the EPOR-dependent proliferation of BAF3/EPOR cells in the absence of its own receptor c-MPL thus suggesting that TPO can bind and activate EPOR (28). Nevertheless, previous studies failed to evidence the direct binding of TPO or its ability to compete with EPO for the binding to EPOR (29). Although the physical and functional cooperation between EPOR and c-Kit are already well established, further experiments are still required to investigate the physical proximity between c-Kit and c-MPL as well as whether c-Kit activation by TPO is initiated by the binding of TPO to c-MPL, EPOR or possibly to another receptor.

Our finding that Masitinib slightly enhances Pf4 transcript levels and induces G1ME cells polyploidization is an indication that TPO-mediated c-Kit activation not only stimulates

proliferation but could also contribute to inhibit terminal megakaryocytic differentiation. This finding is in agreement with a previous study showing that another tyrosine kinase receptors' inhibitor Dasatinib also enhances megakaryocytic differentiation *in vivo*(30). One important remaining question is to determine whether this stimulation of megakaryocytic differentiation by Masitinib or Dasatinib is really due to c-Kit inhibition or to the inhibition of another kinase such as Lyn kinase as previously suggested (30-32). Actually, the repressive effect of Lyn on megakaryocytic differentiation, as well as the inhibition of Lyn by Dasatinib and Masitinib is well established (31, 32). However, two recent studies cast some doubt on the real functional inhibition of Lyn by Masitinib at least in erythroid cells. Indeed, if Lyn is inhibited by Masitinib and given that Lyn kinase down-regulates c-Kit (33), one would expect that Masitinib leads to the up-regulation of c-Kit, though the quite opposite effect has been reported in the erythroid cell line UT7-EPO (34). In agreement with this latter study, we also observed the down regulation of c-Kit in response to Masitinib treatment of G1ME cells. Moreover, Masitinib has been shown to accelerate terminal erythroid differentiation in the presence of EPO highlighting an interesting parallel with the stimulating effect of Masitinib on megakaryocytic differentiation that could be related to the common property of EPO and TPO to activate c-Kit. We therefore favor the interpretation that the stimulation of megakaryocytic differentiation by Masitinib is probably not mediated through the inhibition of Lyn, but additional experiments are still required to firmly establish the implication of c-Kit inhibition.

The third major original finding of our study is the intriguing implication of CD9 in the down regulation of c-Kit present at the cell membrane. The evidence for this implication is based on a clear-cut dose-dependent increase of c-Kit expression that was induced by CD9 knock-down when using specific siRNA (Figure 7). Interestingly, a previous study already reported that a fraction of c-Kit receptor can be trapped into tetraspanin network including CD9 in MO7e megakaryoblastic cells (16) and showed that this trapped fraction of c-Kit displayed low constitutive phosphorylation but no kinase activity and was unresponsive to SCF stimulation. Besides, CD9 is known as the major component of exosomes and recent studies reported that c-Kit can be secreted with exosomes by different types of cells (35-38). Moreover, exosomal secretion of several other known interactors of CD9, like □-catenin (39) or EGFR (40) have been shown to be modulated by changes in CD9 levels whereas loss of CD9 has been associated with a decreased production of exosomes (39). All together, these data suggest the exciting possibility that CD9 levels might modulate c-Kit levels present at the membrane

through the regulation of its secretion by exosomes. Importantly, a very recent study evidenced a surprising decrease in CD9 membrane expression during primary myelofibrosis megakaryopoiesis and demonstrated the implication of CD9 in dysmegakaryopoiesis and in reciprocal interactions between stroma and progenitors in this pathology (41). Our present study raises the other intriguing possibility that these pathological consequences of reduced CD9 levels may be related to the upregulation of c-Kit and/or altered exosomes secretion by megakaryocytic progenitors or even altered exosome-mediated exchanges between megakaryocytic progenitors and stroma cells.

In summary, the three most important findings of this study are that TPO-induced c-Kit activation contributes to stimulate proliferation and at the same time to restrict terminal megakaryocytic differentiation, whereas CD9 which is massively increased during terminal differentiation is involved in the down regulation of c-Kit. Based on these findings, we suggest the working model wherein terminal megakaryocytic differentiation may be induced once progenitors reach a threshold level of CD9 sufficient to stop the proliferation effect of TPO through the down regulation of c-Kit (Figure 8).

References

1. Deutsch VR, Tomer A. Megakaryocyte development and platelet production. British journal of haematology. 2006 Sep;134(5):453-66.

2. Kuter DJ. Milestones in understanding platelet production: a historical overview. British journal of haematology. 2014 Apr;165(2):248-58.

3. Chou FS, Mulloy JC. The thrombopoietin/MPL pathway in hematopoiesis and leukemogenesis. Journal of cellular biochemistry. 2011 Jun;112(6):1491-8.

4. Kuter DJ. The biology of thrombopoietin and thrombopoietin receptor agonists. International journal of hematology. 2013 Jul;98(1):10-23.

5. Fichelson S, Freyssinier JM, Picard F, Fontenay-Roupie M, Guesnu M, Cherai M, et al. Megakaryocyte growth and development factor-induced proliferation and differentiation are regulated by the mitogen-activated protein kinase pathway in primitive cord blood hematopoietic progenitors. Blood. 1999 Sep 1;94(5):1601-13.

6. Guerriero R, Parolini I, Testa U, Samoggia P, Petrucci E, Sargiacomo M, et al. Inhibition of TPO-induced MEK or mTOR activity induces opposite effects on the ploidy of human differentiating megakaryocytes. Journal of cell science. 2006 Feb 15;119(Pt 4):744-52.

7. Rojnuckarin P, Drachman JG, Kaushansky K. Thrombopoietin-induced activation of the mitogen-activated protein kinase (MAPK) pathway in normal megakaryocytes: role in endomitosis. Blood. 1999 Aug 15;94(4):1273-82.

8. Kaushansky K. Determinants of platelet number and regulation of thrombopoiesis. Hematology / the Education Program of the American Society of Hematology American Society of Hematology Education Program. 2009:147-52.

9. Antonchuk J, Hyland CD, Hilton DJ, Alexander WS. Synergistic effects on erythropoiesis, thrombopoiesis, and stem cell competitiveness in mice deficient in thrombopoietin and steel factor receptors. Blood. 2004 Sep 1;104(5):1306-13.

10. Chen J, Li XB, Su R, Song L, Wang F, Zhang JW. ZNF16 (HZF1) promotes erythropoiesis and megakaryocytopoiesis via regulation of the c-KIT gene. The Biochemical journal. 2014 Feb 15;458(1):171-83.

11. Munugalavadla V, Dore LC, Tan BL, Hong L, Vishnu M, Weiss MJ, et al. Repression of c-kit and its downstream substrates by GATA-1 inhibits cell proliferation during erythroid maturation. Molecular and cellular biology. 2005 Aug;25(15):6747-59.

12. Lorenz P, Dietmann S, Wilhelm T, Koczan D, Autran S, Gad S, et al. The ancient mammalian KRAB zinc finger gene cluster on human chromosome 8q24.3 illustrates principles of C2H2 zinc finger evolution associated with unique expression profiles in human tissues. BMC genomics. 2010;11:206.

13. Shin JY, Hu W, Naramura M, Park CY. High c-Kit expression identifies hematopoietic stem cells with impaired self-renewal and megakaryocytic bias. The Journal of experimental medicine. 2014 Feb 10;211(2):217-31.

14. Clay D, Rubinstein E, Mishal Z, Anjo A, Prenant M, Jasmin C, et al. CD9 and megakaryocyte differentiation. Blood. 2001 Apr 1;97(7):1982-9.

15. Le Naour F, Francastel C, Prenant M, Lantz O, Boucheix C, Rubinstein E. Upregulation of CD9 expression during TPA treatment of K562 cells. Leukemia. 1997 Aug;11(8):1290-7.

16. Anzai N, Lee Y, Youn BS, Fukuda S, Kim YJ, Mantel C, et al. C-kit associated with the transmembrane 4 superfamily proteins constitutes a functionally distinct subunit in human hematopoietic progenitors. Blood. 2002 Jun 15;99(12):4413-21.

17. Stachura DL, Chou ST, Weiss MJ. Early block to erythromegakaryocytic development conferred by loss of transcription factor GATA-1. Blood. 2006 Jan 1;107(1):87-97.

18. Dubreuil P, Letard S, Ciufolini M, Gros L, Humbert M, Casteran N, et al. Masitinib (AB1010), a potent and selective tyrosine kinase inhibitor targeting KIT. PloS one. 2009;4(9):e7258.

19. Na YJ, Baek HS, Ahn SM, Shin HJ, Chang IS, Hwang JS. [4-t-butylphenyl]-N-(4-imidazol-1-yl phenyl)sulfonamide (ISCK03) inhibits SCF/c-kit signaling in 501mel human melanoma cells and abolishes melanin production in mice and brownish guinea pigs. Biochemical pharmacology. 2007 Sep 1;74(5):780-6.

20. Herraiz C, Journe F, Abdel-Malek Z, Ghanem G, Jimenez-Cervantes C, Garcia-Borron JC. Signaling from the human melanocortin 1 receptor to ERK1 and ERK2 mitogen-activated protein kinases involves transactivation of cKIT. Molecular endocrinology. 2011 Jan;25(1):138-56.

21. Kamlah F, Hanze J, Arenz A, Seay U, Hasan D, Juricko J, et al. Comparison of the effects of carbon ion and photon irradiation on the angiogenic response in human lung adenocarcinoma cells. International journal of radiation oncology, biology, physics. 2011 Aug 1;80(5):1541-9.

22. Yoshinaga K, Nishikawa S, Ogawa M, Hayashi S, Kunisada T, Fujimoto T, et al. Role of c-kit in mouse spermatogenesis: identification of spermatogonia as a specific site of c-kit expression and function. Development. 1991 Oct;113(2):689-99.

23. Weston W, Zayas J, Perez R, George J, Jurecic R. Dynamic equilibrium of heterogeneous and interconvertible multipotent hematopoietic cell subsets. Scientific reports. 2014;4:5199.

24. England SJ, McGrath KE, Frame JM, Palis J. Immature erythroblasts with extensive ex vivo self-renewal capacity emerge from the early mammalian fetus. Blood. 2011 Mar 3;117(9):2708-17.

25. Munugalavadla V, Kapur R. Role of c-Kit and erythropoietin receptor in erythropoiesis. Critical reviews in oncology/hematology. 2005 Apr;54(1):63-75.

26. Ye ZJ, Gulcicek E, Stone K, Lam T, Schulz V, Weissman SM. Complex interactions in EML cell stimulation by stem cell factor and IL-3. Proceedings of the National Academy of Sciences of the United States of America. 2011 Mar 22;108(12):4882-7.

27. Drube S, Heink S, Walter S, Lohn T, Grusser M, Gerbaulet A, et al. The receptor tyrosine kinase c-Kit controls IL-33 receptor signaling in mast cells. Blood. 2010 May 13;115(19):3899-906.

28. Rouleau C, Cui K, Feldman L. A functional erythropoietin receptor is necessary for the action of thrombopoietin on erythroid cells lacking c-mpl. Experimental hematology. 2004 Feb;32(2):140-8.

29. Broudy VC, Lin NL, Sabath DF, Papayannopoulou T, Kaushansky K. Human platelets display high-affinity receptors for thrombopoietin. Blood. 1997 Mar 15;89(6):1896-904.

30. Mazharian A, Ghevaert C, Zhang L, Massberg S, Watson SP. Dasatinib enhances megakaryocyte differentiation but inhibits platelet formation. Blood. 2011 May 12;117(19):5198-206.

31. Lannutti BJ, Drachman JG. Lyn tyrosine kinase regulates thrombopoietin-induced proliferation of hematopoietic cell lines and primary megakaryocytic progenitors. Blood. 2004 May 15;103(10):3736-43.

32. Lannutti BJ, Minear J, Blake N, Drachman JG. Increased megakaryocytopoiesis in Lyn-deficient mice. Oncogene. 2006 Jun 1;25(23):3316-24.

33. Kosmider O, Buet D, Gallais I, Denis N, Moreau-Gachelin F. Erythropoietin down-regulates stem cell factor receptor (Kit) expression in the leukemic proerythroblast: role of Lyn kinase. PloS one. 2009;4(5):e5721.

34. D'Allard D, Gay J, Descarpentries C, Frisan E, Adam K, Verdier F, et al. Tyrosine kinase inhibitors induce down-regulation of c-Kit by targeting the ATP pocket. PloS one. 2013;8(4):e60961.

35. Atay S, Banskota S, Crow J, Sethi G, Rink L, Godwin AK. Oncogenic KIT-containing exosomes increase gastrointestinal stromal tumor cell invasion. Proceedings of the National Academy of Sciences of the United States of America. 2014 Jan 14;111(2):711-6.

36. Atay S, Godwin AK. Tumor-derived exosomes: A message delivery system for tumor progression. Communicative & integrative biology. 2014 Jan 1;7(1):e28231.

37. Lopatina T, Bruno S, Tetta C, Kalinina N, Porta M, Camussi G. Platelet-derived growth factor regulates the secretion of extracellular vesicles by adipose mesenchymal stem cells and enhances their angiogenic potential. Cell communication and signaling : CCS. 2014;12:26.

38. Xiao H, Lasser C, Shelke G, Wang J, Radinger M, Lunavat T, et al. Mast cell exosomes promote lung adenocarcinoma cell proliferation inverted question mark role of KIT-stem cell factor signaling. Cell communication and signaling : CCS. 2014 Oct 14;12(1):64.

39. Chairoungdua A, Smith DL, Pochard P, Hull M, Caplan MJ. Exosome release of beta-catenin: a novel mechanism that antagonizes Wnt signaling. The Journal of cell biology. 2010 Sep 20;190(6):1079-91.

40. Tang M, Yin G, Wang F, Liu H, Zhou S, Ni J, et al. Downregulation of CD9 promotes pancreatic cancer growth and metastasis through upregulation of epidermal growth factor on the cell surface. Oncology reports. 2015 May 7.

41. Desterke C, Martinaud C, Guerton B, Pieri L, Bogani C, Clay D, et al. Tetraspanin CD9 participates in dysmegakaryopoiesis and stromal interactions in primary myelofibrosis. Haematologica. 2015 Jun;100(6):757-67.

Legends to figures

Figure 1

c-Kit specific inhibitors reduce TPO-dependent G1ME cells proliferation

G1ME cells were cultured in the presence of recombinant TPO with or without increasing doses of c-Kit inhibitors ISCK03 (1.5 or 10 μM) (**A**) or Masitinib (0.15. 1 or 3 μM) (**B**) or control DMSO during 4 days. Cell concentration and cell viability were assessed every day of the kinetic, allowing the maintenance of cell concentration at 2.5 10^5 cells/mL. The cumulated number of viable cells generated from the initial number of cells seeded was calculated based on the amplification factor from day to day. Means and standard deviations from 3 independent experiments. Statistically significant differences in day 4 cell numbers between the indicated conditions (brackets) are indicated by asterisks (* p < 1%; ** p < 0.5%; *** p < 0.05%).

Figure 2

Masitinib but not ISCK03 reduces c-Kit expression at the plasma membrane

A: G1ME cells were cultured in the presence of TPO from Cos7 conditioned mediumand in the presence or absence of c-Kit inhibitors ISCK03 at10 □ M (left panel) or Masitinib at3 μM (right panel) and c-Kit expression levels were determined by FACS analysis every day during 4 days. Each panel presents the superposed fluorescence profiles of c-Kit labeling obtained at day 4 for untreated (dark-grey areas) or treated (light-grey areas) cells as well as profiles obtained after labeling with isotype control IgG of the same untreated or treated cells (white areas). Histogram shows the relative levels of c-Kit Median fluorescence intensity (MFI) in untreated (white boxes) cells or cells treated with either 10 □ M ISCK03 (black boxes) or 3 □ M Masitinib (grey boxes).

B: Western blot analysis showing the decrease of c-Kit phosphorylated at position Y719 in G1ME cells cultured for 4 days in the presence of TPO and either 10 □ M ISCK03 (left panel) of 3 □ M Masitinib (right panel). Numbers below each panel indicate the relative decrease in pY719-cKit signal standardized to □-actin signal (used as loading control) in treated compared to untreated cells (mean from two independent experiments).

Figure 3

Knock down of c-Kit reduces G1ME cells proliferation in response to TPO

G1ME cells were submitted to 2 rounds of transfection at 24 hours interval with either c-Kit siRNA or control luciferase siRNA and re-seeded in medium containing TPO from Cos7 conditioned medium with or without 3 μM Masitinib. **A:** Proliferation curve presenting the cumulated number of viable cells over 4 days after the first transfection. **B. C .D:** Relative decreases of the cumulated number of viable cells (**B**), of c-Kit mRNA levels (**C**) and of c-Kit mean fluorescence levels (**D**) determined after 48, 72 and 96 hours following the first transfection. Results are expressed as relative values (means and standard deviations from 3 independent experiments) standardized to the values obtained in control condition (transfection with luciferase siRNA without Mastinib). Significant variations from this control condition are indicated by asterisks. * $p<5\%$; ** $p<1\%$.

Figure 4

Exogenous SCF does not contribute to the proliferation of G1ME cells in response to TPO

A: Quantification by Elisa immunoassay of SCF concentration in the supernatant of G1ME cells cultured in the presence of recombinant TPO during 24 hours compared to control medium without G1ME cells. Hatched area indicates the 95 % confidence interval of the mean background value detected in control medium devoid of SCF. Means and standard deviations of 4 independent experiments showing no significant difference of SCF concentration between normal medium and G1ME cells supernatant.

B: Proliferation curves of G1ME cells in the presence of recombinant TPO and either control IgG2bk or increasing doses of c-Kit blocking monoclonal antibody ACK2. Means and standard deviations of three independent experiments showing no difference in the total number of cells generated after 4 days in the presence of control IgG2bk or ACK2 c-Kit antibody.

Figure 5

Stimulation of G1ME cells by TPO induces the phosphorylation of c-Kit receptor

G1ME cells were starved for 6 hours without TPO then re-stimulated by TPO from cos7-conditioned medium **(A)** or recombinant SCF **(B)** during 5, 10, 15 or 30 minutes, followed by Western-Blot analysis of Y719 phosphorylated c-Kit, total c-Kit and β-Actin. NS: Non Starved cells; S: Starved cells.

A: Kinetics analysis of c-Kit phosphorylation in response to TPO. Upper part shows typical Western-Blot obtained after revelation of the same membrane with specific antibodies directed against either phosphorylated c-Kit on tyrosine Y719, or total c-Kit or β-Actin used as loading control. Histogram shown in lower part displays the variations of the ratio of phosphorylated over total c-Kit signals normalized to the ratio determined in the starved condition (means and standard deviations from three independent experiments). Significant variations compared to starved condition are indicated by an asterisk ($p< 5\%$).

B: Kinetics analysis of c-Kit phosphorylation in response to SCF. Same legend as in A. Result from 5 minutes re-stimulation by TPO is included for comparison.

Figure 6

Masitinib stimulates Pf4 late megakaryocytic gene expression and polyploidization

G1ME cells were analyzed after a 2 days culture in the presence of TPO from Cos7 conditioned medium with or without Masitinib as indicated. mRNA levels were determined by qRT-PCR and cell cycle analyses were performed by FACS after EdU pulse labeling followed by double labeling for EdU incorporation by Click-it reagent coupled to Alexafluor-647 and DNA content by propidium iodide.

A: Relative levels of mRNAs encoding late megakaryocytic genes Pf4 and Cd9 normalized to □ □ actin and standardized to the control condition with IgG without Masitinib (means and standard deviations from 3 independent experiments).

B: FACS dot-plots for EdU incorporation and DNA content. Numbers indicate the percentage of cells identified in the different phases of cell cycle including cells undergoing polyploidization (EdU labeled cells with DNA content higher than 4 N).

Figure 7

CD9 actively contributes to reduce c-Kit levels

G1ME cells were submitted to two rounds of transfection at 24 hours interval with either CD9 siRNA or control luciferase siRNA and re-seeded in medium containing TPO from Cos7 conditioned medium.

A: Evolution of the relative values of the median fluorescence of CD9 (grey boxes) or c-Kit (black boxes) following transfection with CD9 siRNA normalized to values obtained in control condition following transfection with luriferase siRNA (white boxes). Means and standard deviations from 3 independent experiments. Significant variations compared to control are shown by asterisks ($p < 0.05$ in Student t-test).

B: Compilation of data from three independent transfection experiments showing the striking correlation between the fold reduction of CD9 and the fold increase in c-Kit.

Figure 8

Working model of the dual control of c-Kit by TPO during megakaryopoiesis

Our results showed that part of the proliferative effect of TPO is mediated through the activation of c-Kit signaling that concomitantly contributes to inhibit CD9 expression and polyploidization while c-Kit itself is under the negative control of CD9. Based on these findings, we suggest that TPO stimulates the proliferation of megakaryocytic progenitors while progressively increasing CD9 expression until reaching a threshold level sufficient to inhibit c-Kit expression, in turn allowing proliferation arrest and terminal differentiation.

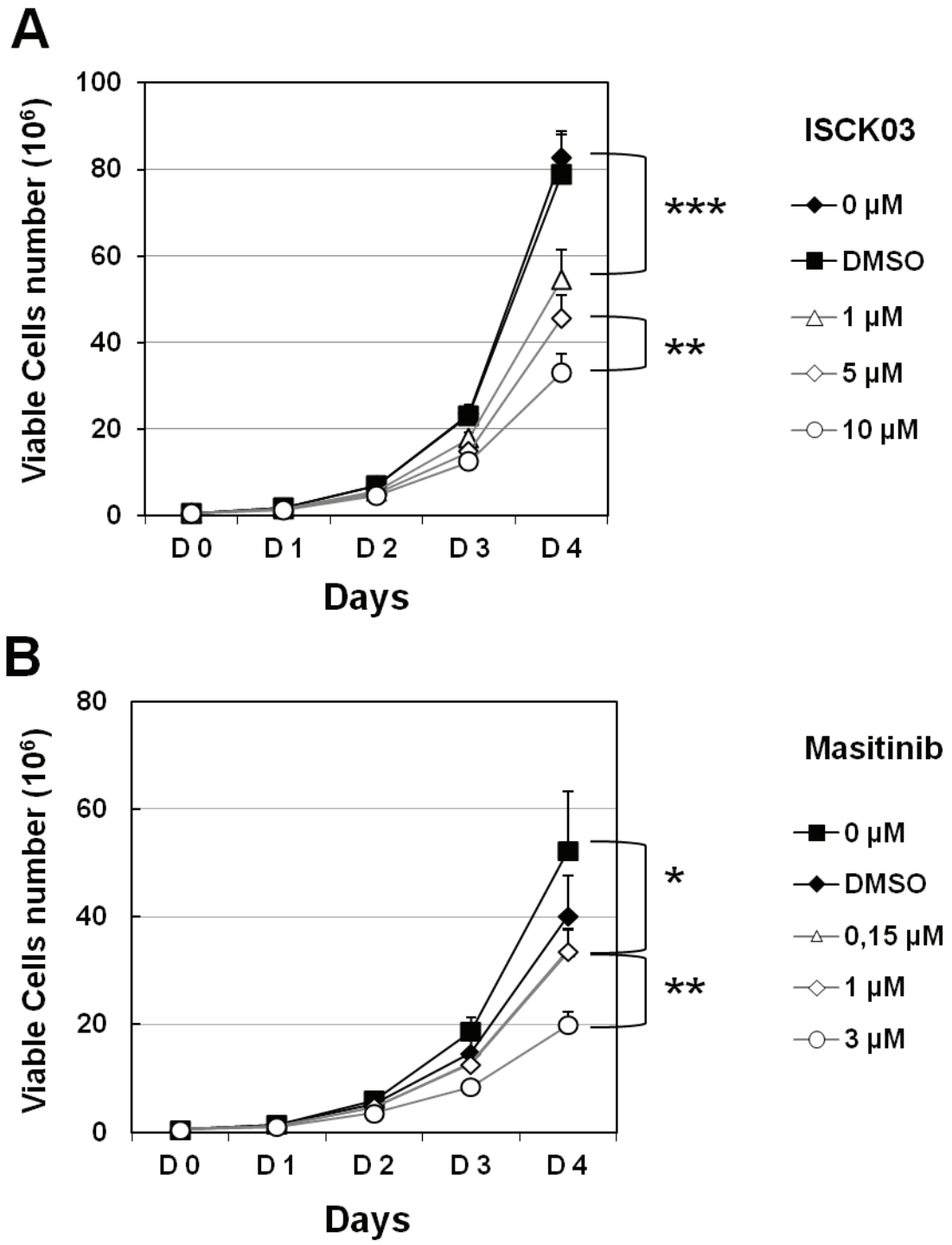
A
Viable Cells number (10⁶)
100
80
60
40
20
0
D 0
D 1
D 2
D 3
D 4
Days
***
**
ISCK03
0 µM
DMSO
1 µM
5 µM
10 µM
B
Viable Cells number (10⁶)
80
60
40
20
0
D 0
D 1
D 2
D 3
D 4
Days
*
**
Masitinib
0 µM
DMSO
0,15 µM
1 µM
3 µM

Figure 1

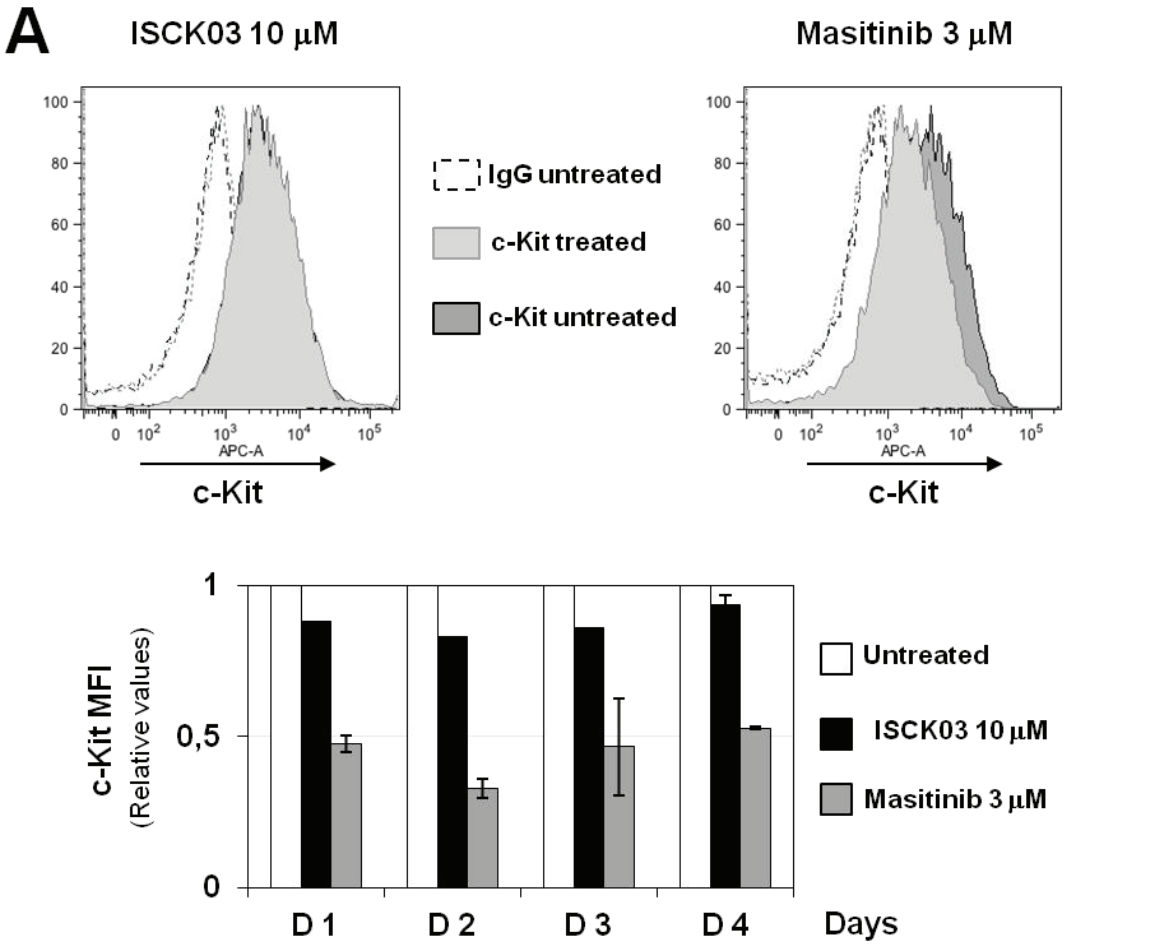
A
ISCK03 10 µM
Masitinib 3 µM
IgG untreated
c-Kit treated
c-Kit untreated
APC-A
c-Kit
c-Kit MFI
(Relative values)
Untreated
ISCK03 10 µM
Masitinib 3 µM
D 1
D 2
D 3
D 4
Days

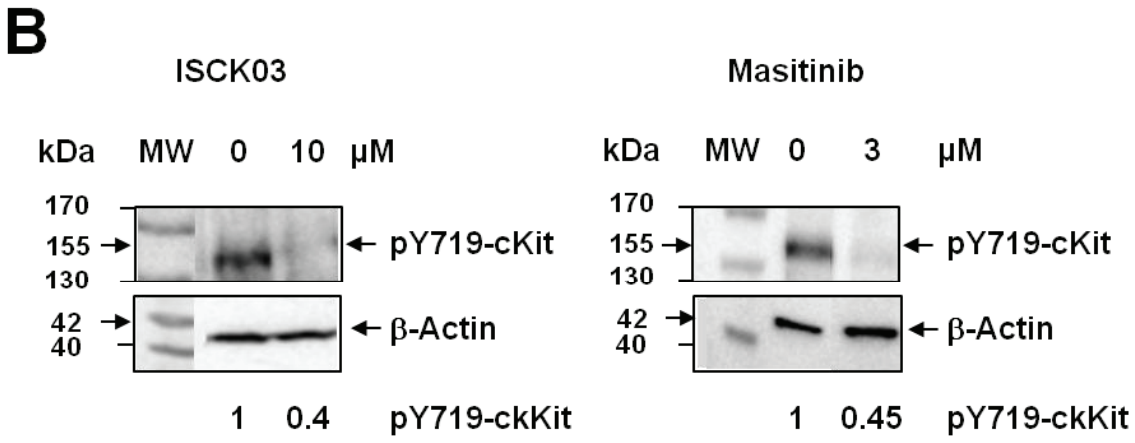
B
ISCK03
Masitinib
kDa
MW
0
10
µM
3
170
155
130
42
40
pY719-cKit
β-Actin
1
0.4
0.45
pY719-ckKit

Figure 2

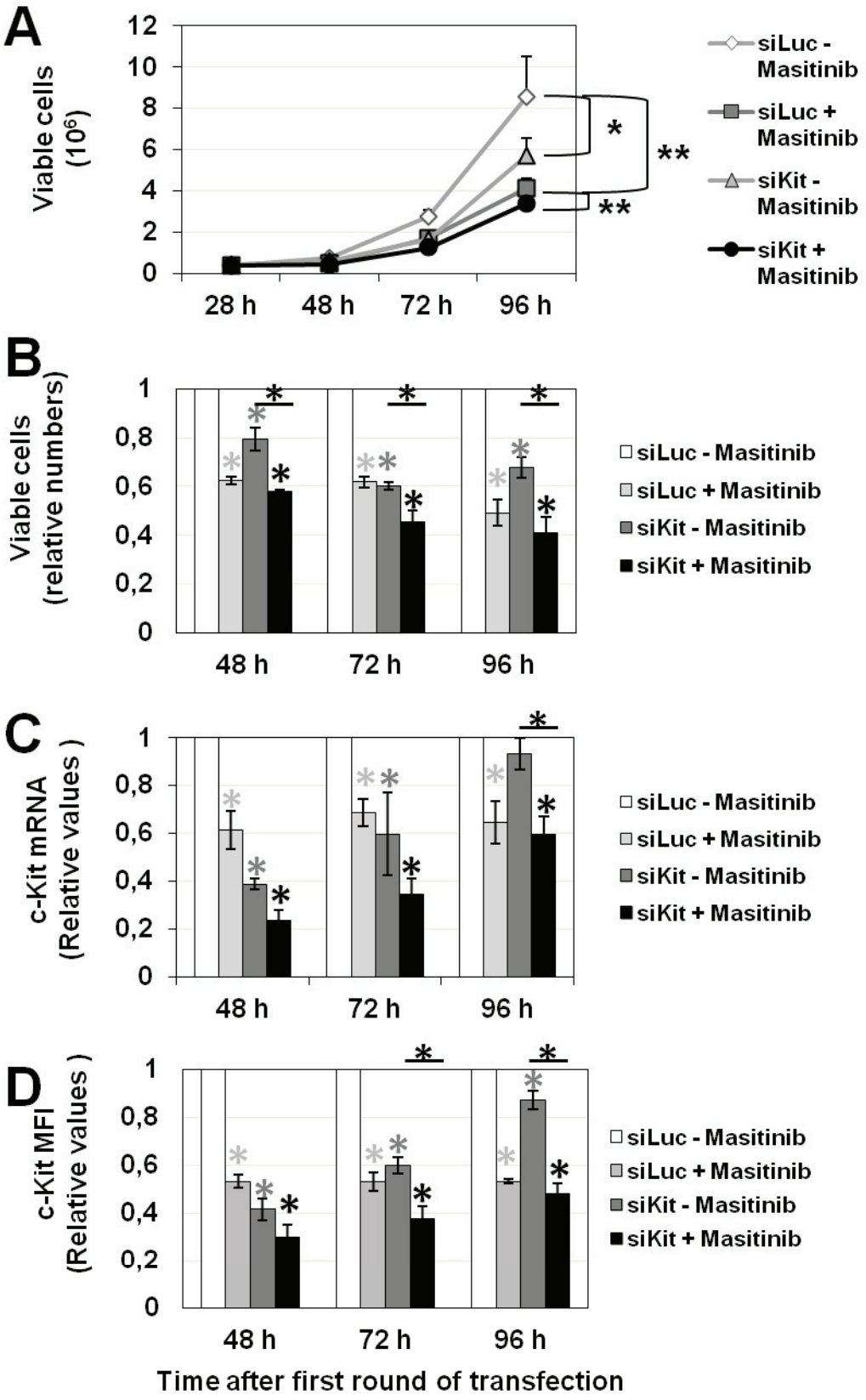
A
Viable cells (10⁶)
12
10
8
6
4
2
0
28 h
48 h
72 h
96 h
*
**
**
siLuc - Masitinib
siLuc + Masitinib
siKit - Masitinib
siKit + Masitinib
B
Viable cells (relative numbers)
1
0,8
0,6
0,4
0,2
0
48 h
72 h
96 h
C
c-Kit mRNA (Relative values)
D
c-Kit MFI (Relative values)
Time after first round of transfection

Figure 3

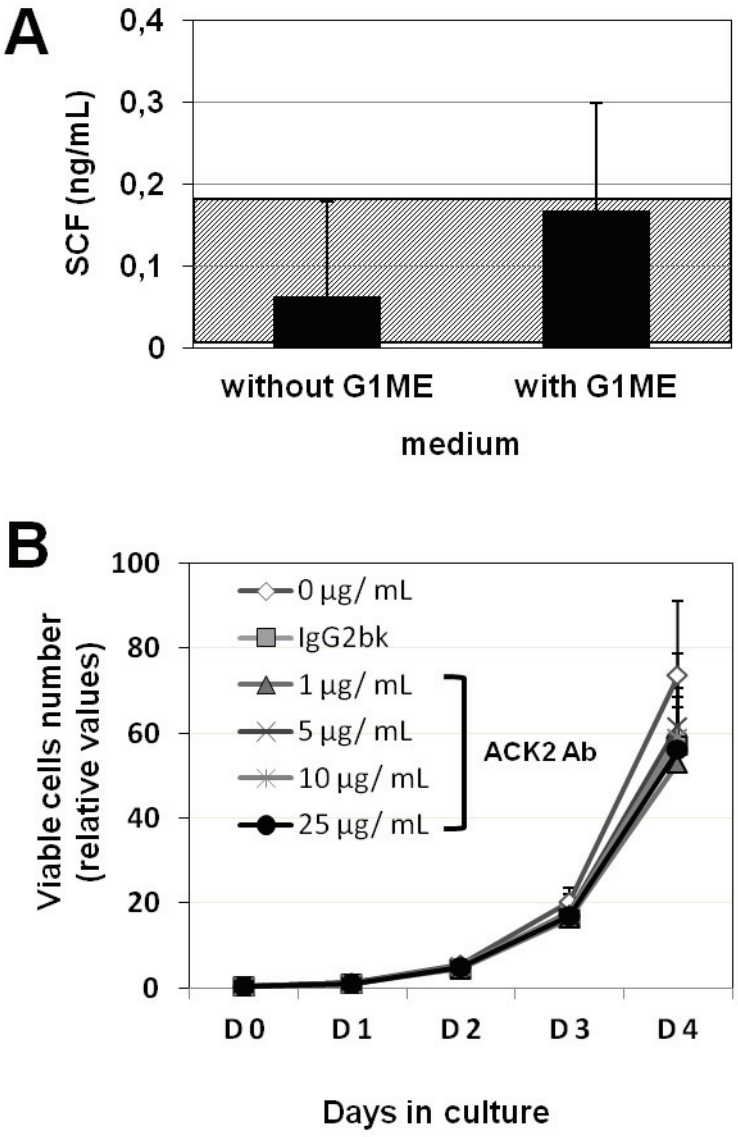
A
0,4
0,3
0,2
0,1
0
SCF (ng/mL)
without G1ME
with G1ME
medium
B
100
80
60
40
20
0
Viable cells number (relative values)
0 µg/ mL
IgG2bk
1 µg/ mL
5 µg/ mL
10 µg/ mL
25 µg/ mL
ACK2 Ab
D 0
D 1
D 2
D 3
D 4
Days in culture

Figure 4

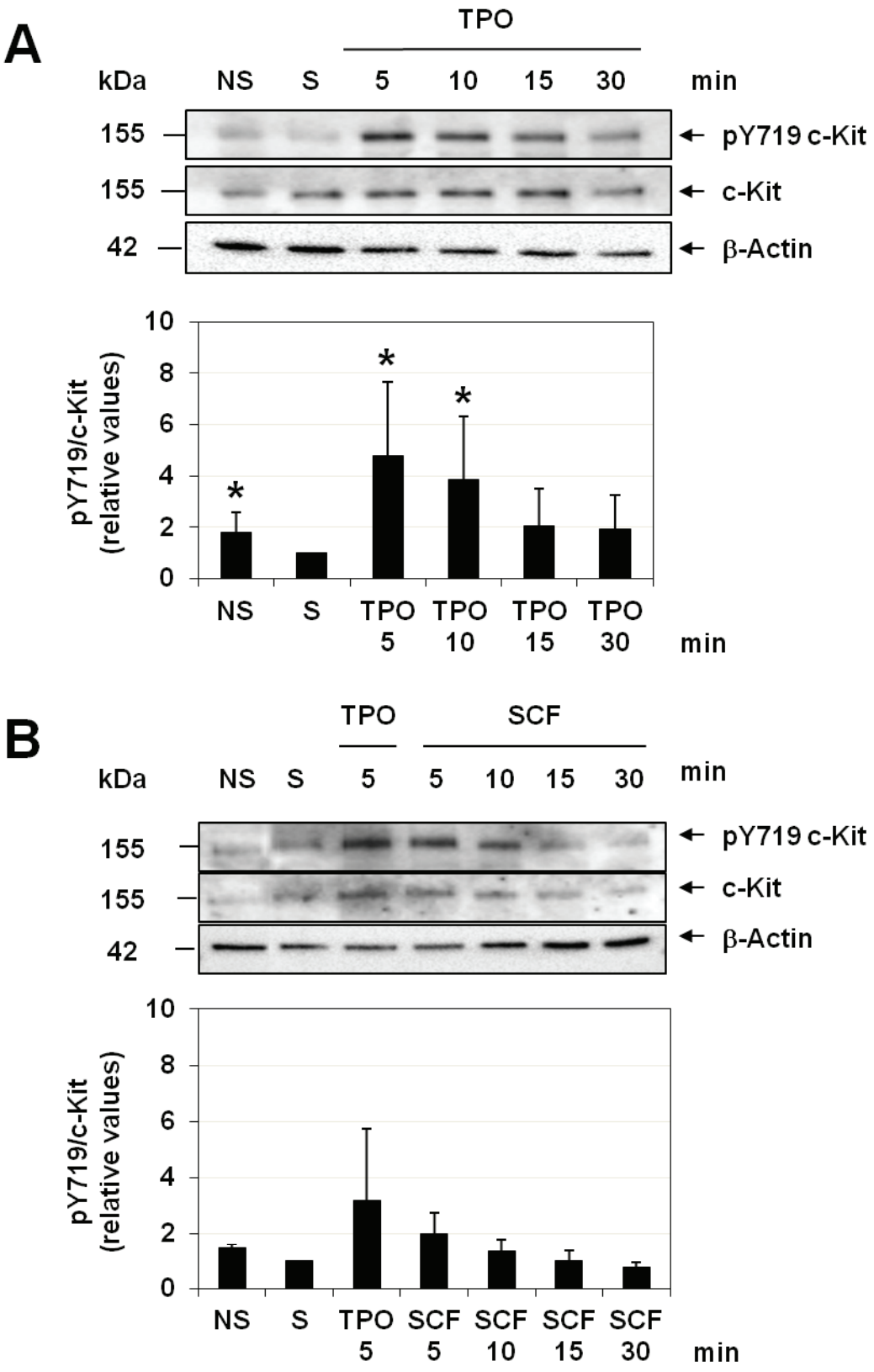
A
TPO
kDa
NS
S
5
10
15
30
min
155
155
42
pY719 c-Kit
c-Kit
β-Actin
pY719/c-Kit
(relative values)
10
8
6
4
2
0
*
*
*
NS
S
TPO 5
TPO 10
TPO 15
TPO 30
min
B
TPO
SCF
kDa
NS
S
5
5
10
15
30
min
155
155
42
pY719 c-Kit
c-Kit
β-Actin
pY719/c-Kit
(relative values)
10
8
6
4
2
0
NS
S
TPO 5
SCF 5
SCF 10
SCF 15
SCF 30
min

Figure 5

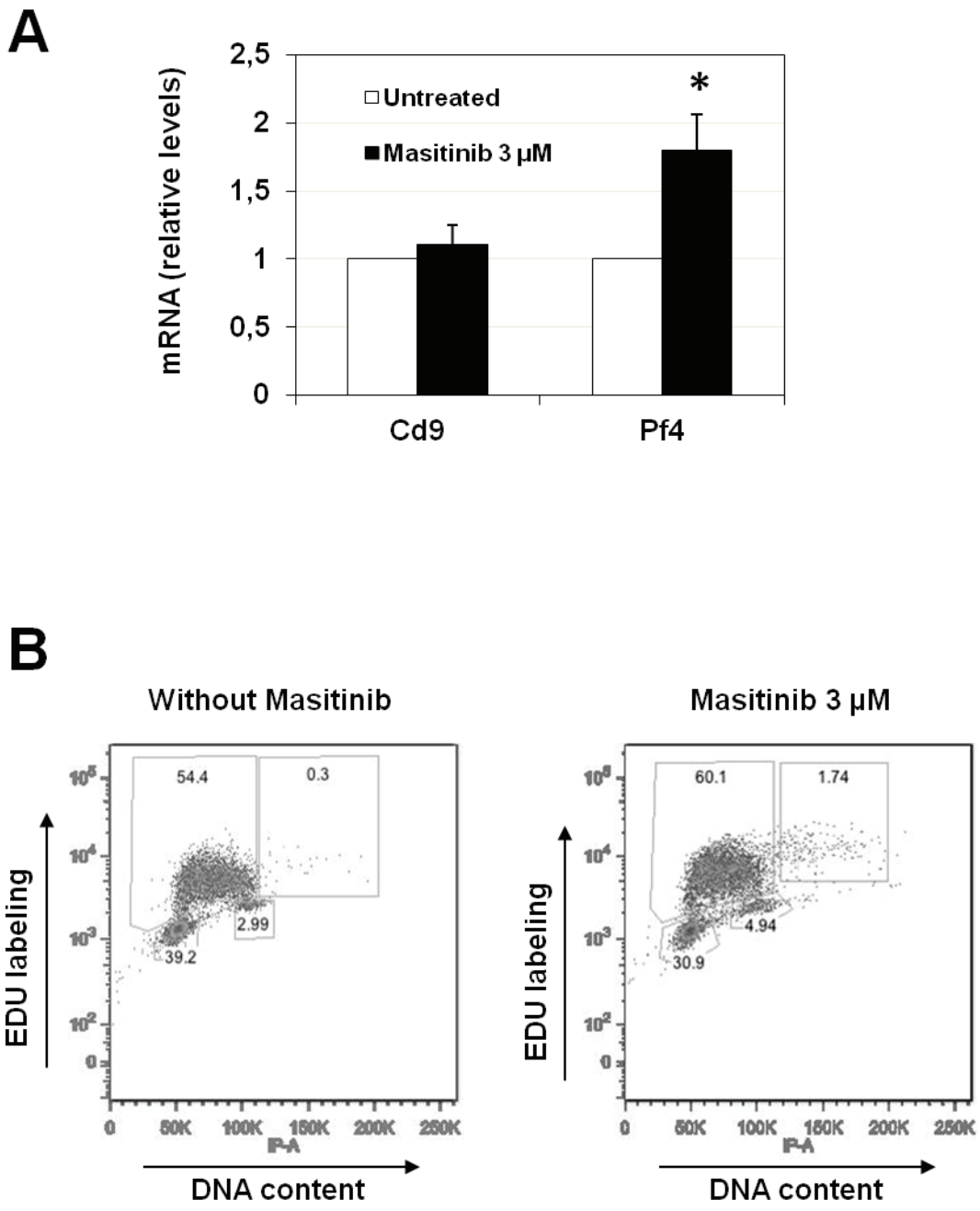
A
mRNA (relative levels)
2,5
2
1,5
1
0,5
0
Untreated
Masitinib 3 µM
*
Cd9
Pf4
B
Without Masitinib
Masitinib 3 µM
EDU labeling
DNA content
54.4
0.3
2.99
39.2
60.1
1.74
4.94
30.9
IP-A

Figure 6

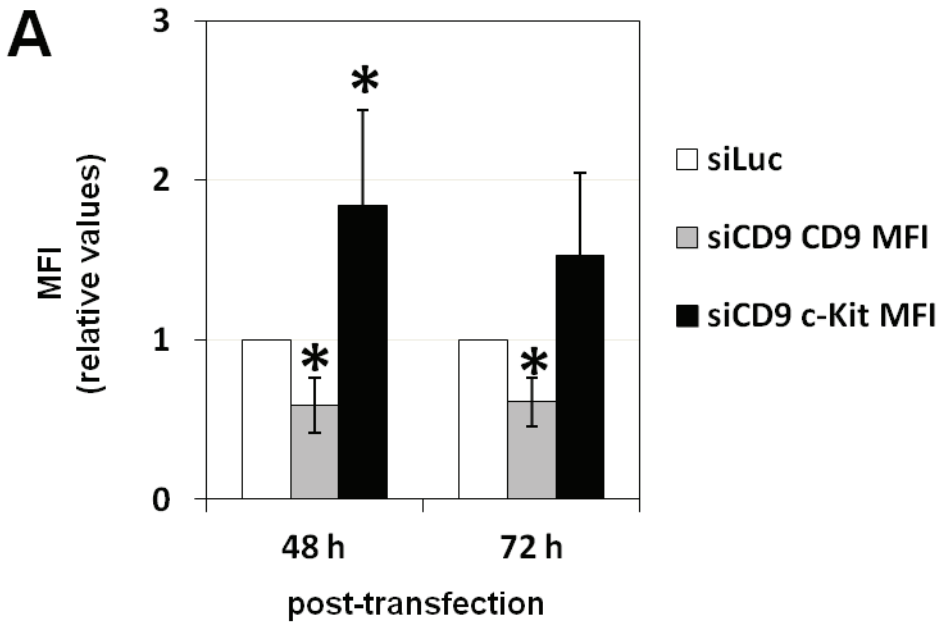
A
3
2
1
0
MFI
(relative values)
*
*
*
siLuc
siCD9 CD9 MFI
siCD9 c-Kit MFI
48 h
72 h
post-transfection

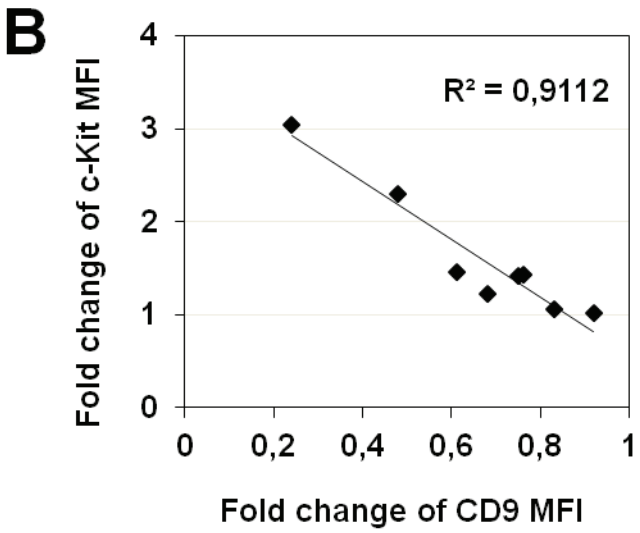
B
4
3
2
1
0
Fold change of c-Kit MFI
R² = 0,9112
0
0,2
0,4
0,6
0,8
1
Fold change of CD9 MFI

Figure 7

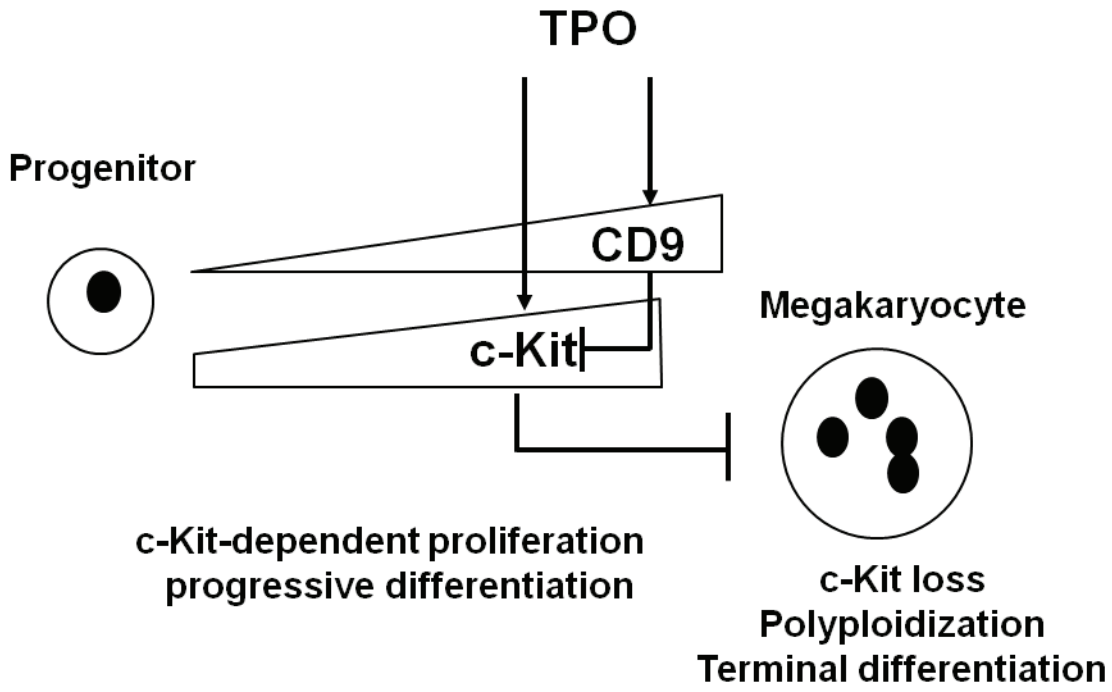
TPO
Progenitor
CD9
c-Kit
Megakaryocyte
c-Kit-dependent proliferation
progressive differentiation
c-Kit loss
Polyploidization
Terminal differentiation

Figure 8

Supplementary Figures and Table

Target	Forward Primer	Reverse Primer
β-actin	5’-TGGGAATGGGTCAGAAGGACTC-3’	5’-CTGGGTCATCTTTTCACGGTTG-3’
c-Kit	5’-GGGCTAGCCAGAGACATCAG-3’	5’-AGGAGAAGAGCTCCCAGAGG-3’
c-Mpl	5’- CCGAGCTCGCTACAGCTT- 3’	5’- CTGTAGTGCGCAGGAAATTG -3’
Cd9	5’- GCTCGAAGATGCTCTTGGTC -3’	5’- GCTCGAAGATGCTCTTGGTC -3’
c-Myc	5’-TCCTGTACCTCGTCTGATTCC-3’	5’-CTCTTCTCCACAGACACCACATC-3’
Fli-1	5’-GACTCTGTCAGGAGAGGAGC-3’	5’-GTCATTTTGAACTCCCCGTTG -3’
Gata1	5’-TTCTTCCACTTCCCCAAATG-3’	5’-AGGCCCAGCTAGCATAAGGT-3’
Gata2	5’-GAATGGACAGAACCGGCC-3’	5’-AGGTGGTGGTTGTCGTCTGA-3’
Hes1	5’-CTACCCCAGCCAGTGTCAAC-3’	5’-CGCCTCTTCTCCATGATAGG-3’
Itga2b	5’-AAGCTCTGAGCACACCCACT-3’	5’-CTCAGCCCTTCACTCTGACC-3’
Jak-2	5’-GATGGCGGTGTTAGACATGA-3’	5’-TGCTGAATGAATCTGCGAAA-3’
Pf4	5’- AGTCCTGAGCTGCTGCTTCT -3’	5’- CAGCTAAGATCTCCATCGCTTT- 3’
Pten	5’-AATTCCCAGTCAGAGGCGCTATGT-3’	5’-GATTGCAAGTTCCGCCACTGAACA-3’
Tal-1	5’-CGGAGGATCTCATTCTTGCTTAG-3’	5’- CTAGGCAGTGGGTTCTTTGGG -3’
tr-Mpl	5’-GAGGACTGGAAGGAGACTGAGGCA-3’	5’-AGGTTGCAGTCCTCTGTAGTCCAT-3’

Table S1

Primer sequences used in qRT-PCR:

Target	Reverse	Forward
c-Kit siRNA.1	5’-CCGUGACAUUCAAGCUUUAdTdT-3’	5’ –UAAACGUUGAAUGUCACGGdTdT-3’
c-Kit siRNA.2	5’-CUGUCUAGAAUUUACUCAAdTdT-3’	5’ –UUGAGUAAAUUCUAGACAGdTdT- 3’
CD9	5’-GAGCAUCUUCGAGCAAGAAdTdT -3’	5’-UUCUUGCUCGAAGAUGCUCdTdT-3’

Table S2

siRNA sequences

Figure S1

G1ME cells do not survive or proliferate in the presence of SCF alone. G1ME cells were cultured during two days either without any cytokine. or in the presence of SCF (100 ng/ mL) or TPO (1% conditioned medium) either alone or combined.

A: % of cell survival assessed by Trypan Blue exclusion at day 2.

B: Cumulated numbers of viable cells during the 2 days culture in the different conditions (means and standard deviations from 3 independent experiments).

Figure S2

Inverse variations of c-Kit and CD9 levels between different hematopoietic cells lines. ESRE (Extensively Self-Renewing Erythroid murine progenitors) (24) and EML (lympho-myeloid multipotent murine cell line) (23) cells were maintained as previously described in their corresponding medium whereas G1ME cells (17) were maintained in the presence of 1% Cos-7 conditioned-medium TPO. **A:** Median of fluorescence intensities (MFI) of CD9**. B:** Median of fluorescence intensities of c-Kit **. C**: CD9/c-Kit MFI ratios.

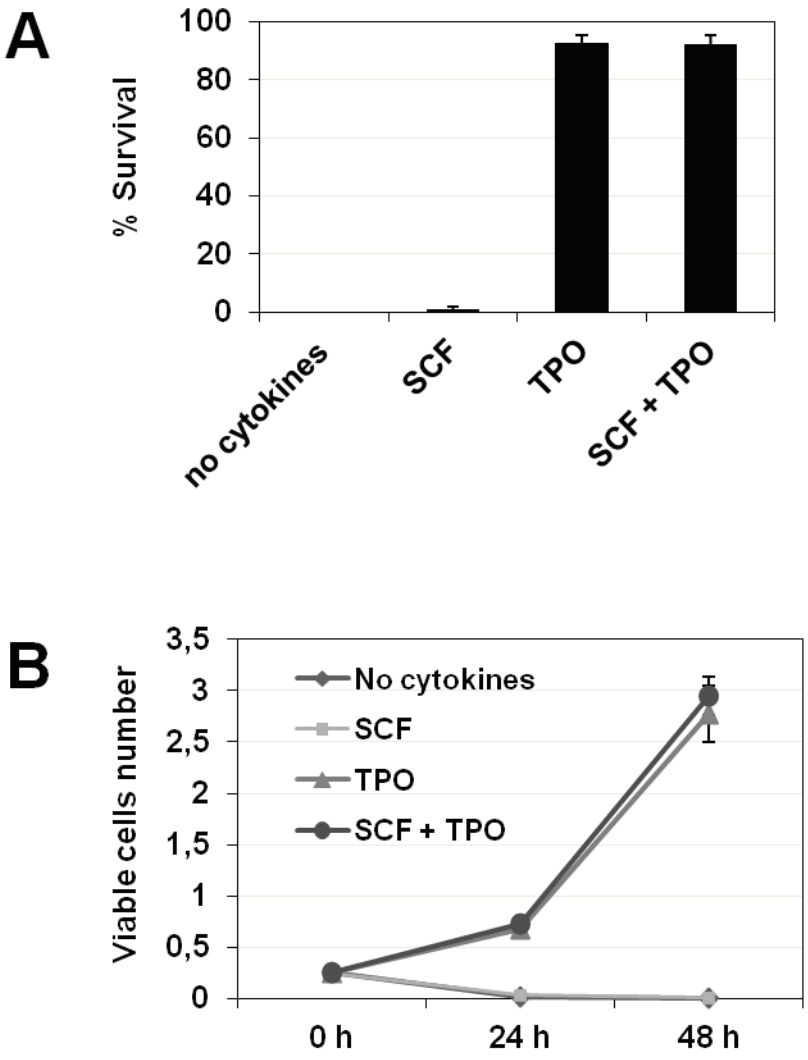
A
100
80
60
40
20
0
% Survival
no cytokines
SCF
TPO
SCF + TPO
B
3,5
3
2,5
2
1,5
1
0,5
0
Viable cells number
No cytokines
SCF
TPO
SCF + TPO
0 h
24 h
48 h

Figure S1

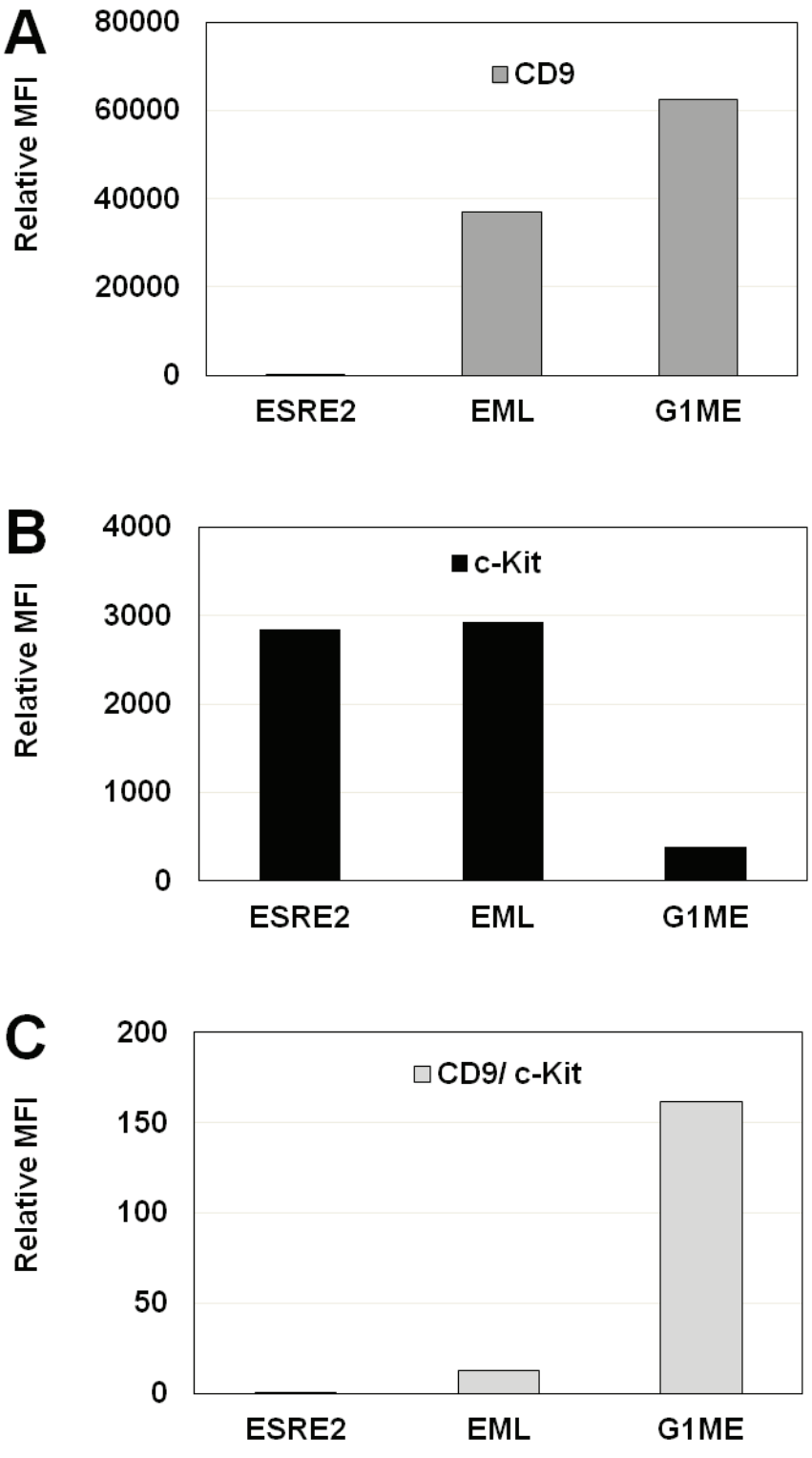
A
Relative MFI
80000
60000
40000
20000
0
CD9
ESRE2
EML
G1ME
B
Relative MFI
4000
3000
2000
1000
0
c-Kit
ESRE2
EML
G1ME
C
Relative MFI
200
150
100
50
0
CD9/ c-Kit
ESRE2
EML
G1ME

Figure S2

DISCUSSION AND PERSPECTIVES

The main interest of our team is to decipher the molecular mechanisms controlling the proliferation/differentiation balance of bipotent and monopotent progenitors. During my thesis, I investigated whether Notch maintains the bipotent state of MEP by acting on the transcription factor GATA1 and whether Notch interacts functionally with TPO and c-Kit pathways during the control of the proliferation versus megakaryocytic differentiation balance.

1. GATA1 Implication downstream of Notch in the control of MEP bipotency and amplification

Before the start of my work, the team evidenced a positive effect of Notch pathway on bipotent MEP progenitors amplification. The first aim of my study was to investigate GATA1 expression and phosphorylation levels implication in this Notch effect. In a first approach, I explored whether Notch was able to regulate GATA1 in L8057 cells. In a second approach, I investigated GATA1 phosphorylation requirement in Notch-dependent maintenance of MEP bipotency and amplification.

Notch activation in L8057 cells did not induce the expression neither the phosphorylation of GATA1. Besides, taking advantage of a murine knock-in model expressing a non-phosphorylable form of GATA1 (S310A) (Rooke and Orkin, 2006), I excluded a GATA1 phosphorylation contribution to Notch-effect on MEP bipotency maintenance.

Nevertheless, contrarily to our starting hypothesis, I observed a negative regulation of GATA1 transcripts and protein levels in Notch-stimulated L8057 megakaryoblastic cells. We also observed a GATA1 downregulation in Notch-stimulated MEP. Thus, convergent results between L8057 and MEP suggest that instead of increasing the expression levels of GATA1 and its availability for its partners Fli-1 and EKLF, Notch reduces GATA1levels.

This observation makes one wonder whether GATA1 decreased levels contributes to Notch effect on the amplification of MEP and whether alternative mechanisms could explain GATA1 modulation by Notch, allowing both erythroid and megakaryocytic differentiation restriction.

1.1 Is GATA1 downregulation implicated in E/MK bipotent progenitors amplification?

Different studies argue for the contribution of a decreased GATA1 expression in MEP proliferation. Indeed, GATA1 decreased expression due to the deletion of a Gata1 enhancer region in the Gata1$^{\Delta NeO\Delta HS}$ murine model induced an increased generation of bipotent progeny derived from fetal liver MEP in semi-solid medium when compared to MEP from wild-type mice (Kuhl et al., 2005). Moreover, Gata1 gene total deletion in murine embryonic stem cells allowed the immortalization of the E/MK bipotent G1ME cells in presence of TPO (Stachura et al., 2006). Furthermore, Gata1 depletion, this time using doxycycline inducible RNA interference, again allowed the immortalization of the bipotent cells G1ME2 in presence of TPO and SCF (Noh et al., 2015).

Nevertheless, the molecular mechanism explaining the contribution of decreased expression or even GATA1 absence to the amplification or immortalization of bipotent E/MK progenitors remains an open question.

The c-Myc transcription factor is a potential candidate as it is negatively regulated by GATA1 (Noh et al., 2015; Rylski et al., 2003) and positively regulated by Notch (Weng et al., 2006), however its expression did not vary in Notch-stimulated G1ME cells (Table 1).

Alternatively, we have more arguments to propose a putative involvement of c-Kit. Indeed, we found in our study that c-Kit is both positively regulated by Notch and implicated in G1ME cells proliferation (detailed in the next paragraphs). In addition, other studies have shown a repression of c-kit expression by GATA1 in erythroid cell line (Munugalavadla et al., 2005). Based on these observations, it seems possible that c-Kit de-repression due to Notchstimulation and subsequently decreased GATA1 levels may contribute to E/MK bipotent progenitors amplification.

1.2 Alternative mechanisms of Notch-dependent regulation of GATA1 activity?

Interestingly, one study reported the negative effect of Notch effector HEY2 on GATA1 transcriptional activity using GATA-dependent reporter assay performed in K562 cells (Elagib et al., 2004). The other Notch effector HES1 has been reported to inhibit GATA1 activity by impeding its recruitment of p300 acetylase (Ishiko et al., 2005). In these two different

studies, the Notch effectors HES1 and HEY2 interact physically with GATA1 thus inhibiting its transcriptional activity.

Based on these observations, we propose a new hypothesis implicating GATA1 in the control of Notch-mediated blockade of MEP differentiation: the interaction between HES or HEY with GATA1 could induce its sequestration and avoid its interaction with its Fli-1 and EKLF partners responsible for the engagement into megakaryocytic and erythrocytic differentiation, respectively.

One experiment allowing to test this hypothesis could be to perform co-immunoprecipitations to analyze whether HES or HEY physically interact with GATA1 and whether this interaction modulates the formation of the differentiation complexes GATA1/ EKLF or GATA1/ Fli-1. In order to approach physiological conditions, this experiment should be performed in bipotent cells such as G1ME2 cells. Indeed, GATA1 expression restoration in these cells approximates physiological levels when compared to fetal liver, and this enables more efficient differentiation even *in vivo*(Noh et al., 2015).

2. c-Kit implication downstream of Notch in the proliferation versus differentiation balance control

Similarly to c-Kit upregulation by Notch observed in MEP, I validated G1ME cells as responsive to Notch stimulation since it induced a HES1 expression increase that was accompanied by c-Kit transcripts and protein levels increase. Furthermore, as in MEP wherein Notch-mediated amplification required SCF/ c-Kit signaling cooperation, I demonstrated in G1ME cells the c-Kit contribution to cell proliferation. These observations raised the questions of c-Kit mechanism of regulation by Notch and whether c-Kit upregulation in GATA1 absence can explain Notch-mediated amplification of bipotent cells.

2.1 By which mechanism Notch regulates c-Kit gene transcription?

In order to determine the level of regulation of c-Kit by Notch, I analyzed c-Kit primary transcripts levels as an early marker of c-Kit gene transcriptionactivation. I observed that Notch-stimulated G1ME cells express higher levels of c-Kit primary transcripts suggesting that c-Kit regulation by Notch is at the transcriptional level. I tried to confirm this result by performing RNA POL II ChIP analyses, though weak enrichment signals on c-Kit gene

hampered this demonstration, whereas positive controls on other promoters showed high enrichment attesting for POL II antibody efficiency. The use of a different POL II antibody could maybe enhance enrichment signals on c-Kit gene. Another approach could be to analyze by ChIP assay for trimethylated Lysine 4 Histone H3 enrichment on c-Kit gene that represents a good evidence of gene transcription activation.

After that, I tried to identify c-Kit regulators modulated by Notch and able to explain its upregulation. Using qRT-PCR and ChIP assays, I excluded the contribution of the two most known c-Kit regulators, GATA2 and SCL, as mediators of Notch during c-Kit up-regulation in G1ME cells as their transcript levels and their enrichment on c-Kit gene were not increased upon Notch activation. Thus, c-Kit regulation mechanism by Notch remains an open question.

Based on available data in the literature, we propose two mechanisms explaining Notch-induced c-Kit upregulation based either on direct activation by RBPJκ or on the repression of a c-Kit negative regulator by HES1.

Analyses of ChIP-seq data (Wang et al., 2011) generated in lymphoid T-ALL cell lines following RBPJκ immunoprecipitation revealed its enrichment on c-Kit promoter. Based on these data, one possibility could be that RBPJκ directly bind to its specific sites on c-Kit regulatory elements thus favoring c-Kit gene transcription in MEP. We could test this hypothesis by analyzing by ChIP assayRBPJκ enrichment on c-Kit regulatory elements in Notch-stimulated G1ME cells.

Alternatively, we could test whether c-Kit upregulation by Notch is dependent on HES1 by analyzing whether this upregulation is cancelled by a Hes1 transcripts targeting siRNA.

Among putative c-Kit repressor candidates, the ZNF16 human transcription factor has been recently reported (Chen et al., 2014a). A first experiment could be to test whether the stimulation of K562 cells by Notch modulates the transcripts levels of Znf16, then whether Notch modulates the enrichment of ZNF16 on c-Kit regulatory elements by ChIP assay. However, being not conserved in mice, ZNF16 could not explain the observed c-Kit upregulation in G1ME cells.

A more interesting candidate is GATA1 that was described as a c-Kit repressor in an erythroid cell line (Munugalavadla et al., 2005). By performing GATA1 ChIP assay, we could test whether this mechanism is conserved in bipotent G1ME2 cells following doxycycline withdrawal and whether Notch stimulation reduces GATA1 enrichment on c-Kit regulatory

elements. A stronger evidence would be to show that c-Kit expression is dependent of the GATA1 levels modulated in G1ME2 cells following their treatment with different doses of doxycycline.

2.2 Does c-Kit de-repression contribute to Notch-mediated amplification of bipotent cells?

Based on our finding that c-Kit contributes to G1ME cells proliferation and that Notch induces the expression of c-Kit as well as the previously described repression of c-Kit by GATA1, it seems possible that Notch-induced amplification of bipotent cells is mediated by GATA1 repression and subsequent induction of c-Kit.

GATA1 expression in G1ME cells needs to be restored in order to explore c-Kit implication downstream of Notch and GATA1. However, I tried this experiment once and observed that HES1 is repressed upon GATA1 restoration (data not shown), which is in agreement with another study that reported the same effect during erythroid differentiation (Ross et al., 2012). GATA1 restoration in G1ME cells was described recently to reach supra-physiological levels (Noh et al., 2015), this suggest that GATA1 restoration in G1ME cells could masks Notch effect on c-Kit, thus limiting the usefulness of G1ME cells in the study of c-Kit role downstream of Notch and GATA1. On the contrary, in G1ME2 cells, doxycycline withdrawal allows GATA1 to be restored at physiological levels and one could expect that GATA1 restored levelscould be modulated by different doses of doxycycline, thus rendering the G1ME2 cells a more powerful model.

Thus, one experiment to test the contribution of c-Kit downstream of Notch and GATA1 in bipotent cells proliferation could be to analyze whether doxycycline dose-dependent GATA1 increase is accompanied by a dose-dependent decrease of c-Kit expression levels as well as more restricted differentiation. Of further interest, we could test whether G1ME2 are responsive to Notch stimulation and whether this stimulation favors cell proliferation in the presence of lower dose of SCF.

3. The role of c-Kit downstream of TPO, Notch and CD9 in the control of the proliferation/ differentiation balance

3.1 TPO activates c-Kit and c-Kit contribute to G1ME cells TPO-dependent proliferation

The convergent results of the two different strategies using either chemical inhibitors of c-Kit or RNA interference led us to conclude to a c-Kit contribution in G1ME cells proliferation. As G1ME cells are cultured in absence of SCF, this observation raised the question of the origin of c-Kit activation. Using ELISA and proliferation assays in the presence of the ACK2 monoclonal antibody that blocks the interaction between c-Kit and SCF, we observed that SCF is not secreted by and does not contribute to G1ME cells proliferation. As G1ME cells are cultured in presence of TPO only, this observation prompted us to examine whether TPO could actually be responsible for c-Kit activation. In order to examine c-Kit activation, I measured by Western-Blot the Y719 phosphorylated over total c-Kit ratio in G1ME cells starved and re-stimulated by TPO. I observed that c-Kit is phosphorylated upon TPO stimulation when compared to starved condition.

Overall, these results suggested that c-Kit was directly activated by TPO and that c-Kit participated to G1ME cells proliferation. However, these observations raise the question of whether c-Kit kinase is actually activated upon TPO-stimulation and whether this activation is required for TPO-dependent proliferation of G1ME cells.

Indeed, I assessed for c-Kit activation only by analyzing the levels of phosphorylation on Y719 residue. This result should be complemented by a kinase assay or by detecting using co-immunoprecipitation assay in TPO stimulated G1ME cells the interaction between c-Kit and its partners recruited exclusively on activated receptor such as the p85 subunit of PI3K. In addition, the clear contribution of c-Kit activated kinase in TPO-dependent G1ME cells proliferation would ultimately require to analyze whether the proliferation is abolished in G1ME cells expressing a dead-kinase mutant and cultured in presence of TPO.

Nevertheless, our finding that TPO induces c-Kit intracellular phosphorylation raises the question of the mechanisms allowing c-Kit activation.

Interestingly, c-Kit activation by other cytokines than SCF has already been reported such as by IL3 (Ye et al., 2011), IL33 (Drube et al., 2010) and EPO (Munugalavadla and Kapur,

2005). In all cases, the documented physical interaction between c-Kit and the corresponding receptors was supposed to facilitate c-Kit trans-phosphorylation. These observations suggest a potential c-Kit activation through physical interaction with c-MPL. Of further interest, TPO has been reported to activate EPOR (Rouleau et al., 2004), suggesting a potential c-Kit activation by the c-MPL/ EPOR complex.

These hypotheses could be tested by two different strategies: a classical biochemical approach of co-immunoprecipitation, or an imaging approach using Proximity Ligation Assay (PLA) or Fluorescence Resonance Energy Transfer (FRET).

In addition, based on the previously reported non-canonical AKT signaling activation by Notch while still at the cell surface (Perumalsamy et al., 2009), we cannot exclude that Notch could be able to activate c-Kit in a non-canonical fashion directly at the cell membrane.

Moreover, since tetraspanins are known to play a clustering role (Hemler, 2003; Larochelle et al., 2012), CD9 could be responsible for Notch, c-Kit and c-MPL clustering at the cell surface, thus forming signaling platform allowing c-Kit activation by these receptors. This hypothesis could be tested using an RNA interference strategy targeting Cd9 and a subsequent co-immunoprecipitation in non-denaturating conditions to analyze the maintenance or not of a physical interaction between these receptors.

3.2 Does c-Kit repress megakaryocytic differentiation?

Given the TPO role in megakaryocytic differentiation and our findings that TPO activates c-Kit which contributes to G1ME cells proliferation, as well as c-Kit downregulation requirement during differentiation, we questioned whether c-Kit also contributes to restrict megakaryocytic differentiation of G1ME cells. To address this question, we analyzed whether c-Kit inhibition by Masitinib affects two aspects of megakaryocytic differentiation: expression of megakaryocytic genes and polyploidization. We found that Masitinib treatment increased polyploid cells proportion (EdU positive and DNA content higher than 4N) and increased late megakaryocytic marker PF4 expression when compared to untreated cells. These results suggest that c-Kit restricts the slight and spontaneous megakaryocytic differentiation of G1ME cells.

However, complementary experiments are required to determine whether Masitinib effect on megakaryocytic differentiation is mediated by c-Kit repression and more various approaches are required to appreciate megakaryocytic differentiation.

Even if Masitinib was used at low dose (Dubreuil et al., 2009) we cannot exclude a potential effect on another tyrosine kinase such as Lyn. Indeed Masitinib was already reported as an inhibitor of Lyn kinase (Lannutti and Drachman, 2004) and Lyn inhibition using either another tyrosine kinase inhibitor Dasatinib (Mazharian et al., 2011) or in knock-out mice (Lannutti et al., 2006) also increased megakaryocytic differentiation. For this reason, we can suspect that megakaryocytic differentiation observed in presence of Masitinib could be due to Lyn kinase and not c-Kit kinase inhibition. Nevertheless, Lyn was reported as a down-regulator of activated c-Kit (Kosmider et al., 2009). Thus, if Masitinib repressed Lyn instead of c-Kit, we would expect Masitinib to increase c-Kit expression, the inverse of what we and others (D'Allard et al., 2013) have observed. Moreover, c-Kit repression using either Masitinib in UT7/EPO cells (D'Allard et al., 2013) or by overexpressing its repressor ZNF16 in K562 cells (Chen et al., 2014a) accelerated erythroid or both erythroid and megakaryocytic differentiation, respectively. For these reasons, it seems more likely that the observed effect of Masitinib on megakaryocytic differentiation is mediated by c-Kit downregulation.

Because we observed that Masitinib induced G1ME cells polyploidization and PF4 late megakaryocytic marker expression, we concluded that c-Kit restricts G1ME cells megakaryopoiesis. Nevertheless, we could complement the demonstration of c-Kit contribution to the repression of megakaryocytic differentiation by clarifying potential Masitinib off-target effect using ISCK03 inhibitor or even specific anti-c-Kit siRNA in a more pertinent cell model that expresses GATA1 and undergoes efficient differentiation such as G1ME2 cells or megakaryocytic progenitors. Furthermore, in these cells, we should assess for megakaryocytic differentiation by complementary methods such as the quantification of more megakaryocytic markers either by qRT-PCR, or FACS acetylcholinesterase staining.

3.3 By which mechanism does CD9 repress c-Kit?

We aimed to decipher the inverse correlation observed between c-Kit and CD9 expression levels following Notch stimulation. I adopted a siRNA strategy targeting Cd9 transcripts and observed that CD9 down-modulation induced an increase of c-Kit expression at the membrane. This observation evidenced a new role for the tetraspanin CD9 in c-Kit receptor level negative regulation and allowed us to propose a new model explaining the dual role of TPO in megakaryopoiesis.

This result also raises the question of the CD9 mode of action allowing c-Kit removal from the plasma membrane. We propose two mechanisms of CD9 action that could either induces c-Kit internalization or induces its internalization followed by exosomal secretion. Based on the following studies, we find more plausible c-Kit secretion into exosomes.

Similarly to our finding that CD9 and c-Kit expression levels at the membrane are inversely correlated, a study recently reported that CD9down-modulation in a non-metastatic pancreatic cell line increase the cell surface expression of EGF-Receptor, associated with increased cell proliferation (Tang et al., 2015). Furthermore, CD9 expression levels down-modulation using doxycycline-inducible specific siRNA or the inhibition of exosomes-production using the inhibitor GW4869 decreased the production of β-catenin containing exosomes. Moreover, CD9 is a known marker of exosomes and a recent study showed that bone-marrow derived dendritic-cells from CD9 -/- mice produced less exosomes when compared to their wild-type counterparts (Chairoungdua et al., 2010). These studies highlight the importance of CD9 levels in the modulation of exosomes production and the control of signaling components expression through exosomal discharge. Besides, the secretion of wild-type c-Kit protein by mast cells has been reported and this secretion induced SCF/ c-Kit activation in lung-recipient cells inducing their proliferation (Xiao et al., 2014). Similarly, the secretion of oncogenic hyper-activated c-Kit protein has also been detected in CD9-positive exosomes derived from GIST-patients (gastrointestinal stromal tumor) and induced the transformation of muscle cells *in vitro*(Atay et al., 2014).

These observations strengthen our hypothesis that CD9 repress c-Kit expression at the cell surface by inducing its secretion in exosomes.

One first essential step to demonstrate this hypothesis is to determine whether G1ME cells supernatant contains exosomes that could be purified by ultracentrifugation (Thery et al., 2006) and whether c-Kit is carried by these exosomes following Western-Blot analysis of its expression in both exosomal fraction and total cell lysate.

Second, we could test whether this mode of secretion of c-Kit is actually dependent on CD9 using specific anti-Cd9 siRNA to quantify both the number of exosomes produced and c-Kit presence into these exosomes. Another approach would be to inhibit exosomes production and test whether c-Kit expression at the cell surface is increased. To do so, among the different pathways controlling vesicles trafficking, ceramide pathway inhibition using GW4869 (Trajkovic et al., 2008) has already been reported as cancelling CD9-dependent

exosomal secretion of β-catenin by HEK 293T cells (Chairoungdua et al., 2010) and of miR-214 by hepatic stellate cells (Chen et al., 2014b). Thus, this inhibitor should be a useful tool to assess a putative ceramide/ CD9-dependent exosomal export of c-Kit.

Besides, similarly to our finding that Masitinib treatment of G1ME cells decreased c-Kit expression at the cell surface, another study (D'Allard et al., 2013) reported the same effect and evidenced that Masitinib induces lysosomal degradation of c-Kit. However, we know that following endocytosis, internalized proteins are targeted either to lysosomes or to multivesicular bodies that will fuse with the cell membrane to liberate exosomes. Thus, we cannot exclude the hypothesis that Masitinib induces exosomal secretion of a fraction of internalized c-Kit. To test this hypothesis, we could quantify the number of exosomes produced in presence of Masitinib.

Of further interest, given that Notch represses CD9 expression and the contribution of CD9 in the control of exosomes production, it seems possible that, in parallel to its repressive effect on GATA1 and positive effect on c-Kit gene transcription, Notch could increase c-Kit expression by repressing CD9 and subsequently the production of c-Kit containing-exosomes. This hypothesis could be tested by measuring the number of exosomes produced following Notch stimulation of G1ME/ G1ME2 cells.

3.4 Is c-Kit repression by CD9 implicated in megakaryocytic differentiation increase?

Interestingly, a recent study associated CD9 expression levels deregulation with unefficient megakaryocytic differentiation in primary myelofibrosis (PMF) patients who present an accumulation of $CD41^{low}$ $CD9^{low}$ megakaryocytes and decreased cell surface expression of CD9 in *in vitro* CD34+ derived-megakaryocytes and in platelets *in vivo*. Furthermore, CD9 decreased expression in megakaryocytic progenitors derived from PMF patients was correlated with deficient communication between megakaryocytes and their stroma (Desterke et al., 2015). These observations raise the question of whether the communication between megakaryocytes and their stroma partly relies on exosomes secretion.

Based on our finding that c-Kit activation contributes to bipotent cells proliferation, whereas it restricts megakaryocytic maturation and given that CD9 levels are progressively increased during megakaryopoiesis, we propose that progression into terminal

megakaryocytic maturation is partly allowed by the CD9-dependent discharge of c-Kit from the cell surface by exosomes.

An experiment allowing to test the implication of CD9-dependent exosomal secretion of c-Kit during megakaryocytic differentiation would be to analyze whether CD9 siRNA-mediated knockdown could reduce exosomes number and the levels of associated c-Kit and whether this effect would be accompanied by accelerated megakaryocytic differentiation of G1ME2 cells or megakaryocytic progenitors.

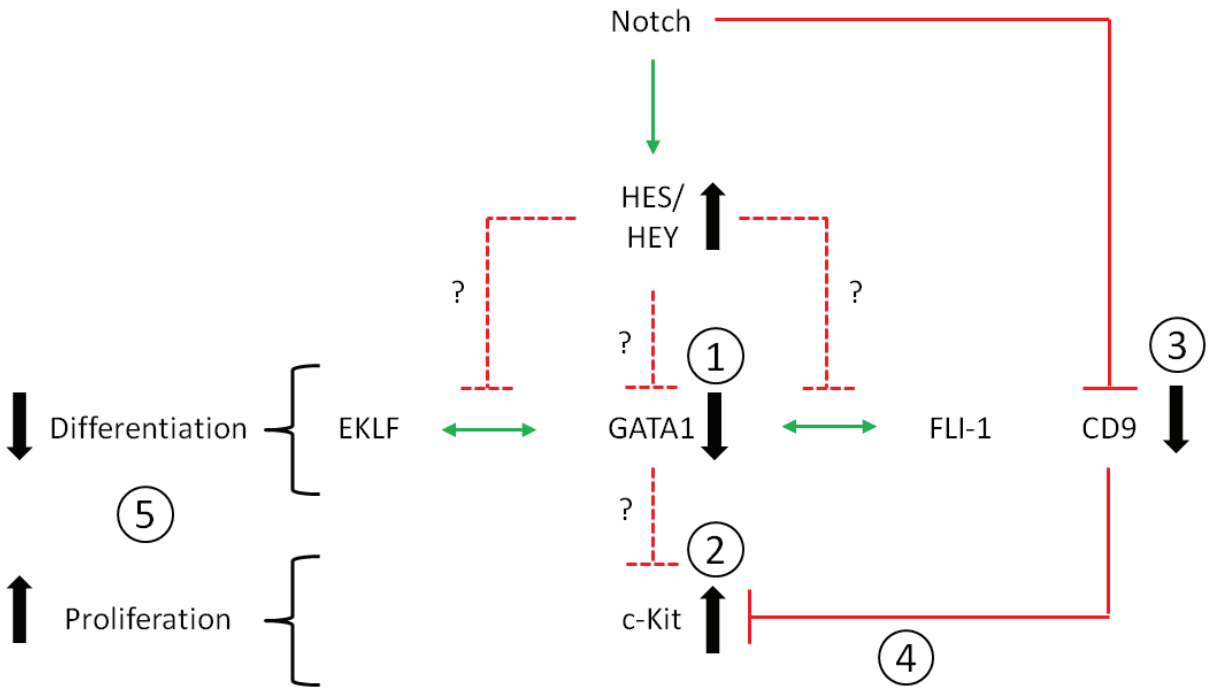

Figure 1: Summary of the proposed hypotheses explaining the positive effect of Notch on the amplification of bipotent MEP progenitors

Regulation network summarizing some results obtained during my thesis (solid and double arrows) and subsequently presumed mechanisms (dotted arrows) participating to the maintenance of a bipotent state interpreted as a blockade of differentiation and increased proliferation. Positive effects are presented by green arrows and negative effects either on expression or activity are presented by red inhibition symbol. During my thesis, I evidenced that Notch represses the expression of GATA1 (1) and CD9 (3), while inducing c-Kit expression (2). I also evidenced the negative regulation of c-Kit by CD9 (4). My results suggest that c-Kit contributes to bipotent cells amplification while restricting their differentiation (5). Besides, previous studies described the requirement for GATA1 interaction (double way arrow) with FLI-1 or EKLF to induce megakaryocytic or erythrocytic differentiation, respectively. Other studies reported that HES/HEY Notch effectors interact with GATA1 inhibiting its transcriptional activity. Based on these data, we propose that on one hand Notch effectors HES/HEY interacts with GATA1 which becomes unable to interact with its partners FLI-1 and EKLF thus repressing both erythrocytic and megakaryocytic differentiation of bipotent progenitors and allowing the maintenance of the bipotent state. On the other hand, Notch effectors HES/HEY would indirectly activate c-Kit by repressing either GATA1 or CD9 thus allowing bipotent cells amplification.

GENERAL CONCLUSION

During my thesis, I investigated the molecular mechanisms allowing the Notch pathway to maintain MEP bipotency by restricting their differentiation and favoring their amplification. My thesis work evidenced Notch role in both GATA1 and CD9 expression levels decrease and positive regulation of c-Kit at the transcriptional level. Further investigation suggested a major c-Kit contribution to TPO-dependent bipotent cells proliferation and restriction of their megakaryocytic differentiation. Additionally, I evidenced a new role of the CD9 tetraspanin in repressing c-Kit cell surface levels.

As recapitulated in Figure 1, these results suggest different modes of action of the Notch/c-Kit axis on bipotent cells maintenance. We presume that MEP differentiation repression would allow the sequestration of GATA1 by HES/ HEY Notch effectors, thus inhibiting its formation of differentiating complexes with FLI-1 or EKLF. On the other hand, both Notch and c-Kit allows E/MK bipotent cells amplification and we propose different modes of c-Kit activation by Notch, either directly through ICN/ RBPJ or indirectly through HES/ HEY Notch effectors. HES and HEY being transcriptional repressors, they can induce c-Kit expression by repressing a negative regulator of c-Kit such as CD9 or GATA1.

In summary, my thesis work highlighted Notch and TPO signals integration on the regulation of GATA1, c-Kit and CD9 and their role in favoring bipotent cells proliferation while restricting their megakaryocytic differentiation.

Based on these observations we propose that while maturing under TPO stimulation, megakaryocytes increase their expression of CD9 which in turn causes a progressive c-Kit discharge from the plasma membrane. This decrease of c-Kit expression would eventually contribute to suppress proliferative at the benefit of differentiating signals and promote the irrevocable engagement into terminal maturation.

Besides, megakaryocytes membrane was shown to be continuously blebbing and releasing microparticles (Flaumenhaft et al., 2009). In addition to the formation of membrane extensions called pro-platelets that are shed to generate circulating platelets in normal conditions, in stress-condition and independently of TPO, megakaryocyte membrane is ruptured allowing the production of enlarged stress-platelets (Nishimura et al., 2015).

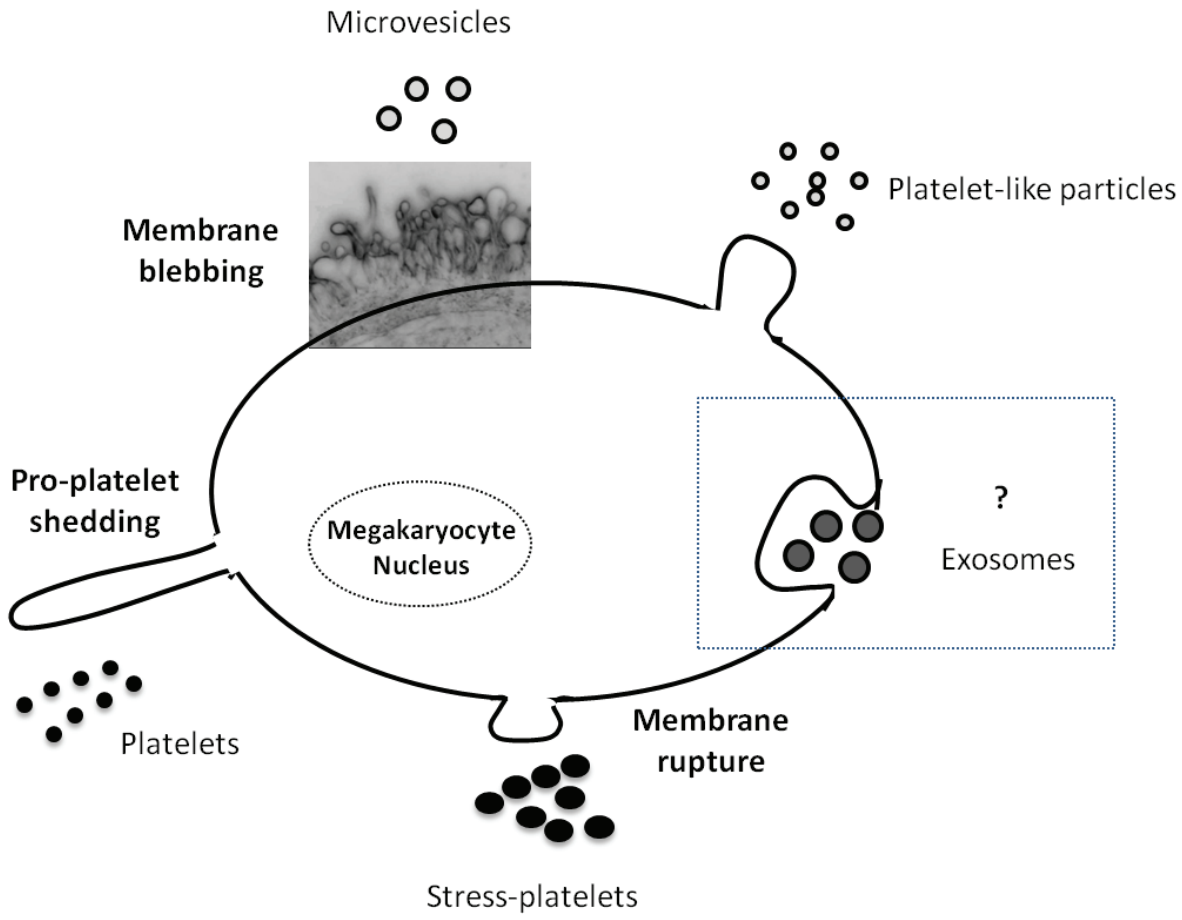

Figure 2: Megakaryocytes are highly active secreting cells

We already know that megakaryocytes are able to secrete micro-vesicles by continuous membrane blebbing, platelets by pro-platelets shedding, stress-platelets by membrane rupture, as well as platelet-like particles. In addition, our results suggest that megakaryocytes may also produce exosomes (Dotted rectangle).

Additionally, based on the studies presented in the previous section, our studies suggest that megakaryocytic progenitors would be able to secrete exosomal vesicles.

Interestingly, these observations highlight the very active and diversified modes of secretion by megakaryocytes (Figure 2). Moreover, platelets and platelet-like-particles have been shown to be released by megakaryocytic cell line and incorporated by hepatocyte cell line inducing their proliferation (Kirschbaum et al., 2015). Furthermore, CD9 has been implicated in the communication between megakaryocytes and their stromal environment (Desterke et al., 2015).

Overall, these data suggest that during their progression toward megakaryocytic maturation, megakaryocytes continuously release vesicles that influence either their direct microenvironment or even in later stage stress or normal platelets influence the balance proliferation/ differentiation of more distant tissues.

MATERIALS AND METHODS

1. Co-culture on OP9 or OP9-Dll1

L8057 cells (Ishida et al., 1993) were cultured in half IMDM half RPMI-1640 (PAA) medium supplemented by 15% of fetal calf serum, 1% of Penistreptomycin (PAA) and 1% of L-Glutamine (PAA) and were maintained between 2.5 10^5 to 1.5 10^6 cells/ mL by dilution every two days. OP9 and OP9-Dll1 (De Smedt et al., 2004) cells were cultured in α-MEM medium supplemented by 20% of fetal calf serum (PAA), 50 µM of β-mercaptoethanol, 0.2 % of sodium bicarbonate and 1 % of Penistreptomycin. OP9 and OP9-Dll1 cells adherent cells were maintained between 5.10^4 cells/ mL and 10^6 cells/ mL, diluted following trypsinization and numeration twice per week and thrown after 11 passages. All cells were cultured at 37°C and 5% CO2. OP9 or OP9-Dll1 adherent cells were plated at 10^5 cell/ mL the day before L8057 were seeded at 1:1 ratio. The day following their seeding, L8057 cells were harvested following their detachment from adherent OP9 cells by flushing then potentially remaining adherent cells were allowed to re-adhere during 30 minutes at 37°C and L8057 suspended cells were harvested again. Further exclusion of OP9 cells was performed by filtering the harvested L8057 cells on cellular sieve of 40 µm (Corning). L8057 cells were counted, then proceeded for either RNA or protein extraction. OP9 contamination was also estimated by quantification of Gfp expression by qRT-PCR.

2. Extraction of nuclear and cytoplasmic proteins

L8057 cells were harvested, counted and washed in PBS supplemented by protease (Roche) and both Ser/ Thr and Tyr phosphatases inhibitors (1 mM sodium pyrophosphate (Sigma), 25 mM sodium beta-glycerophosphate (Sigma) and 50 mM of sodium fluoride (Sigma)). Following their centrifugation, pellets were suspended in a proportional volume (5 times pellet volume) of Hepes buffer (10 mM pH 7.6, 3 mM of MgCl2, 10 mM KCl, 5 % of Glycerol and 0.5 % of NP-40) supplemented by protease and phosphatases inhibitors and incubated on ice during 10 minutes, centrifuged at 6000 rpm for 5 minutes then cytoplasmic extracts were harvested to be stored at (-80 °C). Cell pellets were then suspended in a proportional (3 times pellet volume) volume of Hepes buffer supplemented by protease and phosphatase inhibitors and 300 mM instead of 10 mM of KCl. Following 45 minutes incubation on ice and centrifugation at 6000 rpm for 5 minutes, nuclear protein extracts in the supernatant were

harvested and stored in aliquots at (-80 °C). The concentration of protein extracts was quantified by Bradford assay and equal amount of proteins was charged per condition.

3. Lentiviral infection

MIGR and MIGR-Gata1 retrorviral vectors were generously provided by . Concentrated preparations of retroviruses were prepared at the platform U3444 (Gerland, Lyon) and stored at (-80°C) before use. 5 10^4 G1ME cells (Stachura et al., 2006) per condition were seeded in 96 culture plates. The next day, G1ME cells were transduced either by MIGR or MIGR-GATA1 retroviruses at M.O.I 20 in presence of 4 µg/mL of polybrene. GFP expressing cells were sorted the following day (Considered as Day 0) at the Flow Cytometry platform (AniRA Gerland, Lyon) and were seeded in their culture medium complemented by a full cocktail of E/MK cytokines (mSCF 50 ng/mL, huEPO 2 U/mL, mTPO 20 ng/mL, mIL3 20 ng/mL, mIL6 5 ng/mL mIL11 10 ng/mL). On day 1 post sorting, G1ME cells were harvested for qRT-PCR analysis and on day 1, 2 and 3 post sorting, cells were harvested for Ter119 and CD42b labeling and FACS analysis.

4. G1ME cells stimulation by Notch coated rDll1 ligand

Cultures were performed as described previously (Poirault-Chassac et al., 2010) .Briefly, 24-well plates were pre-coated by a mix of 10 µg/ mL of goat F(ab')2 anti human IgG1 Fc specific (Rockland) and 25 µg/ mL retronectin (Takara) resuspended in phosphate buffered saline (PBS) for 2 hours at 37°C. After two washes in PBS, wells were blocked by 1% of bovine serum albumin (BSA) (Sigma) in PBS for 1 hour and washed once. Wells were coated by 10 µg/ mL of either recombinant IgG1 or DLL1 (Adipogen) for 2 hours and then washed twice with PBS. Coated plates were kept overnight with full-medium at 37°C, 5% CO_2 before cells seeding. G1ME cells were seeded at 2.5 10^5 cells/ mL in presence or absence of 10 µM of ϒ-secretase inhibitor DAPT (Sigma) and diluted by half at 24 h. At 48 hours post-stimulation, cells were counted, viability was assessed, and equal number of cells per condition was harvested for RNA extraction, flow cytometry and Western-Blot analyses.

5. Chromatin Immuno-Precipitation (ChIP)

G1ME cells were harvested following 2 days of co-culture on OP9 or OP9-Dll1, filtered and counted and then proceed for classical ChIP (Letting et al., 2004) .Briefly, cells were fixed in 1% Formaldehyde (Sigma) during 10 minutes and the reaction was stopped by the addition of 125 mM of Glycine (Sigma). Following centrifugation, cell pellets were washed three times in PBS supplemented by protease inhibitors (Roche) and dried cell pellets were conserved at (-80 °C). ChIP was performed following manufacturers' instructions (Millipore # 16-157). $10\text{^}7$ cells per condition was lysed in lysis buffer, then sonicated three times during 3 minutes at 3W and 15V with 3 minutes of pause between each cycle (Bioblock scientific VibraCell 72405). Following centrifugation at 13200 rpm, a fraction was kept for check sonication efficiency and the remainder was diluted and pre-cleared using ProteinA/ Agarose salmon sperm beads during 30 minutes on rotation at 4°C. A fraction was kept for input control and the remainder was proceeded overnight for immuno-precipitation either with rabbit Ig control (Millipore # 12-370) or with the following antibodies PolII (scbt # sc-9001), GATA-2 (scbt # sc-9008) or SCL (a kind gift of C. Porcher) before the addition of ProteinA/ Agarose salmon sperm beads. Beads were washed successively by High Salt, low salt, LiCl and TE buffer (Millipore, # 16-157). Precipitated DNA was eluted twice using elution buffer containing 10% SDS and 100mM of Sodium bicarbonate. Crosslink was reversed by the addition of 200mM of NaCl (Sigma) and incubation 4 h at 65°C. The reaction was stopped by the addition of TE buffer (Tris pH 6.5 40 mM; EDTA 10 mM) and proteins digested by Proteinase K (Roche) enzyme allowed to react 1h at 45°C before storage at (-20 °C). Immunoprecipitated DNA was extracted by phenol/ chloroforme (Sigma) method, the DNA pellet was visualized by the addition of Glycogen (Roche), washed in Ethanol 70° and suspended in water (Sigma). qPCR was performed using the primers detailed in the table below.

Gene	Forward	Reverse
Gata1 HS -3.5	5'-CCGGGTTGAAGCGTCTTCT-3'	5'-TCAGGGAAGGATCCAAGGAA-3'
Rpl18 promoter	5'-ATAGAGTGTTCCCGCATTGCG-3'	5'-TCAGCGAGCTTACCATGATGG-3'
c-Kit - 146	5'-AGAAGGTGCCCCGAGTGTATAA-3'	5'-GCACAGCTCCTTACCTTGCAAT-3'
c-Kit -114	5'-TGCCAGGCTAATGTGTTGTC-3'	5'-ATAAGAAGGCGGCTGTTCTG-3'
c-Kit -35.8	5'-AGAGAACCGAAGGTCGGATAC-3'	5'-TTGATGGAAGCATTAGAAAAAGAATTT-3'
c-Kit -21.1	5'-GATCAAAGATAATGACCCCAAGTGA-3'	5'-GGGAGGAATCAGTTATTTTGAGGTTT-3'
c-Kit 0	5'-CTCCAGGCTAATGTGGTTGTC-3'	5'-ATAAGAAGGCGGCTGTTCTG-3'
c-Kit + 4.7	5'-GGCTGGAAACCACTGCCTTA-3'	5'-AGCCTTGCCTGTGCTTAAGC-3'
c-Kit + 9.7	5'-CCGGGTGGGCCTGAGT-3'	5'-GGCATGGGCTTACAGTGTCA-3'
c-Kit + 16.2	5'-TCTTGGTGAATGGTCGGATAC-3'	5'-AACTGTTGCGGGGCATTAT-3'
c-Kit + 33.1	5'-TGGCAGTCCTGGTTGTAGCA-3'	5'-GCTGCAAGCATGCGATCA-3'
c-Kit + 58.1	5'-GCAGTTCTCCAGGTTGAGTCAGA-3'	5'-GGAGGAGTTAGGGAATATGTCGATAG-3'
c-Kit + 60.2	5'-GAACAGTGGACTCGTAGGAGCAT-3'	5'-AGAGAGGCCCAGCGTATGG-3'
c-Kit + 72.9	5'-AACTGAAGCGAGTACAGCATTCC-3'	5'-TGCTTTTGCTTGTGTACTGTTAACTG-3'
c-Kit + 77.8	5'-CACGCGCTATGCACATCCT-3'	5'-TGCCCAGCACATGACAACTT-3'

6. Micro-RNA extraction and qRT-PCR

Small RNA and total RNA were extracted using miRNeasy micro kit (Qiagen) following the manufacturers' instructions. RT and qPCR primers for miR-221, miR-451 and U6 were purchased from Applied Biosystems (Life Technologies). RT was performed usingTaqMan microRNA Reverse Transcription Kit (# 4366596) and qRT-PCR was performed using TaqMan Universal PCR Master Mix, both from Applied Biosystems (Life Technologies).

Target	Forward Primer	Reverse Primer
-actin	5’-TGGGAATGGGTCAGAAGGACTC-3’	5’-CTGGGTCATCTTTTCACGGTTG-3’
c-Kit	5’-GGGCTAGCCAGAGACATCAG-3’	5’-AGGAGAAGAGCTCCCAGAGG-3’
c-Kit Intron 1	5'-TGGGAAAAGCCAACAGCTAC-3'	5'-GAAAGAGCGGCAGACAAGAG-3'
c-Mpl	5’- CCGAGCTCGCTACAGCTT- 3’	5’- CTGTAGTGCGCAGGAAATTG -3’
Cd9	5’- GCTCGAAGATGCTCTTGGTC -3’	5’- GCTCGAAGATGCTCTTGGTC -3’
c-Myc	5’-TCCTGTACCTCGTCTGATTCC-3’	5’-CTCTTCTCCACAGACACCACATC-3’
Fli-1	5’-GACTCTGTCAGGAGAGGAGC-3’	5’-GTCATTTTGAACTCCCCGTTG -3’
Gata1	5’-TTCTTCCACTTCCCCAAATG-3’	5’-AGGCCCAGCTAGCATAAGGT-3’
Gata2	5’-GAATGGACAGAACCGGCC-3’	5’-AGGTGGTGGTTGTCGTCTGA-3’
Hes1	5’-CTACCCCAGCCAGTGTCAAC-3’	5’-CGCCTCTTCTCCATGATAGG-3’
Itga2b	5’-AAGCTCTGAGCACACCCACT-3’	5’-CTCAGCCCTTCACTCTGACC-3’
Jak-2	5’-GATGGCGGTGTTAGACATGA-3’	5’-TGCTGAATGAATCTGCGAAA-3’
Pf4	5’- AGTCCTGAGCTGCTGCTTCT -3’	5’- CAGCTAAGATCTCCATCGCTTT- 3’
Pten	5’-AATTCCCAGTCAGAGGCGCTATGT-3’	5’-GATTGCAAGTTCCGCCACTGAACA-3’
Tal-1	5’-CGGAGGATCTCATTCTTGCTTAG-3’	5’- CTAGGCAGTGGGTTCTTTGGG -3’
tr-Mpl	5’-GAGGACTGGAAGGAGACTGAGGCA-3’	5’-AGGTTGCAGTCCTCTGTAGTCCAT-3’

ANNEX 1
Manuscript 1: Unexpected plasticity of committed megakaryocytic progenitors revealed upon Notch stimulation

Title: Unexpected plasticity of committed megakaryocytic progenitors revealed upon Notch stimulation

Running title: Notch-inducedmegakaryocyte progenitors plasticity

Authors: Michèle Weiss-Gayet[1], Joëlle Starck[1], Azza Chaabouni, Bénédicte Chazaud and François Morlé*

1 Equal contribution

Authors affiliations: CGPhiMC, CNRS UMR5534 Université Claude Bernard Lyon1, France

*** Corresponding author:**

Francois Morlé,

CGPhiMC, CNRS UMR5534, Bat G Mendel, 16 Rue Dubois, 69622 Villeurbanne, France. Tel : 33 (0)4 72 43 36 37; Fax : 33 (0)4 72 43 26 85; email: francois.morle@univ-lyon1.fr

Scientific category: Hematopoiesis and Stem Cells

Text words count: 4360

Abstract words count: 202

Number of Figures: 7

Number of references: 41

Key points

- Notch favors erythrocytic commitment and stimulates SCF-dependent self-renewal of bipotent and committed erythrocytic and late megakaryocytic progenitors.

- Megakaryocytes can be induced to resume cell divisions and regenerate megakaryocytic, erythrocytic and bipotent progenitors upon Notch activation.

Abstract

The aim of this study was to reinvestigate the controversial contribution of Notch signaling to megakaryocytic lineage development. For that purpose, we analyzed the progeny of purified megakaryocyte-erythroid progenitors (MEP) in short-term cultures performed on recombinant Notch ligand rDll1. Upon short Notch activation, MEP generated an increased number of $Kit^{+}/CD41^{Low}$ progenitors expressing increased levels of Kit. Moreover, Notch activation reduced both the number of differentiated megakaryocytic cells and their expression of CD41 and CD42b. Colony assays showed that Notch favored both the expansion of bipotent progenitors and their erythrocytic commitment as well as the expansion of committed erythrocytic and late megakaryocytic progenitors. We identified a $CD9^{High}$ MEP subset that spontaneously generated almost exclusively megakaryocytic progeny including single megakaryocytes and few megakaryocytic colonies. Colony assays and single cell progeny analyses showed that upon Notch activation, this $CD9^{High}$ subset generated an increased number of megakaryocytic, erythrocytic, bipotent and even granulo-monocytic colonies at the expense of single megakaryocytes. These results evidence that Notch contributes to the self-renewal of all bipotent and committed erythrocytic and megakaryocytic progenitors and strengthen the emerging view that committed megakaryocytic progenitors actually remain competent to resume cell divisions and regenerate alternative lineages until the very last division before terminal megakaryocytic polyploidization.

Introduction

Notch signaling is involved in many proliferation/differentiation and/or lineage commitment decisions during development, including hematopoiesis [1-3]. Notably, Notch1 is required for the generation of the first definitive hematopoietic stem cells (HSC). Notch1 is also required for T-cell lineage development occurring at the expense of B-cell lineage [4]. Moreover, deregulated Notch signaling induces T-cell leukemia in mouse and human [5].

Concordant *in vitro* results have shown that stimulation by Notch ligands (Jag1, Jag2, Dll1 or Dll4)[6-12], as well as enforced expression of Notch intracellular domain (NICD) [7] or that of its target HES1 [13] stimulate HSC self-renewal at the expense of their differentiation [14]. In apparent contradiction, most *in vivo* studies have shown that the steady state number of HSCs is not affected by the suppression of Notch signaling by either conditional deletion of Notch1[15], Notch2 [16], Notch1 and Notch2 [17], RBP-Jk [18], Jag1 [19] or Hes1 nor by enforced expression of the pan-Notch inhibitor dnMAML [20]. However, deletion of Notch2 (but not Notch1) reduces the rate of bone marrow reconstitution including repopulation of HSCs after injury thus suggesting a specific role for Notch2 during stress hematopoiesis [16].

Whether Notch also controls lineage commitment and/or self-renewal divisions of multipotent and/or committed monopotent progenitors remains more controversial. Recent studies showed that Notch activation induces selective apoptosis of granulo-monocytic (GMP) progenitors [21] while loss of Notch signaling induces myelo-monocytic leukemia in mouse and chronic myelo-monocytic leukemia (CMML) in human [21-25]. On the opposite, other studies have shown that Notch activation increases the number of $CD41^+$ megakaryocytic cells generated by murine Lin-/$Sca\text{-}1^+$/$c\text{-}Kit^+$ (LSK), common myeloid (CMP) or MEP progenitors indicating the positive contribution of Notch to the megakaryocytic specification [26]. Further studies have shown that Notch pathway activates AKT that in turn suppresses the inhibitory action of FOXO factors on Notch targets during megakaryocyte development particularly in CMP [27]. Intriguingly in both of these studies [26,27], the positive effect of Notch on megakaryocytic development was systematically associated with an increased MEP and a decreased GMP numbers that were interpreted as the successive contributions of Notch to the megakaryocytic commitments of CMP and MEP. However, intriguingly, Notch does not promote megakaryocytic commitment of human $CD34^+$ pluripotent cells but inhibits terminal megakaryocyte maturation in contrast to what is observed in mouse [28]. These discrepancies

were tentatively attributed to differences in the contribution of Notch to the control of megakaryocytic lineage between mouse and human [29]. Similarly, contradictory results have also been reported regarding the role of Notch during erythropoiesis with some studies indicating increased apoptosis [30,31] and many others indicating either inhibition of erythrocytic differentiation [32-35] and/or increased self-renewal of committed erythrocytic progenitors [35,36].

The aim of this study was to reinvestigate the real impact of Notch signaling in megakaryocytic lineage development. For this purpose, we took advantage of purified bipotent MEP progenitors, which offer the precise deciphering of megakaryocytic commitment, expansion and differentiation through progeny analysis. Moreover, to avoid the side effects associated with the use of Dll1-expressing cells, MEP progenitors were shortly activated *in vitro* with recombinant Notch ligand rDll1,

Material and methods

Mice

Mice (genetic background C57BL/6J-129) were bred and maintained under specific-pathogen-free conditions at the ALECS-SFP animal facilities of the Faculté de Médecine Lyon-Est (Université Claude Bernard, Lyon1, France) and experimentations were performed according to procedures approved by the local animal care and experimentation authorities(Ministère Délégué de la Recherche etdes Nouvelles Technologies, agreement no. 4936; Direction des ServicesVétérinaires, agreement n^{o} 69266317 and 7462).

Flow cytometry

Bone marrow cells (BMC) were flushed from femurs and tibiae in Iscove's Modified Dulbecco's Medium (IMDM) containing 2 % fetal calf serum (FCS), treated with red blood cells ACK lysing buffer (Lonza) and filtered through a 40 □ m cell strainer (BD Biosciences) to obtain single-cell suspensions. BMC suspensions were labeled with a cocktail of biotinylated lineage antibodies (Lineage cell depletion Kit, Miltenyi Biotec) supplemented with biotinylated anti-Sca-1 (BD Pharmingen), anti-CD3 (BD Pharmingen), anti-IL7R (eBiosciences), anti-Ter119 (eBiosciences) and anti-CD19 (Serotec). Lin^{-}/Sca1^{-} cell suspensions were isolated by magnetic depletion of lineage and Sca-1 positive cells using LS

columns (Miltenyi Biotec). For MEP preparation, $Lin^-/Sca1^-$ cells were further labeled with streptavidin-PE-Cy7 (BD Pharmingen) for the elimination of residual biotinylated stained cells and with anti-c-Kit-APC (BD Pharmingen), anti-CD34-FITC (e-Biosciences) and anti-Fc□-RII/III-PE (BD Pharmingen) antibodies and sorted with gating window $Lin^-/Sca1^-/Kit^+$ Fc□-$RII/III^{low}/CD34^{low}$ (Figure S1) as previously described [37] using FACSAria cell sorter and DIVA software (BD Biosciences). MEP subsets expressing different levels of CD9 were sorted using anti-cKit-efluor 450 and anti-CD9-APC antibodies. For cell cycle analyses, sorted $CD9^{High}$ and $CD9^{Med}$ MEP were centrifuged at 400g for 10 minutes, fixed using Foxp3/Transcription Factor Staining Buffer Set (eBioscience), treated with DNAse free RNAseA (100 □ g/mL for 30 min at room temperature) and labeled using FITC mouse anti-human Ki-67 Set (BD Pharmingen) and 50 □ g/mL propidium iodide followed by FACS analysis. 2N and 4N $CD9^{High}$ and $CD9^{Med}$ MEP subsets were sorted after labeling using anti-CD9-APC and anti-cKit-PerCP-efluor 710 (eBioscience) antibodies followed by DNA staining with Hoechst 33342 (20 □ g/mL Eurogentec) during 45 min at 37°C just before sorting.

Colony assays

Colony assays were performed by duplicate seeding of 1000 or 2000 cells into 3 mL final volume of $MethoCult^R$ M3234 (StemCell Technologies) supplemented with 30% FCS, mIL3 (10 ng/mL), mSCF (50 ng/mL), mFlt3l (5 ng/mL), mGM-CSF (5 ng/mL), mIL11 (50 ng/mL), huEPO (4 U/mL) and mTPO (50 ng/mL) allowing the growth of all types of myeloid progenitors. Mixed erythro-megakaryocytic, erythrocytic, megakaryocytic and myeloid colonies were scored under microscope after 7 days of culture at 37°C, 5% CO_2. All cytokines were purchased from PeproTech except huEPO (kindly provided by F Nicolini).

Batch cultures of progenitors on recombinant rDll1 and control IgG1.

Cultures were performed as previously described with minor modifications [10]. Briefly, wells of untreated culture plates were pre-coated for 1 h at 37°C with 10 □ g/mL of goat F(ab')2 anti-human IgG1 Fc specific (Rockland) and of 25 □ g/mL Retronectin (Takara) in phosphate buffered saline(PBS). Wells were washed twice with PBS, blocked with 1 % bovine serum albumin (BSA) in PBS, incubated with 10 □ g/mLof either IgG1 or rDll1 (Adipogen) in PBS for 2 h at 37°C and washed extensively with PBS. Coated wells were seeded at day 0 with 2000 progenitor cells in 1 mL of IMDM medium supplemented with 10% FCS, mIL3 (10 ng/mL), mSCF (30 ng/mL), mFlt3l (25 ng/mL), mGM-CSF (10 ng/mL),

mIL11 (25 ng/mL), huEPO (4 U/mL) and mTPO (25 ng/mL) with or without 10 □ M DAPT (□-secretase inhibitor, Sigma). At day 2, the totality of the cells from each well, representing the total progeny generated by the initial 2000 cells seeded at day 0, were collected and analyzed by colony assay. Alternatively, cells were numbered and analyzed by flow cytometry after labeling with appropriate antibodies at day 5 or 6.

Single cell liquid cultures

Sorted $CD9^{High}$ or $CD9^{Med}$ MEP subsets were seeded as single cell in wells of 96 wells culture plates coated with either IgG or rDll1 and cultured in IMDM medium supplemented as above. Colonies were scored after 7 days under bright field microscope as described previously [37].

qRT-PCR analyses

Total RNA was extracted using the Rneasy PLUS microkit (Qiagen) and reverse transcribed using a Quantitect reverse transcription kit (Qiagen). qPCR reactions were performed on a Mx3000P qPCR instrument (Stratagene) using Light-cycler 480 SybR-Green-Master-Roche kit and primers indicated in Table S1. mRNA specific signals were normalized to that of beta-actin mRNA.

Statistics

The data were analyzed by Student t-test. Differences were considered statistically significant at $P < 0.05$.

Results

Sorted MEP generate an increased number of Kit+ progenitors and a decreased number of less differentiated megakaryocytic cells upon Notch stimulation

FACS-sorted mouse bone marrow MEP progenitors ($lin^-/Sca1^-/Kit^+/CD16/32^{low}/CD34^{low}$; Figure S1) were cultured for 5 days in liquid medium supplemented with a complete cocktail of myeloid cytokines (IL3, Ftl3l, GM-CSF, SCF, IL11, EPO, TPO) in culture wells coated with recombinant Notch ligand rDll1. Cultures

performed in the presence of the □-secretase inhibitor DAPT or on coated IgG instead of rDll1 were used as negative controls of the Notch activation. Despite variations between different MEP preparations, the total number of cells (Figure 1A) as well as the number (Figure 1B) and the relative proportions (Figure 1C) of Kit^+ progenitors were significantly higher in cultures performed on rDll1 than on IgG and were reduced in the presence of Notch inhibitor. qRT-PCR analyses performed at day 2 confirmed the expected increase in Hes1 transcripts attesting Notch pathway activation in the presence of rDll1 and its partial repression by DAPT (Figure S2). Further analyses showed that the Kit^+ progenitors amplified upon Notch activation were characterized by the expression of low levels of CD41 (Figure 2A) and higher levels of Kit detected at both protein (Figure 1D, E) and transcript levels (Figure S2). This amplification of $Kit^+/CD41^{Low}$ progenitors upon Notch activation was strictly dependent on the presence of SCF. Interestingly the increase in Kit expression was readily observed in the absence of SCF (Figure 1D) thus indicating a real contribution of Notch to the up-regulation of Kit expression rather than a simple preferential amplification of progenitors expressing higher levels of Kit. Taken together, these results indicate that activation of the Notch pathway in MEP progenitors increases their Kit expression and stimulates the SCF-dependent amplification of their Kit^+ progeny.

Complementary analyses of the same MEP cultures revealed that Notch stimulation was also associated with a reduced number of megakaryocytic $Kit^-/CD41^+/CD42b^+$ cells (Figure 2A and 2B). Moreover, although still $CD41^+/CD42b^+$, these megakaryocytic cells expressed lower levels of CD41 and CD42b (Figure 2A and 2C), indicative of a less differentiated state upon Notch activation. Thus, Notch activation both reduced the number and slowed down the differentiation of megakaryocytic cells generated by MEP.

Notch activation stimulates the amplification of bipotent and erythrocytic progenitors from MEP population

Colony assays performed in methylcellulose supplemented with the same complete cocktail of myeloid cytokines revealed that 25% of freshly sorted MEP generated a progeny including 50% of pure erythrocytic colonies, 25% of pure megakaryocytic and 25% of mixed erythro-megakaryocytic colonies (Figure 3A, Day 0). These results confirmed previous studies, that the MEP population (which be referenced as Day 0 in the present study) is

actually composed of a mixture of pure erythrocytic and megakaryocytic progenitors in addition to truly bipotent progenitors.

The same colony assay was used to quantify the variations in the number of each type of progenitors induced by a two days culture in liquid medium on either IgG or rDll1 (Figure 3A). The only change observed after the two days culture on IgG was a symmetrical slight increase in megakaryocytic colonies and reproducible but not significant decrease of erythrocytic colonies (Figure 3B) that could suggest spontaneous commitment of bipotent progenitors towards megakaryocytic differentiation. In contrast, the two days culture on rDll1 induced a marked increase in both mixed and erythrocytic colonies and much smaller decrease in megakaryocytic colonies (Figure 3C), these effects being blunted in the presence of DAPT (Figure 3A). This strongly asymmetrical large increase in erythrocytic versus small decrease in megakaryocytic colonies observed on rDll1 cannot be explained only by the simple erythrocytic commitment of bipotent progenitors but indicates a concomitant preferential amplification of erythrocytic progenitors upon Notch activation. As expected, this amplification of bipotent and erythrocytic progenitors induced by Notch activation was also strictly SCF-dependent (Figure S3).

Identification of a specific CD9High MEP subset strongly responding to Notch activation

Although the number of bipotent and erythrocytic progenitors invariably increased in the presence of rDll1, we noticed that the extent of this increase varied (from 1.2 to 3 fold) from a MEP preparation to the other. Surprisingly, the fold increase in erythrocytic and bipotent progenitors observed upon Notch activation positively correlated with the megakaryocytic differentiation bias of the parent MEP populations (Figure 4). The more the native MEP population was biased toward the generation of megakaryocytic colonies, i.e. contained megakaryocytic progenitors, the more it was responding to Notch activation, assessed by increased bipotent (Figure 4A) and erythrocytic (Figure 4C) colonies. This intriguing observation prompted us to isolate MEP subsets differing in their megakaryocytic differentiation bias in order to compare their response to Notch. An interesting previous study reported the existence of a $CD150^{+}$ /$CD9^{High}$ subset of Lin^{-} /Kit^{+} /$Sca1^{-}$ mouse bone marrow cell population displaying obvious erythro-megakaryocytic bipotency while being strongly biased towards megakaryocytic differentiation [38]. Since most of bipotent progenitors present in the MEP gate are $CD150^{+}$[39], CD9 appeared as a very good candidate marker for

the sorting of MEP cells according to their megakaryocytic bias. As shown in Figure 5A, MEP cells displayed a roughly bimodal distribution of CD9 level allowing us to sort three different subsets according to their CD9 expression level ($CD9^{Low}$, $CD9^{Med}$ and $CD9^{High}$). Colony assays performed on these 3 sorted subsets showed an expected increase in the proportion of megakaryocytic colonies correlated with the increase of CD9 expression level reaching more than 90% for the $CD9^{High}$ subset associated with a reduced clonogenicity (Figure 5B). Since the $CD9^{Low}$ subset appeared to be slightly contaminated by a few proportion of granulo-monocytic progenitors (see Figure 5B), we focused the next analyses on the comparison of the Notch response between $CD9^{Med}$ and $CD9^{High}$ subsets that contained most of the erythrocytic-megakaryocytic potential without detectable granulo-monocytic contamination. For that purpose we followed the same protocol described in Figure 2 and the results obtained with three independent preparations of $CD9^{Med}$ or $CD9^{High}$ are presented in Figure 5C and 5D respectively. As expected, the $CD9^{Med}$ (which represented about 50% of MEP), roughly reproduced results obtained with the unfractionated MEP population namely an increase of erythrocytic and bipotent colonies and slight decrease of megakaryocytic colonies after the two days culture on rDll1 (Figure 5C). In marked contrast, the very low numbers of erythrocytic and bipotent colonies generated by $CD9^{High}$ MEP at day 0 were spectacularly enhanced (up to 10 and 40 fold respectively) after the two days culture on rDll1 (Figure 5D) while the numbers of megakaryocytic colonies were again slightly reduced. Moreover, as observed with the unfractionated MEP population (Figure 4) the fold increase in bipotent(Figure 5E) and erythrocytic (Figure 5G) colonies upon Notch activation still correlated with the megakaryocytic bias of the initial $CD9^{High}$ MEP population.

Such a spectacular increase in bipotent and erythrocytic colonies led us to hypothesize that the $CD9^{High}$ subset might actually include quiescent progenitors that would be reactivated by Notch activation. Unexpectedly, FACS analyses performed after double DNA and Ki67 labeling revealed that up to 80% of $CD9^{Med}$ cells were in G1 phase of cell cycle including 30% in G0 as compared with $CD9^{High}$ population which contained only 60% of cells in G1 and 4.7% of cells in G0 (Figure S4A and S4C). In contrast, while both subsets displayed the same proportion of cells in S phase, the $CD9^{High}$ subset was characterized by an increased proportion of cells in G2/M including cells with reduced Ki67 expression. Moreover, the $CD9^{High}$ subset was also characterized by 5% of binucleated cells that may correspond to megakaryocytes transiently paused during the process of their polyploidization (Figure S4B and S4D). Taken together, these observations prompted us to investigate the possibility that

late megakaryocyte progenitors - megakaryocytes present in the $CD9^{High}$ subset might resume cell divisions and re-express erythrocytic program upon Notch activation.

CD9High megakaryocytes can resume cell divisions to generate megakaryocytic precursors upon Notch activation

To explore the role of Notch in the sequential steps of megakaryocytic commitment/expansion/differentiation, we sorted the 2N and 4N fractions of the $CD9^{Med}$ and $CD9^{High}$ MEP subsets and used colony assay to score only the megakaryocytic progenies generated after a two days culture on IgG or rDll1. Colonies containing from 1 (single megakaryocyte) to over 8 megakaryocytes were counted (Figure 6). As expected, the total megakaryocytic progeny of the 2N or 4N $CD9^{High}$ MEP subsets generated on IgG was around 4 fold higher than that of the corresponding $CD9^{Med}$ MEP subsets. However, single megakaryocytes contributed to most (65%) of the 2N $CD9^{High}$ progeny compared to only 33% for the 2N $CD9^{Med}$ (Figure 6B). This difference in the proportion of single megakaryocytes obtained from $CD9^{High}$ versus $CD9^{Med}$ MEP subsets was also observed in their 4N fractions (89% vs 43% respectively, Figure 6B). Most importantly, the two days culture on rDll1 did not significantly change the total megakaryocytic progeny in neither subset. However, Notch activation led to a decrease in the proportion of single megakaryocytes and concomitant increase of colonies containing higher numbers of megakaryocytes (Figure 6B). These results thus indicated that Notch activation was able to reprogram late megakaryocytic progenitors, representing most of megakaryocytic progenitors present in $CD9^{High}$, to resume cell divisions instead of going on towards terminal megakaryocytic growth without division.

Single CD9High MEP cells can generate megakaryocytic, erythrocytic, bipotent and tri-potent progenitors upon Notch activation

Single cell progeny analyses were then performed to directly determine if Notch activation was also able to induce lineage reprogramming. For that purpose, single $CD9^{Med}$ or $CD9^{High}$ MEP were individually seeded in each well of 96 well culture plates coated with either IgG or rDll1 still in the presence of a complete cocktail of myeloid cytokines for 1 week. Cell progenies were scored by careful inspection of all culture wells using bright-field microscope after 7 days of culture as previously described [37] and the qualification of the colony (megakaryocytic, erythrocytic, mixed colonies, granulo-monocytic) raised by one

single cell is given as a percentage of all single cells that were seeded (Figure 7). The culture on either IgG or rDll1 did not significantly change the proportion of $CD9^{Med}$ cells generating colonies including erythrocytic, megakaryocytic, mixed and few granulo-monocytic colonies (Figure 7A), indicating no effect of Notch on $CD9^{Med}$ MEP survival. However, the proportion of $CD9^{Med}$ MEP cells that led to erythrocytic colonies increased at the expense of those giving rise to megakaryocytic colonies (only colonies containing over 4 cells were scored) in the presence of rDll1 as compared to IgG (Figure 7B) thus indicating preferential commitment of $CD9^{Med}$ MEP towards erythrocytic lineage upon Notch activation. This confirmed the colony assay performed with the bulk $CD9^{Med}$ MEP subset (Figure 5C).

Similarly as observed with the whole $CD9^{High}$ MEP population (Figure 5D), single $CD9^{High}$ MEP cells generated upon Notch activation a higher proportion of colonies, including megakaryocytic colonies containing more than 4 cells (Figure 7C, colored bars). However, when considering also $CD9^{High}$ MEP generating at least one single megakaryocyte, the amount of $CD9^{High}$ MEP cells generating a viable progeny did not change significantly on IgG (77%) or rDll1 (71%) (Figure 7C). Remarkably, whereas the progeny of single $CD9^{High}$ MEP cells on IgG was exclusively megakaryocytic, up to 15% of this progeny was committed into erythrocytic, erythro-megakaryocytic or even granulo-monocytic colonies on rDll1 (Figure 7C and 7D). This indicates a reprogramming of megakaryocytic-biased $CD9^{High}$ MEP towards bipotent and erythrocytic lineages upon Notch activation.

In one of these single cell progeny analyses, we further scored the colonies including a detailed analysis of megakaryocytic colonies containing from 1 to more than 4 megakaryocytes. As observed in Figure 6 for the bulk population upon Notch activation, single $CD9^{High}$ MEP cells generated a decreased proportion of single megakaryocytes and increased proportion of megakaryocytic colonies (Figure 7 E and 7F). These results indicate that Notch activation not only stimulates cell divisions of committed megakaryocytic progenitors but also induces their reprogramming towards erythrocytic or granulo-monocytic lineages.

Discussion

The aim of this study was to investigate the effect of the Notch pathway on the development of the megakaryocytic lineage. To specifically answer this question, we used pure bipotent MEP progenitors that were shortly treated with recombinant Dll1.

First, we confirmed the heterogeneity of purified MEP populations actually composed of a mixture of erythrocytic, megakaryocytic in addition to truly bipotent progenitors. Our results showed that activation of the Notch pathway (evidenced by increased levels of the Notch target Hes1 mRNA) stimulated the amplification of $Kit^{+}/CD41^{Low}$ progenitorsin short-term cultures of MEP performed on rDll1. Colony assays further showed that amplified progenitors are mainly bipotent and erythrocytic progenitors whereas the number of megakaryocytic progenitors slightly decreased. The strong asymmetry between the large increase in erythrocytic progenitors versus the small decrease in megakaryocytic progenitors indicated that Notch activation stimulates the amplification of committed erythrocytic progenitors independently on its contribution to the commitment of bipotent progenitors towards the erythrocytic lineage (Figure 7). Importantly, this preferential amplification of bipotent and erythrocytic progenitors was strictly SCF-dependent and associated with the increased expression of Kit receptor detected at both transcriptional and protein levels. Moreover, this increased Kit expression was also observed in the absence of SCF suggesting that it is functionally involved rather than being the simple consequence of the SCF-dependent progenitor amplification induced by Notch. Taken together, these results indicate that Notch activation allows the SCF-dependent amplification of bipotent and erythrocytic progenitors mediated at least partially through the up regulation of Kit. This conclusion corroborates two recent studies showing the contribution of Notch to the SCF-dependent amplification of human erythrocytic progenitors *in vitro*[35] as well as murine erythrocytic progenitors during stress erythropoiesis *in vivo*[36]. Our results also help to resolve some controversies about the apparent divergent effects of Notch signaling on megakaryocytic differentiation between mouse and human [29]. In particular, our results confirm that Notch activation actually favors erythrocytic instead of megakaryocytic commitment as recently shown by for PreMegE progenitors [36]. In opposite, another study concluded that Notch activation favors megakaryocytic development based on the observation of an increased production of $CD41^{+}$ and MEP progenitors by LSK or CMP multipotent progenitors upon Notch activation [27]. However, based on the present data demonstrating that Notch not only increases the self-renewal of bipotent MEP, committed erythrocytic progenitors but also that

of committed late megakaryocytic progenitors (as evidenced by the size increase of megakaryocytic colonies), we suggest that the increased production of MEP and $CD41^+$ progenitors observed in this previous study can be best explained by this contribution of Notch to self-renewal instead of by a true contribution of Notch to the preferential commitment towards megakaryocytic lineage [27]. In addition and in agreement with previous results obtained with human $CD34^+$ cells [28], the present study further showed that Notch stimulation also partially inhibits murine terminal megakaryocytic differentiation as evidenced by the production of a reduced number of double positive CD41/CD42b cells expressing lower level of CD42b.

The most original finding of our study is the unexpected plasticity of the $CD9^{High}$ subset of MEP progenitors revealed by Notch activation. Indeed, in contrast to $CD9^{Med}$ MEP, the progeny of $CD9^{High}$ MEP generated in the absence of Notch stimulation was almost exclusively megakaryocytic including a large majority of single large mature megakaryocytes and few megakaryocytic colonies harboring a reduced number of mature megakaryocytes, indicating an advanced stage of megakaryocytic differentiation. Importantly, Notch stimulation not only increased the size of megakaryocytic colonies but also reduced the proportion of single megakaryocytes. Taken together, these results indicate that the strong megakaryocytic bias of $CD9^{High}$ MEP is associated with reduced self-renewal efficiency that can be reversed by Notch activation acting until the very last division before terminal differentiation, thus allowing progenitors to resume cell divisions instead of endoploidization. Interestingly, previous studies reported that binucleated megakaryocytes are able to resume cell divisions at very low efficiency [40] thus raising the possibility that the 5% of binucleated cells detected in the $CD9^{High}$ MEP populationmight be preferentially involved in the Notch response. Although this possibility cannot be excluded, our finding that Notch also increased the size of megakaryocytic colonies generated by both $CD9^{Med}$ and $CD9^{High}$ diploid subsets already indicates that binucleated megakaryocytes are most probably not the unique Notch target cells explaining increased self-renewal of megakaryocytic progenitors.

The other intriguing property of $CD9^{High}$ MEP is their capacity to restore the generation of mixed, erythrocytic and even few myeloid colonies in response to Notch activation contrasting with their almost exclusive megakaryocytic progeny when these cells are untreated. The most trivial origin of these non-megakaryocytic colonies could be the reactivation and/or the strong preferential amplification of a small number of quiescent bipotent and/or multipotent contaminant progenitors. However, we failed to detect quiescent

G0 cells in the $CD9^{High}$ subset while such G0 cells were readily detected in the $CD9^{Med}$ subset. Moreover, the up to 40 fold increase in bipotent colonies observed after only two days on rDll1 (see Figure 5E) would imply a very short cell cycle of around 8-9 hours that seems very unlikely for the reactivation of quiescent cells. On the other hand, the three independent experiments performed, totalizing the analysis of 252 $CD9^{High}$ single cell progeny, revealed exclusively megakaryocytic progeny when cultured on IgG whereas up to 15% of non-megakaryocytic cells appeared at the expense of the megakaryocytic progeny in cultures on rDll1 (Figure 7). Although these results cannot formally exclude the minor contribution of a small number (less than 1 out of 252) of quiescent/contaminant pluripotent progenitors (possibly $CD9^{High}$ CMP), they already indicate that around 10% of $CD9^{High}$ progenitors can be diverted from terminal megakaryocytic towards erythrocytic or mixed differentiation upon Notch activation. This strongly supports the emerging view [38] that megakaryocytic progenitors actually remain at least bipotent until the very last division before terminal endoploidization, an interpretation that is further strengthened by the only slight decrease of several erythroid specific genes (KLF1, TFRC, KEL) in single $CD9^{+}$ MEP as compared with $CD9^{-}$ MEP (Figure S5)[41]. Interestingly, transient amplification of $CD150^{+/}CD9^{High}$ bipotent progenitors has been shown to accompany platelets recovery in mice injected with anti-platelet serum [38]. Another study recently reported that stress erythropoiesis depends on Notch signaling [36]. The present study raises the intriguing possibility that $CD9^{High}$ MEP progenitors might constitute a common dormant reservoir allowing rapid Notch-dependent regeneration of red cells or platelets in response to hematopoietic stress.

In summary (Figure S6), this study shows that Notch activation favors the erythrocytic commitment of bipotent MEP progenitors and stimulates their SCF-dependent self-renewal as well as that of all committed erythrocytic and late megakaryocytic progenitors in association with increased expression of Kit. Most importantly, this study reveals the unexpected plasticity of $CD9^{High}$ late megakaryocytic progenitors that can, upon Notch activation, be diverted to resume cell division instead of terminal endo-polyploidization/differentiation to regenerate progenitors not only with megakaryocytic but also with erythroid, mixed or even myeloid potential. These data demonstrate Notch signaling as a key regulator of the homeostasis of erythrocytic/megakaryocytic lineages.

Acknowledgments

This work has been supported by grants from the CNRS and Université Claude Bernard Lyon1 and by specific grants from the Ligue Nationale contre le Cancer (Equipe labellisée 2009-2012 and Comités du Rhône, de la Drôme et du Cantal). MW and JS are permanent employees of CNRS while FM and BC are permanent employees of INSERM. AC PhD student has been supported by a three years salary from the Ligue Nationale contre le Cancer (2011-2014) and by a 6 months salary from the Société Française d'Hématologie (2014-2015). Authors acknowledge Thibault Andrieu and Sébastien Dussurgey from the AniRA-Cytometry platform for their expert help in FACS analyses and sorting. All authors are also greatly grateful to Boris Guyot, Gaetan Juban, Guy Mouchiroud and Rémi Mounier for helpful discussions and critical reading of the manuscript as wells as to Thomas Mercher for his warm encouragement and helpful suggestions at the beginning of this study.

Authorship contributions

MW and JS contributed to the design and performed most of the experiments, interpreted the results and reviewed the written manuscript. AC contributed to some of the experiment interpreted the results and reviewed the written manuscript. BC critically reviewed and edited the manuscript. FM designed the study, interpreted the results and wrote the manuscript.

Conflict of Interest Disclosures

None of the authors have conflict of interests.

References

1. Yuan JS, Kousis PC, Suliman S, Visan I, Guidos CJ (2010) Functions of notch signaling in the immune system: consensus and controversies. Annu Rev Immunol 28: 343-365.

2. Bigas A, Espinosa L (2012) Hematopoietic stem cells: to be or Notch to be. Blood 119: 3226-3235.

3. Pajcini KV, Speck NA, Pear WS (2011) Notch signaling in mammalian hematopoietic stem cells. Leukemia 25: 1525-1532.

4. Radtke F, Fasnacht N, Macdonald HR (2010) Notch signaling in the immune system. Immunity 32: 14-27.

5. Koch U, Radtke F (2011) Notch in T-ALL: new players in a complex disease. Trends Immunol 32: 434-442.

6. Varnum-Finney B, Purton LE, Yu M, Brashem-Stein C, Flowers D, et al. (1998) The Notch ligand, Jagged-1, influences the development of primitive hematopoietic precursor cells. Blood 91: 4084-4091.

7. Carlesso N, Aster JC, Sklar J, Scadden DT (1999) Notch1-induced delay of human hematopoietic progenitor cell differentiation is associated with altered cell cycle kinetics. Blood 93: 838-848.

8. Ohishi K, Varnum-Finney B, Bernstein ID (2002) Delta-1 enhances marrow and thymus repopulating ability of human CD34(+)CD38(-) cord blood cells. J Clin Invest 110: 1165-1174.

9. Dando JS, Tavian M, Catelain C, Poirault S, Bennaceur-Griscelli A, et al. (2005) Notch/Delta4 interaction in human embryonic liver CD34+ CD38- cells: positive influence on BFU-E production and LTC-IC potential maintenance. Stem Cells 23: 550-560.

10. Lauret E, Catelain C, Titeux M, Poirault S, Dando JS, et al. (2004) Membrane-bound delta-4 notch ligand reduces the proliferative activity of primitive human hematopoietic CD34+CD38low cells while maintaining their LTC-IC potential. Leukemia 18: 788-797.

11. Karanu FN, Murdoch B, Gallacher L, Wu DM, Koremoto M, et al. (2000) The notch ligand jagged-1 represents a novel growth factor of human hematopoietic stem cells. J Exp Med 192: 1365-1372.

12. Benveniste P, Serra P, Dervovic D, Herer E, Knowles G, et al. (2013) Notch signals are required for in vitro but not in vivo maintenance of human hematopoietic stem cells and delay the appearance of multipotent progenitors. Blood.

13. Kunisato A, Chiba S, Nakagami-Yamaguchi E, Kumano K, Saito T, et al. (2003) HES-1 preserves purified hematopoietic stem cells ex vivo and accumulates side population cells in vivo. Blood 101: 1777-1783.

14. Dahlberg A, Delaney C, Bernstein ID (2011) Ex vivo expansion of human hematopoietic stem and progenitor cells. Blood 117: 6083-6090.

15. Radtke F, Wilson A, Stark G, Bauer M, van Meerwijk J, et al. (1999) Deficient T cell fate specification in mice with an induced inactivation of Notch1. Immunity 10: 547-558.

16. Varnum-Finney B, Halasz LM, Sun M, Gridley T, Radtke F, et al. (2011) Notch2 governs the rate of generation of mouse long- and short-term repopulating stem cells. J Clin Invest 121: 1207-1216.

17. Besseyrias V, Fiorini E, Strobl LJ, Zimber-Strobl U, Dumortier A, et al. (2007) Hierarchy of Notch-Delta interactions promoting T cell lineage commitment and maturation. J Exp Med 204: 331-343.

18. Han H, Tanigaki K, Yamamoto N, Kuroda K, Yoshimoto M, et al. (2002) Inducible gene knockout of transcription factor recombination signal binding protein-J reveals its essential role in T versus B lineage decision. Int Immunol 14: 637-645.

19. Mancini SJ, Mantei N, Dumortier A, Suter U, MacDonald HR, et al. (2005) Jagged1-dependent Notch signaling is dispensable for hematopoietic stem cell self-renewal and differentiation. Blood 105: 2340-2342.

20. Maillard I, Koch U, Dumortier A, Shestova O, Xu L, et al. (2008) Canonical notch signaling is dispensable for the maintenance of adult hematopoietic stem cells. Cell Stem Cell 2: 356-366.

21. Klinakis A, Lobry C, Abdel-Wahab O, Oh P, Haeno H, et al. (2011) A novel tumour-suppressor function for the Notch pathway in myeloid leukaemia. Nature 473: 230-233.

22. Lobry C, Oh P, Aifantis I (2011) Oncogenic and tumor suppressor functions of Notch in cancer: it's NOTCH what you think. J Exp Med 208: 1931-1935.

23. Walkley CR, Izon DJ, Purton LE (2011) Taking HSCs down a Notch in leukemia. Cell Stem Cell 8: 602-603.

24. Kalaitzidis D, Armstrong SA (2011) Cancer: The flipside of Notch. Nature 473: 159-160.

25. Alderton GK (2011) Leukaemia: Notch has commitment issues. Nat Rev Cancer 11: 385.

26. Mercher T, Cornejo MG, Sears C, Kindler T, Moore SA, et al. (2008) Notch signaling specifies megakaryocyte development from hematopoietic stem cells. Cell Stem Cell 3: 314-326.

27. Cornejo MG, Mabialah V, Sykes SM, Khandan T, Lo Celso C, et al. (2011) Crosstalk between NOTCH and AKT signaling during murine megakaryocyte lineage specification. Blood 118: 1264-1273.

28. Poirault-Chassac S, Six E, Catelain C, Lavergne M, Villeval JL, et al. (2010) Notch/Delta4 signaling inhibits human megakaryocytic terminal differentiation. Blood 116: 5670-5678.

29. Malinge S, Crispino J (2010) Notch: of mice and men? Blood 116: 5438-5439.

30. Shelly LL, Fuchs C, Miele L (1999) Notch-1 inhibits apoptosis in murine erythroleukemia cells and is necessary for differentiation induced by hybrid polar compounds. J Cell Biochem 73: 164-175.

31. Jang MS, Miao H, Carlesso N, Shelly L, Zlobin A, et al. (2004) Notch-1 regulates cell death independently of differentiation in murine erythroleukemia cells through multiple apoptosis and cell cycle pathways. J Cell Physiol 199: 418-433.

32. Kumano K, Chiba S, Shimizu K, Yamagata T, Hosoya N, et al. (2001) Notch1 inhibits differentiation of hematopoietic cells by sustaining GATA-2 expression. Blood 98: 3283-3289.

33. Ishiko E, Matsumura I, Ezoe S, Gale K, Ishiko J, et al. (2005) Notch signals inhibit the development of erythroid/megakaryocytic cells by suppressing GATA-1 activity through the induction of HES1. J Biol Chem 280: 4929-4939.

34. Elagib KE, Xiao M, Hussaini IM, Delehanty LL, Palmer LA, et al. (2004) Jun blockade of erythropoiesis: role for repression of GATA-1 by HERP2. Mol Cell Biol 24: 7779-7794.

35. Zeuner A, Francescangeli F, Signore M, Venneri MA, Pedini F, et al. (2011) The Notch2-Jagged1 interaction mediates stem cell factor signaling in erythropoiesis. Cell Death Differ 18: 371-380.

36. Oh P, Lobry C, Gao J, Tikhonova A, Loizou E, et al. (2013) In vivo mapping of notch pathway activity in normal and stress hematopoiesis. Cell Stem Cell 13: 190-204.

37. Starck J, Weiss-Gayet M, Gonnet C, Guyot B, Vicat JM, et al. (2010) Inducible Fli-1 gene deletion in adult mice modifies several myeloid lineage commitment decisions and accelerates proliferation arrest and terminal erythrocytic differentiation. Blood 116: 4795-4805.

38. Ng AP, Kauppi M, Metcalf D, Di Rago L, Hyland CD, et al. (2012) Characterization of thrombopoietin (TPO)-responsive progenitor cells in adult mouse bone marrow with in vivo megakaryocyte and erythroid potential. Proc Natl Acad Sci U S A 109: 2364-2369.

39. Rieger MA, Smejkal BM, Schroeder T (2009) Improved prospective identification of megakaryocyte-erythrocyte progenitor cells. Br J Haematol 144: 448-451.

40. Leysi-Derilou Y, Robert A, Duchesne C, Garnier A, Boyer L, et al. (2010) Polyploid megakaryocytes can complete cytokinesis. Cell Cycle 9: 2589-2599.

41. Guo G, Luc S, Marco E, Lin TW, Peng C, et al. (2013) Mapping cellular hierarchy by single-cell analysis of the cell surface repertoire. Cell Stem Cell 13: 492-505.

Legends to Figures

Figure 1. ***Notch signaling stimulates the SCF-dependent amplification MEP-derived progenitors expressing increased Kit expression.*** 2000 cells from purified MEP populations were cultured in culture plates coated with either recombinant IgG or rDll1 with or without □-secretase inhibitor DAPT in liquid medium supplemented by a complete cocktail of myeloid cytokines (IL3, EPO, GM-CSF, TPO, Flt3l, IL11) including or not SCF as indicated. MEP cell progenies collected after 5-6 days of culture were then numbered and Kit expression was analyzed by FACS. Except for the percentages of Kit^+ cells (C), all results are expressed as relative values standardized to the IgG + SCF condition (means and standard deviations from 3 and 8 independent experiments in the absence or presence of SCF respectively). Statistically significant variations between the IgG and rDll1 or rDll1+DAPT conditions are indicated by asterisks ($p \leq 0.05$ in t-test). **A**: Histogram showing the relative numbers of total cells. **B**: Histogram showing the relative numbers of Kit^+ cells. **C**: Histogram showing the percentage of Kit^+ cells of total MEP cells. **D**: Histogram showing the relative values of Kit median fluorescence intensity (MFI) of Kit^+ cells. **E**: Representative FACS profiles showing the distribution of Kit levels in the various conditions.

Figure 2. ***Under Notch stimulation, MEP generates an increased number of $Kit^+/CD41^{Low}$ progenitors and a reduced number of $Kit^-/CD41^+/CD42b^+$ megakaryocytic cells that harbored a less differentiated phenotype.*** Purified MEP were cultured for 6 days in liquid medium supplemented with a complete cocktail of myeloid cytokines in culture wells coated with either recombinant IgG or rDll1 in the presence or absence of Notch inhibitor DAPT. Cells were then analyzed by FACS for their expression of Kit, CD41 and CD42b. **A**: Typical FACS diagram showing the expression levels of CD41 and CD42b in the Kit negative (black dots) and the Kit positive (red dots) cells at day 6. Percentages indicate the proportion of the $CD41^+/CD42b^+$ double positive differentiated megakaryocytic cells. **B**: Histogram showing the relative percentages of $CD41^+/CD42b^+$ megakaryocytic cells (relative values standardized to the IgG condition). **C**: Histogram showing the relative fluorescence intensities of CD41 and CD42b in the Kit-/CD41+/CD42b cells at the end of the culture (relative values standardized to the IgG condition; means and standard deviations from 4 independent experiments). Asterisks indicate statistically significant differences between IgG and rDll1 conditions ($p<0.05$ in Student t-test).

Figure 3. ***Notch signaling stimulates bipotent and erythrocytic progenitors amplification.*** 2000 bone marrow MEP were cultured for two days in the presence of a complete cocktail of myeloid cytokines (IL3, SCF, EPO, GM-CSF, TPO, Flt3l, IL11) in culture wells coated with either control IgG or recombinant rDll1 in the presence or absence of DAPT as indicated. Total numbers of the different types of progenitors present in the initial untreated population (Day 0) and after the two days culture in the different conditions were determined by colony assays performed in semi-solid medium in the presence of the same complete cocktail of cytokines. **A**: Piled histograms showing the respective numbers of the various types of colonies generated from untreated cells (Day 0) and after a two days culture on IgG, rDll1 or rDll1 + DAPT (mean and standard deviations from 5 independent MEP preparations). **B**: Histograms showing the variations of the numbers of the different types of colonies generated after two days of culture on IgG as compared with Day 0 cells (same experiments as those described in A). **C**: Histograms showing the variations of the numbers of the different types of colonies generated after two days of culture on rDll1 as compared to Day 0 cells (same experiments as those described in A). Statistically significant variations are indicated by asterisks ($p \leq 0.05$ in t-test).

Figure 4. ***The rate of progenitors amplification upon Notch stimulation correlates with the megakaryocytic versus erythrocytic bias of the initial MEP population.***

Dot-plot showing the fold variations of the numbers of the different progenitors induced by Notch ligand as a function of the ratio of megakaryocytic/erythrocytic progenitors present in the native MEP preparation (compiled data from all experiments performed on rDll1 shown in Figure 2). Determinant coefficients and significance of the linear regressions (Fisher F test) are indicated by R^2 and p-values respectively.

Figure 5. ***Notch most responsive bipotent and erythrocytic progenitors are present in the CD9^{High} fraction of the MEP population.*** **A**: FACS diagram showing the gating windows used for the sorting of MEP CD9^{Low}, CD9^{High} and CD9^{Med} fractions. (**B-G)** Progeny of equal numbers of sorted CD9^{Low}, CD9^{High} and CD9^{Med}MEP populations were analyzed by colony assays before (Day 0) and after a two days culture either on IgG or rDll1 with or without DAPT as described in Figure 2. **B**: Progeny analysis of the whole MEP population and of the CD9^{Low}, CD9^{Med} and CD9^{High} MEP subsets immediately after sorting (Day 0). **C, D**: Progeny analysis of the CD9^{Med} (C) and CD9^{High} (D) populations before (Day 0) and after a two days culture on IgG or rDll1 with or without DAPT inhibitor. Piled histograms showing the means

and standard deviations of the number of each type of colonies obtained with three independent MEP preparations. Means and standard deviations from 3 different experiments; statistically significant variations are indicated by asterisks ($p \leq 0.05$ in t-test). **E, F, G**: Plots of the fold variations of the number of mixed (E), megakaryocytic (F) or erythrocytic (G) progenitors after two days on rDll1 as a function of the ratio of megakaryocytic/erythrocytic progenitors present in the initial $CD9^{High}$ and $CD9^{Med}$ MEP populations.

Figure 6. ***Notch signaling increases the size of MEP-derived megakaryocytic colonies.*** MEP were FACS sorted into four subsets according to their CD9 expression levels ($CD9^{High}$ or $CD9^{Med}$) and to their DNA content (2N or 4N) and cultured for two days on IgG or rDll1 before performing colony assay as described in Figure 2. The number and the size of megakaryocytic colonies, according to the numbers of mature megakaryocytes they contain (from 1 to more than 8) were recorded (mean results obtained from two independent preparations of each subset are presented). **A**: Numbers of megakaryocytic colonies harboring the indicated number of megakaryocytes (MK1 for single megakaryocytes to MK>=8 for more than 8 megakaryocytes per colony) obtained per 1000 seeded cells of the indicated subsets. **B**: Relative percentages of megakaryocytic colonies obtained in A as a percentage of total colonies.

Figure 7. ***Single cell progeny analyses of $CD9^{Med}$ MEP and $CD9^{High}$ MEP with or without Notch pathway activation.*** Single MEP $CD9^{Med}$ or MEP $CD9^{High}$ were individually seeded in 96 wells culture plate that have been coated with either IgG or rDll1 and containing medium supplemented with a complete cocktail of myeloid cytokines. The different types of developed colonies were numbered at day 7 by visual inspection of under bright light microscope. **A, B**: Repartition of the indicated type of colony as a percentage of all single seeded $CD9^{Med}$ MEP (A) and as a percentage of $CD9^{Med}$ MEPraising colonies (B) (means and standard deviations from 3 independent experiments; statistically significant variations are indicated by asterisks; $p \leq 0.05$ in t-test). **C, D**: Repartition of the indicated type of colony as a percentage of all single seeded $CD9^{High}$ MEP (C) and as a percentage of $CD9^{High}$ MEPraising colonies (D) (means and standard deviations from 3 independent experiments; statistically significant variations are indicated by asterisks; $p \leq 0.05$ in t-test). **E, F**: Detailed results from one of the three experiments performed in A and C, in which megakaryocytic colonies were further scored according to their content in mature megakaryocytes (form 1 to more than 4), expressed as a percentage of all single seeded $CD9^{High}$ or $CD9^{Med}$ MEP (E) and as a percentage of $CD9^{High}$ or $CD9^{Med}$ MEPraising colonies (F).

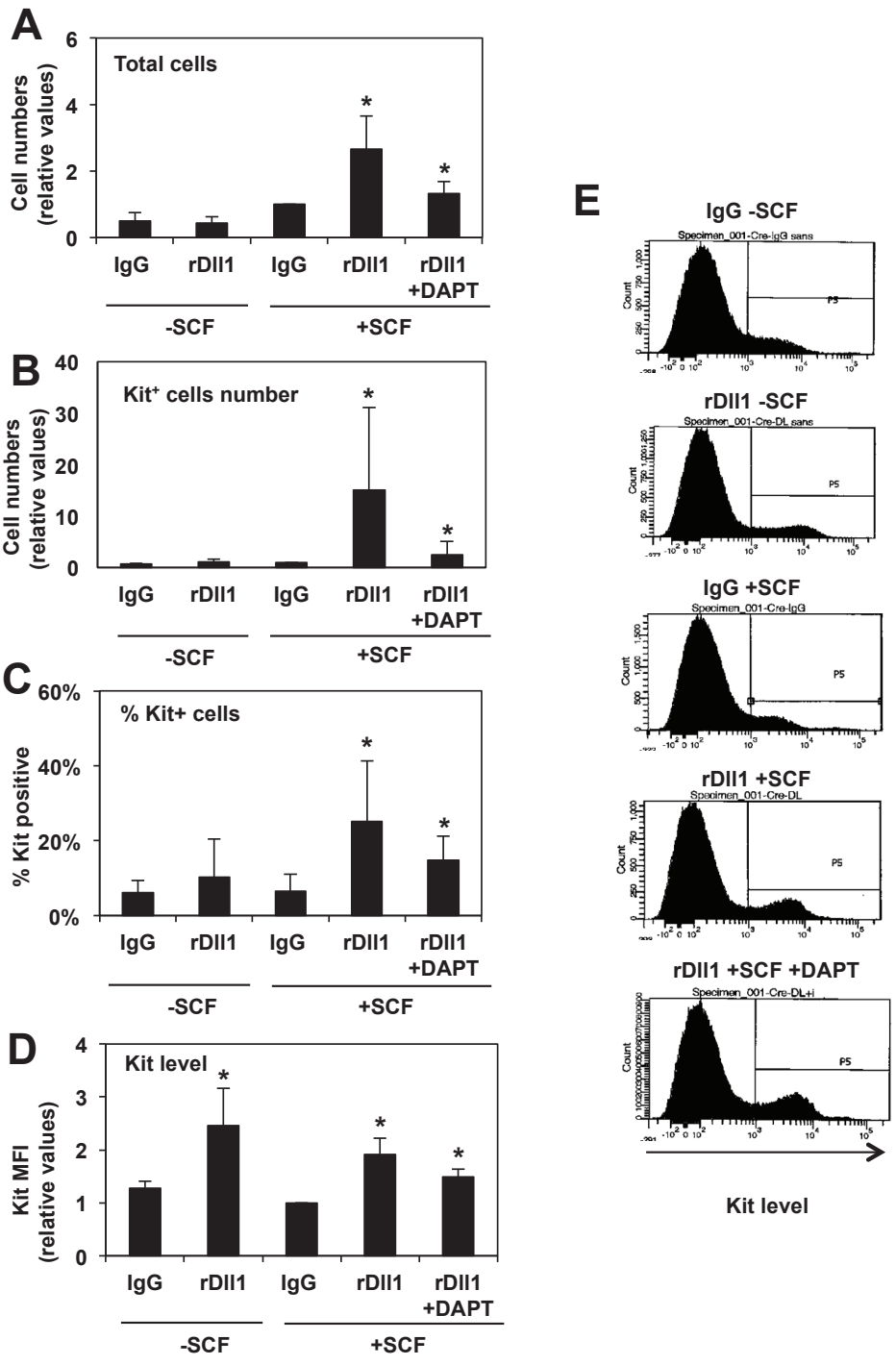
A
Total cells
Cell numbers (relative values)
6
4
2
0
IgG
rDll1
IgG
rDll1
rDll1 +DAPT
-SCF
+SCF
B
Kit+ cells number
Cell numbers (relative values)
40
30
20
10
0
C
% Kit+ cells
% Kit positive
60%
40%
20%
0%
D
Kit level
Kit MFI (relative values)
4
3
2
1
0
E
IgG -SCF
rDll1 -SCF
IgG +SCF
rDll1 +SCF
rDll1 +SCF +DAPT
Count
P5
Kit level

Figure 1

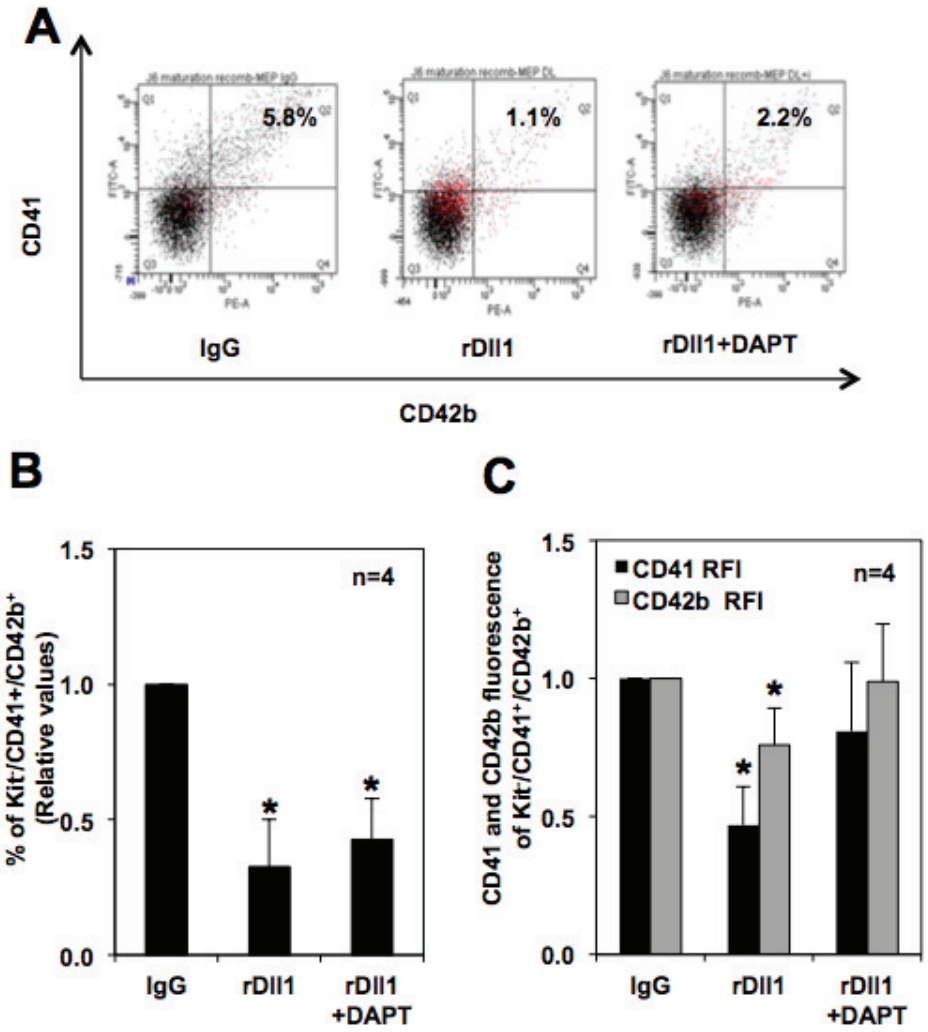
A
CD41
5.8%
1.1%
2.2%
IgG
rDll1
rDll1+DAPT
CD42b
B
% of Kit-/CD41+/CD42b+ (Relative values)
1.5
1.0
0.5
0.0
n=4
*
*
IgG
rDll1
rDll1 +DAPT
C
CD41 and CD42b fluorescence of Kit-/CD41+/CD42b+
CD41 RFI
CD42b RFI
n=4
1.5
1.0
0.5
0.0
*
*
IgG
rDll1
rDll1 +DAPT

Figure 2

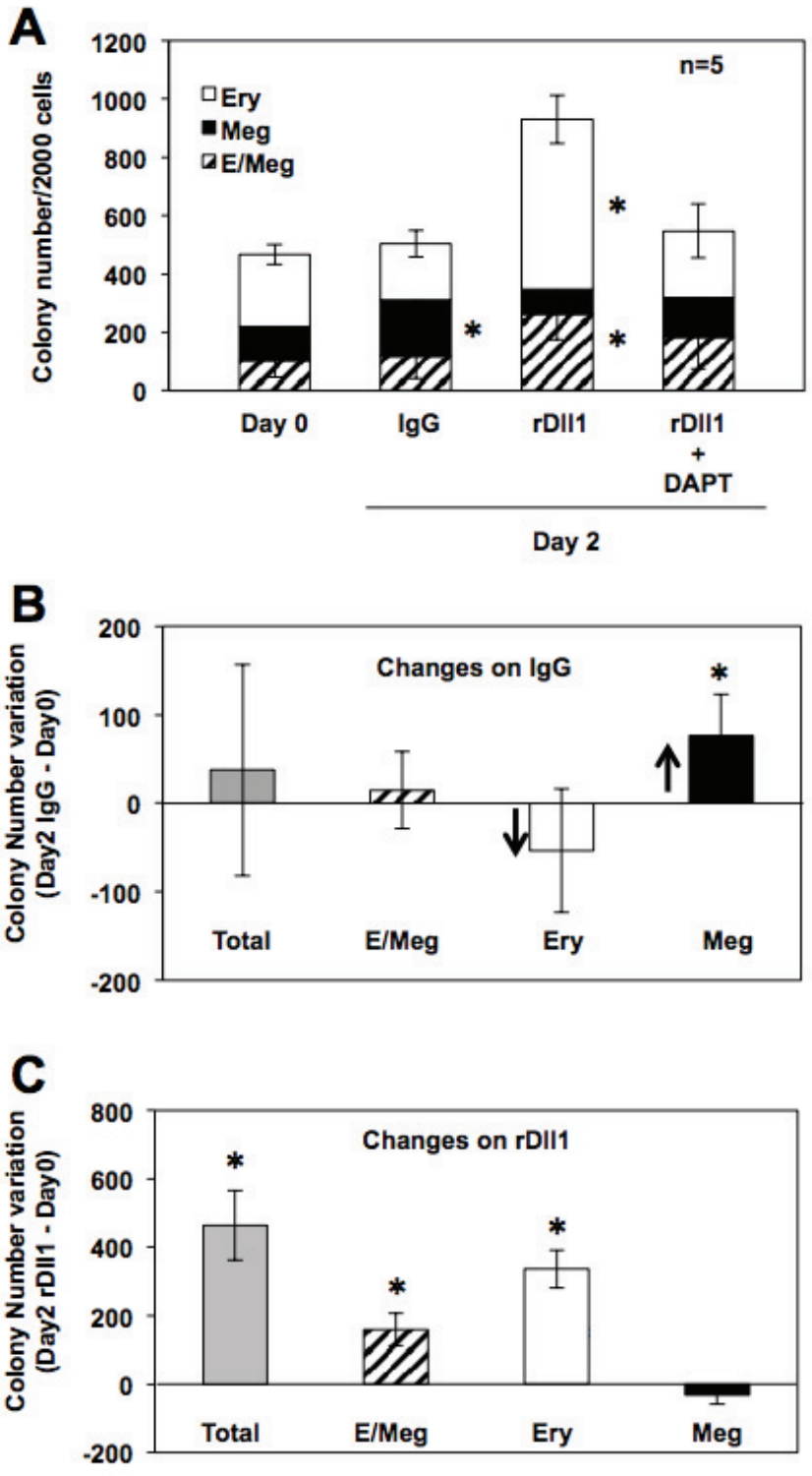
A
Colony number/2000 cells
1200
1000
800
600
400
200
0
Ery
Meg
E/Meg
n=5
*
*
*
Day 0
IgG
rDll1
rDll1
+
DAPT
Day 2
B
Colony Number variation
(Day2 IgG - Day0)
200
100
0
-100
-200
Changes on IgG
*
Total
E/Meg
Ery
Meg
C
Colony Number variation
(Day2 rDll1 - Day0)
800
600
400
200
0
-200
Changes on rDll1
*
*
*
Total
E/Meg
Ery
Meg

Figure 3

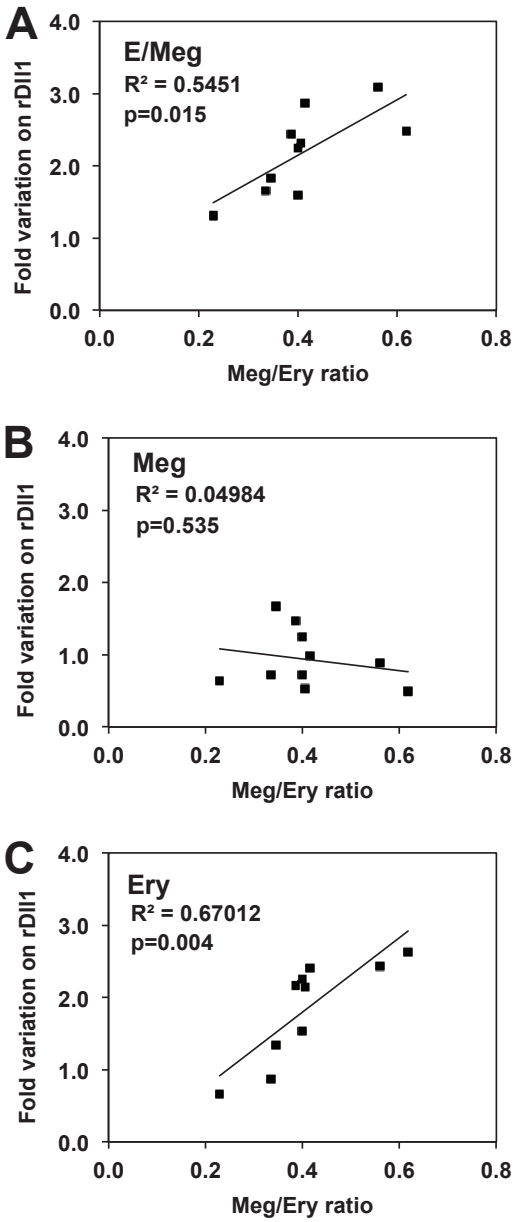
A
E/Meg
R² = 0.5451
p=0.015
Fold variation on rDll1
Meg/Ery ratio
B
Meg
R² = 0.04984
p=0.535
Fold variation on rDll1
Meg/Ery ratio
C
Ery
R² = 0.67012
p=0.004
Fold variation on rDll1
Meg/Ery ratio
0.0
1.0
2.0
3.0
4.0
0.2
0.4
0.6
0.8

Figure 4

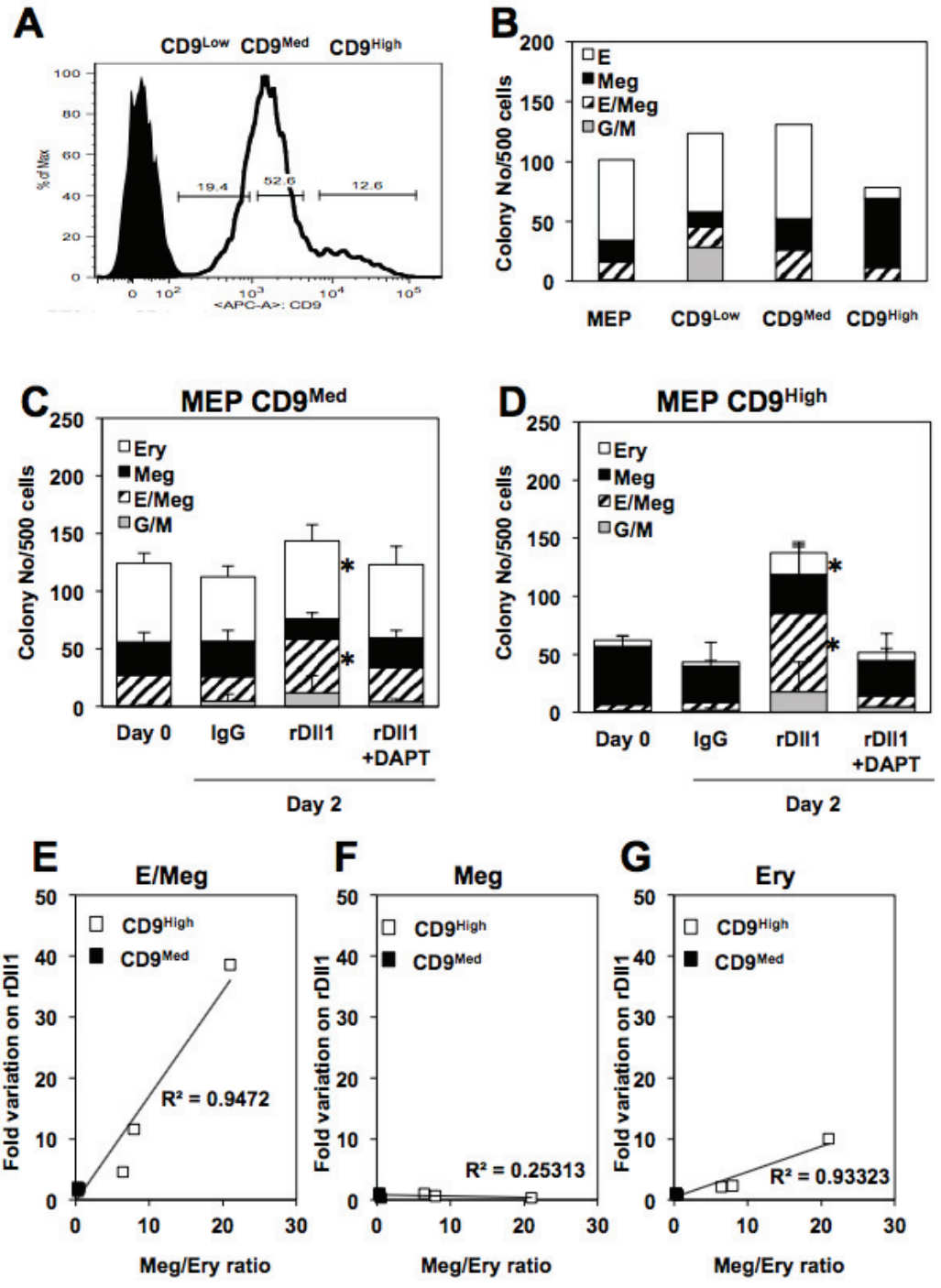
A
CD9Low CD9Med CD9High
% of Max
19.4
52.6
12.6
<APC-A>: CD9
B
Colony No/500 cells
E
Meg
E/Meg
G/M
MEP
CD9Low
CD9Med
CD9High
C
MEP CD9Med
Colony No/500 cells
Ery
Meg
E/Meg
G/M
Day 0
IgG
rDll1
rDll1 +DAPT
Day 2
D
MEP CD9High
Colony No/500 cells
Ery
Meg
E/Meg
G/M
Day 0
IgG
rDll1
rDll1 +DAPT
Day 2
E
E/Meg
CD9High
CD9Med
R² = 0.9472
Fold variation on rDll1
Meg/Ery ratio
F
Meg
CD9High
CD9Med
R² = 0.25313
Fold variation on rDll1
Meg/Ery ratio
G
Ery
CD9High
CD9Med
R² = 0.93323
Fold variation on rDll1
Meg/Ery ratio

Figure 5

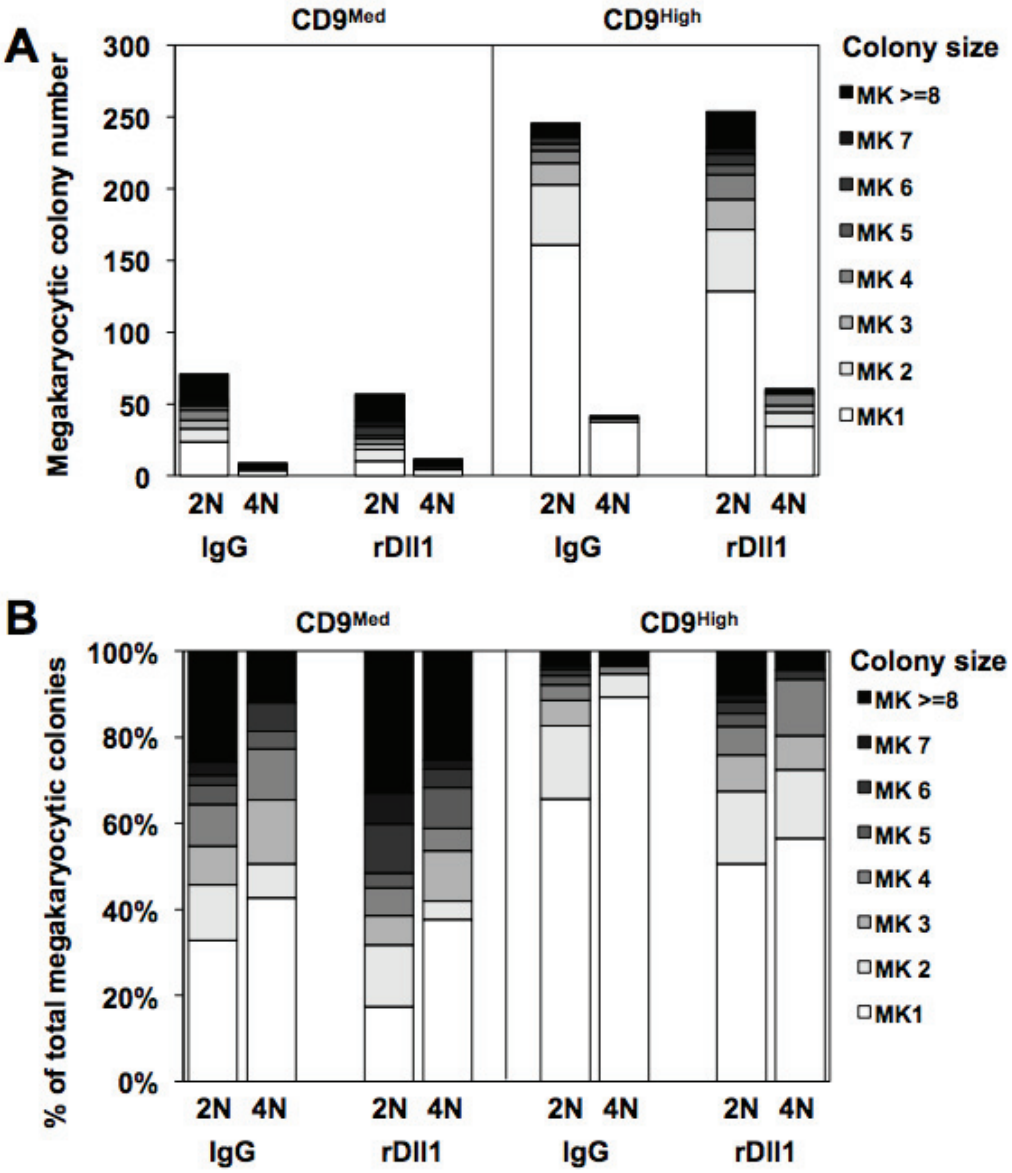
A
CD9Med
CD9High
Megakaryocytic colony number
300
250
200
150
100
50
0
2N 4N
IgG
rDll1
Colony size
MK >=8
MK 7
MK 6
MK 5
MK 4
MK 3
MK 2
MK1
B
% of total megakaryocytic colonies
100%
80%
60%
40%
20%
0%

Figure 6

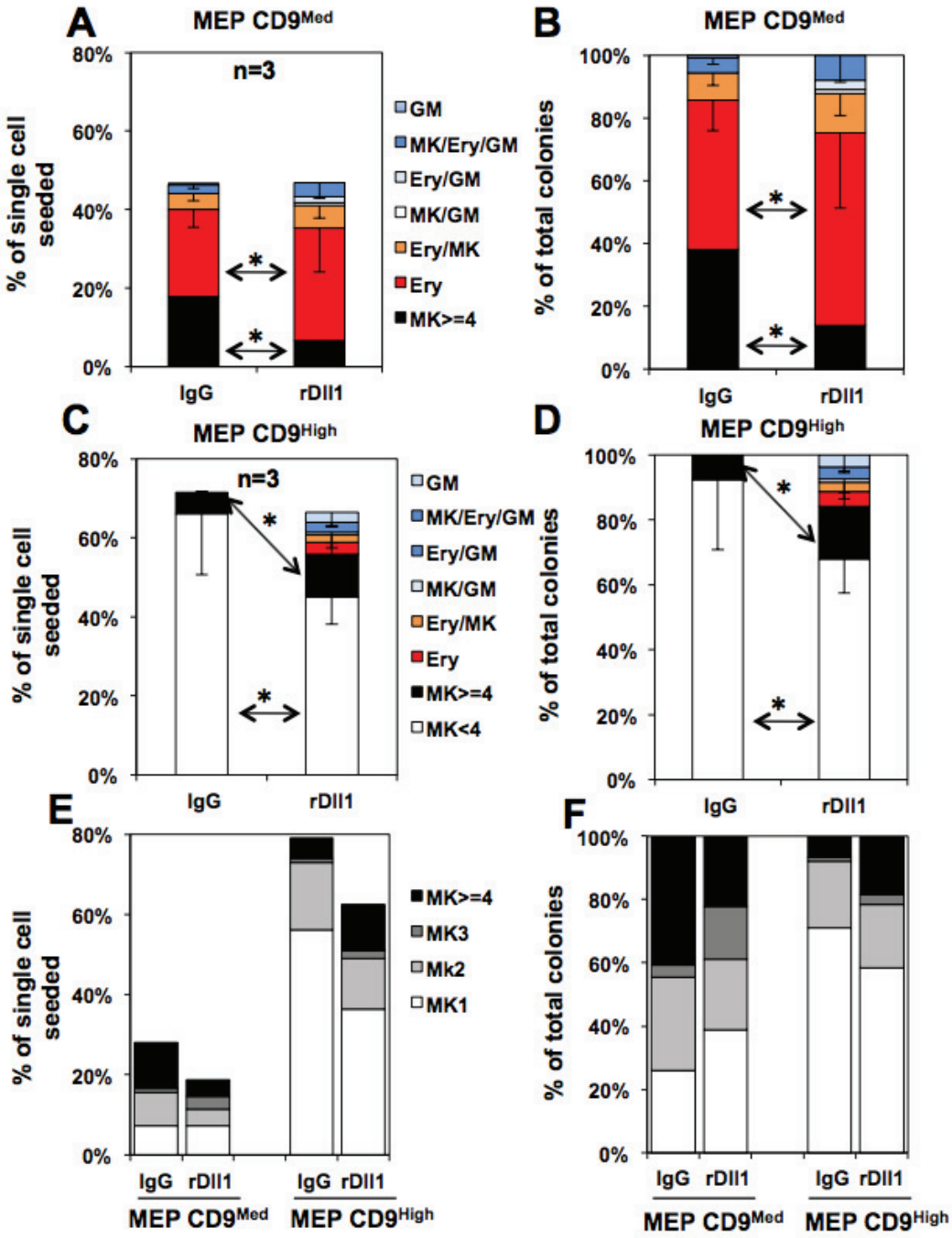
A
MEP CD9Med
n=3
% of single cell seeded
80%
60%
40%
20%
0%
GM
MK/Ery/GM
Ery/GM
MK/GM
Ery/MK
Ery
MK>=4
IgG
rDll1
B
MEP CD9Med
% of total colonies
100%
80%
60%
40%
20%
0%
C
MEP CD9High
n=3
MK<4
D
MEP CD9High
E
MK3
Mk2
MK1
IgG rDll1
MEP CD9Med
MEP CD9High
F

Figure 7

Supplementary figures legends

Figure S1

FACS diagram illustrating the gating strategy used for the sorting of bone marrow MEP and the 2N and 4N subsets expressing various levels of CD9.

Figure S2

Transcript levels changes induced by rDll1

Transcript levels were determined by qRT-PCR after two days cultures of MEP cells on the indicated conditions using β-actin as a reference. Results are presented as relative levels standardized to the culture condition on IgG (means and standard deviations obtained from 3 independent cultures). Statistically significant differences are indicated by asterisks, $p \leq 0.05$ in t-test.

Figure S3

The Amplification of bipotent and erythrocytic progenitors stimulated by Notch signaling is dependent on the Kit/SCF signaling.Equal numbers of MEP were cultured for two days in the presence or absence of SCF and their progenies were analyzed by colony assay as described in Figure 2. Results are expressed as fold variations of the number of each type of progenitors between Day 0 and Day 2 in presence (black boxes) or absence of SCF (white boxes). **A**: Bipotent colonies. **B**: Megakaryocytic colonies. **C**: Erythrocytic colonies. Means and standard deviations from three different experiments; statistically significant variations are indicated by asterisks; $p \leq 0.05$ in t-test.

Figure S4

Cell cycle analyses of $CD9^{High}$ MEP and $CD9^{Med}$ MEPbefore and after two days culture in the presence of absence of Notch ligand

A: FACS diagrams of $CD9^{Med}$ MEP (left panel) and $CD9^{High}$ MEP (right panel) after double labeling for DNA content (Propidium Iodide) and Ki67 expression immediately following their purification.

Percentages indicate the proportion of diploid and Ki67 negative cells corresponding to classical G0 quiescent cells. Arrow indicates tetraploid cells expressing low levels of Ki67 suggesting quiescent G2/M cells that were present specifically in the MEP $CD9^{High}$ subset. **B**: Cytospins of MEP $CD9^{Med}$ (left side) and MEP $CD9^{High}$ cells (right side) after May Gründvald Giemsa staining. Arrow indicates binucleated cells specifically present in the MEP $CD9^{High}$ subset. **C**: Histograms showing the repartition of $CD9^{Med}$ and $CD9^{High}$ cells in the G0/G1, S and G2/M phases of cell cycle before (Day 0) and after a two day culture (Day 2) on either IgG or rDll1 (Mean results from two independent experiments are shown). **D**: Histogram showing the selective presence of 5% of binucleated cells in the MEP $CD9^{High}$ subset.

Figure S5

Retrospective transcriptome comparison between $CD9^{+}$ and $CD9^{-}$ MEP

A: Heatmap of genes upregulated (top) or downregulated (bottom) in $CD9^{+}$ compared to $CD9^{-}$ MEP. Analysis of transcriptome row data from the 64 single MEP recently published by Guo et al [41] allowed us to identify and to virtually sort 16 and 48 single MEP expressing or not CD9 respectively. Heatmap presented here is limited to genes which mean expression levels were found statistically different between these virtually sorted $CD9^{+}$ and $CD9^{-}$ MEP subsets (p-value < 0.05 by Student t-test). Genes names and p-values are indicated on the left and right of the heatmap respectively. Mean expression levels of genes are indicated by numbers in table cells and further illustrated by increasing red color intensity. Note the marked difference between the contrasted differential expression of genes up-regulated compared to the modest differential expression of down regulated genes in $CD9^{+}$MEP.

B: Expression profiles of genes differentially expressed between $CD9^{+}$ and $CD9^{-}$ MEP. Expression profiles of genes differentially expressed between $CD9^{+}$ and $CD9^{-}$ MEP were collected for stem cells (LT-HSC or ST-HSC), erythro-megakaryocytic bipotent (MKE), megakaryocytic (MKP) or erythrocytic (PreCFUE, CFUe and ProE) committed progenitors from Hemaexplorer database [42]. Heatmap presented here corresponds to relative expression levels (mean of all specific probes levels for each given gene) normalized to the median expression level of the 7 different populations (number in table cells correspond to LOG(2) of normalized expression levels). Genes names are indicated on the left of the heatmap and are ordered separately for up-regulated and down regulated genes by decreasing expression levels in LT-HSC. Note that all genes up-regulated in $CD9^{+}$ MEP correspond to genes displaying contrasted higher levels in LT-HSC and lower levels in committed erythrocytic

progenitors while most slightly down-regulated genes (Downb subset) display contrasted lower expression levels in LT-HSC and higher levels in committed erythrocytic progenitors.

Figure S6

Diagram summarizing the effect of Notch on the different progenitors present in the MEP population

Known filiation between the different progenitors is indicated by thin arrows while their different potential are indicated by different colors (Red for pure erythrocytic, yellow for pure megakaryocytic, orange for bipotent and light orange for bipotent with high megakaryocytic bias). Thick blacks arrows indicate self-renewal efficiency in the absence of Notch ligand. Thick green arrows indicate the different effects induced by Notch ligand numbered as follows:

(1) Increase of Kit expression

(2) SCF-dependent increase of self-renewal

(3) Preferential commitment of $CD9^{Med}$ bipotent progenitors towards erythrocytic lineage

(4) Redirection of $CD9^{High}$ bipotent progenitors from endomitosis and terminal megakaryocytic differentiation to the resumption of cell divisions leading to the amplification of megakaryocytic progenitors and concomitant emergence of few progenitors with erythrocytic, mixed and possibly granulo-monocytic potential. Whether the emergence of these progenitors simply reflects persistent bi/multipotency of $CD9^{High}$ progenitors until the last division before endomitosis or results from a true reprogramming process (5) remains an open question.

Table S1Primer sequences used in qRT-PCR

Target	Forward Primer	Reverse Primer
β-Actin	5'-TGGGAATGGGTCAGAAGGACTC-3'	5'-CTGGGTCATCTTTTCACGGTTG-3'
Hes1	5'-CTACCCCAGCCAGTGTCAAC-3'	5'-CGCCTCTTCTCCATGATAGG-3'
Gata1	5'-TTCTTCCACTTCCCCAAATG-3'	AGGCCCAGCTAGCATAAGGT-3'
Gata2	5'-GAATGGACAGAACCGGCC-3'	5'-AGGTGGTGGTTGTCGTCTGA-3'
Pten	5'-AATTCCCAGTCAGAGGCGCTATGT-3'	5'-GATTGCAAGTTCCGCCACTGAACA-3'
cMyc	5'-TCCTGTACCTCGTCTGATTCC-3'	5'-CTCTTCTCCACAGACACCACATC-3'

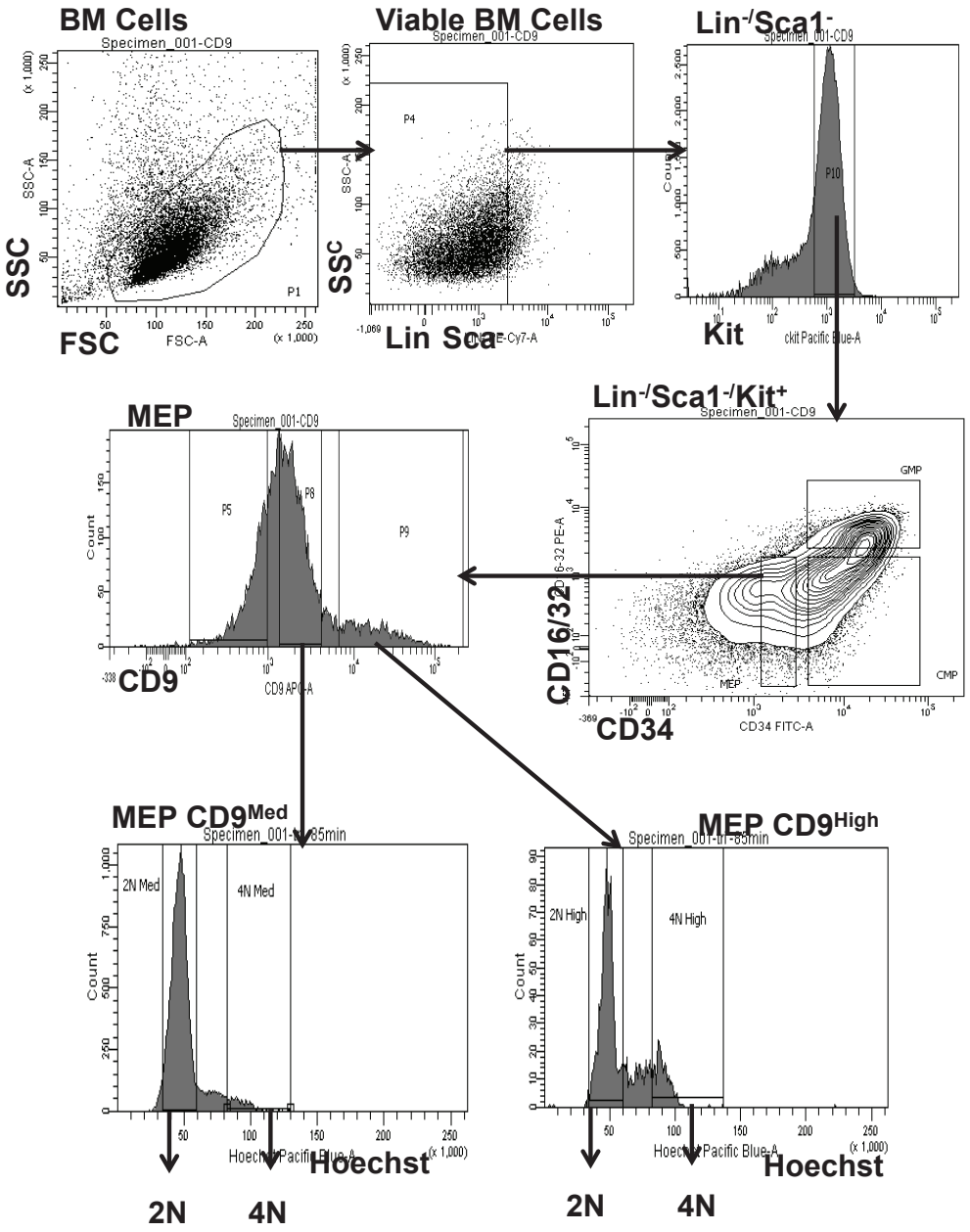
BM Cells
Viable BM Cells
Lin-/Sca1-
SSC
FSC
Lin Sca
Kit
Lin-/Sca1-/Kit+
MEP
CD9
CD16/32
CD34
GMP
CMP
MEP
MEP CD9Med
MEP CD9High
2N Med
4N Med
2N High
4N High
Hoechst
2N
4N

Figure S1

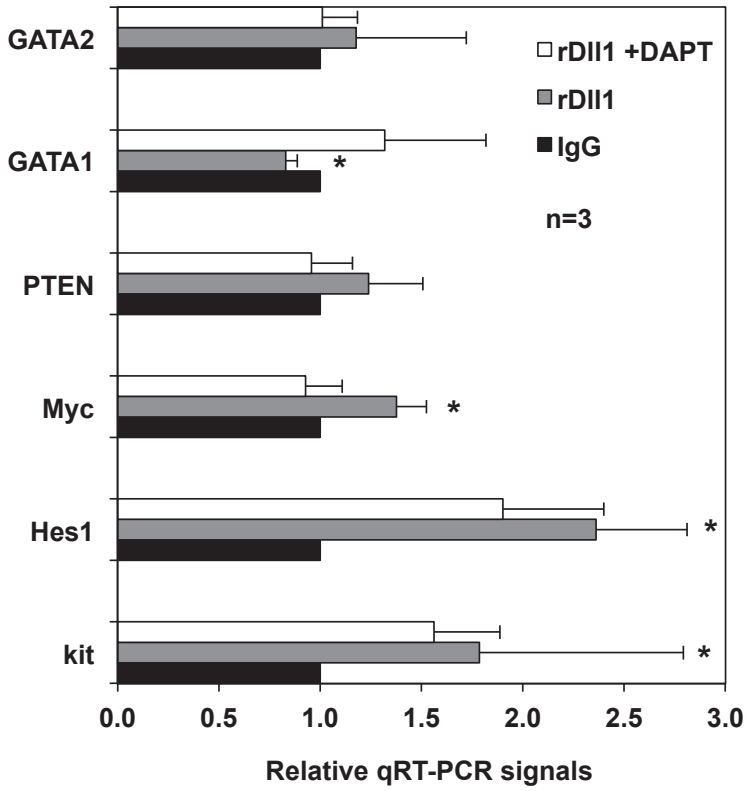
GATA2
GATA1
PTEN
Myc
Hes1
kit
rDll1 +DAPT
rDll1
IgG
n=3
*
*
*
*
0.0
0.5
1.0
1.5
2.0
2.5
3.0
Relative qRT-PCR signals

Figure S2

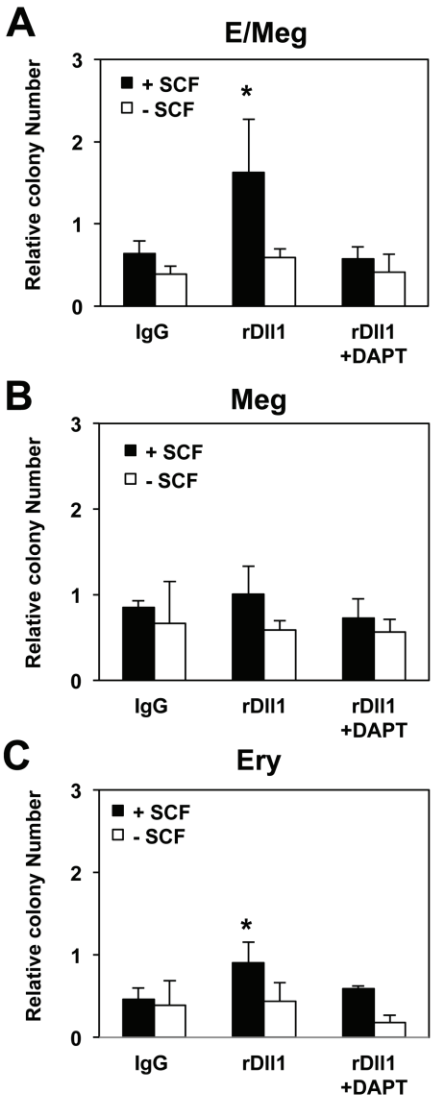
A
E/Meg
Relative colony Number
3
2
1
0
+ SCF
- SCF
*
IgG
rDll1
rDll1
+DAPT
B
Meg
Relative colony Number
3
2
1
0
+ SCF
- SCF
IgG
rDll1
rDll1
+DAPT
C
Ery
Relative colony Number
3
2
1
0
+ SCF
- SCF
*
IgG
rDll1
rDll1
+DAPT

Figure S3

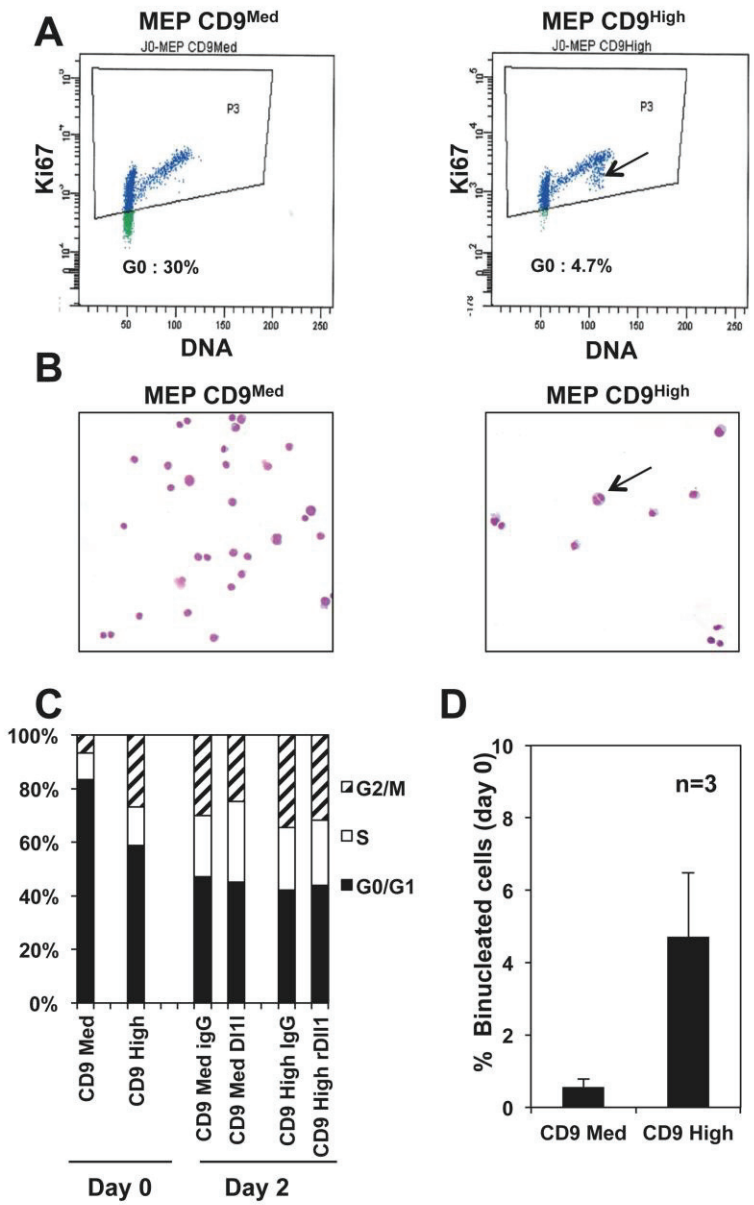
A
MEP CD9Med
J0-MEP CD9Med
P3
Ki67
G0 : 30%
DNA
MEP CD9High
J0-MEP CD9High
P3
Ki67
G0 : 4.7%
DNA
B
MEP CD9Med
MEP CD9High
C
100%
80%
60%
40%
20%
0%
G2/M
S
G0/G1
CD9 Med
CD9 High
CD9 Med igG
CD9 Med Dl1l
CD9 High IgG
CD9 High rDll1
Day 0
Day 2
D
% Binucleated cells (day 0)
n=3
CD9 Med
CD9 High

Figure S4

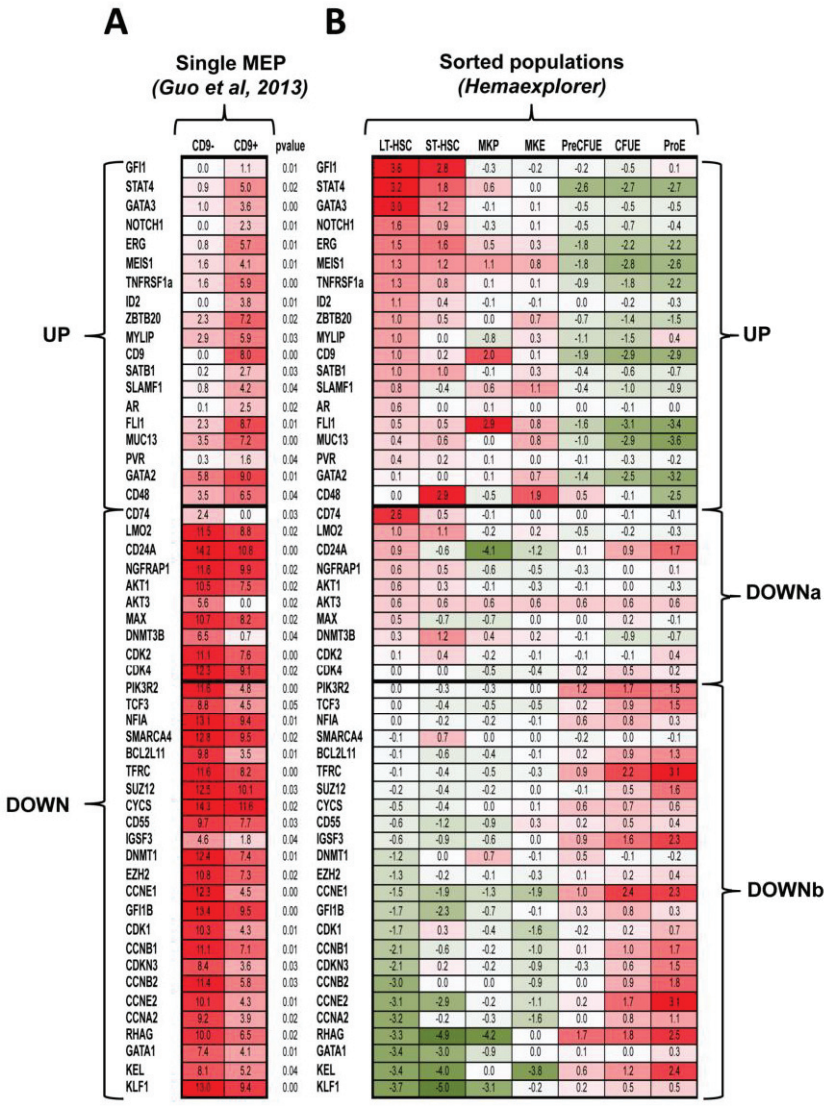
A
Single MEP
(Guo et al, 2013)
CD9-
CD9+
pvalue
B
Sorted populations
(Hemaexplorer)
LT-HSC
ST-HSC
MKP
MKE
PreCFUE
CFUE
ProE
UP
DOWN
UP
DOWNa
DOWNb
GFI1 0.0 1.1 0.01 3.6 2.8 -0.3 -0.2 -0.2 -0.5 0.1
STAT4 0.9 5.0 0.02 3.2 1.8 0.6 0.0 -2.6 -2.7 -2.7
GATA3 1.0 3.6 0.00 3.0 1.2 -0.1 0.1 -0.5 -0.5 -0.5
NOTCH1 0.0 2.3 0.01 1.6 0.9 -0.3 0.1 -0.5 -0.7 -0.4
ERG 0.8 5.7 0.01 1.5 1.6 0.5 0.3 -1.8 -2.2 -2.2
MEIS1 1.6 4.1 0.01 1.3 1.2 1.1 0.8 -1.8 -2.8 -2.6
TNFRSF1a 1.6 5.9 0.00 1.3 0.8 0.1 0.1 -0.9 -1.8 -2.2
ID2 0.0 3.8 0.01 1.1 0.4 -0.1 -0.1 0.0 -0.2 -0.3
ZBTB20 2.3 7.2 0.02 1.0 0.5 0.0 0.7 -0.7 -1.4 -1.5
MYLIP 2.9 5.9 0.03 1.0 0.0 -0.8 0.3 -1.1 -1.5 0.4
CD9 0.0 8.0 0.00 1.0 0.2 2.0 0.1 -1.9 -2.9 -2.9
SATB1 0.2 2.7 0.03 1.0 1.0 -0.1 0.3 -0.4 -0.6 -0.7
SLAMF1 0.8 4.2 0.04 0.8 -0.4 0.6 1.1 -0.4 -1.0 -0.9
AR 0.1 2.5 0.02 0.6 0.0 0.1 0.0 0.0 -0.1 0.0
FLI1 2.3 8.7 0.01 0.5 0.5 2.9 0.8 -1.6 -3.1 -3.4
MUC13 3.5 7.2 0.00 0.4 0.6 0.0 0.8 -1.0 -2.9 -3.6
PVR 0.3 1.6 0.04 0.4 0.2 0.1 0.0 -0.1 -0.3 -0.2
GATA2 5.8 9.0 0.01 0.1 0.0 0.1 0.7 -1.4 -2.5 -3.2
CD48 3.5 6.5 0.04 0.0 2.9 -0.5 1.9 0.5 -0.1 -2.5
CD74 2.4 0.0 0.03 2.6 0.5 -0.1 0.0 0.0 -0.1 -0.1
LMO2 11.5 8.8 0.02 1.0 1.1 -0.2 0.2 -0.5 -0.2 -0.3
CD24A 14.2 10.8 0.00 0.9 -0.6 -4.1 -1.2 0.1 0.9 1.7
NGFRAP1 11.6 9.9 0.02 0.6 0.5 -0.6 -0.5 -0.3 0.0 0.1
AKT1 10.5 7.5 0.02 0.6 0.3 -0.1 -0.3 -0.1 0.0 -0.3
AKT3 5.6 0.0 0.02 0.6 0.6 0.6 0.6 0.6 0.6 0.6
MAX 10.7 8.2 0.02 0.5 -0.7 -0.7 0.0 0.0 0.2 -0.1
DNMT3B 6.5 0.7 0.04 0.3 1.2 0.4 0.2 -0.1 -0.9 -0.7
CDK2 11.1 7.6 0.00 0.1 0.4 -0.2 -0.1 -0.1 -0.1 0.4
CDK4 12.3 9.1 0.02 0.0 0.0 -0.5 -0.4 0.2 0.5 0.2
PIK3R2 11.8 4.8 0.00 0.0 -0.3 -0.3 0.0 1.2 1.7 1.5
TCF3 8.8 4.5 0.05 0.0 -0.4 -0.5 -0.5 0.2 0.9 1.5
NFIA 13.1 9.4 0.01 0.0 -0.2 -0.2 -0.1 0.6 0.8 0.3
SMARCA4 12.8 9.5 0.02 -0.1 0.7 0.0 0.0 -0.2 0.0 -0.1
BCL2L11 9.8 3.5 0.01 -0.1 -0.6 -0.4 -0.1 0.2 0.9 1.3
TFRC 11.6 8.2 0.00 -0.1 -0.4 -0.5 -0.3 0.9 2.2 3.1
SUZ12 12.5 10.1 0.03 -0.2 -0.4 -0.2 0.0 -0.1 0.5 1.6
CYCS 14.3 11.6 0.02 -0.5 -0.4 0.0 0.1 0.6 0.7 0.6
CD55 9.7 7.7 0.03 -0.6 -1.2 -0.9 0.3 0.2 0.5 0.4
IGSF3 4.6 1.8 0.04 -0.6 -0.9 -0.6 0.0 0.9 1.6 2.3
DNMT1 12.4 7.4 0.01 -1.2 0.0 0.7 -0.1 0.5 -0.1 -0.2
EZH2 10.8 7.3 0.02 -1.3 -0.2 -0.1 -0.3 0.1 0.2 0.4
CCNE1 12.3 4.5 0.00 -1.5 -1.9 -1.3 -1.9 1.0 2.4 2.3
GFI1B 13.4 9.5 0.00 -1.7 -2.3 -0.7 -0.1 0.3 0.8 0.3
CDK1 10.3 4.3 0.01 -1.7 0.3 -0.4 -1.6 -0.2 0.2 0.7
CCNB1 11.1 7.1 0.01 -2.1 -0.6 -0.2 -1.0 0.1 1.0 1.7
CDKN3 8.4 3.6 0.03 -2.1 0.2 -0.2 -0.9 -0.3 0.6 1.5
CCNB2 11.4 5.8 0.03 -3.0 0.0 0.0 -0.9 0.0 0.9 1.8
CCNE2 10.1 4.3 0.01 -3.1 -2.9 -0.2 -1.1 0.2 1.7 3.1
CCNA2 9.2 3.9 0.02 -3.2 -0.2 -0.3 -1.6 0.0 0.8 1.1
RHAG 10.0 6.5 0.02 -3.3 -4.9 -4.2 0.0 1.7 1.8 2.5
GATA1 7.4 4.1 0.01 -3.4 -3.0 -0.9 0.0 0.1 0.0 0.3
KEL 8.1 5.2 0.04 -3.4 -4.0 0.0 -3.8 0.6 1.2 2.4
KLF1 13.0 9.4 0.00 -3.7 -5.0 -3.1 -0.2 0.2 0.5 0.5

Figure S5

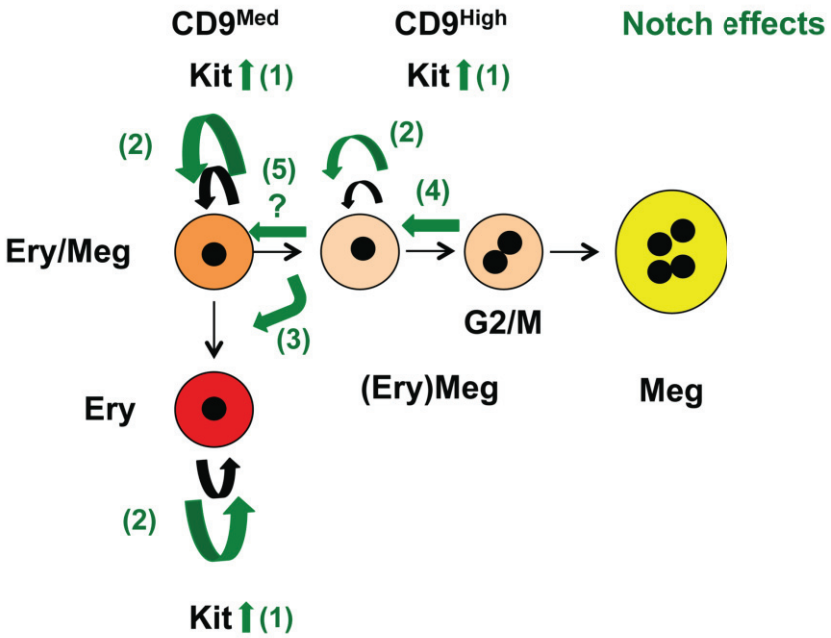
CD9Med
CD9High
Notch effects
Kit (1)
Kit (1)
(2)
(5)
?
(2)
(4)
Ery/Meg
G2/M
(3)
Ery
(Ery)Meg
Meg
(2)
Kit (1)

Figure S6

BIBLIOGRAPHIC REFERENCES

Adamia, S., M. Bar-Natan, B. Haibe-Kains, P.M. Pilarski, C. Bach, S. Pevzner, T. Calimeri, H. Avet-Loiseau, L. Lode, S. Verselis, E.A. Fox, I. Galinsky, S. Mathews, I. Dagogo-Jack, M. Wadleigh, D.P. Steensma, G. Motyckova, D.J. Deangelo, J. Quackenbush, D.G. Tenen, R.M. Stone, and J.D. Griffin. 2014. NOTCH2 and FLT3 gene mis-splicings are common events in patients with acute myeloid leukemia (AML): new potential targets in AML. *Blood*. 123:2816-2825.

Adolfsson, J., R. Mansson, N. Buza-Vidas, A. Hultquist, K. Liuba, C.T. Jensen, D. Bryder, L. Yang, O.J. Borge, L.A. Thoren, K. Anderson, E. Sitnicka, Y. Sasaki, M. Sigvardsson, and S.E. Jacobsen. 2005. Identification of Flt3+ lympho-myeloid stem cells lacking erythro-megakaryocytic potential a revised road map for adult blood lineage commitment. *Cell*. 121:295-306.

Aerbajinai, W., J. Zhu, C. Kumkhaek, K. Chin, and G.P. Rodgers. 2009. SCF induces gamma-globin gene expression by regulating downstream transcription factor COUP-TFII. *Blood*. 114:187-194.

Akashi, K., D. Traver, T. Miyamoto, and I.L. Weissman. 2000. A clonogenic common myeloid progenitor that gives rise to all myeloid lineages. *Nature*. 404:193-197.

Albu, R.I., and S.N. Constantinescu. 2011. Extracellular domain N-glycosylation controls human thrombopoietin receptor cell surface levels. *Frontiers in endocrinology*. 2:71.

Alexander, W.S., A.W. Roberts, A.B. Maurer, N.A. Nicola, A.R. Dunn, and D. Metcalf. 1996. Studies of the c-Mpl thrombopoietin receptor through gene disruption and activation. *Stem cells*. 14 Suppl 1:124-132.

Antonchuk, J., C.D. Hyland, D.J. Hilton, and W.S. Alexander. 2004. Synergistic effects on erythropoiesis, thrombopoiesis, and stem cell competitiveness in mice deficient in thrombopoietin and steel factor receptors. *Blood*. 104:1306-1313.

Anzai, N., Y. Lee, B.S. Youn, S. Fukuda, Y.J. Kim, C. Mantel, M. Akashi, and H.E. Broxmeyer. 2002. C-kit associated with the transmembrane 4 superfamily proteins constitutes a functionally distinct subunit in human hematopoietic progenitors. *Blood*. 99:4413-4421.

Arcaro, A., M. Aubert, M.E. Espinosa del Hierro, U.K. Khanzada, S. Angelidou, T.D. Tetley, A.G. Bittermann, M.C. Frame, and M.J. Seckl. 2007. Critical role for lipid raft-associated Src kinases in activation of PI3K-Akt signalling. *Cellular signalling*. 19:1081-1092.

Arcasoy, M.O., and X. Jiang. 2005. Co-operative signalling mechanisms required for erythroid precursor expansion in response to erythropoietin and stem cell factor. *British journal of haematology*. 130:121-129.

Atay, S., S. Banskota, J. Crow, G. Sethi, L. Rink, and A.K. Godwin. 2014. Oncogenic KIT-containing exosomes increase gastrointestinal stromal tumor cell invasion. *Proceedings of the National Academy of Sciences of the United States of America*. 111:711-716.

Ayaz, F., and B.A. Osborne. 2014. Non-canonical notch signaling in cancer and immunity. *Frontiers in oncology*. 4:345.

Bartucci, M., R. Dattilo, D. Martinetti, M. Todaro, G. Zapparelli, A. Di Virgilio, M. Biffoni, R. De Maria, and A. Zeuner. 2011. Prevention of chemotherapy-induced anemia and thrombocytopenia by constant administration of stem cell factor. *Clinical cancer research : an official journal of the American Association for Cancer Research*. 17:6185-6191.

Benveniste, P., C. Frelin, S. Janmohamed, M. Barbara, R. Herrington, D. Hyam, and N.N. Iscove. 2010. Intermediate-term hematopoietic stem cells with extended but time-limited reconstitution potential. *Cell stem cell*. 6:48-58.

Bersenev, A., C. Wu, J. Balcerek, and W. Tong. 2008. Lnk controls mouse hematopoietic stem cell self-renewal and quiescence through direct interactions with JAK2. *The Journal of clinical investigation*. 118:2832-2844.

Besancenot, R., D. Roos-Weil, C. Tonetti, H. Abdelouahab, C. Lacout, F. Pasquier, C. Willekens, P. Rameau, Y. Lecluse, J.B. Micol, S.N. Constantinescu, W. Vainchenker, E. Solary, and S. Giraudier. 2014. JAK2 and MPL protein levels determine TPO-induced megakaryocyte proliferation vs differentiation. *Blood*. 124:2104-2115.

Bessis, M. 1958. [Electron microscopy of the fate of a molecule in the organism: ferritin & iron hemoglobin cycle]. *Bulletin de l'Academie nationale de medecine*. 142:629-643.

Boer, A.K., A.L. Drayer, and E. Vellenga. 2003. Stem cell factor enhances erythropoietin-mediated transactivation of signal transducer and activator of transcription 5 (STAT5) via the PKA/CREB pathway. *Experimental hematology*. 31:512-520.

Bouilloux, F., G. Juban, N. Cohet, D. Buet, B. Guyot, W. Vainchenker, F. Louache, and F. Morle. 2008. EKLF restricts megakaryocytic differentiation at the benefit of erythrocytic differentiation. *Blood*. 112:576-584.

Boulais, P.E., and P.S. Frenette. 2015. Making sense of hematopoietic stem cell niches. *Blood*. 125:2621-2629.

Bowers, M., B. Zhang, Y. Ho, P. Agarwal, C.C. Chen, and R. Bhatia. 2015. Osteoblast ablation reduces normal long-term hematopoietic stem cell self-renewal but accelerates leukemia development. *Blood*. 125:2678-2688.

Bowie, M.B., D.G. Kent, M.R. Copley, and C.J. Eaves. 2007. Steel factor responsiveness regulates the high self-renewal phenotype of fetal hematopoietic stem cells. *Blood*. 109:5043-5048.

Brannan, C.I., S.D. Lyman, D.E. Williams, J. Eisenman, D.M. Anderson, D. Cosman, M.A. Bedell, N.A. Jenkins, and N.G. Copeland. 1991. Steel-Dickie mutation encodes a c-kit ligand lacking transmembrane and cytoplasmic domains. *Proceedings of the National Academy of Sciences of the United States of America*. 88:4671-4674.

Brizzi, M.F., P. Dentelli, A. Rosso, Y. Yarden, and L. Pegoraro. 1999. STAT protein recruitment and activation in c-Kit deletion mutants. *The Journal of biological chemistry*. 274:16965-16972.

Broudy, V.C. 1997. Stem cell factor and hematopoiesis. *Blood*. 90:1345-1364.

Broudy, V.C., N.L. Lin, G.V. Priestley, K. Nocka, and N.S. Wolf. 1996. Interaction of stem cell factor and its receptor c-kit mediates lodgment and acute expansion of hematopoietic cells in the murine spleen. *Blood*. 88:75-81.

Broudy, V.C., N.L. Lin, D.F. Sabath, T. Papayannopoulou, and K. Kaushansky. 1997. Human platelets display high-affinity receptors for thrombopoietin. *Blood*. 89:1896-1904.

Bruns, I., D. Lucas, S. Pinho, J. Ahmed, M.P. Lambert, Y. Kunisaki, C. Scheiermann, L. Schiff, M. Poncz, A. Bergman, and P.S. Frenette. 2014. Megakaryocytes regulate hematopoietic stem cell quiescence through CXCL4 secretion. *Nature medicine*. 20:1315-1320.

Bunting, S., R. Widmer, T. Lipari, L. Rangell, H. Steinmetz, K. Carver-Moore, M.W. Moore, G.A. Keller, and F.J. de Sauvage. 1997. Normal platelets and megakaryocytes are produced in vivo in the absence of thrombopoietin. *Blood*. 90:3423-3429.

Butler, J.M., D.J. Nolan, E.L. Vertes, B. Varnum-Finney, H. Kobayashi, A.T. Hooper, M. Seandel, K. Shido, I.A. White, M. Kobayashi, L. Witte, C. May, C. Shawber, Y. Kimura, J. Kitajewski, Z. Rosenwaks, I.D. Bernstein, and S. Rafii. 2010. Endothelial cells are essential for the self-renewal and repopulation of Notch-dependent hematopoietic stem cells. *Cell stem cell*. 6:251-264.

Cairns, L.A., E. Moroni, E. Levantini, A. Giorgetti, F.G. Klinger, S. Ronzoni, L. Tatangelo, C. Tiveron, M. De Felici, S. Dolci, M.C. Magli, B. Giglioni, and S. Ottolenghi. 2003. Kit regulatory elements required for expression in developing hematopoietic and germ cell lineages. *Blood*. 102:3954-3962.

Calvi, L.M., G.B. Adams, K.W. Weibrecht, J.M. Weber, D.P. Olson, M.C. Knight, R.P. Martin, E. Schipani, P. Divieti, F.R. Bringhurst, L.A. Milner, H.M. Kronenberg, and D.T. Scadden. 2003. Osteoblastic cells regulate the haematopoietic stem cell niche. *Nature*. 425:841-846.

Carver-Moore, K., H.E. Broxmeyer, S.M. Luoh, S. Cooper, J. Peng, S.A. Burstein, M.W. Moore, and F.J. de Sauvage. 1996. Low levels of erythroid and myeloid progenitors in thrombopoietin-and c-mpl-deficient mice. *Blood*. 88:803-808.

Catelain, C., F. Michelet, A. Hattabi, S. Poirault-Chassac, T. Kortulewski, D. Tronik-Le Roux, W. Vainchenker, and E. Lauret. 2014. The Notch Delta-4 ligand helps to maintain the quiescence

and the short-term reconstitutive potential of haematopoietic progenitor cells through activation of a key gene network. *Stem cell research*. 13:431-441.

Chairoungdua, A., D.L. Smith, P. Pochard, M. Hull, and M.J. Caplan. 2010. Exosome release of beta-catenin: a novel mechanism that antagonizes Wnt signaling. *The Journal of cell biology*. 190:1079-1091.

Chang, Y., D. Bluteau, N. Debili, and W. Vainchenker. 2007. From hematopoietic stem cells to platelets. *Journal of thrombosis and haemostasis : JTH*. 5 Suppl 1:318-327.

Chasis, J.A., and N. Mohandas. 2008. Erythroblastic islands: niches for erythropoiesis. *Blood*. 112:470-478.

Chen, J., X.B. Li, R. Su, L. Song, F. Wang, and J.W. Zhang. 2014a. ZNF16 (HZF1) promotes erythropoiesis and megakaryocytopoiesis via regulation of the c-KIT gene. *The Biochemical journal*. 458:171-183.

Chen, L., A. Charrier, Y. Zhou, R. Chen, B. Yu, K. Agarwal, H. Tsukamoto, L.J. Lee, M.E. Paulaitis, and D.R. Brigstock. 2014b. Epigenetic regulation of connective tissue growth factor by MicroRNA-214 delivery in exosomes from mouse or human hepatic stellate cells. *Hepatology*. 59:1118-1129.

Chiang, M.Y., O. Shestova, L. Xu, J.C. Aster, and W.S. Pear. 2013. Divergent effects of supraphysiologic Notch signals on leukemia stem cells and hematopoietic stem cells. *Blood*. 121:905-917.

Chou, S.T., E. Khandros, L.C. Bailey, K.E. Nichols, C.R. Vakoc, Y. Yao, Z. Huang, J.D. Crispino, R.C. Hardison, G.A. Blobel, and M.J. Weiss. 2009. Graded repression of PU.1/Sfpi1 gene transcription by GATA factors regulates hematopoietic cell fate. *Blood*. 114:983-994.

Chow, A., M. Huggins, J. Ahmed, D. Hashimoto, D. Lucas, Y. Kunisaki, S. Pinho, M. Leboeuf, C. Noizat, N. van Rooijen, M. Tanaka, Z.J. Zhao, A. Bergman, M. Merad, and P.S. Frenette. 2013. CD169(+) macrophages provide a niche promoting erythropoiesis under homeostasis and stress. *Nature medicine*. 19:429-436.

Ciau-Uitz, A., R. Monteiro, A. Kirmizitas, and R. Patient. 2014. Developmental hematopoiesis: ontogeny, genetic programming and conservation. *Experimental hematology*. 42:669-683.

Cocault, L., D. Bouscary, C. Le Bousse Kerdiles, D. Clay, F. Picard, S. Gisselbrecht, and M. Souyri. 1996. Ectopic expression of murine TPO receptor (c-mpl) in mice is pathogenic and induces erythroblastic proliferation. *Blood*. 88:1656-1665.

Coers, J., C. Ranft, and R.C. Skoda. 2004. A truncated isoform of c-Mpl with an essential C-terminal peptide targets the full-length receptor for degradation. *The Journal of biological chemistry*. 279:36397-36404.

Cornejo, M.G., V. Mabialah, S.M. Sykes, T. Khandan, C. Lo Celso, C.K. Lopez, P. Rivera-Munoz, P. Rameau, Z. Tothova, J.C. Aster, R.A. DePinho, D.T. Scadden, D.G. Gilliland, and T. Mercher. 2011. Crosstalk between NOTCH and AKT signaling during murine megakaryocyte lineage specification. *Blood*. 118:1264-1273.

Cortin, V., A. Garnier, N. Pineault, R. Lemieux, L. Boyer, and C. Proulx. 2005. Efficient in vitro megakaryocyte maturation using cytokine cocktails optimized by statistical experimental design. *Experimental hematology*. 33:1182-1191.

Cruz, A.C., B.T. Frank, S.T. Edwards, P.F. Dazin, J.J. Peschon, and K.C. Fang. 2004. Tumor necrosis factor-alpha-converting enzyme controls surface expression of c-Kit and survival of embryonic stem cell-derived mast cells. *The Journal of biological chemistry*. 279:5612-5620.

Csaszar, E., W. Wang, T. Usenko, W. Qiao, C. Delaney, I.D. Bernstein, and P.W. Zandstra. 2014. Blood stem cell fate regulation by Delta-1-mediated rewiring of IL-6 paracrine signaling. *Blood*. 123:650-658.

D'Allard, D., J. Gay, C. Descarpentries, E. Frisan, K. Adam, F. Verdier, C. Floquet, P. Dubreuil, C. Lacombe, M. Fontenay, P. Mayeux, and O. Kosmider. 2013. Tyrosine kinase inhibitors induce down-regulation of c-Kit by targeting the ATP pocket. *PloS one*. 8:e60961.

D'Souza, B., L. Meloty-Kapella, and G. Weinmaster. 2010. Canonical and non-canonical Notch ligands. *Current topics in developmental biology*. 92:73-129.

Dando, J.S., M. Tavian, C. Catelain, S. Poirault, A. Bennaceur-Griscelli, F. Sainteny, W. Vainchenker, B. Peault, and E. Lauret. 2005. Notch/Delta4 interaction in human embryonic liver CD34+ CD38- cells: positive influence on BFU-E production and LTC-IC potential maintenance. *Stem cells*. 23:550-560.

de Graaf, C.A., and D. Metcalf. 2011. Thrombopoietin and hematopoietic stem cells. *Cell cycle*. 10:1582-1589.

de Laval, B., P. Pawlikowska, D. Barbieri, C. Besnard-Guerin, A. Cico, R. Kumar, M. Gaudry, V. Baud, and F. Porteu. 2014. Thrombopoietin promotes NHEJ DNA repair in hematopoietic stem cells through specific activation of Erk and NF-kappaB pathways and their target, IEX-1. *Blood*. 123:509-519.

de Laval, B., P. Pawlikowska, L. Petit-Cocault, C. Bilhou-Nabera, G. Aubin-Houzelstein, M. Souyri, F. Pouzoulet, M. Gaudry, and F. Porteu. 2013. Thrombopoietin-increased DNA-PK-dependent DNA repair limits hematopoietic stem and progenitor cell mutagenesis in response to DNA damage. *Cell stem cell*. 12:37-48.

De Maria, R., U. Testa, L. Luchetti, A. Zeuner, G. Stassi, E. Pelosi, R. Riccioni, N. Felli, P. Samoggia, and C. Peschle. 1999. Apoptotic role of Fas/Fas ligand system in the regulation of erythropoiesis. *Blood*. 93:796-803.

de Paulis, A., G. Minopoli, E. Arbustini, G. de Crescenzo, F. Dal Piaz, P. Pucci, T. Russo, and G. Marone. 1999. Stem cell factor is localized in, released from, and cleaved by human mast cells. *Journal of immunology*. 163:2799-2808.

de Sauvage, F.J., K. Carver-Moore, S.M. Luoh, A. Ryan, M. Dowd, D.L. Eaton, and M.W. Moore. 1996. Physiological regulation of early and late stages of megakaryocytopoiesis by thrombopoietin. *The Journal of experimental medicine*. 183:651-656.

de Sauvage, F.J., P.E. Hass, S.D. Spencer, B.E. Malloy, A.L. Gurney, S.A. Spencer, W.C. Darbonne, W.J. Henzel, S.C. Wong, W.J. Kuang, and et al. 1994. Stimulation of megakaryocytopoiesis and thrombopoiesis by the c-Mpl ligand. *Nature*. 369:533-538.

De Sepulveda, P., K. Okkenhaug, J.L. Rose, R.G. Hawley, P. Dubreuil, and R. Rottapel. 1999. Socs1 binds to multiple signalling proteins and suppresses steel factor-dependent proliferation. *The EMBO journal*. 18:904-915.

De Smedt, M., I. Hoebeke, and J. Plum. 2004. Human bone marrow CD34+ progenitor cells mature to T cells on OP9-DL1 stromal cell line without thymus microenvironment. *Blood cells, molecules & diseases*. 33:227-232.

Debili, N., L. Coulombel, L. Croisille, A. Katz, J. Guichard, J. Breton-Gorius, and W. Vainchenker. 1996. Characterization of a bipotent erythro-megakaryocytic progenitor in human bone marrow. *Blood*. 88:1284-1296.

Deshpande, S., B. Bosbach, Y. Yozgat, C.Y. Park, M.A. Moore, and P. Besmer. 2013. KIT receptor gain-of-function in hematopoiesis enhances stem cell self-renewal and promotes progenitor cell expansion. *Stem cells*. 31:1683-1695.

Desterke, C., C. Martinaud, B. Guerton, L. Pieri, C. Bogani, D. Clay, F. Torossian, J.J. Lataillade, H.C. Hasselbach, H. Gisslinger, J.L. Demory, B. Dupriez, C. Boucheix, E. Rubinstein, S. Amsellem, A.M. Vannucchi, and M.C. Le Bousse-Kerdiles. 2015. Tetraspanin CD9 participates in dysmegakaryopoiesis and stromal interactions in primary myelofibrosis. *Haematologica*. 100:757-767.

Deutsch, V.R., and A. Tomer. 2013. Advances in megakaryocytopoiesis and thrombopoiesis: from bench to bedside. *British journal of haematology*. 161:778-793.

Dias, S., R. Mansson, S. Gurbuxani, M. Sigvardsson, and B.L. Kee. 2008. E2A proteins promote development of lymphoid-primed multipotent progenitors. *Immunity*. 29:217-227.

Ding, L., T.L. Saunders, G. Enikolopov, and S.J. Morrison. 2012. Endothelial and perivascular cells maintain haematopoietic stem cells. *Nature*. 481:457-462.

Dongre, A., L. Surampudi, R.G. Lawlor, A.H. Fauq, L. Miele, T.E. Golde, L.M. Minter, and B.A. Osborne. 2014. Non-Canonical Notch Signaling Drives Activation and Differentiation of Peripheral CD4(+) T Cells. *Frontiers in immunology*. 5:54.

Dore, L.C., T.M. Chlon, C.D. Brown, K.P. White, and J.D. Crispino. 2012. Chromatin occupancy analysis reveals genome-wide GATA factor switching during hematopoiesis. *Blood*. 119:3724-3733.

Drachman, J.G., K.M. Millett, and K. Kaushansky. 1999. Thrombopoietin signal transduction requires functional JAK2, not TYK2. *The Journal of biological chemistry*. 274:13480-13484.

Drayer, A.L., A.K. Boer, E.L. Los, M.T. Esselink, and E. Vellenga. 2005. Stem cell factor synergistically enhances thrombopoietin-induced STAT5 signaling in megakaryocyte progenitors through JAK2 and Src kinase. *Stem cells*. 23:240-251.

Drube, S., S. Heink, S. Walter, T. Lohn, M. Grusser, A. Gerbaulet, L. Berod, J. Schons, A. Dudeck, J. Freitag, S. Grotha, D. Reich, O. Rudeschko, J. Norgauer, K. Hartmann, A. Roers, and T. Kamradt. 2010. The receptor tyrosine kinase c-Kit controls IL-33 receptor signaling in mast cells. *Blood*. 115:3899-3906.

Dubreuil, P., S. Letard, M. Ciufolini, L. Gros, M. Humbert, N. Casteran, L. Borge, B. Hajem, A. Lermet, W. Sippl, E. Voisset, M. Arock, C. Auclair, P.S. Leventhal, C.D. Mansfield, A. Moussy, and O. Hermine. 2009. Masitinib (AB1010), a potent and selective tyrosine kinase inhibitor targeting KIT. *PloS one*. 4:e7258.

Dykstra, B., and G. de Haan. 2008. Hematopoietic stem cell aging and self-renewal. *Cell and tissue research*. 331:91-101.

Eaves, C.J. 2015. Hematopoietic stem cells: concepts, definitions, and the new reality. *Blood*. 125:2605-2613.

Elagib, K.E., M. Xiao, I.M. Hussaini, L.L. Delehanty, L.A. Palmer, F.K. Racke, M.J. Birrer, G. Shanmugasundaram, M.A. McDevitt, and A.N. Goldfarb. 2004. Jun blockade of erythropoiesis: role for repression of GATA-1 by HERP2. *Molecular and cellular biology*. 24:7779-7794.

Elliott, S., T. Lorenzini, S. Asher, K. Aoki, D. Brankow, L. Buck, L. Busse, D. Chang, J. Fuller, J. Grant, N. Hernday, M. Hokum, S. Hu, A. Knudten, N. Levin, R. Komorowski, F. Martin, R. Navarro, T. Osslund, G. Rogers, N. Rogers, G. Trail, and J. Egrie. 2003. Enhancement of therapeutic protein in vivo activities through glycoengineering. *Nature biotechnology*. 21:414-421.

Ema, H., Y. Morita, and T. Suda. 2014. Heterogeneity and hierarchy of hematopoietic stem cells. *Experimental hematology*. 42:74-82 e72.

Endo, T., A. Odb, I. Satoh, Y. Haseyama, M. Nishio, K. Koizumi, H. Takashima, K. Fujimoto, Y. Amasaki, H. Fujita, T. Koike, and K. Sawada. 2001. Stem cell factor protects c-kit+ human primary erythroid cells from apoptosis. *Experimental hematology*. 29:833-841.

Endo, T.A., M. Masuhara, M. Yokouchi, R. Suzuki, H. Sakamoto, K. Mitsui, A. Matsumoto, S. Tanimura, M. Ohtsubo, H. Misawa, T. Miyazaki, N. Leonor, T. Taniguchi, T. Fujita, Y. Kanakura, S. Komiya, and A. Yoshimura. 1997. A new protein containing an SH2 domain that inhibits JAK kinases. *Nature*. 387:921-924.

Engin, F., Z. Yao, T. Yang, G. Zhou, T. Bertin, M.M. Jiang, Y. Chen, L. Wang, H. Zheng, R.E. Sutton, B.F. Boyce, and B. Lee. 2008. Dimorphic effects of Notch signaling in bone homeostasis. *Nature medicine*. 14:299-305.

Fabriek, B.O., M.M. Polfliet, R.P. Vloet, R.C. van der Schors, A.J. Ligtenberg, L.K. Weaver, C. Geest, K. Matsuno, S.K. Moestrup, C.D. Dijkstra, and T.K. van den Berg. 2007. The macrophage CD163 surface glycoprotein is an erythroblast adhesion receptor. *Blood*. 109:5223-5229.

Ferrao, P.T., T.J. Gonda, and L.K. Ashman. 2003. Constitutively active mutant D816VKit induces megakayocyte and mast cell differentiation of early haemopoietic cells from murine foetal liver. *Leukemia research*. 27:547-555.

Fibbe, W.E., D.P. Heemskerk, L. Laterveer, J.F. Pruijt, D. Foster, K. Kaushansky, and R. Willemze. 1995. Accelerated reconstitution of platelets and erythrocytes after syngeneic transplantation of

bone marrow cells derived from thrombopoietin pretreated donor mice. *Blood*. 86:3308-3313.

Fichelson, S., J.M. Freyssinier, F. Picard, M. Fontenay-Roupie, M. Guesnu, M. Cherai, S. Gisselbrecht, and F. Porteu. 1999. Megakaryocyte growth and development factor-induced proliferation and differentiation are regulated by the mitogen-activated protein kinase pathway in primitive cord blood hematopoietic progenitors. *Blood*. 94:1601-1613.

Flaumenhaft, R., J.R. Dilks, J. Richardson, E. Alden, S.R. Patel-Hett, E. Battinelli, G.L. Klement, M. Sola-Visner, and J.E. Italiano, Jr. 2009. Megakaryocyte-derived microparticles: direct visualization and distinction from platelet-derived microparticles. *Blood*. 113:1112-1121.

Foster, D., and S. Lok. 1996. Biological roles for the second domain of thrombopoietin. *Stem cells*. 14 Suppl 1:102-107.

Foudi, A., K. Hochedlinger, D. Van Buren, J.W. Schindler, R. Jaenisch, V. Carey, and H. Hock. 2009. Analysis of histone 2B-GFP retention reveals slowly cycling hematopoietic stem cells. *Nature biotechnology*. 27:84-90.

Fox, N., G. Priestley, T. Papayannopoulou, and K. Kaushansky. 2002. Thrombopoietin expands hematopoietic stem cells after transplantation. *The Journal of clinical investigation*. 110:389-394.

Frontelo, P., D. Manwani, M. Galdass, H. Karsunky, F. Lohmann, P.G. Gallagher, and J.J. Bieker. 2007. Novel role for EKLF in megakaryocyte lineage commitment. *Blood*. 110:3871-3880.

Fryer, C.J., J.B. White, and K.A. Jones. 2004. Mastermind recruits CycC:CDK8 to phosphorylate the Notch ICD and coordinate activation with turnover. *Molecular cell*. 16:509-520.

Fujiki, H., T. Kimura, H. Minamiguchi, S. Harada, J. Wang, M. Nakao, S. Yokota, Y. Urata, Y. Ueda, H. Yamagishi, and Y. Sonoda. 2002. Role of human interleukin-9 as a megakaryocyte potentiator in culture. *Experimental hematology*. 30:1373-1380.

Gabbianelli, M., O. Morsilli, A. Massa, L. Pasquini, P. Cianciulli, U. Testa, and C. Peschle. 2008. Effective erythropoiesis and HbF reactivation induced by kit ligand in beta-thalassemia. *Blood*. 111:421-429.

Gabbianelli, M., U. Testa, O. Morsilli, E. Pelosi, E. Saulle, E. Petrucci, G. Castelli, S. Giovinazzi, G. Mariani, M.E. Fiori, G. Bonanno, A. Massa, C.M. Croce, L. Fontana, and C. Peschle. 2010. Mechanism of human Hb switching: a possible role of the kit receptor/miR 221-222 complex. *Haematologica*. 95:1253-1260.

Garcia, J., J. de Gunzburg, A. Eychene, S. Gisselbrecht, and F. Porteu. 2001. Thrombopoietin-mediated sustained activation of extracellular signal-regulated kinase in UT7-Mpl cells requires both Ras-Raf-1- and Rap1-B-Raf-dependent pathways. *Molecular and cellular biology*. 21:2659-2670.

Geissler, E.N., E.C. McFarland, and E.S. Russell. 1981. Analysis of pleiotropism at the dominant white-spotting (W) locus of the house mouse: a description of ten new W alleles. *Genetics*. 97:337-361.

Gekas, C., and T. Graf. 2013. CD41 expression marks myeloid-biased adult hematopoietic stem cells and increases with age. *Blood*. 121:4463-4472.

Gering, M., and R. Patient. 2010. Notch signalling and haematopoietic stem cell formation during embryogenesis. *Journal of cellular physiology*. 222:11-16.

Goldberg, L.R., M.S. Dooner, K.W. Johnson, E.F. Papa, M.G. Pereira, M. Del Tatto, D.M. Adler, J.M. Aliotta, and P.J. Quesenberry. 2014. The murine long-term multi-lineage renewal marrow stem cell is a cycling cell. *Leukemia*. 28:813-822.

Gommerman, J.L., D. Sittaro, N.Z. Klebasz, D.A. Williams, and S.A. Berger. 2000. Differential stimulation of c-Kit mutants by membrane-bound and soluble Steel Factor correlates with leukemic potential. *Blood*. 96:3734-3742.

Gothot, A., R. Pyatt, J. McMahel, S. Rice, and E.F. Srour. 1997. Functional heterogeneity of human CD34(+) cells isolated in subcompartments of the G0 /G1 phase of the cell cycle. *Blood*. 90:4384-4393.

Gotoh, A., H. Takahira, C. Mantel, S. Litz-Jackson, H.S. Boswell, and H.E. Broxmeyer. 1996. Steel factor induces serine phosphorylation of Stat3 in human growth factor-dependent myeloid cell lines. *Blood*. 88:138-145.

Grass, J.A., M.E. Boyer, S. Pal, J. Wu, M.J. Weiss, and E.H. Bresnick. 2003. GATA-1-dependent transcriptional repression of GATA-2 via disruption of positive autoregulation and domain-wide chromatin remodeling. *Proceedings of the National Academy of Sciences of the United States of America*. 100:8811-8816.

Grinenko, T., K. Arndt, M. Portz, N. Mende, M. Gunther, K.N. Cosgun, D. Alexopoulou, N. Lakshmanaperumal, I. Henry, A. Dahl, and C. Waskow. 2014. Clonal expansion capacity defines two consecutive developmental stages of long-term hematopoietic stem cells. *The Journal of experimental medicine*. 211:209-215.

Guerriero, R., I. Parolini, U. Testa, P. Samoggia, E. Petrucci, M. Sargiacomo, C. Chelucci, M. Gabbianelli, and C. Peschle. 2006. Inhibition of TPO-induced MEK or mTOR activity induces opposite effects on the ploidy of human differentiating megakaryocytes. *Journal of cell science*. 119:744-752.

Guiu, J., R. Shimizu, T. D'Altri, S.T. Fraser, J. Hatakeyama, E.H. Bresnick, R. Kageyama, E. Dzierzak, M. Yamamoto, L. Espinosa, and A. Bigas. 2013. Hes repressors are essential regulators of hematopoietic stem cell development downstream of Notch signaling. *The Journal of experimental medicine*. 210:71-84.

Guo, G., S. Luc, E. Marco, T.W. Lin, C. Peng, M.A. Kerenyi, S. Beyaz, W. Kim, J. Xu, P.P. Das, T. Neff, K. Zou, G.C. Yuan, and S.H. Orkin. 2013. Mapping cellular hierarchy by single-cell analysis of the cell surface repertoire. *Cell stem cell*. 13:492-505.

Gurney, A.L., K. Carver-Moore, F.J. de Sauvage, and M.W. Moore. 1994. Thrombocytopenia in c-mpl-deficient mice. *Science*. 265:1445-1447.

Hanspal, M., Y. Smockova, and Q. Uong. 1998. Molecular identification and functional characterization of a novel protein that mediates the attachment of erythroblasts to macrophages. *Blood*. 92:2940-2950.

Harandi, O.F., S. Hedge, D.C. Wu, D. McKeone, and R.F. Paulson. 2010. Murine erythroid short-term radioprotection requires a BMP4-dependent, self-renewing population of stress erythroid progenitors. *The Journal of clinical investigation*. 120:4507-4519.

Hasemann, M.S., F.K. Lauridsen, J. Waage, J.S. Jakobsen, A.K. Frank, M.B. Schuster, N. Rapin, F.O. Bagger, P.S. Hoppe, T. Schroeder, and B.T. Porse. 2014. C/EBPalpha is required for long-term self-renewal and lineage priming of hematopoietic stem cells and for the maintenance of epigenetic configurations in multipotent progenitors. *PLoS genetics*. 10:e1004079.

Heazlewood, S.Y., R.J. Neaves, B. Williams, D.N. Haylock, T.E. Adams, and S.K. Nilsson. 2013. Megakaryocytes co-localise with hemopoietic stem cells and release cytokines that up-regulate stem cell proliferation. *Stem cell research*. 11:782-792.

Heissig, B., K. Hattori, S. Dias, M. Friedrich, B. Ferris, N.R. Hackett, R.G. Crystal, P. Besmer, D. Lyden, M.A. Moore, Z. Werb, and S. Rafii. 2002. Recruitment of stem and progenitor cells from the bone marrow niche requires MMP-9 mediated release of kit-ligand. *Cell*. 109:625-637.

Hemler, M.E. 2003. Tetraspanin proteins mediate cellular penetration, invasion, and fusion events and define a novel type of membrane microdomain. *Annual review of cell and developmental biology*. 19:397-422.

Hilton, M.J., X. Tu, X. Wu, S. Bai, H. Zhao, T. Kobayashi, H.M. Kronenberg, S.L. Teitelbaum, F.P. Ross, R. Kopan, and F. Long. 2008. Notch signaling maintains bone marrow mesenchymal progenitors by suppressing osteoblast differentiation. *Nature medicine*. 14:306-314.

Hitchcock, I.S., M.M. Chen, J.R. King, and K. Kaushansky. 2008. YRRL motifs in the cytoplasmic domain of the thrombopoietin receptor regulate receptor internalization and degradation. *Blood*. 112:2222-2231.

Hodge, D., E. Coghill, J. Keys, T. Maguire, B. Hartmann, A. McDowall, M. Weiss, S. Grimmond, and A. Perkins. 2006. A global role for EKLF in definitive and primitive erythropoiesis. *Blood*. 107:3359-3370.

Huang, E.J., K.H. Nocka, J. Buck, and P. Besmer. 1992. Differential expression and processing of two cell associated forms of the kit-ligand: KL-1 and KL-2. *Molecular biology of the cell*. 3:349-362.

Huang, Z., T.D. Richmond, A.G. Muntean, D.L. Barber, M.J. Weiss, and J.D. Crispino. 2007. STAT1 promotes megakaryopoiesis downstream of GATA-1 in mice. *The Journal of clinical investigation*. 117:3890-3899.

Huddleston, H., B. Tan, F.C. Yang, H. White, M.J. Wenning, A. Orazi, M.C. Yoder, R. Kapur, and D.A. Ingram. 2003. Functional p85alpha gene is required for normal murine fetal erythropoiesis. *Blood*. 102:142-145.

Hunt, P., K.M. Zsebo, M.M. Hokom, A. Hornkohl, N.C. Birkett, J.C. del Castillo, and F. Martin. 1992. Evidence that stem cell factor is involved in the rebound thrombocytosis that follows 5-fluorouracil treatment. *Blood*. 80:904-911.

Ingley, E. 2008. Src family kinases: regulation of their activities, levels and identification of new pathways. *Biochimica et biophysica acta*. 1784:56-65.

Ishibashi, T., H. Kimura, T. Uchida, S. Kariyone, P. Friese, and S.A. Burstein. 1989. Human interleukin 6 is a direct promoter of maturation of megakaryocytes in vitro. *Proceedings of the National Academy of Sciences of the United States of America*. 86:5953-5957.

Ishida, Y., J. Levin, G. Baker, P.E. Stenberg, Y. Yamada, H. Sasaki, and T. Inoue. 1993. Biological and biochemical characteristics of murine megakaryoblastic cell line L8057. *Experimental hematology*. 21:289-298.

Ishiko, E., I. Matsumura, S. Ezoe, K. Gale, J. Ishiko, Y. Satoh, H. Tanaka, H. Shibayama, M. Mizuki, T. Era, T. Enver, and Y. Kanakura. 2005. Notch signals inhibit the development of erythroid/megakaryocytic cells by suppressing GATA-1 activity through the induction of HES1. *The Journal of biological chemistry*. 280:4929-4939.

Iso, T., L. Kedes, and Y. Hamamori. 2003. HES and HERP families: multiple effectors of the Notch signaling pathway. *Journal of cellular physiology*. 194:237-255.

Iwasaki, H., S. Mizuno, R.A. Wells, A.B. Cantor, S. Watanabe, and K. Akashi. 2003. GATA-1 converts lymphoid and myelomonocytic progenitors into the megakaryocyte/erythrocyte lineages. *Immunity*. 19:451-462.

Jing, H., C.R. Vakoc, L. Ying, S. Mandat, H. Wang, X. Zheng, and G.A. Blobel. 2008. Exchange of GATA factors mediates transitions in looped chromatin organization at a developmentally regulated gene locus. *Molecular cell*. 29:232-242.

Jordan, C.T., J.P. McKearn, and I.R. Lemischka. 1990. Cellular and developmental properties of fetal hematopoietic stem cells. *Cell*. 61:953-963.

Joshi, I., L.M. Minter, J. Telfer, R.M. Demarest, A.J. Capobianco, J.C. Aster, P. Sicinski, A. Fauq, T.E. Golde, and B.A. Osborne. 2009. Notch signaling mediates G1/S cell-cycle progression in T cells via cyclin D3 and its dependent kinases. *Blood*. 113:1689-1698.

Kadri, Z., L. Maouche-Chretien, H.M. Rooke, S.H. Orkin, P.H. Romeo, P. Mayeux, P. Leboulch, and S. Chretien. 2005. Phosphatidylinositol 3-kinase/Akt induced by erythropoietin renders the erythroid differentiation factor GATA-1 competent for TIMP-1 gene transactivation. *Molecular and cellular biology*. 25:7412-7422.

Kadri, Z., R. Shimizu, O. Ohneda, L. Maouche-Chretien, S. Gisselbrecht, M. Yamamoto, P.H. Romeo, P. Leboulch, and S. Chretien. 2009. Direct binding of pRb/E2F-2 to GATA-1 regulates maturation and terminal cell division during erythropoiesis. *PLoS biology*. 7:e1000123.

Kapur, R., and L. Zhang. 2001. A novel mechanism of cooperation between c-Kit and erythropoietin receptor. Stem cell factor induces the expression of Stat5 and erythropoietin receptor, resulting in efficient proliferation and survival by erythropoietin. *The Journal of biological chemistry*. 276:1099-1106.

Karanu, F.N., B. Murdoch, L. Gallacher, D.M. Wu, M. Koremoto, S. Sakano, and M. Bhatia. 2000. The notch ligand jagged-1 represents a novel growth factor of human hematopoietic stem cells. *The Journal of experimental medicine*. 192:1365-1372.

Karanu, F.N., L. Yuefei, L. Gallacher, S. Sakano, and M. Bhatia. 2003. Differential response of primitive human CD34- and CD34+ hematopoietic cells to the Notch ligand Jagged-1. *Leukemia*. 17:1366-1374.

Karlsson, G., E. Rorby, C. Pina, S. Soneji, K. Reckzeh, K. Miharada, C. Karlsson, Y. Guo, C. Fugazza, R. Gupta, J.H. Martens, H.G. Stunnenberg, S. Karlsson, and T. Enver. 2013. The tetraspanin CD9 affords high-purity capture of all murine hematopoietic stem cells. *Cell reports*. 4:642-648.

Kaushansky, K. 2005. The molecular mechanisms that control thrombopoiesis. *The Journal of clinical investigation*. 115:3339-3347.

Kaushansky, K. 2009. Determinants of platelet number and regulation of thrombopoiesis. *Hematology / the Education Program of the American Society of Hematology. American Society of Hematology. Education Program*:147-152.

Kaushansky, K., V.C. Broudy, A. Grossmann, J. Humes, N. Lin, H.P. Ren, M.C. Bailey, T. Papayannopoulou, J.W. Forstrom, and K.H. Sprugel. 1995. Thrombopoietin expands erythroid progenitors, increases red cell production, and enhances erythroid recovery after myelosuppressive therapy. *The Journal of clinical investigation*. 96:1683-1687.

Kiel, M.J., O.H. Yilmaz, T. Iwashita, O.H. Yilmaz, C. Terhorst, and S.J. Morrison. 2005. SLAM family receptors distinguish hematopoietic stem and progenitor cells and reveal endothelial niches for stem cells. *Cell*. 121:1109-1121.

Kieran, M.W., A.C. Perkins, S.H. Orkin, and L.I. Zon. 1996. Thrombopoietin rescues in vitro erythroid colony formation from mouse embryos lacking the erythropoietin receptor. *Proceedings of the National Academy of Sciences of the United States of America*. 93:9126-9131.

Kim, Y.W., B.K. Koo, H.W. Jeong, M.J. Yoon, R. Song, J. Shin, D.C. Jeong, S.H. Kim, and Y.Y. Kong. 2008. Defective Notch activation in microenvironment leads to myeloproliferative disease. *Blood*. 112:4628-4638.

Kimura, S., A.W. Roberts, D. Metcalf, and W.S. Alexander. 1998. Hematopoietic stem cell deficiencies in mice lacking c-Mpl, the receptor for thrombopoietin. *Proceedings of the National Academy of Sciences of the United States of America*. 95:1195-1200.

Kirito, K., and K. Kaushansky. 2005. Thrombopoietin stimulates vascular endothelial cell growth factor (VEGF) production in hematopoietic stem cells. *Cell cycle*. 4:1729-1731.

Kirito, K., M. Osawa, H. Morita, R. Shimizu, M. Yamamoto, A. Oda, H. Fujita, M. Tanaka, K. Nakajima, Y. Miura, K. Ozawa, and N. Komatsu. 2002. A functional role of Stat3 in in vivo megakaryopoiesis. *Blood*. 99:3220-3227.

Kirschbaum, M., G. Karimian, J. Adelmeijer, B.N. Giepmans, R.J. Porte, and T. Lisman. 2015. Horizontal RNA transfer mediates platelet-induced hepatocyte proliferation. *Blood*.

Klinakis, A., C. Lobry, O. Abdel-Wahab, P. Oh, H. Haeno, S. Buonamici, I. van De Walle, S. Cathelin, T. Trimarchi, E. Araldi, C. Liu, S. Ibrahim, M. Beran, J. Zavadil, A. Efstratiadis, T. Taghon, F. Michor, R.L. Levine, and I. Aifantis. 2011. A novel tumour-suppressor function for the Notch pathway in myeloid leukaemia. *Nature*. 473:230-233.

Kosmider, O., D. Buet, I. Gallais, N. Denis, and F. Moreau-Gachelin. 2009. Erythropoietin down-regulates stem cell factor receptor (Kit) expression in the leukemic proerythroblast: role of Lyn kinase. *PloS one*. 4:e5721.

Kovall, R.A., and S.C. Blacklow. 2010. Mechanistic insights into Notch receptor signaling from structural and biochemical studies. *Current topics in developmental biology*. 92:31-71.

Kuhl, C., A. Atzberger, F. Iborra, B. Nieswandt, C. Porcher, and P. Vyas. 2005. GATA1-mediated megakaryocyte differentiation and growth control can be uncoupled and mapped to different domains in GATA1. *Molecular and cellular biology*. 25:8592-8606.

Kumano, K., S. Chiba, A. Kunisato, M. Sata, T. Saito, E. Nakagami-Yamaguchi, T. Yamaguchi, S. Masuda, K. Shimizu, T. Takahashi, S. Ogawa, Y. Hamada, and H. Hirai. 2003. Notch1 but not

Notch2 is essential for generating hematopoietic stem cells from endothelial cells. *Immunity*. 18:699-711.

Kunisaki, Y., I. Bruns, C. Scheiermann, J. Ahmed, S. Pinho, D. Zhang, T. Mizoguchi, Q. Wei, D. Lucas, K. Ito, J.C. Mar, A. Bergman, and P.S. Frenette. 2013. Arteriolar niches maintain haematopoietic stem cell quiescence. *Nature*. 502:637-643.

Kunisato, A., S. Chiba, E. Nakagami-Yamaguchi, K. Kumano, T. Saito, S. Masuda, T. Yamaguchi, M. Osawa, R. Kageyama, H. Nakauchi, M. Nishikawa, and H. Hirai. 2003. HES-1 preserves purified hematopoietic stem cells ex vivo and accumulates side population cells in vivo. *Blood*. 101:1777-1783.

Lannutti, B.J., and J.G. Drachman. 2004. Lyn tyrosine kinase regulates thrombopoietin-induced proliferation of hematopoietic cell lines and primary megakaryocytic progenitors. *Blood*. 103:3736-3743.

Lannutti, B.J., A. Epp, J. Roy, J. Chen, and N.C. Josephson. 2009. Incomplete restoration of Mpl expression in the mpl-/- mouse produces partial correction of the stem cell-repopulating defect and paradoxical thrombocytosis. *Blood*. 113:1778-1785.

Lannutti, B.J., J. Minear, N. Blake, and J.G. Drachman. 2006. Increased megakaryocytopoiesis in Lyn-deficient mice. *Oncogene*. 25:3316-3324.

Larochelle, A., J.M. Gillette, R. Desmond, B. Ichwan, A. Cantilena, A. Cerf, A.J. Barrett, A.S. Wayne, J. Lippincott-Schwartz, and C.E. Dunbar. 2012. Bone marrow homing and engraftment of human hematopoietic stem and progenitor cells is mediated by a polarized membrane domain. *Blood*. 119:1848-1855.

Laurenti, E., C. Frelin, S. Xie, R. Ferrari, C.F. Dunant, S. Zandi, A. Neumann, I. Plumb, S. Doulatov, J. Chen, C. April, J.B. Fan, N. Iscove, and J.E. Dick. 2015. CDK6 levels regulate quiescence exit in human hematopoietic stem cells. *Cell stem cell*. 16:302-313.

Lazo, P.A. 2007. Functional implications of tetraspanin proteins in cancer biology. *Cancer science*. 98:1666-1677.

Lecuyer, E., S. Herblot, M. Saint-Denis, R. Martin, C.G. Begley, C. Porcher, S.H. Orkin, and T. Hoang. 2002. The SCL complex regulates c-kit expression in hematopoietic cells through functional interaction with Sp1. *Blood*. 100:2430-2440.

Lee, E.J., P. Godara, and D. Haylock. 2014. Biomanufacture of human platelets for transfusion: Rationale and approaches. *Experimental hematology*. 42:332-346.

Leimberg, M.J., E. Prus, A.M. Konijn, and E. Fibach. 2008. Macrophages function as a ferritin iron source for cultured human erythroid precursors. *Journal of cellular biochemistry*. 103:1211-1218.

Lennartsson, J., and L. Ronnstrand. 2012. Stem cell factor receptor/c-Kit: from basic science to clinical implications. *Physiological reviews*. 92:1619-1649.

Lennartsson, J., R. Shivakrupa, and D. Linnekin. 2004. Synergistic growth of stem cell factor and granulocyte macrophage colony-stimulating factor involves kinase-dependent and -independent contributions from c-Kit. *The Journal of biological chemistry*. 279:44544-44553.

Letting, D.L., Y.Y. Chen, C. Rakowski, S. Reedy, and G.A. Blobel. 2004. Context-dependent regulation of GATA-1 by friend of GATA-1. *Proceedings of the National Academy of Sciences of the United States of America*. 101:476-481.

Leung, K.T., K.Y. Chan, P.C. Ng, T.K. Lau, W.M. Chiu, K.S. Tsang, C.K. Li, C.K. Kong, and K. Li. 2011. The tetraspanin CD9 regulates migration, adhesion, and homing of human cord blood CD34+ hematopoietic stem and progenitor cells. *Blood*. 117:1840-1850.

Liao, W.R., R.H. Hsieh, K.W. Hsu, M.Z. Wu, M.J. Tseng, R.T. Mai, Y.H. Wu Lee, and T.S. Yeh. 2007. The CBF1-independent Notch1 signal pathway activates human c-myc expression partially via transcription factor YY1. *Carcinogenesis*. 28:1867-1876.

Lin, K.K., L. Rossi, N.C. Boles, B.E. Hall, T.C. George, and M.A. Goodell. 2011. CD81 is essential for the re-entry of hematopoietic stem cells to quiescence following stress-induced proliferation via deactivation of the Akt pathway. *PLoS biology*. 9:e1001148.

Linden, H.M., and K. Kaushansky. 2000. The glycan domain of thrombopoietin enhances its secretion. *Biochemistry*. 39:3044-3051.

Linnekin, D., C.S. DeBerry, and S. Mou. 1997. Lyn associates with the juxtamembrane region of c-Kit and is activated by stem cell factor in hematopoietic cell lines and normal progenitor cells. *The Journal of biological chemistry*. 272:27450-27455.

Liu, H., A.W. Chi, K.L. Arnett, M.Y. Chiang, L. Xu, O. Shestova, H. Wang, Y.M. Li, A. Bhandoola, J.C. Aster, S.C. Blacklow, and W.S. Pear. 2010a. Notch dimerization is required for leukemogenesis and T-cell development. *Genes & development*. 24:2395-2407.

Liu, J., C. Sato, M. Cerletti, and A. Wagers. 2010b. Notch signaling in the regulation of stem cell self-renewal and differentiation. *Current topics in developmental biology*. 92:367-409.

Liu, W., M. Wang, D.C. Tang, I. Ding, and G.P. Rodgers. 1999. Thrombopoietin has a differentiative effect on late-stage human erythropoiesis. *British journal of haematology*. 105:459-469.

Lok, S., K. Kaushansky, R.D. Holly, J.L. Kuijper, C.E. Lofton-Day, P.J. Oort, F.J. Grant, M.D. Heipel, S.K. Burkhead, J.M. Kramer, and et al. 1994. Cloning and expression of murine thrombopoietin cDNA and stimulation of platelet production in vivo. *Nature*. 369:565-568.

Longley, B.J., Jr., D.D. Metcalfe, M. Tharp, X. Wang, L. Tyrrell, S.Z. Lu, D. Heitjan, and Y. Ma. 1999. Activating and dominant inactivating c-KIT catalytic domain mutations in distinct clinical forms of human mastocytosis. *Proceedings of the National Academy of Sciences of the United States of America*. 96:1609-1614.

Longley, B.J., Jr., G.S. Morganroth, L. Tyrrell, T.G. Ding, D.M. Anderson, D.E. Williams, and R. Halaban. 1993. Altered metabolism of mast-cell growth factor (c-kit ligand) in cutaneous mastocytosis. *The New England journal of medicine*. 328:1302-1307.

Maillard, I., U. Koch, A. Dumortier, O. Shestova, L. Xu, H. Sai, S.E. Pross, J.C. Aster, A. Bhandoola, F. Radtke, and W.S. Pear. 2008. Canonical notch signaling is dispensable for the maintenance of adult hematopoietic stem cells. *Cell stem cell*. 2:356-366.

Malaise, M., D. Steinbach, and S. Corbacioglu. 2009. Clinical implications of c-Kit mutations in acute myelogenous leukemia. *Current hematologic malignancy reports*. 4:77-82.

Malinge, S., and J. Crispino. 2010. Notch: of mice and men? *Blood*. 116:5438-5439.

Malinge, S., C. Ragu, V. Della-Valle, D. Pisani, S.N. Constantinescu, C. Perez, J.L. Villeval, D. Reinhardt, J. Landman-Parker, L. Michaux, N. Dastugue, A. Baruchel, W. Vainchenker, J.P. Bourquin, V. Penard-Lacronique, and O.A. Bernard. 2008. Activating mutations in human acute megakaryoblastic leukemia. *Blood*. 112:4220-4226.

Malinge, S., C. Thiollier, T.M. Chlon, L.C. Dore, L. Diebold, O. Bluteau, V. Mabialah, W. Vainchenker, P. Dessen, S. Winandy, T. Mercher, and J.D. Crispino. 2013. Ikaros inhibits megakaryopoiesis through functional interaction with GATA-1 and NOTCH signaling. *Blood*. 121:2440-2451.

Mancini, S.J., N. Mantei, A. Dumortier, U. Suter, H.R. MacDonald, and F. Radtke. 2005. Jagged1-dependent Notch signaling is dispensable for hematopoietic stem cell self-renewal and differentiation. *Blood*. 105:2340-2342.

Mansson, R., A. Hultquist, S. Luc, L. Yang, K. Anderson, S. Kharazi, S. Al-Hashmi, K. Liuba, L. Thoren, J. Adolfsson, N. Buza-Vidas, H. Qian, S. Soneji, T. Enver, M. Sigvardsson, and S.E. Jacobsen. 2007. Molecular evidence for hierarchical transcriptional lineage priming in fetal and adult stem cells and multipotent progenitors. *Immunity*. 26:407-419.

Marcelo, K.L., T.M. Sills, S. Coskun, H. Vasavada, S. Sanglikar, L.C. Goldie, and K.K. Hirschi. 2013. Hemogenic endothelial cell specification requires c-Kit, Notch signaling, and p27-mediated cell-cycle control. *Developmental cell*. 27:504-515.

Masson, K., E. Heiss, H. Band, and L. Ronnstrand. 2006. Direct binding of Cbl to Tyr568 and Tyr936 of the stem cell factor receptor/c-Kit is required for ligand-induced ubiquitination, internalization and degradation. *The Biochemical journal*. 399:59-67.

Matsuoka, Y., Y. Sasaki, R. Nakatsuka, M. Takahashi, R. Iwaki, Y. Uemura, and Y. Sonoda. 2011. Low level of c-kit expression marks deeply quiescent murine hematopoietic stem cells. *Stem cells*. 29:1783-1791.

Mazharian, A., C. Ghevaert, L. Zhang, S. Massberg, and S.P. Watson. 2011. Dasatinib enhances megakaryocyte differentiation but inhibits platelet formation. *Blood*. 117:5198-5206.

McCulloch, E.A., L. Siminovitch, J.E. Till, E.S. Russell, and S.E. Bernstein. 1965. The cellular basis of the genetically determined hemopoietic defect in anemic mice of genotype Sl-Sld. *Blood*. 26:399-410.

Mercher, T., M.G. Cornejo, C. Sears, T. Kindler, S.A. Moore, I. Maillard, W.S. Pear, J.C. Aster, and D.G. Gilliland. 2008. Notch signaling specifies megakaryocyte development from hematopoietic stem cells. *Cell stem cell*. 3:314-326.

Mercher, T., G.D. Raffel, S.A. Moore, M.G. Cornejo, D. Baudry-Bluteau, N. Cagnard, J.L. Jesneck, Y. Pikman, D. Cullen, I.R. Williams, K. Akashi, H. Shigematsu, J.P. Bourquin, M. Giovannini, W. Vainchenker, R.L. Levine, B.H. Lee, O.A. Bernard, and D.G. Gilliland. 2009. The OTT-MAL fusion oncogene activates RBPJ-mediated transcription and induces acute megakaryoblastic leukemia in a knockin mouse model. *The Journal of clinical investigation*. 119:852-864.

Mide, S.M., P. Huygens, C.E. Bozzini, and J.A. Fernandez Pol. 2001. Effects of human recombinant erythropoietin on differentiation and distribution of erythroid progenitor cells on murine medullary and splenic erythropoiesis during hypoxia and post-hypoxia. *In vivo*. 15:125-132.

Miller, B.A., S.P. Perrine, A. Bernstein, S.D. Lyman, D.E. Williams, L.L. Bell, and N.F. Olivieri. 1992. Influence of steel factor on hemoglobin synthesis in sickle cell disease. *Blood*. 79:1861-1868.

Minamiguchi, H., T. Kimura, Y. Urata, H. Miyazaki, T. Bamba, T. Abe, and Y. Sonoda. 2001. Simultaneous signalling through c-mpl, c-kit and CXCR4 enhances the proliferation and differentiation of human megakaryocyte progenitors: possible roles of the PI3-K, PKC and MAPK pathways. *British journal of haematology*. 115:175-185.

Miyazawa, K., K. Toyama, A. Gotoh, P.C. Hendrie, C. Mantel, and H.E. Broxmeyer. 1994. Ligand-dependent polyubiquitination of c-kit gene product: a possible mechanism of receptor down modulation in M07e cells. *Blood*. 83:137-145.

Mohandas, N., and M. Prenant. 1978. Three-dimensional model of bone marrow. *Blood*. 51:633-643.

Morita, Y., H. Ema, and H. Nakauchi. 2010. Heterogeneity and hierarchy within the most primitive hematopoietic stem cell compartment. *The Journal of experimental medicine*. 207:1173-1182.

Muller-Sieburg, C.E., R.H. Cho, M. Thoman, B. Adkins, and H.B. Sieburg. 2002. Deterministic regulation of hematopoietic stem cell self-renewal and differentiation. *Blood*. 100:1302-1309.

Munugalavadla, V., L.C. Dore, B.L. Tan, L. Hong, M. Vishnu, M.J. Weiss, and R. Kapur. 2005. Repression of c-kit and its downstream substrates by GATA-1 inhibits cell proliferation during erythroid maturation. *Molecular and cellular biology*. 25:6747-6759.

Munugalavadla, V., and R. Kapur. 2005. Role of c-Kit and erythropoietin receptor in erythropoiesis. *Critical reviews in oncology/hematology*. 54:63-75.

Muta, K., S.B. Krantz, M.C. Bondurant, and C.H. Dai. 1995. Stem cell factor retards differentiation of normal human erythroid progenitor cells while stimulating proliferation. *Blood*. 86:572-580.

Myers, J., Y. Huang, L. Wei, Q. Yan, A. Huang, and L. Zhou. 2010. Fucose-deficient hematopoietic stem cells have decreased self-renewal and aberrant marrow niche occupancy. *Transfusion*. 50:2660-2669.

Nakamura-Ishizu, A., H. Takizawa, and T. Suda. 2014a. The analysis, roles and regulation of quiescence in hematopoietic stem cells. *Development*. 141:4656-4666.

Nakamura-Ishizu, A., K. Takubo, M. Fujioka, and T. Suda. 2014b. Megakaryocytes are essential for HSC quiescence through the production of thrombopoietin. *Biochemical and biophysical research communications*. 454:353-357.

Neben, T.Y., J. Loebelenz, L. Hayes, K. McCarthy, J. Stoudemire, R. Schaub, and S.J. Goldman. 1993. Recombinant human interleukin-11 stimulates megakaryocytopoiesis and increases peripheral platelets in normal and splenectomized mice. *Blood*. 81:901-908.

Ng, A.P., M. Kauppi, D. Metcalf, L. Di Rago, C.D. Hyland, and W.S. Alexander. 2012. Characterization of thrombopoietin (TPO)-responsive progenitor cells in adult mouse bone marrow with in vivo megakaryocyte and erythroid potential. *Proceedings of the National Academy of Sciences of the United States of America*. 109:2364-2369.

Ng, A.P., M. Kauppi, D. Metcalf, C.D. Hyland, E.C. Josefsson, M. Lebois, J.G. Zhang, T.M. Baldwin, L. Di Rago, D.J. Hilton, and W.S. Alexander. 2014. Mpl expression on megakaryocytes and platelets is dispensable for thrombopoiesis but essential to prevent myeloproliferation. *Proceedings of the National Academy of Sciences of the United States of America*. 111:5884-5889.

Ng, S.Y., T. Yoshida, J. Zhang, and K. Georgopoulos. 2009. Genome-wide lineage-specific transcriptional networks underscore Ikaros-dependent lymphoid priming in hematopoietic stem cells. *Immunity*. 30:493-507.

Nibley, W.E., and G.J. Spangrude. 1998. Primitive stem cells alone mediate rapid marrow recovery and multilineage engraftment after transplantation. *Bone marrow transplantation*. 21:345-354.

Nicoli, S., C.P. Knyphausen, L.J. Zhu, A. Lakshmanan, and N.D. Lawson. 2012. miR-221 is required for endothelial tip cell behaviors during vascular development. *Developmental cell*. 22:418-429.

Nishikii, H., Y. Kanazawa, T. Umemoto, Y. Goltsev, Y. Matsuzaki, K. Matsushita, M. Yamato, G.P. Nolan, R. Negrin, and S. Chiba. 2015. Unipotent megakaryopoietic pathway bridging hematopoietic stem cells and mature megakaryocytes. *Stem cells*.

Nishimura, S., M. Nagasaki, S. Kunishima, A. Sawaguchi, A. Sakata, H. Sakaguchi, T. Ohmori, I. Manabe, J.E. Italiano, Jr., T. Ryu, N. Takayama, I. Komuro, T. Kadowaki, K. Eto, and R. Nagai. 2015. IL-1alpha induces thrombopoiesis through megakaryocyte rupture in response to acute platelet needs. *The Journal of cell biology*. 209:453-466.

Nishio, M., A. Oda, K. Koizumi, I. Satoh, Y. Sato, T. Endoh, A. Tsutsumi, M. Fujihara, K. Ikebuchi, H. Ikeda, T. Koike, and K.I. Sawada. 2001. Stem cell factor prevents Fas-mediated apoptosis of human erythroid precursor cells with Src-family kinase dependency. *Experimental hematology*. 29:19-29.

Noh, J.Y., S. Gandre-Babbe, Y. Wang, V. Hayes, Y. Yao, P. Gadue, S.K. Sullivan, S.T. Chou, K.R. Machlus, J.E. Italiano, Jr., M. Kyba, D. Finkelstein, J.C. Ulirsch, V.G. Sankaran, D.L. French, M. Poncz, and M.J. Weiss. 2015. Inducible Gata1 suppression expands megakaryocyte-erythroid progenitors from embryonic stem cells. *The Journal of clinical investigation*. 125:2369-2374.

Nombela-Arrieta, C., and L.E. Silberstein. 2014. The science behind the hypoxic niche of hematopoietic stem and progenitors. *Hematology / the Education Program of the American Society of Hematology. American Society of Hematology. Education Program*. 2014:542-547.

Odai, H., K. Sasaki, Y. Hanazono, H. Ueno, T. Tanaka, K. Miyagawa, K. Mitani, Y. Yazaki, and H. Hirai. 1995. c-Cbl is inducibly tyrosine-phosphorylated by epidermal growth factor stimulation in fibroblasts, and constitutively tyrosine-phosphorylated and associated with v-Src in v-src-transformed fibroblasts. *Japanese journal of cancer research : Gann*. 86:1119-1126.

Oguro, H., L. Ding, and S.J. Morrison. 2013. SLAM family markers resolve functionally distinct subpopulations of hematopoietic stem cells and multipotent progenitors. *Cell stem cell*. 13:102-116.

Oh, P., C. Lobry, J. Gao, A. Tikhonova, E. Loizou, J. Manent, B. van Handel, S. Ibrahim, J. Greve, H. Mikkola, S. Artavanis-Tsakonas, and I. Aifantis. 2013. In vivo mapping of notch pathway activity in normal and stress hematopoiesis. *Cell stem cell*. 13:190-204.

Olson, T.S., A. Caselli, S. Otsuru, T.J. Hofmann, R. Williams, P. Paolucci, M. Dominici, and E.M. Horwitz. 2013. Megakaryocytes promote murine osteoblastic HSC niche expansion and stem cell engraftment after radioablative conditioning. *Blood*. 121:5238-5249.

Orfao, A., A.C. Garcia-Montero, L. Sanchez, L. Escribano, and Rema. 2007. Recent advances in the understanding of mastocytosis: the role of KIT mutations. *British journal of haematology*. 138:12-30.

Osawa, M., K. Hanada, H. Hamada, and H. Nakauchi. 1996. Long-term lymphohematopoietic reconstitution by a single CD34-low/negative hematopoietic stem cell. *Science*. 273:242-245.

Panuganti, S., E.T. Papoutsakis, and W.M. Miller. 2010. Bone marrow niche-inspired, multiphase expansion of megakaryocytic progenitors with high polyploidization potential. *Cytotherapy*. 12:767-782.

Panuganti, S., A.C. Schlinker, P.F. Lindholm, E.T. Papoutsakis, and W.M. Miller. 2013. Three-stage ex vivo expansion of high-ploidy megakaryocytic cells: toward large-scale platelet production. *Tissue engineering. Part A*. 19:998-1014.

Papadimitriou, C.A., M.S. Topp, H. Serve, E. Oelmann, M. Koenigsmann, J. Maurer, D. Oberberg, B. Reufi, E. Thiel, and W.E. Berdel. 1995. Recombinant human stem cell factor does exert minor stimulation of growth in small cell lung cancer and melanoma cell lines. *European journal of cancer*. 31A:2371-2378.

Parmar, K., P. Mauch, J.A. Vergilio, R. Sackstein, and J.D. Down. 2007. Distribution of hematopoietic stem cells in the bone marrow according to regional hypoxia. *Proceedings of the National Academy of Sciences of the United States of America*. 104:5431-5436.

Paronetto, M.P., J.P. Venables, D.J. Elliott, R. Geremia, P. Rossi, and C. Sette. 2003. Tr-kit promotes the formation of a multimolecular complex composed by Fyn, PLCgamma1 and Sam68. *Oncogene*. 22:8707-8715.

Pase, L., J.E. Layton, W.P. Kloosterman, D. Carradice, P.M. Waterhouse, and G.J. Lieschke. 2009. miR-451 regulates zebrafish erythroid maturation in vivo via its target gata2. *Blood*. 113:1794-1804.

Passegue, E., A.J. Wagers, S. Giuriato, W.C. Anderson, and I.L. Weissman. 2005. Global analysis of proliferation and cell cycle gene expression in the regulation of hematopoietic stem and progenitor cell fates. *The Journal of experimental medicine*. 202:1599-1611.

Pearce, K.H., Jr., B.J. Potts, L.G. Presta, L.N. Bald, B.M. Fendly, and J.A. Wells. 1997. Mutational analysis of thrombopoietin for identification of receptor and neutralizing antibody sites. *The Journal of biological chemistry*. 272:20595-20602.

Pedersen, M., T. Lofstedt, J. Sun, L. Holmquist-Mengelbier, S. Pahlman, and L. Ronnstrand. 2008. Stem cell factor induces HIF-1alpha at normoxia in hematopoietic cells. *Biochemical and biophysical research communications*. 377:98-103.

Perry, J.M., O.F. Harandi, and R.F. Paulson. 2007. BMP4, SCF, and hypoxia cooperatively regulate the expansion of murine stress erythroid progenitors. *Blood*. 109:4494-4502.

Perumalsamy, L.R., M. Nagala, P. Banerjee, and A. Sarin. 2009. A hierarchical cascade activated by non-canonical Notch signaling and the mTOR-Rictor complex regulates neglect-induced death in mammalian cells. *Cell death and differentiation*. 16:879-889.

Petit-Cocault, L., C. Volle-Challier, M. Fleury, B. Peault, and M. Souyri. 2007. Dual role of Mpl receptor during the establishment of definitive hematopoiesis. *Development*. 134:3031-3040.

Poirault-Chassac, S., E. Six, C. Catelain, M. Lavergne, J.L. Villeval, W. Vainchenker, and E. Lauret. 2010. Notch/Delta4 signaling inhibits human megakaryocytic terminal differentiation. *Blood*. 116:5670-5678.

Poulos, M.G., P. Guo, N.M. Kofler, S. Pinho, M.C. Gutkin, A. Tikhonova, I. Aifantis, P.S. Frenette, J. Kitajewski, S. Rafii, and J.M. Butler. 2013. Endothelial Jagged-1 is necessary for homeostatic and regenerative hematopoiesis. *Cell reports*. 4:1022-1034.

Pronk, C.J., D.J. Rossi, R. Mansson, J.L. Attema, G.L. Norddahl, C.K. Chan, M. Sigvardsson, I.L. Weissman, and D. Bryder. 2007. Elucidation of the phenotypic, functional, and molecular topography of a myeloerythroid progenitor cell hierarchy. *Cell stem cell*. 1:428-442.

Proulx, C., L. Boyer, D.R. Hurnanen, and R. Lemieux. 2003. Preferential ex vivo expansion of megakaryocytes from human cord blood CD34+-enriched cells in the presence of thrombopoietin and limiting amounts of stem cell factor and Flt-3 ligand. *Journal of hematotherapy & stem cell research*. 12:179-188.

Qian, H., N. Buza-Vidas, C.D. Hyland, C.T. Jensen, J. Antonchuk, R. Mansson, L.A. Thoren, M. Ekblom, W.S. Alexander, and S.E. Jacobsen. 2007. Critical role of thrombopoietin in maintaining adult quiescent hematopoietic stem cells. *Cell stem cell*. 1:671-684.

Qyang, Y., S.M. Chambers, P. Wang, X. Xia, X. Chen, M.A. Goodell, and H. Zheng. 2004. Myeloproliferative disease in mice with reduced presenilin gene dosage: effect of gamma-secretase blockage. *Biochemistry*. 43:5352-5359.

Racke, F.K., K. Lewandowska, S. Goueli, and A.N. Goldfarb. 1997. Sustained activation of the extracellular signal-regulated kinase/mitogen-activated protein kinase pathway is required for megakaryocytic differentiation of K562 cells. *The Journal of biological chemistry*. 272:23366-23370.

Rajaraman, S., W.S. Davis, A. Mahakali-Zama, H.K. Evans, L.B. Russell, and M.A. Bedell. 2002. An allelic series of mutations in the kit ligand gene of mice. I. Identification of point mutations in seven ethylnitrosourea-induced Kitl(Steel) alleles. *Genetics*. 162:331-340.

Rhodes, M.M., P. Kopsombut, M.C. Bondurant, J.O. Price, and M.J. Koury. 2008. Adherence to macrophages in erythroblastic islands enhances erythroblast proliferation and increases erythrocyte production by a different mechanism than erythropoietin. *Blood*. 111:1700-1708.

Robert-Moreno, A., L. Espinosa, M.J. Sanchez, J.L. de la Pompa, and A. Bigas. 2007. The notch pathway positively regulates programmed cell death during erythroid differentiation. *Leukemia*. 21:1496-1503.

Rooke, H.M., and S.H. Orkin. 2006. Phosphorylation of Gata1 at serine residues 72, 142, and 310 is not essential for hematopoiesis in vivo. *Blood*. 107:3527-3530.

Ross, J., L. Mavoungou, E.H. Bresnick, and E. Milot. 2012. GATA-1 utilizes Ikaros and polycomb repressive complex 2 to suppress Hes1 and to promote erythropoiesis. *Molecular and cellular biology*. 32:3624-3638.

Rossi, D.J., D. Bryder, J.M. Zahn, H. Ahlenius, R. Sonu, A.J. Wagers, and I.L. Weissman. 2005. Cell intrinsic alterations underlie hematopoietic stem cell aging. *Proceedings of the National Academy of Sciences of the United States of America*. 102:9194-9199.

Rossi, P., G. Marziali, C. Albanesi, A. Charlesworth, R. Geremia, and V. Sorrentino. 1992. A novel c-kit transcript, potentially encoding a truncated receptor, originates within a kit gene intron in mouse spermatids. *Developmental biology*. 152:203-207.

Rothenberg, E.V. 2014. Transcriptional control of early T and B cell developmental choices. *Annual review of immunology*. 32:283-321.

Rouleau, C., K. Cui, and L. Feldman. 2004. A functional erythropoietin receptor is necessary for the action of thrombopoietin on erythroid cells lacking c-mpl. *Experimental hematology*. 32:140-148.

Rouyez, M.C., C. Boucheron, S. Gisselbrecht, I. Dusanter-Fourt, and F. Porteu. 1997. Control of thrombopoietin-induced megakaryocytic differentiation by the mitogen-activated protein kinase pathway. *Molecular and cellular biology*. 17:4991-5000.

Rylski, M., J.J. Welch, Y.Y. Chen, D.L. Letting, J.A. Diehl, L.A. Chodosh, G.A. Blobel, and M.J. Weiss. 2003. GATA-1-mediated proliferation arrest during erythroid maturation. *Molecular and cellular biology*. 23:5031-5042.

Sanchez, M., I.L. Weissman, M. Pallavicini, M. Valeri, P. Guglielmelli, A.M. Vannucchi, G. Migliaccio, and A.R. Migliaccio. 2006. Differential amplification of murine bipotent megakaryocytic/erythroid progenitor and precursor cells during recovery from acute and chronic erythroid stress. *Stem cells*. 24:337-348.

Sanjuan-Pla, A., I.C. Macaulay, C.T. Jensen, P.S. Woll, T.C. Luis, A. Mead, S. Moore, C. Carella, S. Matsuoka, T.B. Jones, O. Chowdhury, L. Stenson, M. Lutteropp, J.C. Green, R. Facchini, H. Boukarabila, A. Grover, A. Gambardella, S. Thongjuea, J. Carrelha, P. Tarrant, D. Atkinson, S.A. Clark, C. Nerlov, and S.E. Jacobsen. 2013. Platelet-biased stem cells reside at the apex of the haematopoietic stem-cell hierarchy. *Nature*. 502:232-236.

Sarrazin, S., and M. Sieweke. 2011. Integration of cytokine and transcription factor signals in hematopoietic stem cell commitment. *Seminars in immunology*. 23:326-334.

Sasaki, T., C. Mizuochi, Y. Horio, K. Nakao, K. Akashi, and D. Sugiyama. 2010. Regulation of hematopoietic cell clusters in the placental niche through SCF/Kit signaling in embryonic mouse. *Development*. 137:3941-3952.

Saur, S.J., V. Sangkhae, A.E. Geddis, K. Kaushansky, and I.S. Hitchcock. 2010. Ubiquitination and degradation of the thrombopoietin receptor c-Mpl. *Blood*. 115:1254-1263.

Serve, H., N.S. Yee, G. Stella, L. Sepp-Lorenzino, J.C. Tan, and P. Besmer. 1995. Differential roles of PI3-kinase and Kit tyrosine 821 in Kit receptor-mediated proliferation, survival and cell adhesion in mast cells. *The EMBO journal*. 14:473-483.

Shen, W.F., S. Rozenfeld, A. Kwong, L.G. Kom ves, H.J. Lawrence, and C. Largman. 1999. HOXA9 forms triple complexes with PBX2 and MEIS1 in myeloid cells. *Molecular and cellular biology*. 19:3051-3061.

Shimizu, R., J.D. Engel, and M. Yamamoto. 2008. GATA1-related leukaemias. *Nature reviews. Cancer*. 8:279-287.

Shin, H.M., M.E. Tilahun, O.H. Cho, K. Chandiran, C.A. Kuksin, S. Keerthivasan, A.H. Fauq, T.E. Golde, L. Miele, M. Thome, B.A. Osborne, and L.M. Minter. 2014a. NOTCH1 Can Initiate NF-kappaB Activation via Cytosolic Interactions with Components of the T Cell Signalosome. *Frontiers in immunology*. 5:249.

Shin, J.Y., W. Hu, M. Naramura, and C.Y. Park. 2014b. High c-Kit expression identifies hematopoietic stem cells with impaired self-renewal and megakaryocytic bias. *The Journal of experimental medicine*. 211:217-231.

Shultz, L.D., T.V. Rajan, and D.L. Greiner. 1997. Severe defects in immunity and hematopoiesis caused by SHP-1 protein-tyrosine-phosphatase deficiency. *Trends in biotechnology*. 15:302-307.

Simsek, T., F. Kocabas, J. Zheng, R.J. Deberardinis, A.I. Mahmoud, E.N. Olson, J.W. Schneider, C.C. Zhang, and H.A. Sadek. 2010. The distinct metabolic profile of hematopoietic stem cells reflects their location in a hypoxic niche. *Cell stem cell*. 7:380-390.

Skoda, R.C., D.C. Seldin, M.K. Chiang, C.L. Peichel, T.F. Vogt, and P. Leder. 1993. Murine c-mpl: a member of the hematopoietic growth factor receptor superfamily that transduces a proliferative signal. *The EMBO journal*. 12:2645-2653.

Snow, J.W., N. Abraham, M.C. Ma, N.W. Abbey, B. Herndier, and M.A. Goldsmith. 2002. STAT5 promotes multilineage hematolymphoid development in vivo through effects on early hematopoietic progenitor cells. *Blood*. 99:95-101.

Solar, G.P., W.G. Kerr, F.C. Zeigler, D. Hess, C. Donahue, F.J. de Sauvage, and D.L. Eaton. 1998. Role of c-mpl in early hematopoiesis. *Blood*. 92:4-10.

Soni, S., S. Bala, B. Gwynn, K.E. Sahr, L.L. Peters, and M. Hanspal. 2006. Absence of erythroblast macrophage protein (Emp) leads to failure of erythroblast nuclear extrusion. *The Journal of biological chemistry*. 281:20181-20189.

Soucie, E., F. Brenet, and P. Dubreuil. 2015. Molecular basis of mast cell disease. *Molecular immunology*. 63:55-60.

Soucie, E., K. Hanssens, T. Mercher, S. Georgin-Lavialle, G. Damaj, C. Livideanu, M.O. Chandesris, Y. Acin, S. Letard, P. de Sepulveda, O. Hermine, O.A. Bernard, and P. Dubreuil. 2012. In aggressive forms of mastocytosis, TET2 loss cooperates with c-KITD816V to transform mast cells. *Blood*. 120:4846-4849.

Spencer, J.A., F. Ferraro, E. Roussakis, A. Klein, J. Wu, J.M. Runnels, W. Zaher, L.J. Mortensen, C. Alt, R. Turcotte, R. Yusuf, D. Cote, S.A. Vinogradov, D.T. Scadden, and C.P. Lin. 2014. Direct measurement of local oxygen concentration in the bone marrow of live animals. *Nature*. 508:269-273.

Stachura, D.L., S.T. Chou, and M.J. Weiss. 2006. Early block to erythromegakaryocytic development conferred by loss of transcription factor GATA-1. *Blood*. 107:87-97.

Stier, S., T. Cheng, D. Dombkowski, N. Carlesso, and D.T. Scadden. 2002. Notch1 activation increases hematopoietic stem cell self-renewal in vivo and favors lymphoid over myeloid lineage outcome. *Blood*. 99:2369-2378.

Stockklausner, C., A.C. Klotter, N. Dickemann, I.N. Kuhlee, C.M. Duffert, C. Kerber, N.H. Gehring, and A.E. Kulozik. 2015. The thrombopoietin receptor P106L mutation functionally separates receptor signaling activity from thrombopoietin homeostasis. *Blood*. 125:1159-1169.

Strom, A., P. Castella, J. Rockwood, J. Wagner, and M. Caudy. 1997. Mediation of NGF signaling by post-translational inhibition of HES-1, a basic helix-loop-helix repressor of neuronal differentiation. *Genes & development*. 11:3168-3181.

Sugimoto, A., M. Yamamoto, M. Suzuki, T. Inoue, S. Nakamura, R. Motoda, F. Yamasaki, and K. Orita. 2006. Delta-4 Notch ligand promotes erythroid differentiation of human umbilical cord blood CD34+ cells. *Experimental hematology*. 34:424-432.

Sui, X., S.B. Krantz, M. You, and Z. Zhao. 1998. Synergistic activation of MAP kinase (ERK1/2) by erythropoietin and stem cell factor is essential for expanded erythropoiesis. *Blood*. 92:1142-1149.

Sun, J., A. Ramos, B. Chapman, J.B. Johnnidis, L. Le, Y.J. Ho, A. Klein, O. Hofmann, and F.D. Camargo. 2014. Clonal dynamics of native haematopoiesis. *Nature*. 514:322-327.

Szalai, G., A.C. LaRue, and D.K. Watson. 2006. Molecular mechanisms of megakaryopoiesis. *Cellular and molecular life sciences : CMLS*. 63:2460-2476.

Takubo, K., N. Goda, W. Yamada, H. Iriuchishima, E. Ikeda, Y. Kubota, H. Shima, R.S. Johnson, A. Hirao, M. Suematsu, and T. Suda. 2010. Regulation of the HIF-1alpha level is essential for hematopoietic stem cells. *Cell stem cell*. 7:391-402.

Tallack, M.R., G.W. Magor, B. Dartigues, L. Sun, S. Huang, J.M. Fittock, S.V. Fry, E.A. Glazov, T.L. Bailey, and A.C. Perkins. 2012. Novel roles for KLF1 in erythropoiesis revealed by mRNA-seq. *Genome research*. 22:2385-2398.

Tamir, A., T. Petrocelli, K. Stetler, W. Chu, J. Howard, B.S. Croix, J. Slingerland, and Y. Ben-David. 2000. Stem cell factor inhibits erythroid differentiation by modulating the activity of G1-cyclin-dependent kinase complexes: a role for p27 in erythroid differentiation coupled G1 arrest. *Cell growth & differentiation : the molecular biology journal of the American Association for Cancer Research*. 11:269-277.

Tang, M., G. Yin, F. Wang, H. Liu, S. Zhou, J. Ni, C. Chen, Y. Zhou, and Y. Zhao. 2015. Downregulation of CD9 promotes pancreatic cancer growth and metastasis through upregulation of epidermal growth factor on the cell surface. *Oncology reports*.

Thery, C., S. Amigorena, G. Raposo, and A. Clayton. 2006. Isolation and characterization of exosomes from cell culture supernatants and biological fluids. *Current protocols in cell biology / editorial board, Juan S. Bonifacino ... [et al.]*. Chapter 3:Unit 3 22.

Thoren, L.A., K. Liuba, D. Bryder, J.M. Nygren, C.T. Jensen, H. Qian, J. Antonchuk, and S.E. Jacobsen. 2008. Kit regulates maintenance of quiescent hematopoietic stem cells. *Journal of immunology*. 180:2045-2053.

Tijssen, M.R., and C. Ghevaert. 2013. Transcription factors in late megakaryopoiesis and related platelet disorders. *Journal of thrombosis and haemostasis : JTH*. 11:593-604.

Toki, T., R. Kanezaki, S. Adachi, H. Fujino, G. Xu, T. Sato, K. Suzuki, H. Tauchi, M. Endo, and E. Ito. 2009. The key role of stem cell factor/KIT signaling in the proliferation of blast cells from Down syndrome-related leukemia. *Leukemia*. 23:95-103.

Tong, W., Y.M. Ibarra, and H.F. Lodish. 2007. Signals emanating from the membrane proximal region of the thrombopoietin receptor (mpl) support hematopoietic stem cell self-renewal. *Experimental hematology*. 35:1447-1455.

Trajkovic, K., C. Hsu, S. Chiantia, L. Rajendran, D. Wenzel, F. Wieland, P. Schwille, B. Brugger, and M. Simons. 2008. Ceramide triggers budding of exosome vesicles into multivesicular endosomes. *Science*. 319:1244-1247.

Traver, D., T. Miyamoto, J. Christensen, J. Iwasaki-Arai, K. Akashi, and I.L. Weissman. 2001. Fetal liver myelopoiesis occurs through distinct, prospectively isolatable progenitor subsets. *Blood*. 98:627-635.

Turner, A.M., L.G. Bennett, N.L. Lin, J. Wypych, T.D. Bartley, R.W. Hunt, H.L. Atkins, K.E. Langley, V. Parker, F. Martin, and et al. 1995. Identification and characterization of a soluble c-kit receptor produced by human hematopoietic cell lines. *Blood*. 85:2052-2058.

van Galen, P., A. Kreso, E. Wienholds, E. Laurenti, K. Eppert, E.R. Lechman, N. Mbong, K. Hermans, S. Dobson, C. April, J.B. Fan, and J.E. Dick. 2014. Reduced lymphoid lineage priming promotes human hematopoietic stem cell expansion. *Cell stem cell*. 14:94-106.

Van Vlierberghe, P., and A. Ferrando. 2012. The molecular basis of T cell acute lymphoblastic leukemia. *The Journal of clinical investigation*. 122:3398-3406.

Vannucchi, A.M., F. Paoletti, S. Linari, C. Cellai, R. Caporale, P.R. Ferrini, M. Sanchez, G. Migliaccio, and A.R. Migliaccio. 2000. Identification and characterization of a bipotent (erythroid and megakaryocytic) cell precursor from the spleen of phenylhydrazine-treated mice. *Blood*. 95:2559-2568.

Varnum-Finney, B., L.M. Halasz, M. Sun, T. Gridley, F. Radtke, and I.D. Bernstein. 2011. Notch2 governs the rate of generation of mouse long- and short-term repopulating stem cells. *The Journal of clinical investigation*. 121:1207-1216.

Varnum-Finney, B., L. Wu, M. Yu, C. Brashem-Stein, S. Staats, D. Flowers, J.D. Griffin, and I.D. Bernstein. 2000. Immobilization of Notch ligand, Delta-1, is required for induction of notch signaling. *Journal of cell science*. 113 Pt 23:4313-4318.

Vigon, I., J.P. Mornon, L. Cocault, M.T. Mitjavila, P. Tambourin, S. Gisselbrecht, and M. Souyri. 1992. Molecular cloning and characterization of MPL, the human homolog of the v-mpl oncogene: identification of a member of the hematopoietic growth factor receptor superfamily. *Proceedings of the National Academy of Sciences of the United States of America*. 89:5640-5644.

Walker, L., M. Lynch, S. Silverman, J. Fraser, J. Boulter, G. Weinmaster, and J.C. Gasson. 1999. The Notch/Jagged pathway inhibits proliferation of human hematopoietic progenitors in vitro. *Stem cells*. 17:162-171.

Wang, H., J. Zou, B. Zhao, E. Johannsen, T. Ashworth, H. Wong, W.S. Pear, J. Schug, S.C. Blacklow, K.L. Arnett, B.E. Bernstein, E. Kieff, and J.C. Aster. 2011. Genome-wide analysis reveals conserved and divergent features of Notch1/RBPJ binding in human and murine T-lymphoblastic leukemia cells. *Proceedings of the National Academy of Sciences of the United States of America*. 108:14908-14913.

Wang, L., H. Zhang, S. Rodriguez, L. Cao, J. Parish, C. Mumaw, A. Zollman, M.M. Kamoka, J. Mu, D.Z. Chen, E.F. Srour, B.R. Chitteti, H. HogenEsch, X. Tu, T.M. Bellido, H.S. Boswell, T. Manshouri, S. Verstovsek, M.C. Yoder, R. Kapur, A.A. Cardoso, and N. Carlesso. 2014. Notch-dependent repression of miR-155 in the bone marrow niche regulates hematopoiesis in an NF-kappaB-dependent manner. *Cell stem cell*. 15:51-65.

Weber, J.M., and L.M. Calvi. 2010. Notch signaling and the bone marrow hematopoietic stem cell niche. *Bone*. 46:281-285.

Weber, S., S. Wetzel, J. Prox, T. Lehmann, J. Schneppenheim, M. Donners, and P. Saftig. 2013. Regulation of adult hematopoiesis by the a disintegrin and metalloproteinase 10 (ADAM10). *Biochemical and biophysical research communications*. 442:234-241.

Weng, A.P., J.M. Millholland, Y. Yashiro-Ohtani, M.L. Arcangeli, A. Lau, C. Wai, C. Del Bianco, C.G. Rodriguez, H. Sai, J. Tobias, Y. Li, M.S. Wolfe, C. Shachaf, D. Felsher, S.C. Blacklow, W.S. Pear, and J.C. Aster. 2006. c-Myc is an important direct target of Notch1 in T-cell acute lymphoblastic leukemia/lymphoma. *Genes & development*. 20:2096-2109.

Williams, D.E., J. Eisenman, A. Baird, C. Rauch, K. Van Ness, C.J. March, L.S. Park, U. Martin, D.Y. Mochizuki, H.S. Boswell, and et al. 1990. Identification of a ligand for the c-kit proto-oncogene. *Cell*. 63:167-174.

Wilson, A., E. Laurenti, G. Oser, R.C. van der Wath, W. Blanco-Bose, M. Jaworski, S. Offner, C.F. Dunant, L. Eshkind, E. Bockamp, P. Lio, H.R. Macdonald, and A. Trumpp. 2008. Hematopoietic stem cells reversibly switch from dormancy to self-renewal during homeostasis and repair. *Cell*. 135:1118-1129.

Winkler, I.G., V. Barbier, R. Wadley, A.C. Zannettino, S. Williams, and J.P. Levesque. 2010. Positioning of bone marrow hematopoietic and stromal cells relative to blood flow in vivo: serially reconstituting hematopoietic stem cells reside in distinct nonperfused niches. *Blood*. 116:375-385.

Wormald, S., and D.J. Hilton. 2004. Inhibitors of cytokine signal transduction. *The Journal of biological chemistry*. 279:821-824.

Wu, H., U. Klingmuller, P. Besmer, and H.F. Lodish. 1995. Interaction of the erythropoietin and stem-cell-factor receptors. *Nature*. 377:242-246.

Wu, W., and X.H. Sun. 2012. Janus kinase 3: the controller and the controlled. *Acta biochimica et biophysica Sinica*. 44:187-196.

Xiao, H., C. Lasser, G. Shelke, J. Wang, M. Radinger, T. Lunavat, C. Malmhall, L. Lin, J. Li, L. Li, and J. Lotvall. 2014. Mast cell exosomes promote lung adenocarcinoma cell proliferation inverted question mark role of KIT-stem cell factor signaling. *Cell communication and signaling : CCS*. 12:64.

Xue, X., N.K. Pech, W.C. Shelley, E.F. Srour, M.C. Yoder, and M.C. Dinauer. 2010. Antibody targeting KIT as pretransplantation conditioning in immunocompetent mice. *Blood*. 116:5419-5422.

Yamamoto, R., Y. Morita, J. Ooehara, S. Hamanaka, M. Onodera, K.L. Rudolph, H. Ema, and H. Nakauchi. 2013. Clonal analysis unveils self-renewing lineage-restricted progenitors generated directly from hematopoietic stem cells. *Cell*. 154:1112-1126.

Yan, X.Q., D.L. Lacey, C. Saris, S. Mu, D. Hill, R.G. Hawley, and F.A. Fletcher. 1999. Ectopic overexpression of c-mpl by retroviral-mediated gene transfer suppressed megakaryopoiesis but enhanced erythropoiesis in mice. *Experimental hematology*. 27:1409-1417.

Yao, D., Y. Huang, X. Huang, W. Wang, Q. Yan, L. Wei, W. Xin, S. Gerson, P. Stanley, J.B. Lowe, and L. Zhou. 2011. Protein O-fucosyltransferase 1 (Pofut1) regulates lymphoid and myeloid homeostasis through modulation of Notch receptor ligand interactions. *Blood*. 117:5652-5662.

Ye, Z.J., E. Gulcicek, K. Stone, T. Lam, V. Schulz, and S.M. Weissman. 2011. Complex interactions in EML cell stimulation by stem cell factor and IL-3. *Proceedings of the National Academy of Sciences of the United States of America*. 108:4882-4887.

Yoda, M., T. Kimura, T. Tohmonda, S. Uchikawa, T. Koba, J. Takito, H. Morioka, M. Matsumoto, D.C. Link, K. Chiba, Y. Okada, Y. Toyama, and K. Horiuchi. 2011. Dual functions of cell-autonomous and non-cell-autonomous ADAM10 activity in granulopoiesis. *Blood*. 118:6939-6942.

Yoshida, H., K. Kawane, M. Koike, Y. Mori, Y. Uchiyama, and S. Nagata. 2005. Phosphatidylserine-dependent engulfment by macrophages of nuclei from erythroid precursor cells. *Nature*. 437:754-758.

Yoshihara, H., F. Arai, K. Hosokawa, T. Hagiwara, K. Takubo, Y. Nakamura, Y. Gomei, H. Iwasaki, S. Matsuoka, K. Miyamoto, H. Miyazaki, T. Takahashi, and T. Suda. 2007. Thrombopoietin/MPL signaling regulates hematopoietic stem cell quiescence and interaction with the osteoblastic niche. *Cell stem cell*. 1:685-697.

Zayas, J., D.S. Spassov, R.G. Nachtman, and R. Jurecic. 2008. Murine hematopoietic stem cells and multipotent progenitors express truncated intracellular form of c-kit receptor. *Stem cells and development*. 17:343-353.

Zeng, S., Z. Xu, S. Lipkowitz, and J.B. Longley. 2005. Regulation of stem cell factor receptor signaling by Cbl family proteins (Cbl-b/c-Cbl). *Blood*. 105:226-232.

Zeuner, A., F. Francescangeli, M. Signore, M.A. Venneri, F. Pedini, N. Felli, A. Pagliuca, C. Conticello, and R. De Maria. 2011. The Notch2-Jagged1 interaction mediates stem cell factor signaling in erythropoiesis. *Cell death and differentiation*. 18:371-380.

Zeuner, A., M. Signore, D. Martinetti, M. Bartucci, C. Peschle, and R. De Maria. 2007. Chemotherapy-induced thrombocytopenia derives from the selective death of megakaryocyte progenitors and can be rescued by stem cell factor. *Cancer research*. 67:4767-4773.

Zhao, M., J.M. Perry, H. Marshall, A. Venkatraman, P. Qian, X.C. He, J. Ahamed, and L. Li. 2014. Megakaryocytes maintain homeostatic quiescence and promote post-injury regeneration of hematopoietic stem cells. *Nature medicine*. 20:1321-1326.

Zhao, W., C. Kitidis, M.D. Fleming, H.F. Lodish, and S. Ghaffari. 2006. Erythropoietin stimulates phosphorylation and activation of GATA-1 via the PI3-kinase/AKT signaling pathway. *Blood*. 107:907-915.

Zhou, L., L.W. Li, Q. Yan, B. Petryniak, Y. Man, C. Su, J. Shim, S. Chervin, and J.B. Lowe. 2008. Notch-dependent control of myelopoiesis is regulated by fucosylation. *Blood*. 112:308-319.

Zhu, H.H., K. Ji, N. Alderson, Z. He, S. Li, W. Liu, D.E. Zhang, L. Li, and G.S. Feng. 2011. Kit-Shp2-Kit signaling acts to maintain a functional hematopoietic stem and progenitor cell pool. *Blood*. 117:5350-5361.

Zsebo, K.M., D.A. Williams, E.N. Geissler, V.C. Broudy, F.H. Martin, H.L. Atkins, R.Y. Hsu, N.C. Birkett, K.H. Okino, D.C. Murdock, and et al. 1990. Stem cell factor is encoded at the Sl locus of the mouse and is the ligand for the c-kit tyrosine kinase receptor. *Cell*. 63:213-224.

Régulations divergentes du récepteur c-Kit par la TPO et la tétraspanine CD9 :
Implication dans le contrôle de la balance prolifération/maturation mégacaryocytaire

La thrombopoïétine (TPO) favorise successivement la prolifération et la maturation des progéniteurs mégacaryocytaires, soulevant la question du mécanisme expliquant cette dualité d'action. La signalisation SCF/ c-Kit est essentielle pour la prolifération de tous les progéniteurs hématopoïétiques, alors que l'extinction de l'expression du récepteur c-Kit est requise pour l'engagement en différenciation terminale. Réciproquement, l'équipe a montré que la stimulation de la voie Notch affecte une sous-population de progéniteurs bipotents érythro-mégacaryocytaires exprimant fortement CD9 (tétraspanine induite durant la maturation mégacaryocytaire) et favorise la reprise de leurs divisions au détriment de leur différenciation mégacaryocytaire terminale. Cet effet de la voie Notch s'accompagne d'une augmentation de l'expression de c-Kit. Ces observations m'ont conduite à m'intéresser aux mécanismes de régulation de c-Kit par la TPO en m'appuyant sur un modèle de progéniteurs bipotents immortalisés et dont la prolifération est strictement dépendante de la TPO (cellules G1ME). Les travaux réalisés durant ma thèse m'ont permis d'établir que (i) La stimulation des cellules G1ME par le ligand de Notch DLL1 favorise l'expression de c-Kit et réprime celle de CD9 (ii) L'activation inattendue de c-Kit par la TPO contribue à la prolifération (iii) c-Kit contribue activement à restreindre la polyploïdisation des cellules G1ME en présence de TPO (iv) La tétraspanine CD9 elle-même réprime l'expression de c-Kit à la membrane. Sur la base de ces résultats, nous proposons le modèle selon lequel, la TPO participerait à la fois à la prolifération des progéniteurs du fait de sa capacité à activer c-Kit, mais contribue aussi à l'augmentation de l'expression de CD9 qui en atteignant un seuil suffisant conduit à l'extinction de l'expression de c-Kit à la surface, entrainant alors l'arrêt des divisions et la différenciation mégacaryocytaire terminale.

Mots clés :

Divergent regulations of c-Kit receptor by TPO and CD9 in megakaryocytic cells:
Implication in the dynamic control of the balance proliferation/differentiation

The Thrombopoietin (TPO) favors both the proliferation and the maturation of megakaryocytic progenitors, raising the question of the molecular mechanism explaining its dual function. SCF/ c-Kit signaling is essential for all hematopoietic progenitors amplification, whereas terminal differentiation requires the extinction of c-Kit receptor expression. Reciprocally, we evidenced in our team that Notch stimulation enables the induction of c-Kit expression and act on a particular subpopulation of bipotent erythro-megakaryocytic progenitors highly expressing the tetraspanin CD9 (induced during megakaryocytic maturation) and favors their re-entry in a cycling state by blocking their megakaryocytic maturation. These observations lead to the investigation of the molecular mechanism of c-Kit regulation by TPO in a cellular model of bipotent progenitors immortalized and dependent on TPO, the G1ME cells. During my thesis, I evidenced that: i) Notch stimulation induces the expression of c-Kit while repressing CD9 expression; ii) Surprisingly TPO is able to activate c-Kit allowing its contribution to cell proliferation; iii) c-Kit also represses megakaryocytic polyploidization (endomitosis characterizing megakaryocytic maturation) of G1ME cells; iv) The tetraspanin CD9 represses the expression of c-Kit. The ensemble of these data allows us to propose the following model wherein TPO activates c-Kit allowing the proliferation of megakaryocytic progenitors, while concomitantly induces the expression of the tetraspanin CD9 that will reach a sufficient level to provoke the extinction of c-Kit expression at the cell surface, thus enabling the arrest of cell cycling progress and the engagement into terminal megakaryocytic maturation.

Keywords: